

T
F-86
VER

SIMULATION OF MIXED-FEED LIME SHAFT KILN : PERFORMANCE ANALYSIS AND OPTIMAL DESIGN

A THESIS
submitted in fulfilment of the
requirements for the award of the degree
of
DOCTOR OF PHILOSOPHY
in
CHEMICAL ENGINEERING

By

CHAMAN LAL VERMA




DEPARTMENT OF CHEMICAL ENGINEERING
UNIVERSITY OF ROORKEE
ROORKEE-247 667 (INDIA)

December, 1986


CANDIDATE'S DECLARATION

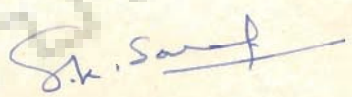
I hereby certify that the work which is being presented in the thesis entitled 'SIMULATION OF MIXED-FEED LIME SHAFT KILN: PERFORMANCE ANALYSIS AND OPTIMAL DESIGN' in fulfilment of the requirement for the award of the Degree of Doctor of Philosophy submitted in the Department of Chemical Engineering of the University is an authentic record of my own work carried out during a period from July, 1979 to December, 1986 under the supervision of Dr. S.K. Saraf and Dr. N.G. Dave.

The matter embodied in this thesis has not been submitted by me for the award of any other Degree.


(CHAMAN LAL VERMA)

This is to certify that the above statement made by the candidate is correct to the best of our knowledge.


(NATWAR G. DAVE)
Scientist (Building Materials)
Central Building Research
Institute, Roorkee (U.P.) 247 667
India


(SHANT KUMAR SARAF)
Professor of Chemical Engineering
University of Roorkee, Roorkee
(U.P.) 247 667 - India

DATE : 26 DECEMBER, 1986

ABSTRACT

The process of endothermic decomposition of calcium carbonate (limestone) to calcium oxide (quick lime) is brought about at elevated temperatures usually exceeding 1173 K under atmospheric pressure conditions. A mixed feed lime shaft kiln is basically a solid fuel-fired moving bed reactor with the upward-flow of hot gases counter-current to the down-flow of a mixed-charge of limestone and fuel particles undergoing calcination and combustion, respectively. A kiln basically has three operating sections, namely, the preheating, the burning and the cooling zones. The feed consisting of limestone and fuel particles is loaded into the kiln at the top, and the calcined product is withdrawn from its bottom. Air at ambient conditions enters at the bottom and the hot kiln (exhaust) gases leave from the top of the kiln.

The literature survey revealed that although the most sophisticated lime shaft kilns have been developed to obtain high productivity, lime quality and thermal efficiency, yet the design of a suitable kiln for a new situation using the basic principles involved in lime burning remains uncertain owing to the complex nature of the process and the uncertainties involved in the operating practices. No published information is available on mathematical modelling and simulation of the mixed-feed limeshaft kilns.

A field survey conducted for the study of lime kilns in India revealed that a major fraction of lime is being produced in the mixed-feed lime shaft kilns in the building and small scale process

industries for capacities generally in the range of 5 to 15 tonnes of quick lime per day. Presently these kilns are designed using thumb rules, based on past experience. For example, the relevant Indian Standards suggest a height-to-diameter ratio in the range of 3 to 4 corresponding to a superficial lime output rate of $2.5 \text{ tonnes}/(\text{m}^2 \text{ day})$ for an efficient mixed-feed vertical lime shaft kiln.

In view of the importance of the mixed-feed lime shaft kilns for lime manufacture in India, the present investigation was undertaken to develop a detailed mathematical model for simulating the performance of such kilns. The effect of different design and operating parameters on the performance of these kilns was then studied to establish optimal design and operating criteria.

Initially an attempt was made to evolve some state-of-the-art process engineering correlations for the mixed feed lime shaft kilns based on published information and the experience gained during the field survey and investigations on some commercially operating kilns. The energy requirements for the preheating and calcination of limestones were correlated with their chemical compositions. For a continuously operated kiln the times required for the preheating of limestone particles, their calcination and cooling of the product quick lime were correlated in terms of the particle diameters and the superficial lime output rates. The heights of the three zones of the lime kiln were estimated through the knowledge of the retention times for the respective zones. On account of the generalized practice

of semi-continuous kiln operation followed for these types of low capacity mixed-feed kilns, a correlation was evolved to estimate the increase in the overall retention time by duly accounting for the time lag of manual over mechanized operation, working (8-hourly) shifts per day, the number of charges or discharges effected per shift, and the average time for each charge or discharge.

Simulation of the mixed-feed lime shaft kiln required a detailed study of the phenomenological behaviour of the process and careful analysis of the design and operating parameters. The important design parameters identified are : Nominal lime production rate, Superficial lime output rate, wall thickness of brick masonry shaft and the exhaust gas temperature. The operating parameters of significance are : the size of limestone particles, the size and composition of the fuel particles, limestone-to-fuel ratio in the mixed-feed (input) and excess air fraction.

The shrinking core model has been assumed for the decomposition of a limestone sphere undergoing calcination. At a given instant, there is a central core of undecomposed calcium carbonate surrounded by a shell of calcium oxide with the reaction occurring at the interface between the core and the shell. Rate of conduction of heat through the lime layer to the limestone core boundary has been taken to be the calcination rate controlling mechanism. The surface of stone exchanges heat with the fuel and

gases by conduction, convection and radiation mechanisms. The undecomposed limestone core is assumed to remain at the calcination temperature (1173 K) after the commencement of the calcination process irrespective of the core size. The net heat received at the surface of the limestone-lime particle is consumed for the dissociation of calcium carbonate and partially for the heating up of the lime layer. The stone particle conduction equation was solved using the usual quasi-steady state assumption for any specified surface temperature and limestone conversion. Development of the model equation with due consideration for the sensible heat accumulation in the lime layer, and accounting for variations in surface temperature and fractional conversion along the axial position in the kiln are the novel features incorporated in the proposed model.

The proximate analysis of coal provides a basic framework for describing its combustion behaviour in a mixed-feed lime shaft kiln. The coal particles get preheated initially to 373 K and thereupon the demosturization starts. The volatile matter is assumed to be driven off linearly with temperature when the fuel temperature lies in the range of 673-1173 K. Instantaneous combustion of the volatile matter is generally assumed when the fuel temperature becomes equal to greater than 948 K, the assumed value of auto-ignition temperature for the volatile matter. The volatile matter released in the fuel temperature range of 673 to 948 K is assumed to escape unburnt resulting in the partial loss of thermal efficiency.

The ignition of the fixed carbon content of a coal particle has been assumed to commence only after the process of devolatilization is completed. The kinetics of shrinking particle size model has been assumed for combustion of the fixed carbon content of the fuel alongwith simultaneous segregation of ash from the fuel particle. An equation to describe the combustion behaviour of the fixed carbon content of the coal particle was used which accounts for the surface reaction rate and oxygen mass transport resistances.

When the fuel temperature reaches 1173 K (assumed ash fusion temperature) and above, the fusion of the ash particles is assumed to result in the formation of a porous ash layer around the shrinking core of fixed carbon interspersed with the fine ash particles. The necessary changes in particle surface areas before and after the ash fusion and increase in the density of the ash layer on account of its shrinkage with increase in the fuel temperature are also incorporated in the model.

Detailed analysis and modelling of the preheating, burning and cooling zones of the coal fired lime shaft kiln are carried out with some realistic assumptions. Comprehensive material and energy balances have been written for a differential volume element of axial width ΔZ at a given axial position (Z) of the kiln in due cognizance of the conditions prevailing in a particular zone of the kiln under

consideration. The complicated interphase modes of the heat and mass transfer processes with or without chemical reactions, the relevant heat transfer coefficients, effectiveness factors for estimating active heat exchange surface areas, variations in specific heats with temperature and composition, variations in gas emissivities for gas-solid radiant heat exchange, etc., are properly accounted for in the analysis of a particular zone. In addition, the bulk movement of gaseous components from one phase to another at appropriate temperatures and their contributions in the energy balances are properly incorporated in the proposed models. The temperatures of bulk gas, limestone and the fuel particles, fractional degree of combustion of the fuel and fractional degree of calcination of the limestone particles are the important output parameters obtained from the solution of the simulation model after applying suitable convergence criteria. Thus, a rigorous, uniquely stable and efficient system has been developed for analyzing the behaviour of a coal fired lime shaft kiln.

The important design and operational parameters investigated, their average values for the base conditions, and their ranges of variation are given in Table-6.1 (Chapter-6).

The effect of variations in the design and operational parameters on the performance of the kiln are extensively discussed. Temperature and conversion profiles pertaining to the base conditions are carefully analyzed. Only one parameter is varied at a time for

parametric sensitivity analysis by choosing the maximum and the minimum values of the ranges investigated apart from the base conditions, maintaining all the other parameters at the values corresponding to the base conditions. The results of the sensitivity analysis are presented in Tables-6.4 through 6.6 (Chapter-6).

The aim of the present investigation was largely to develop a comprehensive, uniquely stable and an efficient simulation system for the mixed feed lime shaft kiln, a stupendous task in itself, and not to carry out rigorous optimization studies for such kilns. But parametric sensitivity analysis led to the identification of the following optimum and most appropriate design and operating conditions from the thermal performance point of view for a nominal lime production rate of 10 tpd :

- (i) Partical size of limestone (d_{P_s}) = 0.100 m
- (ii) Ratio of particle size of fuel to size of limestone
(d_{P_f} / d_{P_s}) = 0.5
- (iii) Superficial lime output rate (P_s) = 3.0 t/(m²) (day)
- (iv) Limestone to fuel ratio (X_r) = 5.8
- (v) Fractional content of volatile matter in
fuel (X_{fv}) = as low as possible, but not exceeding 0.25

(ix)

(vi) Excess air based on total combustion of fixed carbon and total volatile matter (X_{ea})

= - 10 percent

(vii) Wall thickness of masonry shaft (W_{rb}) excluding fire bricks

= 0.46 m

(viii) Exhaust gas temperature (T_{g_o})

= = 813 K

For the above conditions the effective kiln height-to-its-internal diameter ratio is around 6.5.

ACKNOWLEDGEMENTS

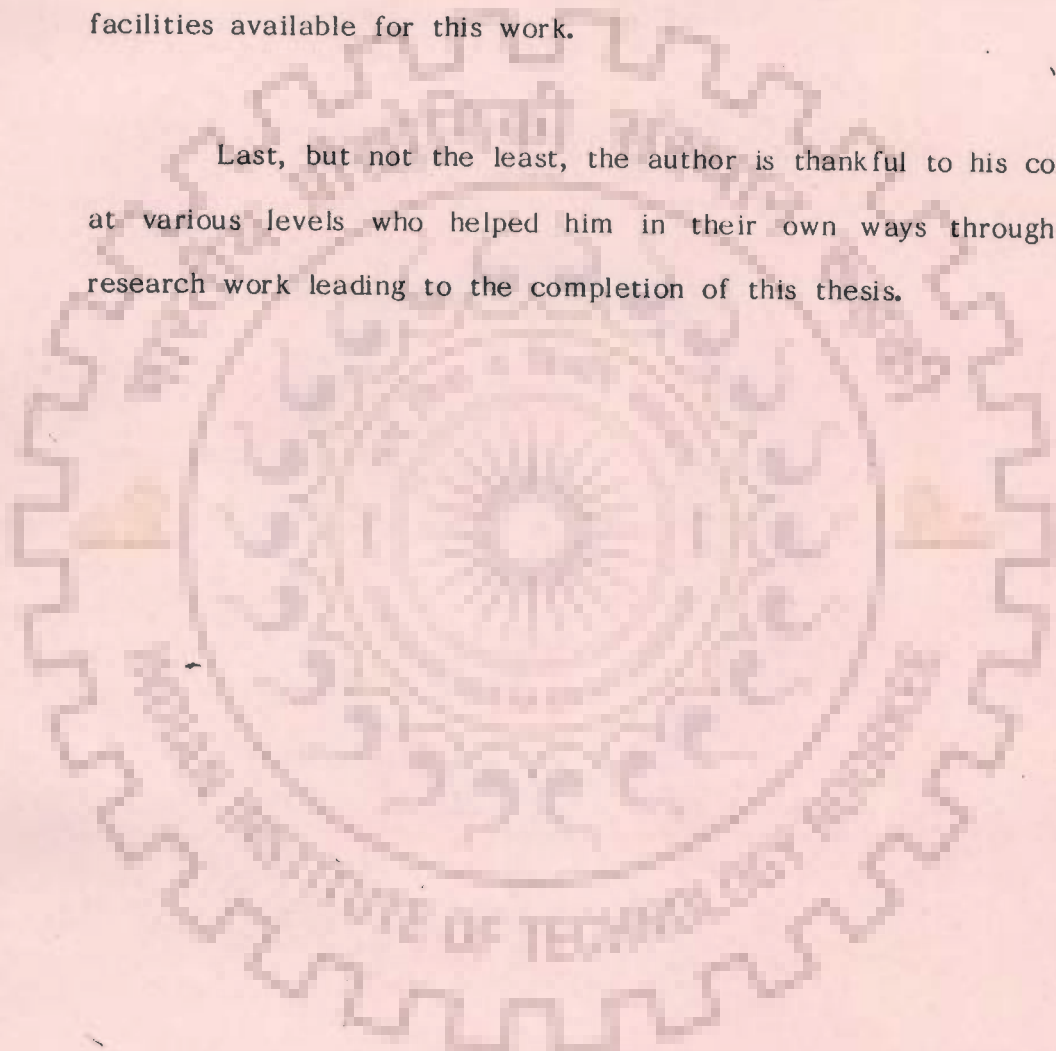
The author wishes to acknowledge with a profound sense of gratitude the inspiring guidance and luminous suggestions rendered by his venerable supervisors, Dr. S.K. Saraf, Professor of Chemical Engineering, University of Roorkee, Roorkee and Dr. N.G. Dave, Scientist (Building Materials), Central Building Research Institute, Roorkee. The critical inspiration and encouragement provided by them during the most crucial phases of the project led to the completion of this problem involving high complexities of analysis.

The author also wishes to express his deep sense of admiration for Dr. A.S. Moharir, presently Senior Research Engineer (Computer Aided Design Centre), Indian Institute of Technology, Bombay for the assistance provided by him in the initial formulation of computer programmes as well as the invaluable suggestions given by him from time to time.

He is grateful to Director, Central Building Research Institute, Roorkee for permitting him to work on this problem and for providing facilities throughout the course of the research work. The timely help provided by Dr. Mohan Rai, Deputy Director and Head, Building Materials Division and Dr. S.S. Wadhwa, Scientist Incharge, CBRI Computer Centre and his staff are humbly acknowledged.

Thanks are also due to Head, Chemical Engineering Department, University of Roorkee, Roorkee for making departmental facilities available for this work.

Last, but not the least, the author is thankful to his colleagues at various levels who helped him in their own ways throughout the research work leading to the completion of this thesis.



CONTENTS

	<u>PAGE</u>
DECLARATION	(i)
ABSTRACT	(ii)
ACKNOWLEDGEMENTS	(x)
LIST OF FIGURES	(xvi)
LIST OF TABLES	(xviii)
NOMENCLATURE	(xxi)
<u>CHAPTER-1</u>	
INTRODUCTION	1
<u>CHAPTER-2</u>	
REVIEW OF LITERATURE	6
2.1 LIMESTONE CALCINATION AND MECHANISM STUDIES	6
2.2 MANUFACTURE OF LIME IN SHAFT KILNS	13
2.3 DEVELOPMENTS ON LIME KILNS IN INDIA	17
2.4 OPERATIONAL PARAMETERS AND THERMAL EFFICIENCIES	21
2.5 PROCESS ENGINEERING IN KILN DESIGN	26
2.6 CRITICAL APPRAISAL	28

CHAPTER-3

PERFORMANCE ESTIMATION OF SOME MIXED-FEED LIME KILNS	30
3.1 FIELD SURVEY	30
3.2 IN-SITU INVESTIGATION	33
3.3 LABORATORY INVESTIGATION	41
3.4 PROCESS ENGINEERING CORRELATIONS : STATE-OF-THE-ART	45
3.5 INFERENCES	62

CHAPTER-4

MODELLING OF COAL FIRED LIME SHAFT KILN	65
4.1 PREAMBLE	65
4.2 ANALYSIS OF THE PREHEATING ZONE	66
4.3 MODEL FOR COMBUSTION BEHAVIOUR OF A COAL PARTICLE	74
4.4 HEAT CONDUCTION THROUGH LIME LAYER OF A CALCINING LIMESTONE PARTICLE	82
4.5 ANALYSIS OF THE BURNING ZONE	90
4.6 ANALYSIS OF THE COOLING ZONE	104

CHAPTER-5

DEVELOPMENT OF SIMULATION PROGRAMME	107
-------------------------------------	-----

5.1	SYSTEM PARAMETERS AND PROPERTIES ESTIMATION	107
-----	---	-----

5.2	HEAT LOSS THROUGH KILN WALL	122
-----	-----------------------------	-----

5.3	SALIENT FEATURES OF COMPUTER PROGRAMMES	125
-----	---	-----

CHAPTER-6

	RESULTS AND DISCUSSION	134
--	------------------------	-----

6.1	CHOICE OF PARAMETERS FOR SIMULATION STUDIES	134
-----	---	-----

6.2	SIMULATION RESULTS FOR THE BASE CONDITIONS	147
-----	--	-----

6.3	EFFECT OF VARIATIONS IN THE DESIGN AND OPERATIONAL PARAMETERS	167
-----	---	-----

6.4	CONDITIONS FOR OPTIMAL DESIGN AND OPERATION	176
-----	---	-----

CHAPTER -7

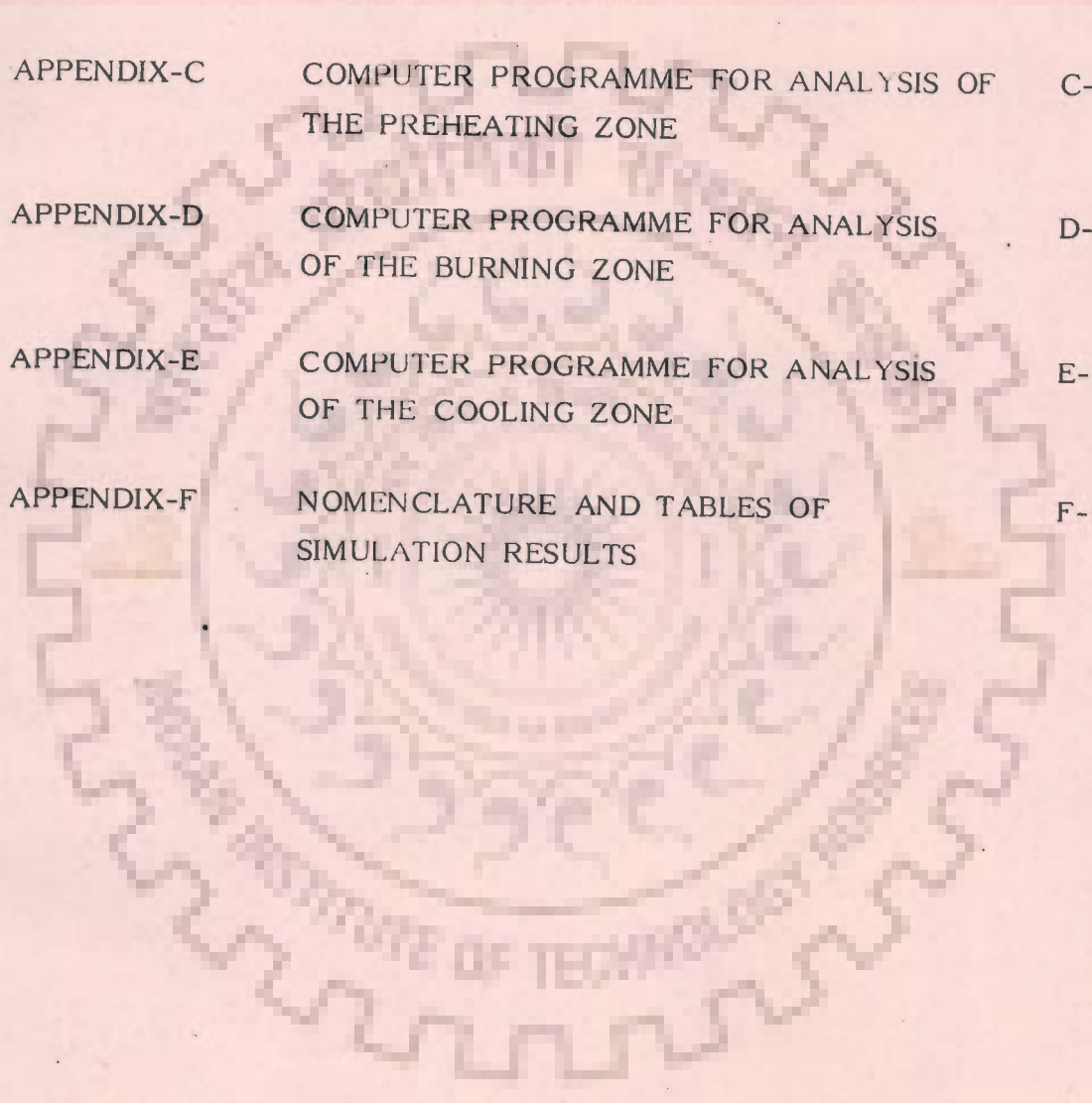
	CONCLUSIONS AND RECOMMENDATIONS	179
--	---------------------------------	-----

7.1	CONCLUSIONS	179
-----	-------------	-----

7.2	RECOMMENDATIONS	181
-----	-----------------	-----

	REFERENCES	183
--	------------	-----

APPENDIX-A	COMPUTER PROGRAMME FOR COMPUTATION OF ENERGY REQUIREMENTS IN LIME BURNING	A-1
APPENDIX-B	COMPUTER PROGRAMME FOR STATE-OF-THE-ART PROCESS ENGINEERING DESIGN COMPUTATIONS	B-1
APPENDIX-C	COMPUTER PROGRAMME FOR ANALYSIS OF THE PREHEATING ZONE	C-1
APPENDIX-D	COMPUTER PROGRAMME FOR ANALYSIS OF THE BURNING ZONE	D-1
APPENDIX-E	COMPUTER PROGRAMME FOR ANALYSIS OF THE COOLING ZONE	E-1
APPENDIX-F	NOMENCLATURE AND TABLES OF SIMULATION RESULTS	F-1



LIST OF FIGURES

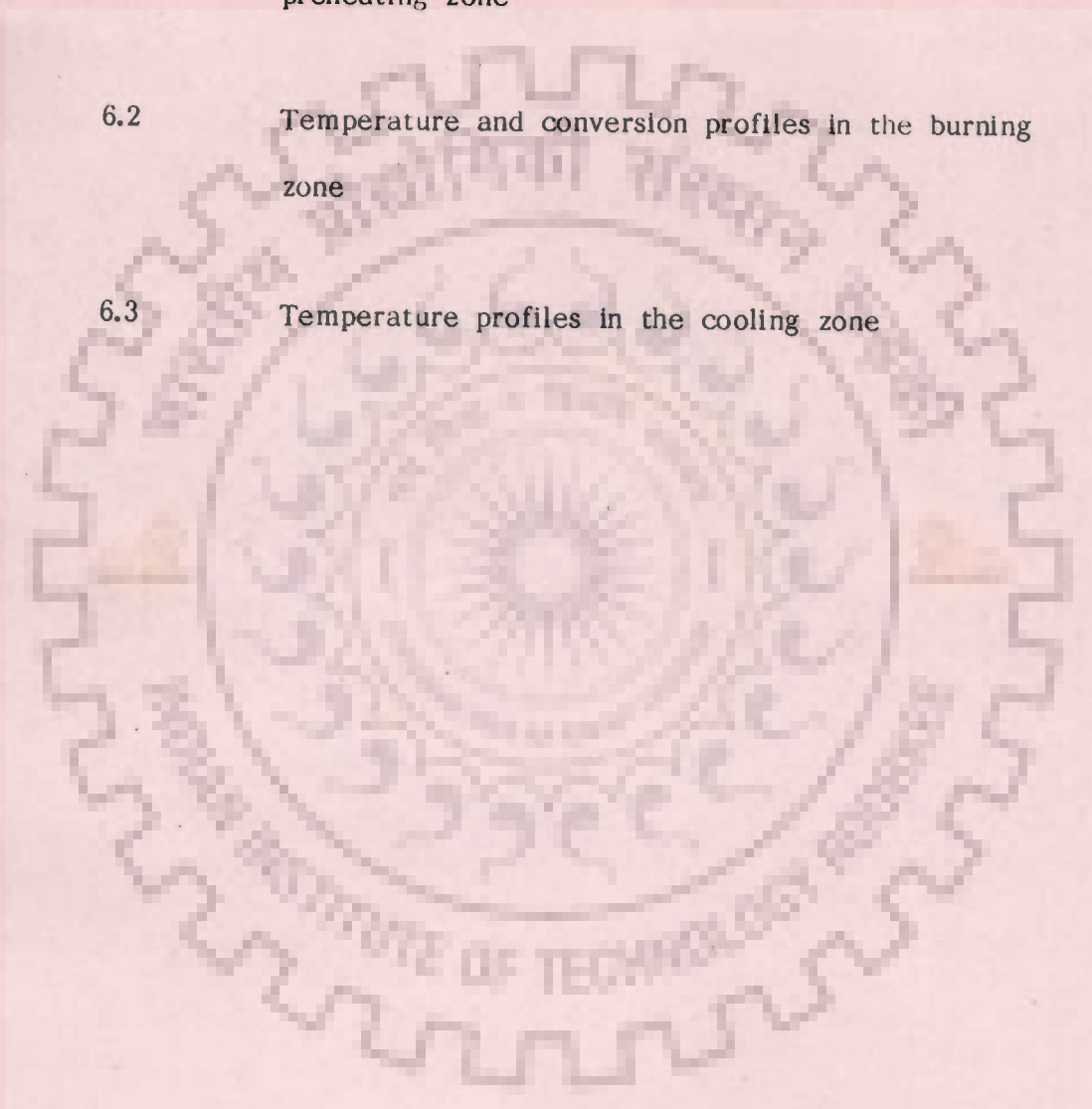
<u>FIG.</u>	<u>DESCRIPTION</u>	<u>PAGE</u>
2.1	A decomposing particle of calcite showing radial temperature profile in calcium oxide layer	6-A
2.2	Schematic diagram of a mixed-feed lime shaft kiln	14-A
3.1	Representative time-temperature graph at preheating section of cinder-fired lime kiln	34-A
3.2	Temperature variations at calcination section	34- B
3.3	Representative time-temperature graph at cooling section of cinder-fired lime kiln	34- C
3.4	Details of bench scale experimental lime kiln	41-A
4.1	Differential volume element in a generalized section of lime shaft kiln	69-A
5.1	Information flow diagram for analysis of the preheating zone	126-A
5.2	Information flow diagram for analysis of the burning zone	129-A

5.3 Information flow diagram for analysis of the cooling zone 132-A

6.1 Temperature profiles and fuel behaviour in the preheating zone 149-A

6.2 Temperature and conversion profiles in the burning zone 151-A

6.3 Temperature profiles in the cooling zone 159-A

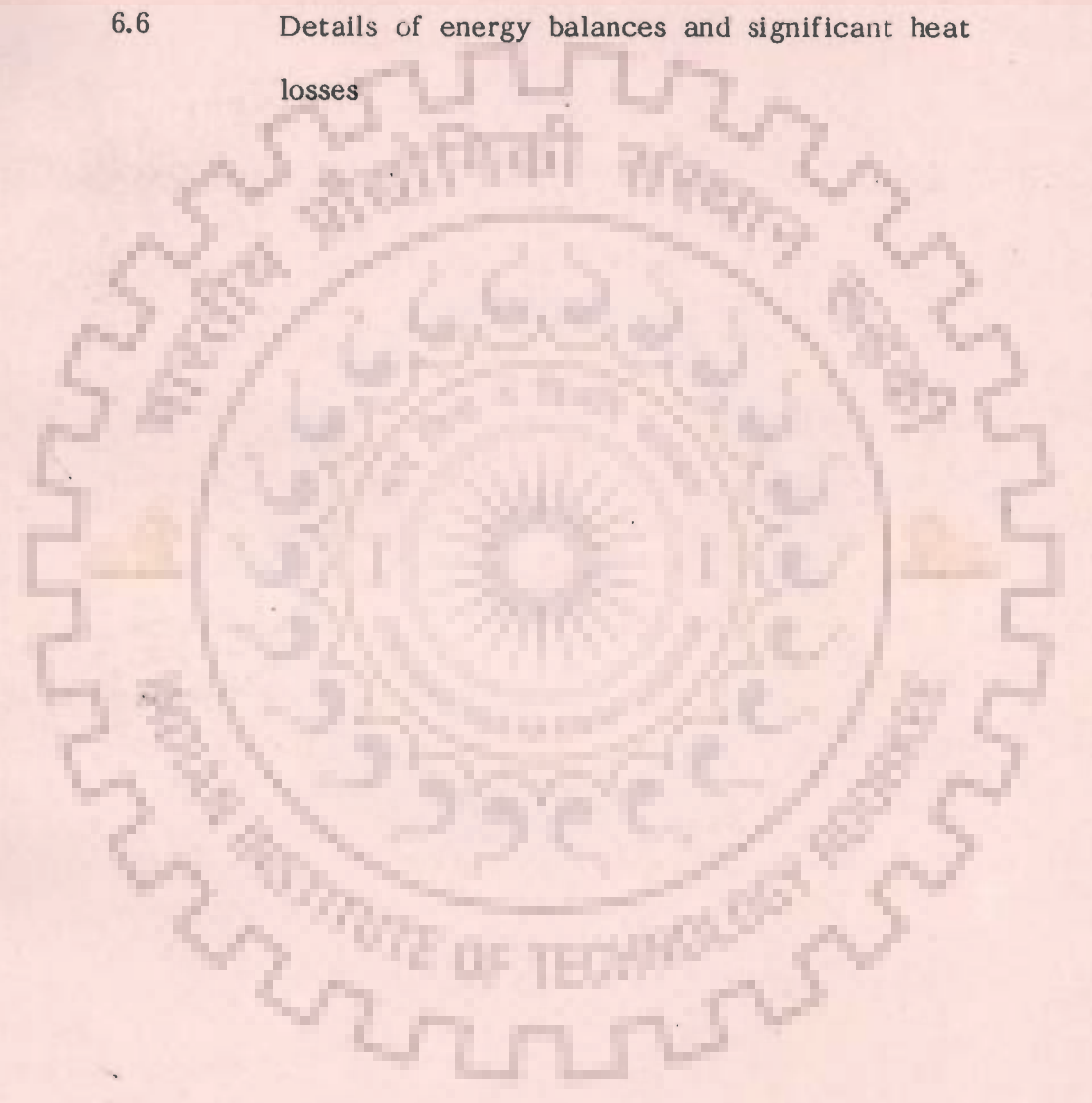


LIST OF TABLES

<u>TABLE</u>	<u>DESCRIPTION</u>	<u>PAGE</u>
3.1	Initial data on some masonry mixed-feed lime shaft kilns	32
3.2	General design specifications of the kilns investigated	35
3.3	Chemical analysis of limestone samples	35
3.4	Proximate analysis of cinders	36
3.5	Representative time-averaged analysis of gas samples	36
3.6	Quality of product in cinder-fired lime kilns	38
3.7	Performance Data for the cinder-fired lime kilns	40
3.8	Chemical analysis of limestone used in bench scale kiln	40
3.9	Proximate analysis of coal used in bench scale kiln	42
3.10	Operating data on the bench scale kiln	42
3.11	Average analysis of flue gas samples from bench scale kiln	44

3.12	Product distribution data in the bench scale kiln	44
3.13	Energy requirements in lime burning	50
3.14	Computed values of preheating times for limestones	53
3.15	Computed values of burning times for limestones	54
3.16	Computed values of cooling times for quick lime (lumps)	55
3.17	Comparison of retention times for field operating kilns	60
3.18	Process engineering design of coal fired lime shaft kiln	61
6.1	Important design and operating conditions : Average values and ranges investigated	135
6.2	Values of major system parameters	137
6.3	Computed parameters of significance	145
6.4	Design and performance results obtained from the simulation system	163

6.5	Details of kiln zonal heights and maximum temperature locations	165
6.6	Details of energy balances and significant heat losses	166



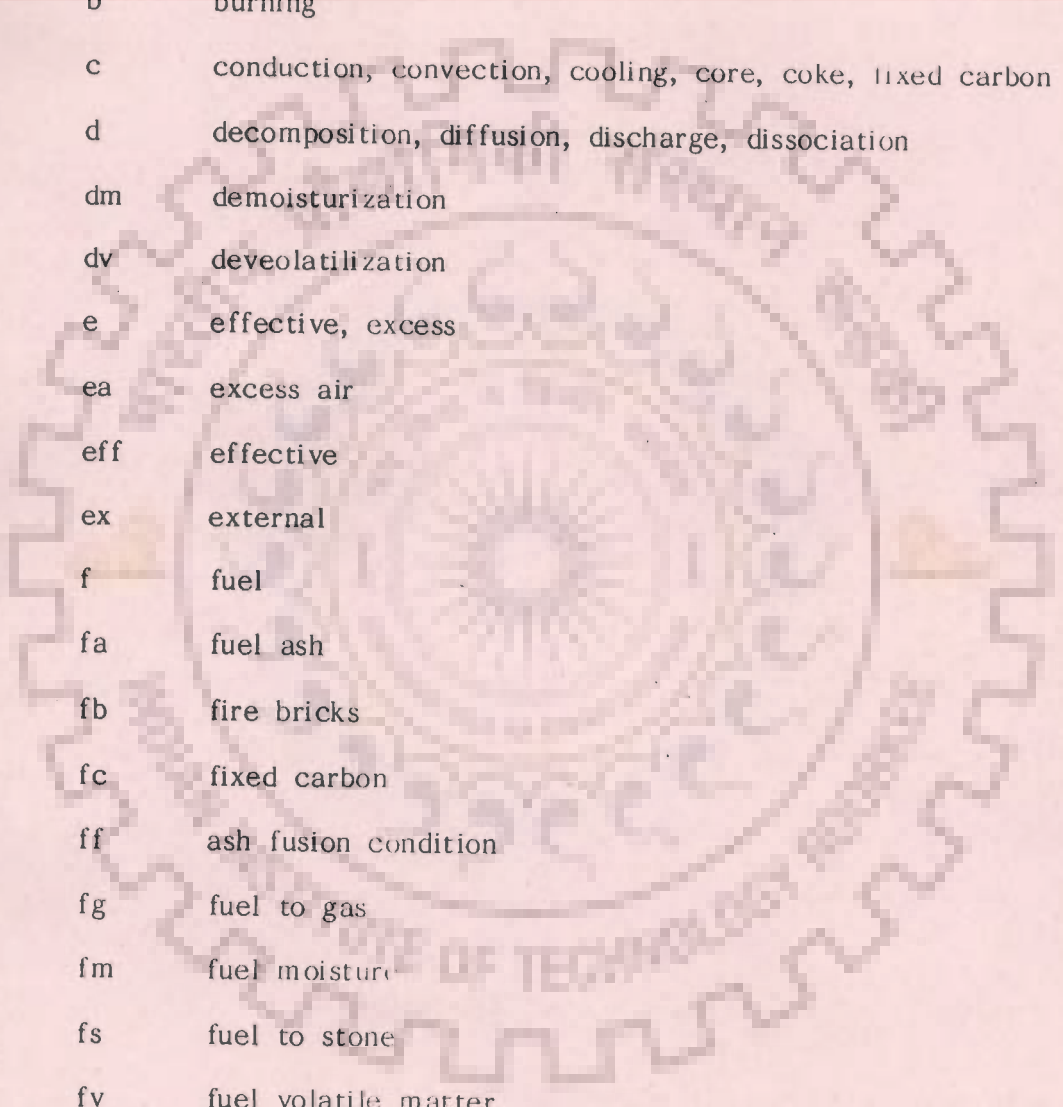
NOMENCLATURE

a	Constant as defined
a_s	Specific interfacial area of limestone particles, m^2/m^3 of bed volume
a_f	Specific interfacial area of fuel particles, m^2/m^3 of bed volume
$A_{l/c}$	Fractional time lag allowance for manual kiln operation over mechanised operation
C, C_p	Specific heat, Kcal/(Kg)(K)
d_p	Average particle diameter, m
D	Diameter, m
E	Energy, specific energy, Kcal/Kg
E_a	Fractional excess air
E_s	Endothermic heat of dissociation of limestone, Kcal/Kg
G	Superficial gas mass velocity based on empty kiln cross-sectional area, $Kg/(m^2)(hr)$
h	Heat transfer coefficient, $Kcal/(hr)(m^2)(K)$
H	Height (Length) of zone, m
H_f	Heating value of fuel, Kcal/Kg
H_l	Heat loss, Kcal/hr
k	Thermal conductivity, $Kcal/(hr)(m)(K)$
k_s	Surface rate constant, $Kg/(m^2)(hr)(atm)$
k_d	Diffusional rate constant, $Kg/(m^2)(hr)(atm)$

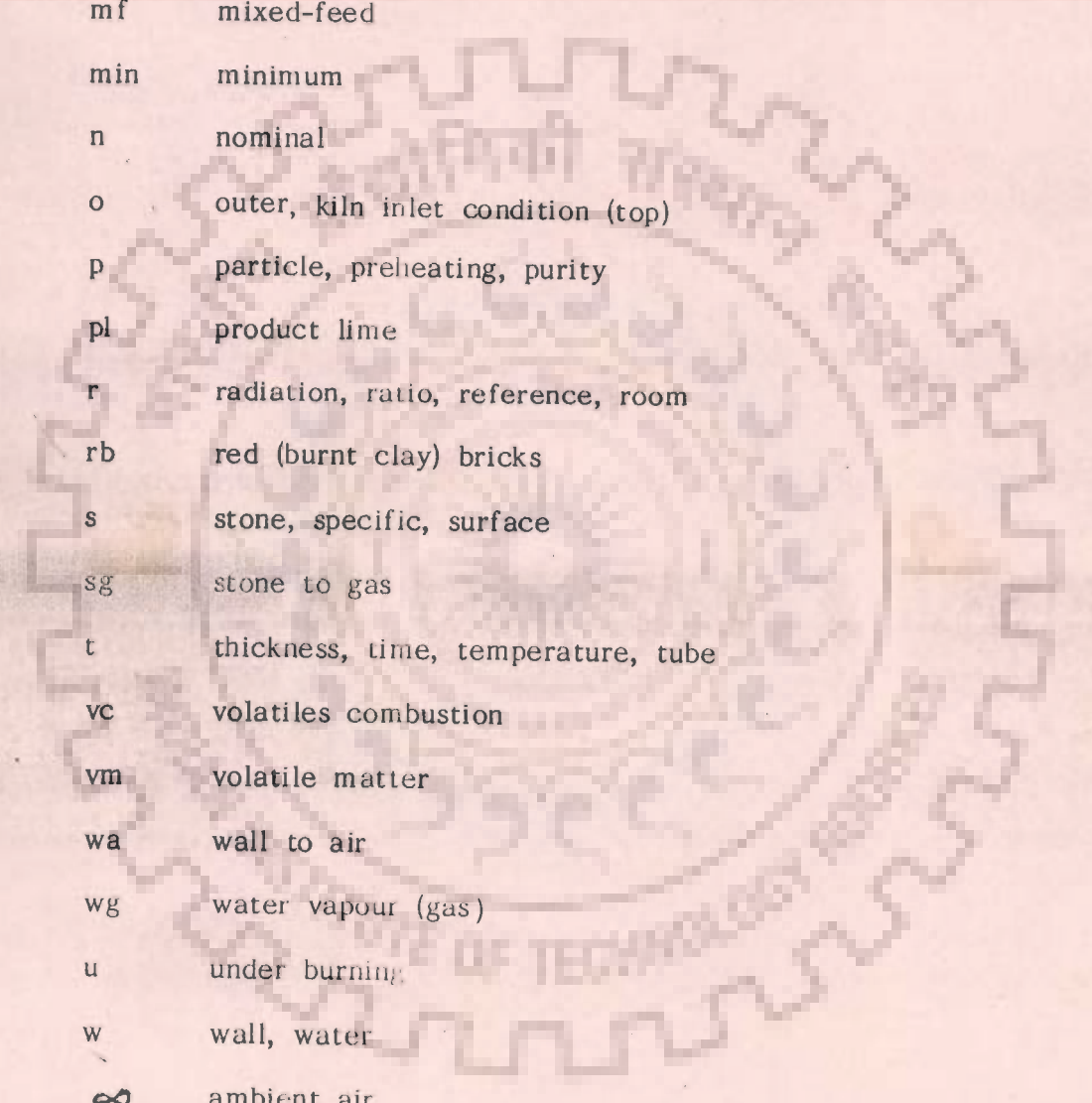
\bar{K}_s	Rate constant for combustion of carbon due to combined effect of surface as well as diffusional resistances, $\text{Kg}/(\text{m}^2)(\text{hr})(\text{atm})$
L	Length, m
m	Mass, Kg
\dot{m}	Mass flow rate (Kg/hr)
n	Number of particles
N _d	Number of discharges effected per shift in semi-continuous kiln operation
N _s	Number of working shifts per day employed in semi-continuous kiln operation
Nu	Nusselt number
p	Partial pressure, atm
P _n	Nominal lime production rate, tonne/day
P _s	Superficial lime output rate based on inner cross-sectional area of empty kiln, $\text{tonne}/(\text{m}^2)(\text{day})$
P _v	Superficial lime output rate based on inner volume of kiln $\text{tonne}/(\text{m}^3)(\text{day})$
Pr	Prantl number
Q	Rate of heat transfer, Kcal/hr
r	Radius, m
r _c	Radius of calcium carbonate core, m
r _p	Radius of particle, m
R	Radius of of kiln, m
R	Gas constant
R _t	Retention time, hr

Re	Reynolds number
s	Surface
S	Sensible heat, Kcal
S_{hl}	Sensible heat content of the lime layer, Kcal
t	Time
t	Tonne (metric)
T	Temperature, K
T_{dm}	Temperature of demosturization, K
T_{ff}	Incipient ash fusion temperature of coal, K
T_{vmc}	Auto-ignition temperature for VM combustion, K
U_i	Overall heat transfer coefficient based on inner wall area, Kcal/(hr)(m ²) (K)
v_{sf}	Volumetric flow rate of stone and fuel, m ³ /hr
V	Volumetric flow rate, m ³ /hr
V	Fractional volatile matter of fuel on dry ash free basis
W	Wall
W_{fb}	Fire bricks wall lining thickness
W_{rb}	Red bricks (clay) wall lining thickness, m
W_t	Wall thickness of the kiln shaft, shaft
x, X	Fractional conversion, weight fraction, fractional content by weight
x_f	Fuel conversion based on original unit mass of fuel
x_s	Fractional degree of calcination of limestone
x_{ff}	Fractional fuel conversion at incipient ash fusion point
X_r	Limestone to fuel ratio by weight

Z	Distance along the axis taken as positive from top/upper section of kiln/zone, m
Δ	Forward finite difference operator
ΔH_1	Wall heat losses, Kcal/hr
ΔZ	Width of differential element along the axis of kiln, m
α	Constant as defined in text
β, γ	Constant as defined in text
θ	Time, hr
θ_d	Average time of each discharge effected in manual kiln operation, hr
$\theta_{r/z}$	Retention time for an operating zone of kiln under semi-continuous operation, hr
$\theta_{t/c}$	Retention time for continuous operation, hr
ϕ	Sphericity of solid particles
η	Effectiveness factor (fraction)
η_1	Fractional thermal efficiency of lime kiln
μ	Viscosity, Kg/(m)(hr)
ρ	Density, bulk density, Kg/m ³
ρ_{ff}	Density of fuel at incipient ash fusion point
λ_w	Heat of desorption of water, Kcal/Kg
λ_{vm}	Heat of devolatilization, Kcal/Kg
σ_r	Radiation constant, Kcal/(m ²)(hr)(K ⁴)
ϵ	Emissivity
ϵ_b	Bed porosity

SUBSCRIPTS

a	air, ash
av	average
b	burning
c	conduction, convection, cooling, core, coke, fixed carbon
d	decomposition, diffusion, discharge, dissociation
dm	demoisturization
dv	deveolatilization
e	effective, excess
ea	excess air
eff	effective
ex	external
f	fuel
fa	fuel ash
fb	fire bricks
fc	fixed carbon
ff	ash fusion condition
fg	fuel to gas
fm	fuel moisture
fs	fuel to stone
fv	fuel volatile matter
g	gas
gf	gas to fuel
gs	gas to stone
gls	general limestone
gw	gas to wall
hl	heat of lime layer



i	inner
l	lime, loss
m	mixture (of limestone and fuel), mean
max	maximum
mf	mixed-feed
min	minimum
n	nominal
o	outer, kiln inlet condition (top)
p	particle, preheating, purity
pl	product lime
r	radiation, ratio, reference, room
rb	red (burnt clay) bricks
s	stone, specific, surface
sg	stone to gas
t	thickness, time, temperature, tube
vc	volatiles combustion
vm	volatile matter
wa	wall to air
wg	water vapour (gas)
u	under burning
w	wall, water
∞	ambient air



CHAPTER-1
INTRODUCTION

Chapter - 1

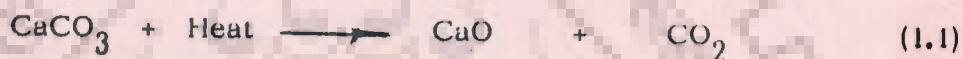
INTRODUCTION

Lime is a basic industrial chemical which is known to mankind, as a building material, since times immemorial. It finds extensive applications in the building, chemical, paper, sugar, pharmaceutical, iron and steel, and numerous other industries. The chemical grade lime is of highest purity and is used, by and large, as captive lime in the soda ash, precipitated chalk, carbide, synthetic rubber, glass, aluminium, magnesium and the aforesaid industries. Building lime has been classified in different grades depending upon its quality and composition (I.S.I., 1973). This material is mostly harnessed in preparation of mortars, plasters, pozzolanas, sand - lime bricks, and for purposes of whitewashing and soil stabilization, etc.

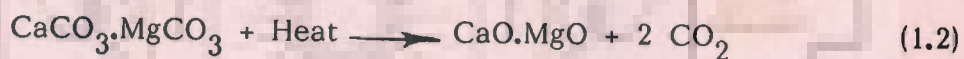
Manufacture of lime is effected by the burning of limestone rocks having significant percentage of calcium carbonate at controlled operating conditions and thus, in the process, driving off carbon dioxide from the parent stone. The impurities present (primarily silica, alumina, iron oxide, etc.) in the stone are non-volatile in nature and remain as contaminants in the lime produced. Limestones generally contain some quantities of magnesium carbonate also, and depending upon the relative proportions of calcium and magnesium carbonates in the stone, different nomenclatures are used to classify the limestone, but two basic types are of commercial importance, namely, calcite and dolomite (Boynton, 1967). The calcitic stone usually contains calcium carbonate exceeding 95 percent and the dolomitic

stone has the magnesium carbonate content of 35 - 40 percent by weight. During the burning operation both the carbonates are converted to their corresponding oxides. Dolomitic lime is used largely in the refractories where a high MgO content is essential.

The endothermic process of decomposition of pure calcium carbonate (limestone) to calcium oxide (quick lime) is represented by the reaction as:



Similarly the representative reaction for the calcination of dolomitic limestone ($\text{CaCO}_3 \cdot \text{MgCO}_3$) to dolomitic quick lime ($\text{CaO} \cdot \text{MgO}$) is:



The average dissociation temperatures for the above two types of limestones under normal atmospheric pressure conditions are 900°C and 725°C , respectively. Associated with the reaction (1.1) and (1.2) are other undesirable side reactions, viz., the sulphur dioxide present in the stone or fuel tends to react with lime and oxygen to form calcium sulphate which is unstable at high temperatures. So for the production of sulphur free lime it is necessary that the lime remains very hot while in contact with the products of combustion. Alumina and silica combine with both CaO and MgO to form silicates and aluminates at very high temperatures. These compounds are water insoluble and are generally undesirable in lime since they represent a loss of not only the oxide values, but also coat the lime particles with a water impervious layer and so reduce its reactivity.

The reactivity of quick lime is also affected by the higher operating temperatures and retention times. It is well known that temperature has a predominant effect on the rate of dissociation of limestone (Boynton, 1967 and Knibbs and Gee, 1959). With the increase in temperature the rate increases and consequently the reaction time decreases. However, maintenance of higher temperatures beyond an optimum limit for extended periods of time leads to overburning of lime. The process of overburning causes sintering, with a consequent increase in density, decrease in surface area and, therefore, the loss in its reactivity. The optimum temperature for maximum kiln efficiency varies with composition for different limestones.

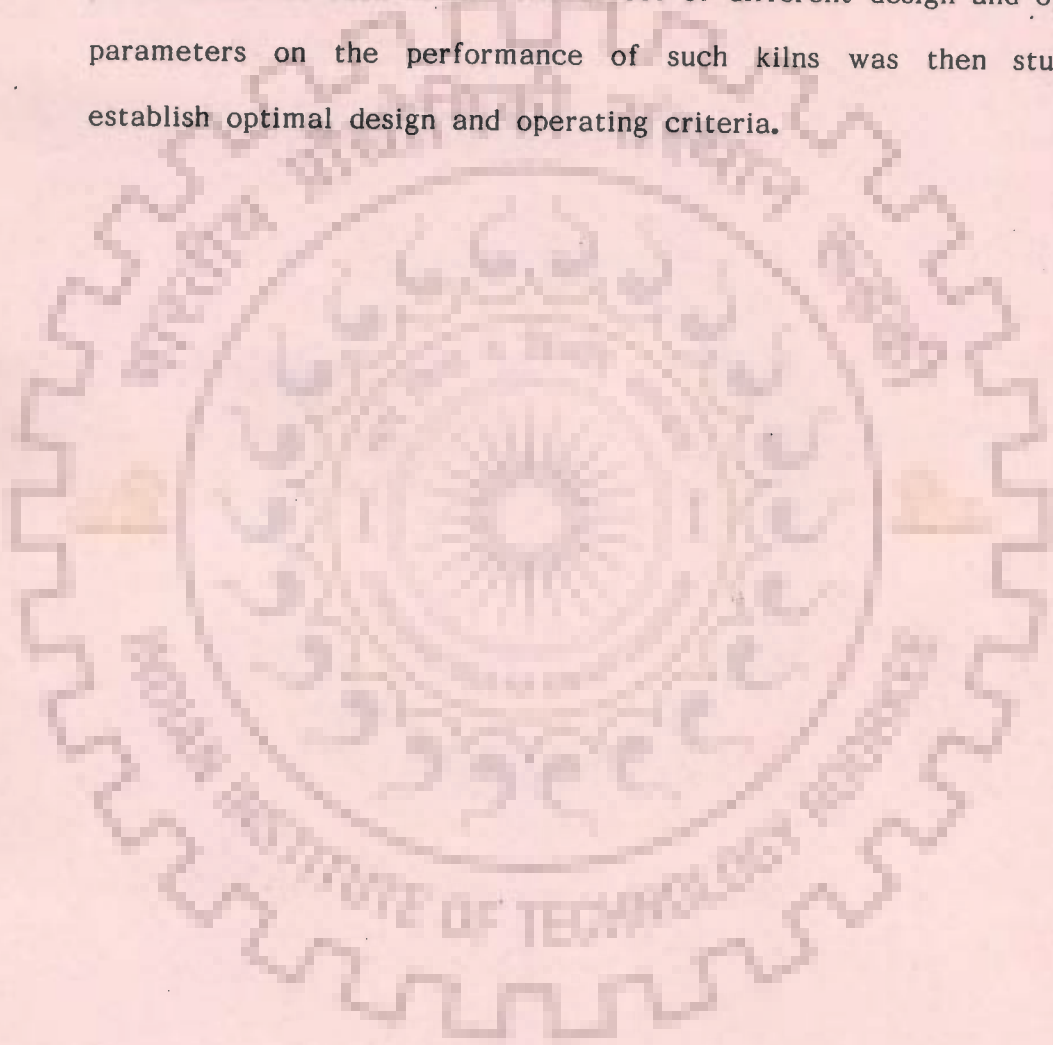
The physical and chemical properties of the limestones and the fuels employed in calcining them play an important role in determining the material and heat requirements of the process for a given type of firing system and draft employed in the kiln. Thus the process engineering design for the manufacture of quick lime involves careful analysis and accurate estimation of raw material properties and optimisation of important variables, which influence the kiln design and its production efficiency. The major parameters to be controlled in the design and operation of a lime burning kiln are the temperature, feed particle size, retention times, kiln draft, feed input rate, the physical properties and chemical compositions of raw materials, lime to fuel ratios, and heat losses.

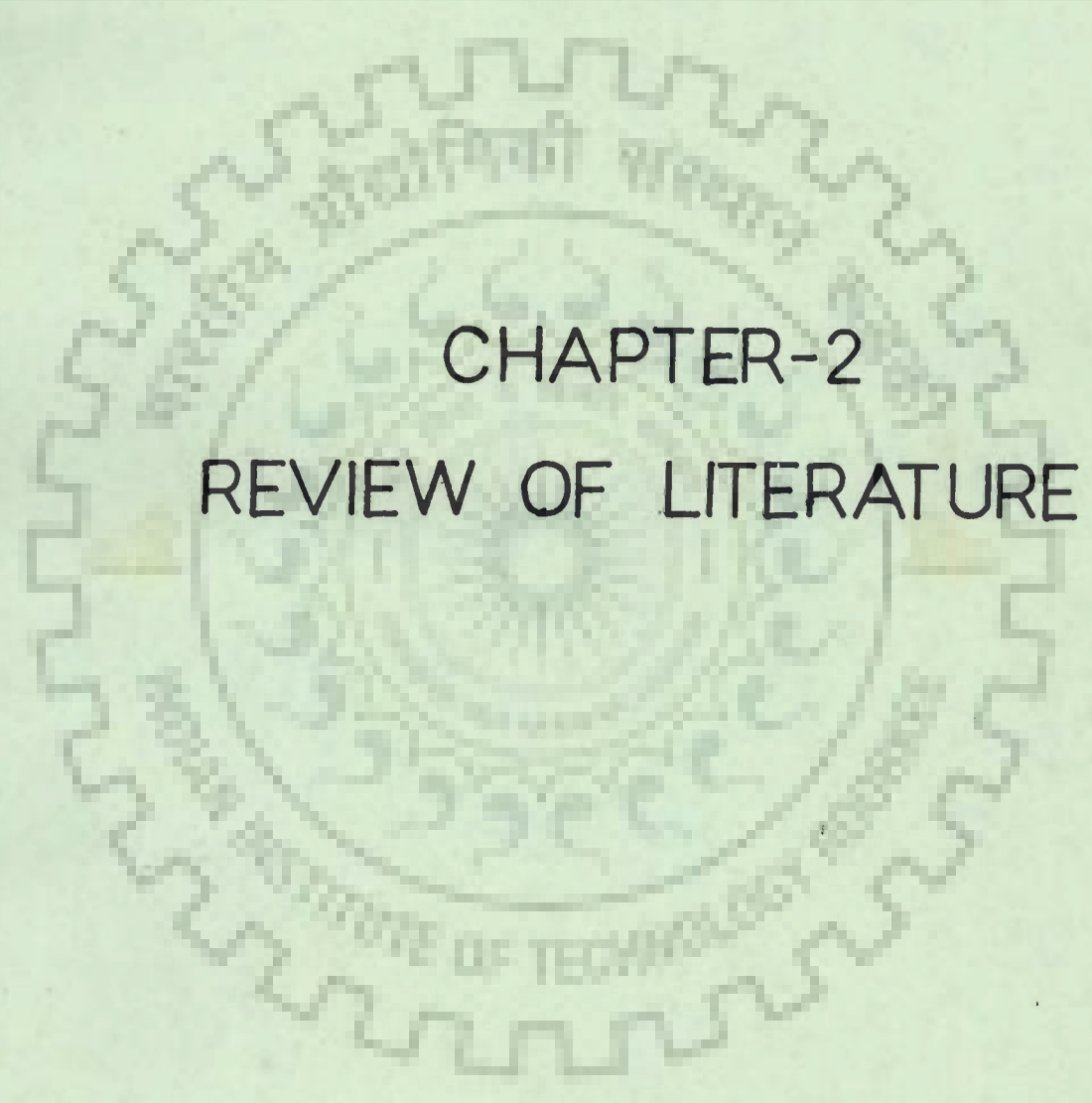
A mixed feed vertical lime shaft kiln is basically a moving bed reactor with the upward flow of hot combustion gases, counter-current to the downflow of a mixed charge of limestone and fuel particles undergoing calcination and combustion, respectively. A kiln basically has three operating zones, namely the preheating, burning and cooling. The feed is loaded into the kiln at the top and the calcined product is withdrawn from its bottom.

Even though the most sophisticated lime shaft kilns have been developed to obtain high productivity, lime quality and thermal efficiency, yet the design of a suitable kiln for a new situation using basic principles involved in lime burning remains uncertain owing to the complex nature of the process and the uncertainties involved in the operational practices. Some fundamental and empirical design correlations have been proposed by some investigators for typical kiln designs, especially for oil or gas firing systems. However, no published information is available on mathematical modelling and simulation of mixed-feed lime shaft kilns.

In India a major fraction of lime is being produced in the mixed-feed lime shaft kilns. Presently these kilns are designed using thumb rules based on past experience. For example, the Indian Standards (ISI, 1961 & 1967) suggest a superficial lime output rate of $2.5 \text{ tonnes}/(\text{m}^2)(\text{day})$ based on empty cross-sectional area and correspondingly height-to-diameter ratio in the range of 3 to 4 for an efficient mixed-feed vertical lime shaft kiln.

In view of the importance of mixed-feed lime shaft kilns for lime manufacture in India, the present investigation was undertaken to develop a detailed mathematical model for simulating the performance of such kilns. The effect of different design and operating parameters on the performance of such kilns was then studied to establish optimal design and operating criteria.





CHAPTER-2
REVIEW OF LITERATURE

Chapter - 2

REVIEW OF LITERATURE

2.1 LIMESTONE CALCINATION AND MECHANISM STUDIES

Studies on the calcination of limestones and the mechanism of calcination have been reported by several investigators, viz., Azbe (1941), Fishwick (1970), Gibbs (1942), Hills (1968), Koloberdin et.al (1972 and 1975), Narsimhan (1961), Satterfield and Feaks (1959), Transtel and Ulrich (1965), and Lee (1976). The decomposition of a limestone sphere, when exposed to high temperatures in a furnace, starts at the surface of the particle and proceeds inwards towards the centre as shown in Fig. 2.1. Temperature gradients develop between the surrounding and the surface of the limestone and between the surface and centre of the lump. At a given instant there is a central core of undecomposed CaCO_3 surrounded by a shell of CaO with a relatively thin reaction front between the core and the shell. The rate of reaction could possibly be controlled by the three simultaneously occurring processes:

(i) Heat transfer to the surface of the stone by radiation and convection and thence to the reaction front through the CaO shell by conduction.

(ii) Initiation of chemical reaction at the surface with the evolution of CO_2 and the movement of reaction front radially inwards as the reaction progresses.

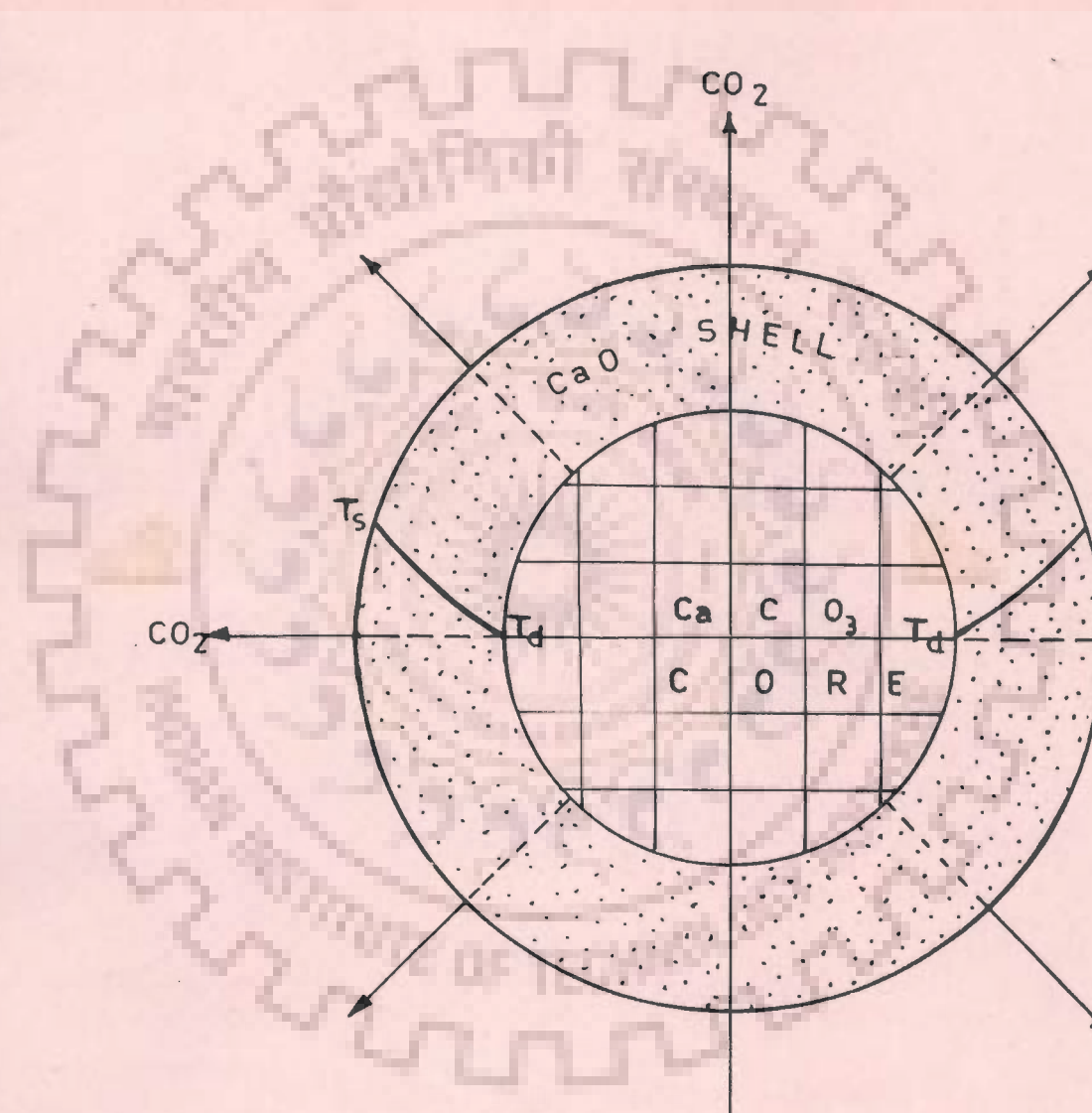


FIG. 2-1- A DECOMPOSING PARTICLE OF CALCITE SHOWING RADIAL TEMPERATURE PROFILE IN CaO LAYER.

(iii) The transfer of CO_2 evolved at the interface by diffusion through the pores of the reactive lime shell covering the unconverted limestone core.

Furnas (1931) studied the rates of calcination by passing streams of hot gases through a sized limestone charge in a furnace. He found that, within a lump of limestone undergoing calcination, (i) the boundary layer between the CaCO_3 core and the surrounding CaO shell is clearly visible, (ii) the boundary layer is sharp and thin, and (iii) its rate of travel inwards from the surface is roughly linear with time, independent of lump size and shape. He observed the rate of travel of the decomposition zone to be a temperature function as :

$$\log R = 0.003145 t - 3.3085 \quad (2.1)$$

where R is the rate of advance in cm/hr, and t is the temperature in $^{\circ}\text{C}$. This equation may be treated as a rough approximation only as it does not fit the results of Satterfield and Feakes (1959).

Satterfield and Feakes (1959) measured the actual temperatures of the decomposing calcium carbonate samples. They observed that the calcination temperature was considerably lower than that of the surroundings, and remained constant during the reaction. Their experiments were conducted in pure CO_2 at one atm pressure and very high temperatures were therefore involved. They concluded that heat transfer was important in controlling the reaction rate at high temperatures. Satterfield and Feakes brought forth the possibility of a chemical control mechanism which involved the cracking of the

original carbonate lattice. They concluded that the effects of CO_2 partial pressure and temperature on reaction rate acted as confirmatory evidence for the proposed mechanisms. According to them a considerable number of previous workers, who proposed a chemical control mechanism suggested the following rate equation for calcination of limestone:

$$M = k e^{-E/RT} \quad (2.2)$$

where M is the reaction rate, expressed as moles/(hr) (sq cm) of reaction area, k is the reaction rate constant, E is the activation energy per g. mole, R is the gas constant and T is the absolute temperature in $^{\circ}\text{K}$. According to Satterfield and Feakes, the earlier workers who assumed the reaction to be a chemical controlled mechanism found the Arrhenius activation energy for the reaction to be about 40 K cal/g mole - approx. equal to the heat of calcination reaction, whereas, they found a much larger activation energy of the order of 360 K cal/g mole. Thus their investigation did not yield any quantitative information on the kinetics of the chemical reaction.

Gibbs (1942) calculated the rate of heat penetration in the stone through the concept of concentric spherical layers assuming that, the specimen is homogenous in structure and composition, the portion of the specimen undergoing active calcination can be considered as a concentric layer in the sphere, this layer penetrating deeper and deeper as the calcination proceeds. Although this zone of active calcination undoubtedly has some depth or thickness, he merely

considered it as a spherical surface. Consequently he interpreted the weight loss during the calcining process as that lost by the volume between the active calcining surface and the surface of the 2 in. sphere used by him in the experiment. The furnace temperature was varied between 1050°F and 2100°F. Gibbs developed an empirical relation between time and penetration which, he professed, could be approximately used for practical purpose:

$$P = a T^2 + b \quad (2.3)$$

where P is the penetration in inches (i.e. distance of the actively calcining surface from the surface of the sphere, T is the time in minutes, a is a constant of value 0.00002875 and b is a constant of value 0.0125.

The rates and activation energies for the decomposition of limestones have generally been determined from a series of isothermal decomposition experiments, but Bijawat (1957) showed that these can be obtained from a single nonisothermal decomposition experiment also. Good agreement was observed for the values obtained by the two methods. The results presented by him are based on the experimental data of Azbe (1942). The movement of the calcination boundary is given by the equation :

$$P = r (1-F)^{1/3} \quad (2.4)$$

where P is the penetration at any time Θ in inches. F is the fraction

of CO_2 left at any time in the decomposing specimen, and r is the radius of the sphere.

Transtel and Ulrich (1965) have discussed the reaction processes when limestone is burnt within the temperature range $900 - 1200^\circ\text{C}$ using various slab stone dimensions and CO_2 contents of the furnace. A mathematical analysis of the reaction process has been made in which it is assumed that the heat requirement of the calcination reaction is provided by conduction in the CaO layer, but is hindered by the outward flow of CO_2 . The equations developed by the theoretical approach can be used to determine the kiln conditions required to produce a given quality of lime. The speed of calcination can be calculated for a given set of conditions. However, they point out that the correction factors must yet be determined which will allow the equations to be applied to pieces of limestones packed closely within the confines of a kiln.

Narsimhan (1961) has advanced theoretical treatments for the calcination of limestones assuming the reaction to be heat transfer, mass transfer, and simultaneous heat and mass transfer controlled. It is assumed that the surface chemical reaction is very fast and as such does not interfere in the determination of the overall decomposition rate. He has derived rigorous expressions based on heat transfer rate and system properties for the prediction of decomposition times for definite geometric shapes such as spheres and cylinders. While deriving his mathematical model for a sphere of calcium carbonate, Narsimhan assumed that the temperature in

the centre of the sphere levels up with the decomposition temperature within a very short time. This assumption has been justified in view of the large magnitude of the thermal diffusivity of calcium carbonate. On this basis there is no internal temperature gradient and all the heat reaching the decomposition plane is used up for the endothermic reaction. The good agreement observed between the actual and predicted values for the burning times bears out the soundness of the decomposition scheme envisaged by him.

The complex theoretical expressions derived by Koloberdin and associates (1972 and 1975) for the thermal decomposition of carbonates could not be experimentally verified. They have derived an equation based on heat transfer to the surface of the limestone particle, thermal conduction through the layer of calcium oxide formed, and on the rate of reaction itself.

An interesting investigation on the subject has been carried out by Hills (1968). His experiments, substantiated with theoretical approach, revealed that the rate of decomposition of limestone spheres is exclusively controlled by heat and mass transfer alone. The definite spherical boundary, that exists between the undecomposed carbonate and a layer of reacted porous lime, maintains its spherical shape and the rate of reaction is solely controlled by the heat transfer to this boundary and by the transfer of CO_2 away from it. He developed a mathematical model of the decomposition process and it was shown to compare favourably with his experimental data. The rate of decomposition of limestone is given as:

$$\text{rate} = 4\pi r^2 \rho_{\text{CO}_2} \frac{dr}{dt}, \text{ moles/time} \quad (2.5)$$

where ρ_{CO_2} is the molar density of carbon dioxide. If dr/dt is constant then according to this identity the rate per unit area of reaction interface is also constant. Hills observed that the approximate constancy of dr/dt had led many a previous worker to propose that the reaction is controlled by a chemical step at the reaction interface. However, he points out that transport controlled reactions can also display some characteristics, symptomatic of chemically controlled reactions, and so they do not provide any evidence to the mechanism controlling the reactions. He developed some mathematical models based on heat and mass transfer for prediction of the rates of decomposition of the limestone particles which were shown to compare very well with the experimental data. According to him the existing theoretical treatments for packed bed processes do not apply to these reactions since their mathematical formulations involve strongly non-linear equations. As manifested by Hills, the equations derived in his paper should enable one to predict the decomposition of calcium carbonate in packed bed conditions.

Li and Coworkers (1976) investigated the rates of decomposition of limestones obtained from four different mines. An empirical formula given for the thermal decomposition of limestone is :

$$Y = a e^{-bt} \quad (2.6)$$

where Y is the percent of limestone remaining undecomposed, t is the decomposition time in minutes, and a and b are constants ($a =$

99.609 - 100.120, $b = 0.066 - 0.0081$) under the conditions of their experiments. The decomposition temperatures of 800 - 900°C have only been reported.

2.2 MANUFACTURE OF LIME IN SHAFT KILNS

The burning of limestone is carried out in what is known as lime kiln. Several types of kilns, such as the shaft, rotary, fluosolids, the calcimatic, etc., are presently being employed for the manufacture of quick lime, but the present review restricts itself to the shaft kilns only. The general details of the manufacturing process have been reported by some investigators, e.g., Azbe (1947), Beckenbach (1971), Flachsenberg (1975), Middlemas (1964), Schwarzkopf (1970) etc. Recent developments in lime shaft kilns have been reviewed by several workers viz. Dandois and Smithwick, 1973; Das, 1974; Fiedler, 1976; Gribbin, 1970; and Verma and Saxena, 1978. Although the manufacturing technique appears to be simple yet the actual process in a lime kiln is extremely complicated.

The mixed-feed lime shaft kilns have been widely used in the European and oriental countries, but they appear to be comparatively less popular in the U.S.A. These kilns exhibit good thermal efficiency and produce effluent gas with high carbon dioxide concentration. Thus industries using both lime and CO₂, such as sugar, refining plants, basic magnesia plants and alkali industry depend entirely

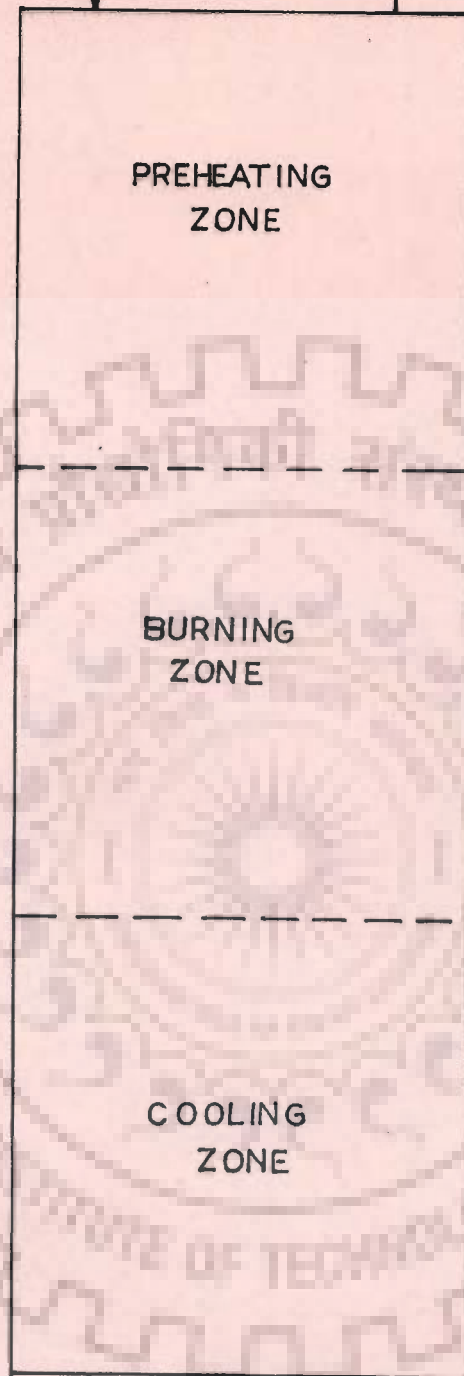
on such kilns. Small scale production for building lime is also carried out in the mixed-feed kilns in many developing countries.

A schematic diagram of a typical mixed-feed lime kiln has been shown in Fig. 2.2. It is usually a tall cylindrical structure lined inside with refractory and insulating bricks. The fuels employed in burning limestone may be coal, coke, charcoal, cinder, or wood. A uniformly mixed-proportion of limestone and fuel is lifted by a skip hoist to the top of the kiln and thence loaded into the kiln. As the burning progresses the charge travels down through the kiln to a rising stream of combustion products. The lime produced is removed from the bottom of the kiln by some suitable means. Generally, the kiln operates in three zones, namely, the preheating, calcining and the cooling zones. The middle calcining zone operates at elevated temperatures in the range of 900-1200°C for obtaining soft burnt lime, and the upcoming gaseous products from this zone preheat the mixture of limestone and fuel. Air for combustion is introduced at the bottom of the kiln and gets preheated while cooling the quick lime in the cooling zone near the bottom. There is always some amount of unavoidable crushing of lime during its downward movement into the kiln, and the material discharged from the kiln consists of lime lumps and powdered lime contaminated with fuel ash and clinkers from coal and coke.

The gas fired vertical shaft kilns are also, in general, cylindrical structures with suitable arrangements for burning the limestone with

LIMESTONE
&
FUEL

EXHAUST GAS 14-A



PRODUCT LIME
+
ASH

AIR

FIG. 2.2 - SCHEMATIC DIAGRAM OF A MIXED-FEED LIME SHAFT KILN

gas. Any fuel gas, such as, natural, blast furnace, or coke oven gas can be used. Similarly in the oil-fired kilns a suitable fuel oil is employed for firing the kiln. The oil is sometimes first gasified by injection into a hot stream of recirculated gas from the kiln top. Combustion of the oil can be effected either in the external combustion chambers or within the kiln body itself, but the heat consumption per Kg. of lime has been reported to be comparatively less in the latter case (Hoffman, 1963). The main advantages of these kilns over the mixed-feed kilns are : higher capacity, better quality and non-contamination of the product lime with fuel ash.

According to Azbe (1945) certain fundamental requirements for obtaining good quality and low cost lime are : (i) proper combustion of fuel and steady supply of heat to the kiln, (ii) proper heat distribution in the kiln, (iii) uniform drawing of lime through the different shaft sections, (iv) complete cooling of lime and recovery of heat, (v) temperature control of the hot zone by economical means, (vi) ample draft to obtain high capacity and (vii) arrangements to facilitate operation. Parson (1964) has reviewed some of the advantages obtained in the vertical shaft kiln. These are : (i) its simplicity of construction and operation, (ii) low first cost, (iii) high thermal efficiency (because of convective heat transfer rather than radiative as in rotary kilns), (iv) high volumetric efficiency, (v) possibly minimum decipitation of solid products & (vi) erosion of refractory

due to slight movement of particles relative to each other. He points out that the gas kiln popular in America has never matched the efficiency of the mixed-feed kiln used in Europe. According to him all the defects of the vertical kiln, namely, irregularity of operation, prevalence of core, overburning, deterioration of refractories, etc., can be blamed on one common characteristic, i.e., channelling. Channelling is the tendency of some parts of the kiln shaft to run at higher temperatures than others. It is a combustion phenomenon that results from the combination of fuel and air in the voids in the kiln charge. He logically deduced that an excess amount of fuel could help in reducing channelling.

Azbe (1941) has briefly described his patented design of a centre burner gas-fired vertical shaft lime kiln with provisions for the control of zonal temperatures, distribution of heat, rate of draw and location of draw. He has divided the lime kiln into six zones, namely, (i) storage and drying zone, (ii) preheating zone, (iii) upper calcining zone, (iv) lower calcining zone, (v) finishing zone, and (vi) cooling zone. Division of the kiln into these zones, he suggests, makes it amenable to effective control that greatly enhances quality, quantity and efficiency.

The annular shaft kilns (Beckenback, 1971 and Flachsenberg, 1970) with nominal outputs in the range of 100 - 300 tpd, came into existence in West Germany in the sixties owing to more exacting demands in regard to reactivity, low ash content, and sulphur content of quick lime. This kiln can be operated either by induced draft or by forced draft and is equally suitable for oil or gas firing. Some

other kilns have also been developed which lend themselves to convenient firing with oil and gas (Middlemas, 1964). A new design of an oil-fired lime shaft kiln based on the 'catagas' system of oil gasification has also been reported by Middlemas (1963). This kiln is basically a conventional gas fired design with catagas units fitted at the bottom of the burning zone.

2.3 DEVELOPMENT ON LIME KILNS IN INDIA

In a recently conducted field survey it was observed that building lime is being produced in India in the small scale and cottage industries. Several types of lime kilns are in vogue, namely, the stack or heap kilns and the intermittent kilns of the batch type (Dave and Masood, 1972; Dave and Coworkers, 1977; Macedo, 1958; Rai and Sharma, 1966; and Verma and Saxena, 1978). These kilns being of the primitive type are highly inefficient and produce lime of unpredictable quality. The improved vertical shaft kiln, constructed in masonry and lined inside with fire bricks is rather a recent development in the country. The use of this type of kiln is being advocated by the Khadi and Village Industries Commission, Bombay and the Central Building Research Institute, Roorkee for the manufacture of building lime for smaller capacities of production. The other advanced type of shaft kilns, the rotary or the fluo-solids kilns have yet to be used on a large scale in the country to achieve much larger capacities of production of the building lime, say exceeding 25 tonnes of quick lime per day. These vertical shaft kilns are of the mixed-feed type generally operating on natural draft. The survey

further indicated that lime for use in the chemical and metallurgical industries is also being produced in the rotary, fluo-solids and cross-flow kilns to some extent in the country. But their designs are proprietary in nature and the know-how is generally being imported.

A symposium was organised by the National Buildings Organisation on the 'Manufacture and Use of Building Lime in India' at Rewa (M.P.) in March, 1958, in which Macedo (1958) presented a paper on the factors in the design and economic operation of a lime kiln. The paper is a general review on the subject. The specific design criteria for any of the kilns based either on theory or practice, are not mentioned in his paper. Macedo remarked that the mixed-feed vertical kiln was a highly heat efficient lime kiln and it was best suited to the Indian conditions.

After a careful analysis of the existing practices of lime burning, Macedo (1967) later observed in another symposium held in New Delhi that most of the building lime produced in the small and cottage scale sectors was costly and the quality of the product was uncertain.

Dave and Masood (1972) presented a paper on the study of existing lime kilns in India in another seminar on 'Lime Manufacture and Uses' held at New Delhi. They reported the construction and operational features of some typical kilns, such as, the country batch

type, the Vindhyan Kiln, the Rajasthan kiln, and the fire-brick lined kiln. They concluded that most of the lime kilns in operation in India were following the age old uneconomic operational practices and needed considerable improvements for efficient operation. These investigators further observed that lime burning is characterised by a large number of operating variables, and optimum performance is achieved by trial and error methods only. The author believes that this degree of uncertainty to obtain optimum kiln performance can be eliminated by a considerable extent if the analysis of design and operation of lime kilns for optimum performance is undertaken to investigate and correlate the effect of numerous parameters which affect the productivity thermal, efficiency and product quality.

Describing the manufacture of lime in India Robin Spence (1974-75) observes that great improvements in efficiency of the lime kilns are possible with the present days' scientific understanding of the fundamental process. In view of the general scarcity of cement in India from time to time, the labour intensive lime industry has been predicted as the hope of the future.

Verma and Saxena (1978) carried out some preliminary studies of the low capacity mixed-feed kilns producing less than 5 tonnes of lime per day. The study revealed that there were significant variations in the design and performance characteristics of these kilns. The prevalent methods of operation were quite inefficient and heat wasteful. They concluded that the performance of the semi-continuously operated kilns in respect of obtainable productivities

could be enhanced by lowering down the retention times under local operating conditions, such as, incorporating frequent charging and discharging schedules at regular intervals of time, contrary to the existing practices of once-a-day charging of the raw material and withdrawal of the product lime.

Dave and Coworkers (1977) have also reported some recent investigations on the design and performance of Indian lime kilns. They observe that the lime industry still works mostly on traditional lines and little improvements in the designs and operational practices have been effected. In order to eliminate the colossal wastes of energies and the loss in productivities they consider it imperative that steps be undertaken to investigate the ways and means of carrying out the necessary improvements.

Gobindakrishnayya (1958) has outlined the salient features of the oil fired lime shaft kilns. The operational advantages of oil firing over solid-fuel firing were outlined. He concluded that for the manufacture of lime as a building material in comparatively small sized shaft kilns, the oil firing system is neither practical nor economical.

Adhia (1952) has reported a nomograph to determine the performance of a mixed-feed coke fired lime kiln used in the chemical industry, such as the alkali and sugar industries where lime and gas

both are used. The nomograph is a general presentation of material balances in a lime kiln. It takes into consideration excess air upto a maximum of five percent, whereas excess air to an extent of about 25 percent and higher is not uncommon for such kilns. No attempt was made to predict important kiln design characteristics such as the thermal efficiency and product quality.

In a recent seminar held at New Delhi, Chopra (1985) has advocated the designing and installation of coal fired mixed-feed vertical shaft kilns in the country for capacities of 50-60 tonnes of quick lime per day. Verma and others (1985) delved on the subject of lime manufacture, fuel utilisation patterns and problems. They have described the modern kilns of high capacities which could be potentially used by the indigenous lime manufacturers with a view to effecting further economies in the consumption of fuels. The technologies mostly being adopted by the indigenous iron and steel industry are of foreign origin.

2.4 OPERATIONAL PARAMETERS AND THERMAL EFFICIENCIES

Azbe (1953-54) has given the effect of temperature on the calcining time, as reported by several investigators, for a 150 mm limestone. Wide variations in the calcination time corresponding to a given firing temperature were observed. Different calcining times

could be obtained by varying the gas velocity, the radiation characteristics, surface orientation of limestone, etc. An increase in temperature enhances the calcination rate by lowering the calcining time and vice versa. The burning of limestone at higher temperature for extended periods of time tends to overburn the product, causing lime shrinkage with consequent reduction in lime reactivity, and thus impairing the product quality.

The draft employed in a lime kiln exerts a tremendous influence on the operation and productivity of the kiln (Azbe, 1941 and Holman, 1950). Azbe (1945, 1953-54) recommended the use of Fanning's equation to estimate the draft loss:

$$\frac{\Delta P}{e} = \frac{(4 f) L V^2}{2 g_c D} \quad (2.7)$$

where ΔP is the pressure drop, f is the friction factor, e is the density of gas, L is the height of bed, V is the gas velocity based on empty cross-section, g_c is the gravitational constant and D is the diameter of passage. The friction factor, f , is governed by Reynolds Number. The gas velocity is directly proportional to the cross-sectional capacity of the kiln, P_s , in $t/(m^2)$ (day) i.e.

$$P_s \propto (\Delta P)^{0.5} \quad (2.8)$$

Thus the production capacity of a kiln can be enhanced by the judicious application of a draft system. On this basis Azbe investigated the effect of various mechanical draft systems, namely, forced, induced and the balanced draft on the kiln capacity. He inferred that the capacity of an existing kiln could be increased two to four times

by proper application of such draft systems, the maximum effect being realized by the combined application of the induced and the forced drafts in the balanced form.

The size, shape and composition of limestone affect the time of preheating, calcining and cooling (Azbe, 1944; Eigen, 1957 and Koloberdin and others, 1976). The physical properties of the limestone such as its specific heat, thermal conductivity, etc. depend to a great extent upon its chemical composition. The passage time in the kiln varies from about 10 hours in modern kilns to as much as 100 hours or even more in some of the older type kilns. Azbe concluded that the heating and calcining times are directly related to the square of the stone size. Because of the requirement of lower calcining time for smaller size of limestone, higher capacities could be achieved through the use of smaller stone sizes. Eigen (1957) has considered the burning of small sized limestone in a cross-current shaft kiln and concluded that small sized limestone in a high coke fired shaft kiln calcines more economically than in the cross-current kiln.

During the operation of a lime kiln, the feed input vis-a-vis product output rates are to be regulated and synchronized with the designed capacity and quality of product keeping in view the retention times in the various zones. Sophisticated kilns have been developed with elaborate arrangements for materials feeding and product withdrawal (Verma and Saxena, 1978). Azbe (1941) has indicated that a kiln with automatic draw to loosen the charge and move the fines

will give about 16 percent higher production over the same kiln, if discharged manually.

The type of fuel used and its method of burning wield a significant influence on the operation and performance of a lime shaft kiln. A gas or oil fired kiln for a unit volume obviously produces greater quantity of lime than the solid fuel fired kiln. The performance of pulverised coal firing over coke firing has been reported by Eigen (1957). High output, low fuel costs, availability of 93 percent free CaO soft burned lime, and ease of separation of flyash by screening have been described.

Reporting his findings on the coke fired lime shaft kilns, Eigen (1957 and 1959) observed that the lime output in tonnes per square meter of cross-section is directly proportional to the depth of the burning zone and intensely proportional to the true burning time. High burning efficiency is achieved for small grained limestone with relatively coarse coke free from fines especially if the limestone and coke are closely classified and effective height is relatively large.

The thermal efficiency of a lime shaft kiln has been defined as the ratio of theoretical heat requirement based on unit weight of lime to that of the total heat supplied into the kiln based on the unit weight of the product (Boynton, 1967; Balazsovics, 1970; and Eigen, 1958). According to Brzakovic (1975), the theoretical heat requirements in lime calcination vary between 690 and 835 Kcal per Kg. of lime and the value of 760 Kcal/Kg is being accepted as the nearest true value. According to Tanskii (1962) kiln efficiency

is primarily a combination of fuel efficiency, refractory life, operating labour, and supply costs and last but not the least, down time. Vertical kilns are practically maintenance free and do not ordinarily have any down time except perhaps for occasional relining with refractories. He suggests that in order to obtain maximum fuel efficiency in a vertical kiln, the requirements to be met are: (i) appropriate size grading of limestone, (ii) availability of adequate draft, (iii) stone to be preheated properly, (iv) proper mixing of combustion gases and air, (v) adequate volume and pressure for introduction of combustible gases and air into the centre burner, (vi) effective cooling of lime and reintroduction into the kiln of the preheated air and (vii) adequate instrumentation to balance out the kiln operation.

Welsz (1952) has given exclusive charts for determining the thermal efficiencies of the lime shaft and cement kilns from studies of gas analysis. He has defined terms like 'equivalent CO_2 ' and 'A' factors which take into account the combustion characteristics, and quality of limestone and burnt lime respectively. Several types of fuels, such as, nonresinous wood, metallurgical coke, bituminous coal, natural gas, blast furnace gas, etc., have been accommodated in his charts.

For obtaining an efficient operation of a lime kiln, the role of instrumentation and control has been emphasized by Azbe (1946) especially for modern kilns incorporating complex design features. He has suggested hot zone recirculation of gases for the temperature control. Separate draft controls are described for kiln fan motor and producer fan motor in a gas fired kiln. The significance of measurement and control engineering has been highlighted by Ruch

(1973). He has enumerated several variables which should be measured by direct or indirect means to execute the process for an optimal operation.

2.5 PROCESS ENGINEERING IN KILN DESIGN

The process engineering problems of lime shaft kilns have been elucidated by Jeschar (1971) who observed that although considerable improvements could in fact be achieved in some plants, yet it is not possible to predict the behaviour of a particular kiln in all respects. He has considered a hypothetical kiln in which the fuel is fed into the region of decarbonation zone, no wall losses take place and the system properties in the gas and solid phases remain the same over the entire cross-section of the kiln. For such an idealized kiln he has obtained the equation to predict the solid and gas temperatures in the preheating and cooling zones of the lime kiln. He has reviewed some equations for the calculation of heat transfer coefficients in bulk materials and presented an approximate equation for computing the length of the decarbonation zone.

Balazsovics (1959) has vividly described the importance of thermotechnical problems in lime burning kilns. The attainable maximum productivity is affected by the formation and operation of the burning zone of a lime shaft kiln. He has investigated the effect of different factors on heat transfer and also on the output

of the lime shaft kiln, and observed that the heat transfer coefficient in the burning zone is proportional to the square-root of the superficial velocity of the exhaust gases based on the empty cross-section of the kiln. Since the gas velocity is directly related to the cross-sectional capacity, the heat transfer coefficient, h in (Kcal) (hr) (m²) (°C), is related to the capacity, P_s in t/(m²) (day), by the correlation :

$$h = K (P_s)^{0.5} \quad (2.9)$$

where K is a constant. Balazsovics recommends that the above heat transfer coefficient must be multiplied by a factor of 0.75 to account for the surface irregularity of limestone and the decrease in available surface for heat transfer under the conditions of packed beds. The time period of burning for the practical shape of stone has been given by the equation

$$t_b = \frac{W \rho_s}{\Delta T_m} \left(\frac{d_p}{6.0 \times 0.75 h} + \frac{d_p^2}{24 k} \right) \quad (2.10)$$

where, W (quantity of heat in K cal/Kg required for the decomposition of 1 Kg limestone), ρ_s (bulk density of limestone, Kg/m³), ΔT_m (mean temperature difference between exhaust gas and dissociation layer of the stone in °C), d_p (diameter of the stone, m), K (thermal conductivity of stone Kcal/(m) (hr) (°C)). He has further observed that for large lumps of stones, the thermal conductivity of the stone decisively affects the kiln output and the mean temperature difference between the exhaust gas and the dissociation layer of stone is very important. He has also reported an equation relating to the behaviour

of burning zone with recycling of the exhaust gas, and concludes that recycling of the exhaust gas in the burning zone is justified only when an overburning of the lime cannot be avoided by other means.

Wuhrer (1963) has discussed the essential requirements for obtaining soft burned lime in coal fired lime shaft kilns. These are: low heat consumption, a continuous and uniform kiln feeding, a good grading of the stone and coal, mixed firing, proper coal size matching the stone size, and a limited mass temperature in the decarbonation zone. The capacity of a kiln is dependent upon the length of the zone of heat exchange i.e. the oxidation zone of coal in the kiln. He has proposed the following thumb rule, duly confirmed by his experiments, for the height of the oxidation zone of lime kiln :

$$H_o = d_c \cdot V_f \cdot 5 \quad (2.11)$$

where H_o is the height of the oxidation zone, d_c is the average diameter of coal particles and V_f is the dilution factor of coal in the poured material. For a coal content of 13 percent V_f is about 6. Values of the burning times for single limestone particles were observed to tally with those obtained by some other workers as claimed by him. The influence of production rate and stone diameter on the residence time has been correlated.

2.6 CRITICAL APPRAISAL

A perusal of the available literature reveals that although some of the most sophisticated lime shaft kilns have been developed

to obtain high productivity, lime quality and thermal efficiency, yet the design of a suitable kiln for a new situation using basic principles involved in lime burning still remains uncertain owing to the complexities of the process and operational behaviour of a lime shaft kiln. Some serious efforts to develop the fundamental or empirical design correlations have been made by some investigators for typical kiln designs, especially for gas or oil firing systems.

Most of the lime production in India is carried out in vertical shaft kilns as per the literature survey and field studies carried out recently. The building lime, by and large, is being produced in the mixed-feed shaft kilns. The design of such kilns is apparently based on thumb rules deduced from the operational behaviour of these kilns (Wuher, 1963). The trial and error procedures are still employed in India after commissioning the kiln to obtain desired capacity and product quality from the building lime kilns. The available Indian Standards (I.S.I., 1961 and 1967) on mixed-feed lime shaft kiln also reflect similar thumb rules.

Process design correlations, based on theoretical and detailed performance analysis have not been evolved nor any kind of simulation studies have been conducted for the mixed-feed coal-fired kilns. It was, therefore, considered essential to analyse the performance of these kilns and develop appropriate design and performance correlations for efficient utilization of these low cost kilns in developing countries, and that some experimental investigations be conducted for estimation of performance vis-a-vis optimal design and operation of the vertical mixed-feed lime shaft kilns.



CHAPTER-3

PERFORMANCE ESTIMATION OF
SOME MIXED-FEED LIME KILNS

Chapter-3

PERFORMANCE ESTIMATION OF SOME MIXED-FEED LIME KILNS

3.1 FIELD SURVEY

For the purpose of the present investigation, the studies have been restricted to the mixed-feed lime shaft kilns operating on natural draft. Design and performance data in respect of a few masonry kilns spread over some important lime manufacturing centres were obtained by visiting plant sites. The major data collected in respect of the physical features of kilns, nominal production rates, size of limestones, size of fuel particles, fuel consumption, etc., are given in Table-3.1, where P_n denotes the nominal production rate in tonnes per day, L_e is the effective height of the kiln (m), D_{av} is the average inner diameter (m), d_{ps} is the size of limestone particles (m); d_{pf} is the size of fuel particles (m), W_t is the average wall thickness including firebricks lining (m), etc.

3.1.1 Design Features

The nominal production capacities of the kilns ranged between 3 and 20 tonnes of quick lime per day. The kilns were constructed in ordinary brick masonry lined inside with 23 mm thick lining of fire bricks. The heights of the kilns varied from about 3 to 15 meters and the inner diameters ranged from 1.5 to 4.0 meters. The thickness of the kiln shafts varied between 0.75 and 2.00 meters.

Four outlet doors of suitable sizes (generally 60 cm wide x 75 cm high) having arches at the top were provided for the discharge of the burnt lime. In some of the kilns poke holes were provided for the measurement of operating temperatures as well as for observing the conditions of firing. Suitably graded pieces of limestones (50 - 125 mm) and coal particles (20 - 50 mm) were taken in stipulated ratios by weight or by volume and were charged into the kilns. Usually the mineral limestones of building or chemical grades were calcined.

3.1.2 Operational Features

The kilns were operated semicontinuously on the natural draft, the air for combustion being induced through the doors at the bottom, usually in one 8 to 12 hours shift per day with twice a day charging and discharging schedules varying from 2 to 4 hours for each schedule. The product consisted of burnt pieces of quick lime, some dust lime containing the ash of the fuel, underburnt and overburnt pieces of limestones, and some ash clinkers or unburnt pieces of coal. Usually the steam coal of grade II or III with gross calorific values ranging between 5,000 and 6,000 Kcal/Kg was used in these kilns. Limestone-to-coal ratio by weight in input feed varied from 4-6.

The kilns were not loaded and discharged during the late evening and night hours with the result that the fire in the kiln travelled to its top surface during the early morning hours resulting in the elimination of the preheating zone altogether. The first morning

TABLE-3.1

INITIAL DATA ON SOME MASONRY MIXED-FEED LIME SHAFT KILNS

Kiln NO.	Identification (Plant, site)	P_n (t/d)	L_e (m)	D_{av} (m)	D_{p_s} (m)	d_{p_f} (m)	X_r (w/w)	W_t (m)	Remarks
1.	KVIC,DDN	3.0	5.50	1.98	.050-.100	.025-.050	4.5-5.5	0.75	Mineral Lime stone (building/ chemical grade) and steam coal (grade II/III) employed
2.	KVIC,DDN	5.0	8.00	1.75	.075-.125	.025-.050	4.5-5.5	0.75	
3.	CBRI,RKE	4.5	4.58	1.54	.075-.100	.040-.050	5.0-6.0	0.85	
4.	PSLW,MRT	3.5	2.95	2.22	.050-.075	.025-.040	4.0-5.0	1.50	-do-
5.	M&C,DDN	9.0	9.15	2.74	.075-.125	.025-.075	4.5-5.0	2.00	-do-
6.	VP,DDN	10.0	10.10	2.74	-do-	-do-	-do-	1.37	-do-
7.	HML,NRNL	15.0	12.00	3.25	.100-.150	.050-.075	5.0-5.5	1.20	-do-
8.	GHLI,RPR	20.0	14.50	4.00	.075-.150	.040-.075	5.5-6.0	1.25	-do-
9.	TLI,MZFNR	10.0	9.50	2.40	.075-.100	.040-.050	-do-	0.95	-do-
10.	HC,PNTSHB	10.0	11.00	2.37	.075-.125	.040-.065	5.0-5.5	1.35	-do-
11.	RC,KLMB	10.0	11.00	2.52	-do-	.040-.060	5.0-5.5	1.35	-do-
12.	PC,MDDN	8.5	11.50	2.50	-do-	-do-	5.0-6.0	0.95	-do-

discharge accounted for a major part (about 60 to 70 percent) of the daily produce which was hand picked (manually) by semi-skilled workers for lumps of quick lime.

3.1.3 General Observations

The superficial lime output rates based on empty kiln cross-sectional areas were computed and observed to lie in the range 1.0 - 2.5 t/(m²) (day). The specific energy consumption was estimated to be in the range of 1,750 - 2,500 Kcal/Kg of lime. The degree of underburning of limestone varied from 10 to 40 percent. The maximum bulk operating temperatures in the burning section of the kilns ranged between 1173 K and 1573 K.

The data obtained for the mixed-feed lime kilns are only indicative in nature as the same are based on the pieces of information supplied by the kiln operators, owners or lime manufacturers. The wide variations in the designs and operational practices of these kilns necessitated performance studies of a few selected kilns in some detail both in the field and in the laboratory.

3.2 IN-SITU INVESTIGATION

3.2.1 Experimental

Two low capacity masonry mixed-feed kilns were investigated at site under the existing field conditions of operation. The general design features of these cinder (waste fuel from steam boilers) fired kilns are indicated in Table-3.2.

Limestone particles of size 15-150 mm and cinders of size 5-25 mm were burnt in the kilns. Samples of representative limestones were analysed for their chemical compositions and the results are reported in Table-3.3. The proximate analysis of cinders as determined in the laboratory are reported in Table-3.4.

The heat values of the fuels were estimated from their proximate analyses using Goutal's Formula (Brame and King, 1955) and the same were computed to be about 3,115 and 2,420 Kcal/Kg for the fuels used in the two kilns respectively.

Temperature measurements were carried out at different time intervals to locate the preheating, calcining and cooling zones using stainless steel sheath type chromel-alumel thermocouples alongwith indicating pyrometers. The bulk averaged operating temperatures were measured along the height of the kiln at appropriate locations in the different zones and the representative curves are given in Figs. 3.1 through 3.3.

Flue gas samples were withdrawn at different times from just above the calcination zone by means of rubber bladder type gas samplers. These gases were analysed with the help of Orsat's apparatus. The representative time averaged analyses of gas samples collected from the two kilns are reported in Table-3.5.

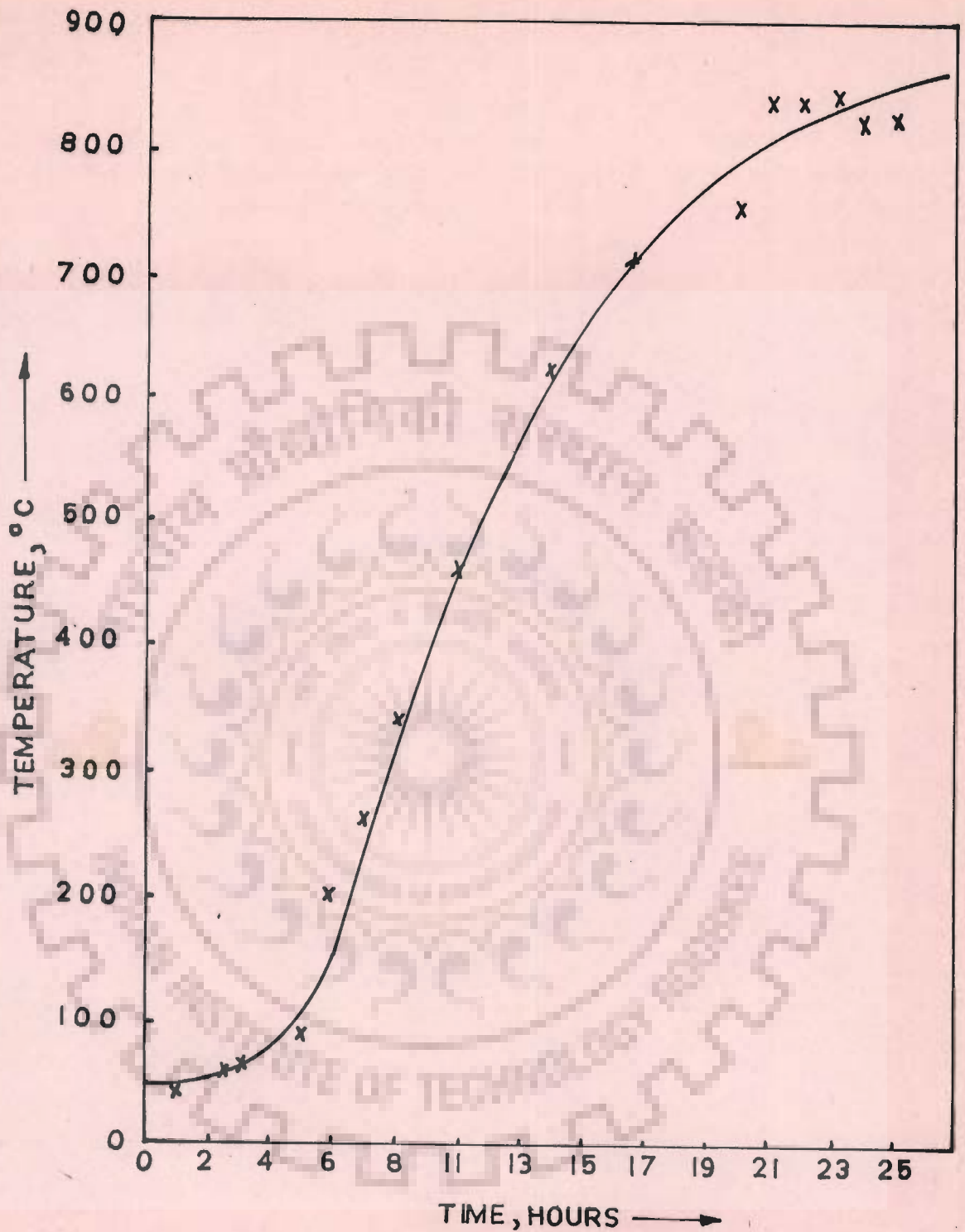


FIG. 3-1 - REPRESENTATIVE TIME-TEMPERATURE GRAPH AT PREHEATING SECTION OF CINDER FIRED KILN

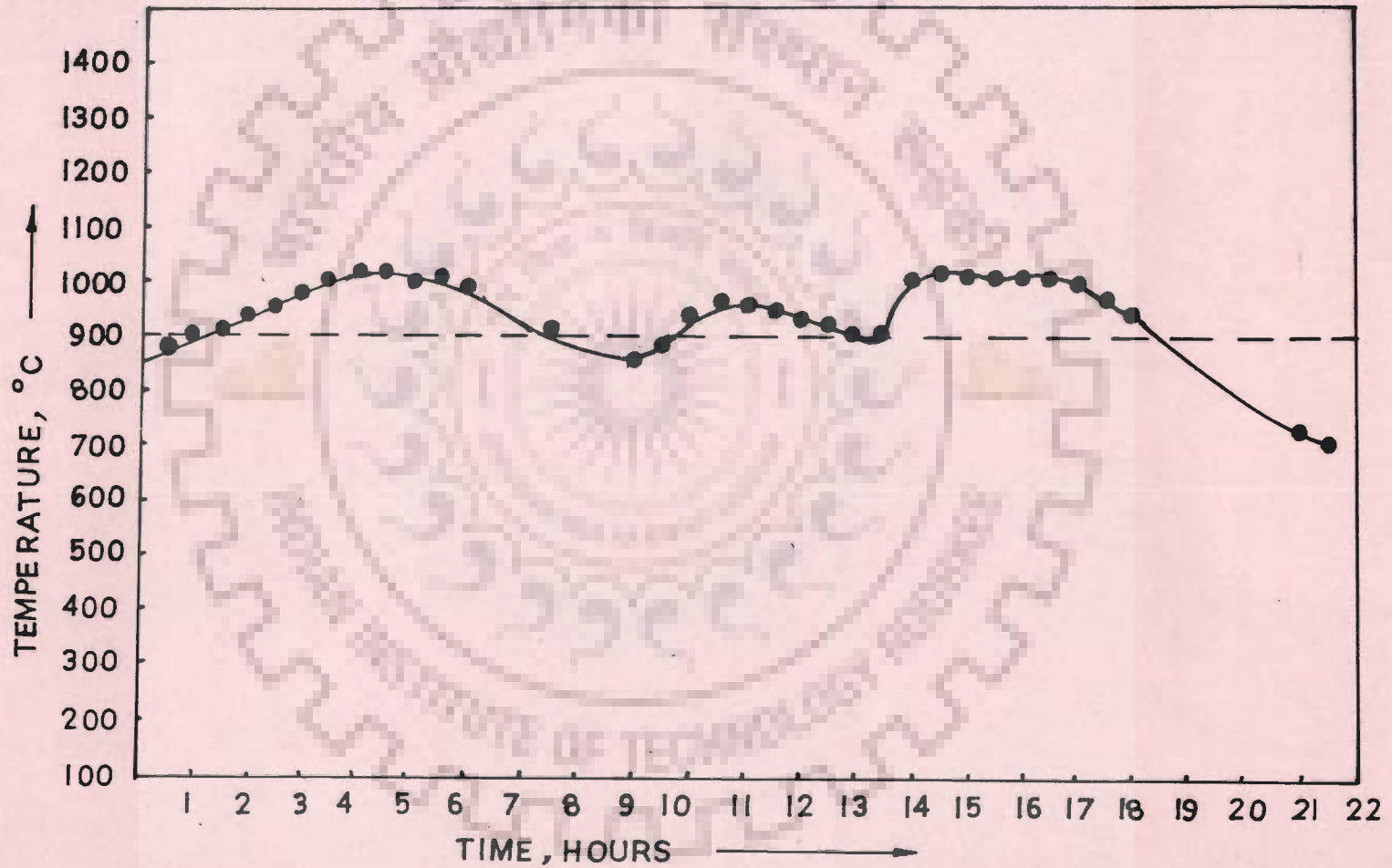


FIG-32— REPRESENTATIVE TEMPERATURE VARIATIONS AT CALCINATION SECTION OF CINDER FIRED KILN

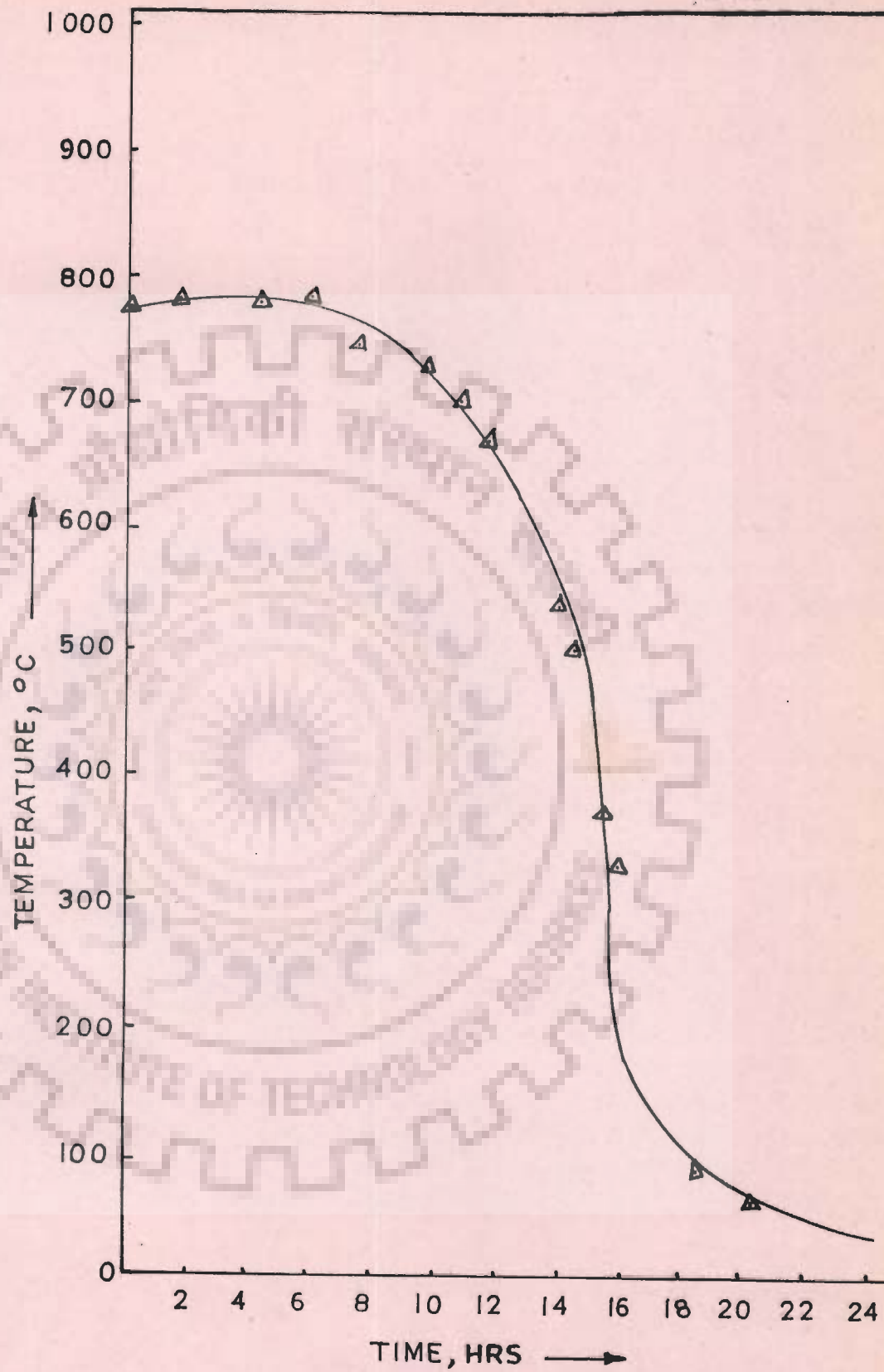


FIG. 3.3 - REPRESENTATIVE TIME-TEMPERATURE GRAPH AT SECTION OF CINDER FIRE KILN

TABLE-3.2

General Design Specifications of the Kiln Investigated

<u>Kiln No.</u>	<u>Average Cap. (t /d)</u>	<u>Height (m)</u>	<u>Av. Inner Dia. (m)</u>	<u>Av. Wall Thickness (m)</u>
-----------------	----------------------------	-------------------	---------------------------	-------------------------------

1.	1.0	3.05	1.85	1.10
2.	2.0	4.17	2.04	1.33

TABLE-3.3

Chemical Analysis of Limestone Samples

<u>Sl. No.</u>	<u>Constituent</u>	<u>Quantity (percent by weight)</u>	
		<u>Kiln No. 1</u>	<u>Kiln No. 2</u>
1.	Loss on Ignition	39.29	42.40
2.	SiO ₂	11.15	1.45
3.	R ₂ O ₃	1.58	0.65
4.	CaO	42.54	53.40
5.	MgO	5.11	1.20
6.	Others	Tr.	Tr.

TABLE-3.4

Proximate Analysis of Cinders

<u>Sl. No</u>	<u>Constituent</u>	<u>Quantity (W/W percent)</u>	
		<u>Kiln No. 1</u>	<u>Kiln No. 2</u>
1.	Moisture	0.00	0.00
2.	Volatile Matter	0.00	0.00
3.	Fixed Carbon	38.00	29.50
4.	Ash	62.00	70.50

TABLE-3.5

Representative Time Averaged Analyses of Gas Samples

<u>Sl. No.</u>	<u>Constituent</u>	<u>Quantity (percent by volume)</u>	
		<u>Kiln No. 1</u>	<u>Kiln No.2</u>
1.	CO ₂	25.3	22.9
2.	O ₂	3.9	5.9
3.	CO	1.6	2.3
4.	N ₂ (by difference)	69.2	68.9

The limestone to fuel ratios in the feed and productions obtained from the two kilns were determined over a period of three days and the average values for the same were estimated. The representative products from the kilns were carefully sampled in sufficient quantities and the lump lime pieces, the unburnt stones, overburnt lime, powdered lime (contaminated with fuel ash) and unburnt fuel pieces were hand picked separately and weighed to assess the product distribution. The data collected on the kilns are reported in Table-3.6.

3.2.2 Performance Results

The performance data obtained from the studies carried out on the two cinder fired lime kilns were analysed and the results are reported in Table-3.7.

The initial four columns of the table represent the relevant productivity data obtained for the two kilns, where P_s is the superficial lime output rate based on cross-sectional area of the kiln, $t/(m^2)(day)$, and P_v is the output rate based on the inner kiln volume, $t/(m^3)(day)$. R_t is the average kiln retention time in hours. It is seen that kiln No. 1 yielded lower sectional and volumetric outputs than those obtained from kiln No. 2. This is on account of (i) the higher retention time of about 90 hours imposed in kiln No. 1 compared to that of about 80 hours in kiln No. 2, (ii) the operational lapses, and (iii) the

TABLE-3.6

Quality of Product in Cinder fired Lime Kilns

Kiln No.	Average Production (tpd)	Stone: fuel by weight (X_p)	Product Distribution (% W/W)				Unburnt Fuel
			Lump Lime	Kiln Dust (Lime + Ash)	Under burnt Stone	Over burnt lime	
1.	1.0	2.5	39.5	52.6	6.6	0.7	0.6
2.	2.0	2.0	39.6	50.2	8.5	0.6	0.7

design of the kiln in respect of geometrical height to average diameter ratio. The greater height of kiln No.2 resulted in increased draft compared to kiln No. 1. Thus it is inferred that maximum attainable output from a kiln can be obtained by an experienced burner through regulation of retention times to an optimum lower limit, i.e., by operating the kilns in as continuous a manner as feasible.

The data on the average quality of the produce obtained from the two kilns are reported in Table-3.6. It is observed the the product is highly contaminated by as much as about 50 percent of kiln dust consisting of powdered lime and fuel ash which is basically attributable to the high amount of ash content in the clinder (Table-3.4). The lime lumps obtained were of the order of about 40 per cent only, but the degree of underburning and overburning was observed to be less than 10 per cent and, therefore, within reasonable limits.

The thermal performance of the lime kilns has also been elucidated in Table-3.7, where E_s is the specific energy consumption in terms of Kcals per Kg. of lime and F_s represents the fuel consumption in tonnes per tonne of lime produced. The average E_s and F_s values were computed to be of the order of 2,450 Kcals/Kg and 0.9 tonne of fuel per tonne of lime, respectively, which are quite high.

-The thermal losses are accounted for by the cumulative effect of several operational interactions. Firstly, the traditional method of

TABLE-3.7

Performance Data for the Cinder-Fired Lime Kilns

Kiln No.	L_e/D Ratio	P_s $t/(m^2)$ (day)	P_y $t/(m^3)$ (day)	R_t (hrs.)	E_s (Kcals/ Kg lime)	F_s (t cinder)
1.	1.43	0.28	0.09	90	2,500	0.8
2.	1.95	0.55	0.13	80	2,420	1.0

TABLE-3.8

Chemical Analysis of Limestone Used in Bench Scale Kiln

<u>Sl.No.</u>	<u>Constituent</u>	<u>Quantity</u> (% W/W)
1.	LOI	41.60
2.	Si O ₂	4.25
3.	R ₂ O ₃	0.98
4.	CaO	51.57
5.	MgO	1.20
6.	Others	0.40

kiln operation with once-a-day charging and discharging schedule made an allowance for the fire zone to reach the top of kiln usually from midnight onwards, and thereby resulting in tremendous sensible heat losses through the flue gases. The temperature of the flue gases was observed to rise, with the upward movement of the fire zone, to as much as 700°C representing significant heat losses. This observation is also corroborated by the findings of some earlier workers (Dave and Masood, 1972). The temperature of the withdrawn lime going to as much as 400°C for the latter half portion of the product withdrawn from the kilns also accounted for the loss of sensible heat. Incomplete combustion of fuel indicated by the presence of CO in the flue gases also contributed to some heat loss as according to an estimate (Boynton, 1967) the presence of one per cent CO in the exhaust gases amounts to a loss of about 55-65 Kcals per Kg. of lime.

3.3 LABORATORY INVESTIGATION

A bench scale prototype kiln, constructed in brick masonry, was set up in the laboratory. The details of this model are shown in Fig. 3.4. Two discharge doors located diametrically opposite to each other were provided. The chemical analysis of limestone and proximate analysis of coal particles burnt in this kiln are given in Tables-3.8 and 3.9 respectively. The kiln was operated by using a predetermined optimum proportion of limestone to coal for the conditions of the experiment.

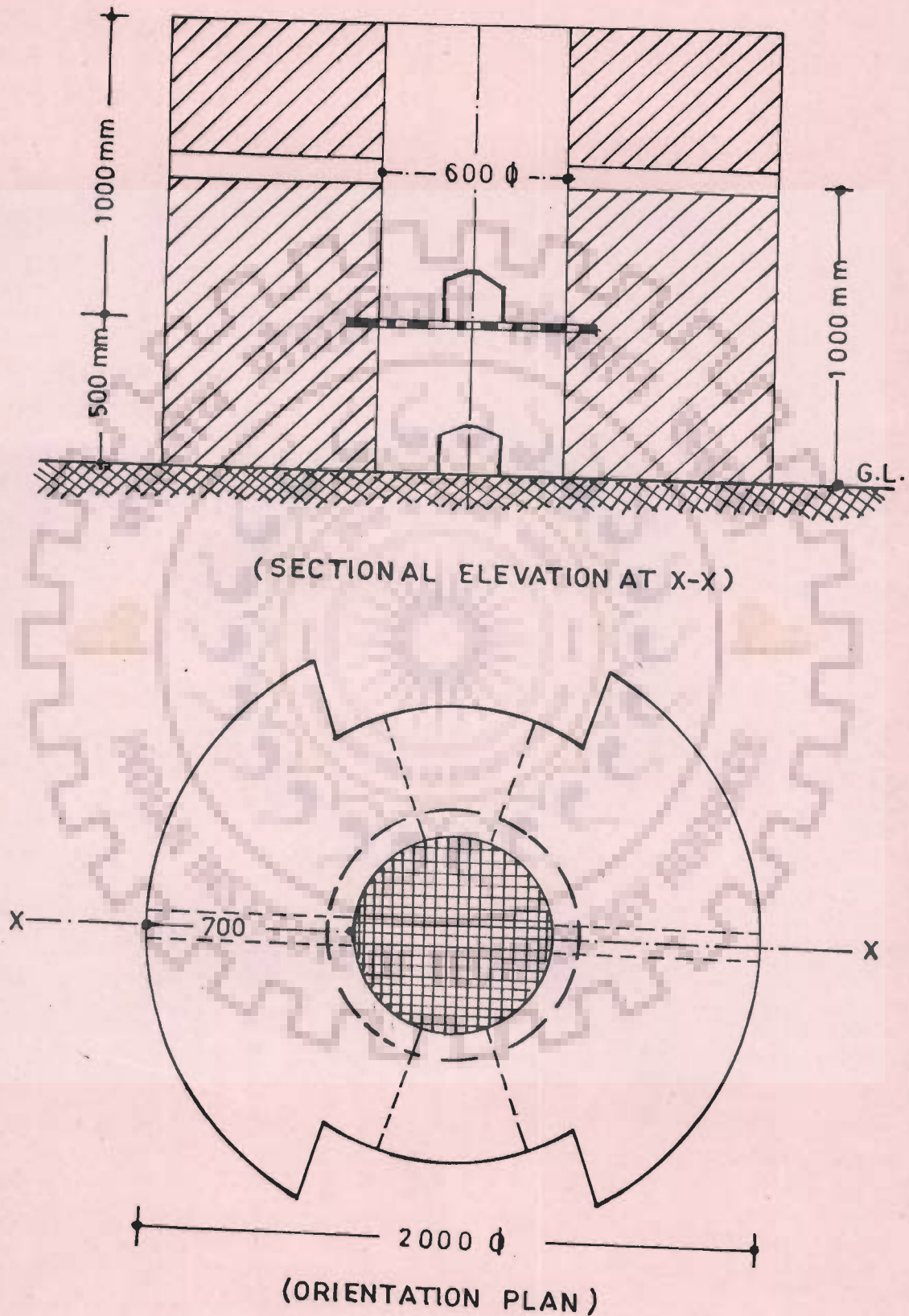


FIG. 3-4 DETAILS OF BENCH SCALE EXPERIMENTAL LIME KILN
 (ALL DIMENSIONS IN MM)

TABLE-3.9

Proximate Analysis of Coal Used in Bench Scale Kiln

<u>Sl. No.</u>	<u>Constituent</u>	<u>Quantity</u> (% W/W)
1.	Moisture	5.33
2.	Volatile Matter	14.95
3.	Fixed Carbon	48.12
4.	Ash	31.60

TABLE-3.10

Operating Data on the Bench Scale Kiln

<u>Sl.No.</u>	<u>Operational Feature</u>	<u>Characteristic Data</u>
1.	size gradation of limestones	40 - 60 mm
2.	Size gradation of coal particles	25 - 50 mm
3.	Feed rate of total charge	25 - 30 Kg/ hr
4.	Limestone to coal ratio (W/W)	3.5 - 3.7
5.	Maximum bulk operating temps.	1020 - 1160 ^o C
6.	Temperatures of exhaust gases	300 - 600 ^o C
7.	Temperature of lime withdrawn	200 - 350 ^o C
8.	Kiln retention time	8 - 10 hrs

The operational data for the kiln is given in Table-3.10. The productivity of the kiln was estimated under pseudo-steady state conditions. During the progress of operation, samples of the produce withdrawn from the kilns were collected and separated to estimate the product distribution. From a knowledge of the burnt (quick) lime obtained and the fuel consumed specific fuel/energy consumptions were determined. The bulk operating temperatures were measured using chromel alumel stainless steel sheaths type thermocouples and consistent controls were exercised throughout the duration of the experimental run.

The exhaust gas samples were collected from the top of the experimental kiln and the same were analysed with the help of Orsat's Apparatus. The time averaged data are indicated in Table-3.11.

Average lime production rate of about 10 Kg/hr with specific energy consumption of the order of 3,500 Kcal/Kg of quick lime were obtained. The distribution of product obtained is outlined in Table-3.12.

The data obtained from the bench scale operation of the lime kiln are only indicative type demonstrating the flexibility in operation of the mixed-feed lime kilns even in the cottage scale industries. The low level of production, however, adds to the operating expenses in terms of higher energy costs.

TABLE-3.11

Average Analysis of Flue Gas Samples from Bench Scale Kiln

<u>Constituent</u>	<u>Quantity</u> (% V/V)
Carbon dioxide	26.6
Oxygen	3.8
Carbon monoxide	0.1
Nitrogen (by difference)	69.5

TABLE-3.12

Product Distribution Data in the Bench Scale Kiln

<u>Sl. No.</u>	<u>Product Constituent</u>	<u>Percent (W/W)</u>
1.	Quick (lump) lime	63.8
2.	Underburnt	11.1
3.	Dust lime (Produced lime + Coal ash)	25.1

3.4 PROCESS ENGINEERING CORRELATIONS : STATE-OF-THE-ART

Initially an attempt was made to evolve some process engineering correlations for the mixed-feed lime shaft kiln based on published information, the experience gained during the field survey and investigation on commercially operating kilns and the bench scale laboratory kiln.

3.4.1 Energy Requirements in Lime Burning

The energy required for the calcination of limestones at a given temperature consists of the heat required for preheating a given sample of limestone from the room temperature to the threshold calcination temperature and the heat of dissociation of the stone for conversion to quick lime. Generally limestones of variable compositions are obtained from various sources. It was thus considered appropriate to evolve correlations for estimation of energy requirements for different types/grades of limestones, notably the calcite, dolomite, magnesian, hydraulic, etc. with a view to providing useful information on state-of-the-art kiln design computations.

3.4.1.1 Preheating of Limestones

The representative composition of a generalized sample of limestone could be represented by the weight fraction of its different

constituents. Ignoring the traces, let x_1 , x_2 , x_3 , x_4 and x_5 be the weight fractions of calcium carbonate, magnesium carbonate, silica, alumina and iron oxide, respectively. Using the specific heat data for the different components (Murray, 1947; Perry and Chilton, 1968), the specific heat of a generalized sample of limestone ($c_{p\text{glS}}$) was evolved from the equation :

$$c_{p\text{glS}} = x_1 c_{p\text{CaCO}_3} + x_2 c_{p\text{MgCO}_3} + x_3 c_{p\text{SiO}_2} + x_4 c_{p\text{Al}_2\text{O}_3} + x_5 c_{p\text{Fe}_2\text{O}_3}, \text{ Kcal}/(\text{Kg}) (^{\circ}\text{C}) \quad (3.1)$$

substitution of the specific heat data leads to

$$c_{p\text{glS}} = \alpha + (\beta T - \gamma/T^2) \quad (3.2)$$

where T is the temperature in K and

$$\alpha = (0.1968 x_1 + 0.1212 x_2 + 0.1812 x_3 + 0.2165 x_4 + 0.1543 x_5)$$

$$\beta = (0.1189 x_1 + 0.3330 x_2 + 0.1452 x_3 + 0.0879 x_4 + 0.1000 x_5)10^{-3}$$

$$\gamma = (0.3076 x_1 + 0.0379 x_2 + 0.4020 x_3 + 0.5125 x_4 + 0.2650 x_5)10^{+4}$$

Thus the energy required for preheating a given sample of limestone

(E_p) from room temperature (T_r) to the dissociation temperature T_d could be computed from the equation

$$(E_p)_{T_d} = \int_{T_r}^{T_d} (\alpha + \beta T - \gamma/T^2) dT \quad (3.3)$$

or

$$(E_p)_{T_d} = \alpha(T_d - T_r) + 0.5\beta(T_d^2 - T_r^2) - \gamma(1/T_r - 1/T_d), \text{ Kcal/Kg} \quad (3.4)$$

The preheating energy requirements per Kg of limestone for various compositions were computed from equation (3.4).

3.4.1.2 Endothermic Heat of Dissociation

The energy required for the dissociation of a given sample of limestone is the summation of the heats of dissociation of calcium carbonate and magnesium carbonate constituents of the stone. The heats of dissociation at reference temperature of 25°C are reported in the literature (Boynton, 1967; Zindeveld and Vandenberg, 1971).

For the dissociation of calcium carbonate and magnesium carbonate, the variations in the heats of dissociations at different dissociating temperatures could be accounted for from the equation:

$$(E_d)_{T_d} = (E_d)_{T_r} + \int_{T_r}^{T_d} \Delta C_p dT \quad (3.5)$$

For the reaction : $\text{Ca CO}_3 \rightarrow \text{CaO} + \text{CO}_2$

$$\Delta C_p = (C_p)_{\text{CaO}} + (C_p)_{\text{CO}_2} - (C_p)_{\text{CaCO}_3}$$

and for the dissociation of MgCO_3



$$\Delta C_p = (C_p)_{\text{MgO}} + (C_p)_{\text{CO}_2} - (C_p)_{\text{MgCO}_3}$$

Using the data on specific heats and maintaining consistency of units, the equations for heats of dissociation for the two carbonates were evolved as:

$$(E_{d_{\text{CaCO}_3}})_{T_d} = (E_{d_{\text{CaCO}_3}})_{T_r} + \left[6.6(T_d - T_r) - 0.02155 (T_d^2 - T_r^2) + 41,000 (1/T_r - 1/T_d) \right] 10^{-3},$$

Kcal/Kg

(3.6)

and

$$(E_{d_{\text{MgCO}_3}})_{T_d} = (E_{d_{\text{MgCO}_3}})_{T_r} + 131.0 (T_d - T_r) - 0.143 (T_d^2 - T_r^2) - 4,430,000 (1/T_r - 1/T_d) \cdot 10^{-3},$$

Kcal/Kg (3.7)

Thus for a generalized sample of limestone, the heat of dissociation is given by the equation:

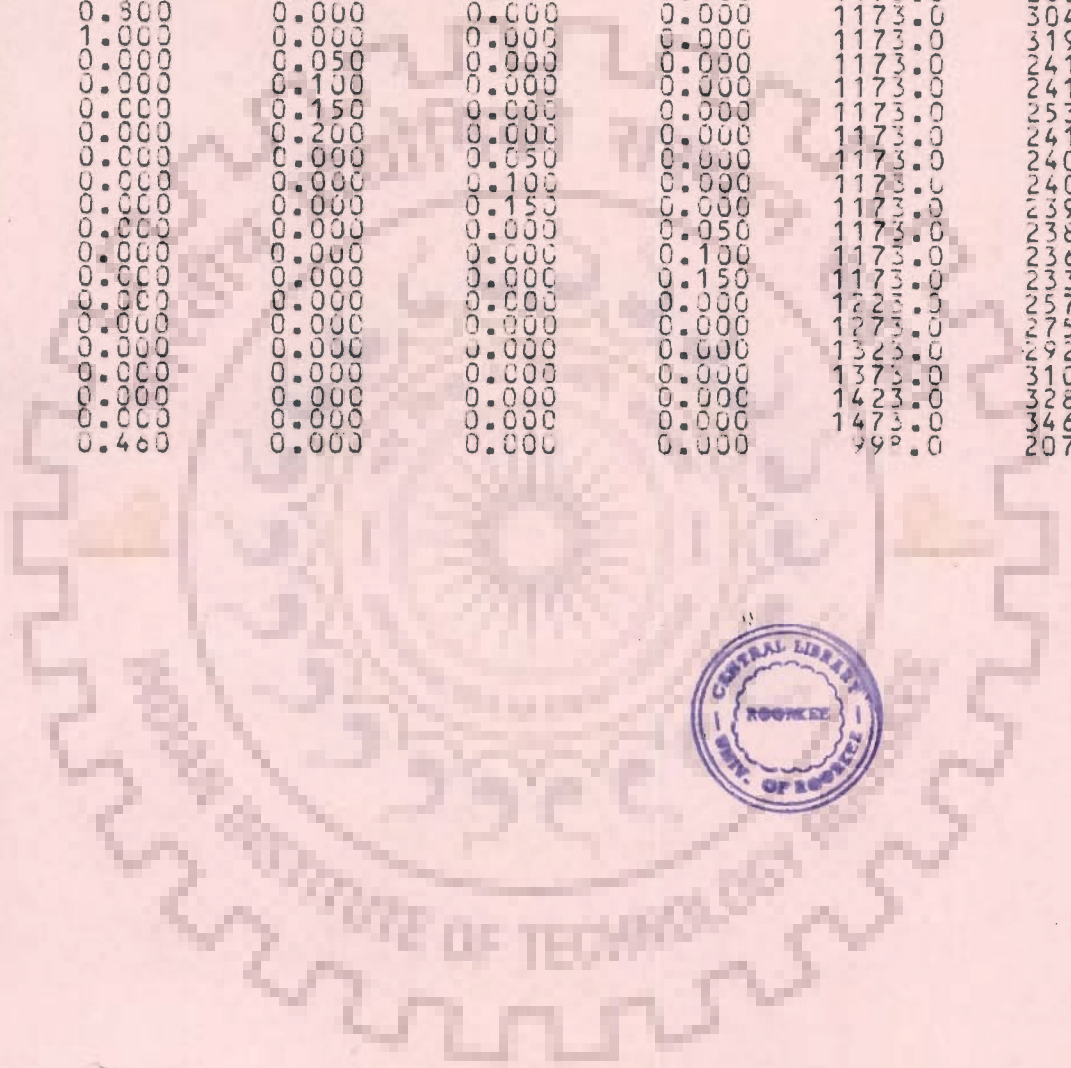
$$(E_{d_{\text{gls}}})_{T_d} = (E_{d_{\text{CaCO}_3}})_{T_d} x_1 + (E_{d_{\text{MgCO}_3}})_{T_d} x_2,$$

Kcal/Kg (3.8)

The energy requirements for preheating and dissociation of various types of limestones were computed using a digital computer (SN-23). Computer programme for the same is given in Appendix-A and the results are given in Table-3.13 where X1, X2, X3, X4, X5 are the weight fractions of calcium carbonate, magnesium carbonate, silica, alumina and iron oxide, respectively in a generalized sample of limestone; HPHLS is the energy required for preheating and HDLSS is the heat of dissociation in Kcal/Kg of limestone. The values computed for calcitic and dolomitic limestones agree fairly well with those reported by various investigators (Boynton, 1967; Knibbs and Gee, 1959; Eigen, 1958).

TABLE-3.13
ENERGY REQUIREMENTS IN LIME BURNING

X1	X2	X3	X4	X5	T(K)	HPHLS	HDL
1.000	0.000	0.000	0.000	0.000	1173.0	241.02	403
0.950	0.050	0.000	0.000	0.000	1173.0	244.96	396
0.900	0.100	0.000	0.000	0.000	1173.0	248.88	389
0.850	0.150	0.000	0.000	0.000	1173.0	252.77	382
0.800	0.200	0.000	0.000	0.000	1173.0	256.63	375
0.750	0.250	0.000	0.000	0.000	1173.0	260.47	368
0.700	0.300	0.000	0.000	0.000	1173.0	264.28	361
0.650	0.350	0.000	0.000	0.000	1173.0	268.06	354
0.600	0.400	0.000	0.000	0.000	1173.0	271.81	347
0.550	0.450	0.000	0.000	0.000	1173.0	275.53	340
0.500	0.500	0.000	0.000	0.000	1173.0	279.22	333
0.450	0.550	0.000	0.000	0.000	1173.0	282.88	326
0.400	0.600	0.000	0.000	0.000	1173.0	286.51	319
0.350	0.650	0.000	0.000	0.000	1173.0	290.11	312
0.300	0.700	0.000	0.000	0.000	1173.0	293.68	305
0.250	0.750	0.000	0.000	0.000	1173.0	297.22	298
0.200	0.800	0.000	0.000	0.000	1173.0	300.73	291
0.150	0.850	0.000	0.000	0.000	1173.0	304.21	284
0.100	0.900	0.000	0.000	0.000	1173.0	307.66	277
0.050	0.950	0.000	0.000	0.000	1173.0	311.08	270
0.000	1.000	0.000	0.000	0.000	1173.0	314.47	263
0.000	0.000	0.000	0.000	0.000	1173.0	317.83	256
0.000	0.000	0.000	0.000	0.000	1173.0	321.16	249
0.000	0.000	0.000	0.000	0.000	1173.0	324.46	242
0.000	0.000	0.000	0.000	0.000	1173.0	327.73	235
0.000	0.000	0.000	0.000	0.000	1173.0	331.00	228
0.000	0.000	0.000	0.000	0.000	1173.0	334.24	221
0.000	0.000	0.000	0.000	0.000	1173.0	337.46	214
0.000	0.000	0.000	0.000	0.000	1173.0	340.65	207



179286
Central Library University of Roorkee
ROORKEE

3.4.2 Feed Mix Ratio

The input to the lime kiln at the top is a mixed feed of limestone and solid fuel in a given ratio (x_r) by weight. The same is proposed to be determined from the following equation based on the definition of thermal efficiency for a given type of lime kiln:

$$X_r = H_f \eta_l [E_d (1-x_u)]^{-1} \quad (3.9)$$

where H_f is the average heat value of the fuel (Kcal/Kg), η_l is the fractional gross thermal efficiency based on output lime, E_d is the endothermic heat of decomposition (Kcal/Kg limestone), and x_u is the fractional degree of underburning acceptable for a given type of kiln and its mode of operation.

3.4.3 Residence Times

On the basis of existing knowledge as summarized in Chapter-2 of this thesis, the available data based on single particle investigations vis-a-vis the semi-empirical approach as attempted in the past were partially modified to compute the design of the coal fired lime shaft kilns by substitution of averaged values of system properties pertinent to this kind of kilns in the indigenous context. The predominant effect

of heat transfer coefficient due to radiation were accounted for in the burning zone by defining effective heat transfer coefficient due to convection and radiation.

For the continuously operated mixed-feed kilns the time required (in hours) under average conditions for the preheating of limestone (θ_p), its burning (θ_b), and the cooling of the product lime lumps (θ_c) are given by the following equations:

$$\theta_p = 686 (d_{p_s}^3 / P_s)^{1/2} \quad (3.10)$$

$$\theta_b = 6350 d_{p_s} \left[0.052 d_{p_s} + (20.25 + 180 d_{p_s} + 6.75 \sqrt{P_s / d_{p_s}})^{-1} \right] \quad (3.11)$$

$$\theta_c = 488 (d_{p_s}^3 / P_s)^{1/2} \quad (3.12)$$

where d_{p_s} is the average size of the stone (m) and P_s is the superficial lime output rate based on average inner cross-sectional area of the kiln. The values of residence times for continuous operation were computed. The results are reported in Tables-3.14 through 3.16.

TABLE-3.14

Computed Values of Preheating Times for Limestones

d_{p_s} (m)	PREHEATING TIME (Hrs)			
	$P_s = 1.0$	$P_s = 15$	$P_s = 2.0$	$P_s = 2.5$
0.010	0.69	0.56	0.49	0.31
0.025	2.67	2.18	1.89	1.20
0.050	7.68	6.28	5.45	3.45
0.075	14.10	11.53	10.00	6.28
0.100	21.60	17.68	15.30	9.65
0.125	30.40	24.90	21.50	13.66
0.150	39.00	31.90	27.60	17.50

TABLE-3.15

Computed Values of Burning Times for Limestones

d_p (m)	BURNING TIME (Hrs)			
	$P_s=1.0$	$P_s=1.5$	$P_s=2.0$	$P_s=2.5$
0.100	0.74	0.64	0.57	0.53
0.025	2.57	2.29	2.10	1.94
0.050	6.12	5.58	5.20	4.92
0.075	9.55	9.22	8.65	7.98
0.100	13.98	13.22	12.65	12.08
0.125	17.90	17.12	16.48	15.93
0.150	22.20	21.30	20.65	20.16

TABLE-3.16

Computed Values of Cooling Time For Quick Lime (Lumps)

d_{P_s} (m)	COOLING TIME (Hrs)			
	$P_s=1.0$	$P_s=1.5$	$P_s=2.0$	$P_s=2.5$
0.010	0.49	0.40	0.35	0.31
0.025	1.90	1.55	1.35	1.20
0.050	5.47	4.47	3.89	3.47
0.075	10.04	8.22	7.12	6.37
0.100	15.37	12.60	10.90	9.37
0.125	21.60	17.70	15.30	13.75
0.150	27.70	22.70	19.65	17.60

3.4.4 Zonal Heights

Heights of the preheating, burning and cooling zones, in meters, based on residence times and system properties could be computed. The correlations evolved are :

$$H_p = 74.3 (1 + X_r) P_s \theta_p / (X_p X_s X_r \rho_{mf}) \quad (3.13)$$

$$H_b = 74.3 (1 + X_r') P_s \theta_b / (X_p X_s X_r' \rho_{mf}') \quad (3.14)$$

$$H_c = \left[41.7 + 74.3 (X_r / X_s X_r) + 74.3 (1 - X_s) / X_s \right] P_s \theta_c / (X_p \rho_{pl}) \quad (3.15)$$

where x_s is the fractional dissociation of limestone to quick lime ($x_s = 1 - x_u$), x_f is the fractional ash content of fuel, x_p is the fractional purity of limestone in terms of CaCO_3 , x_r is the limestone to fuel ratio by weight in the feed input, ρ_{mf} is the bulk density of the mixed-feed (Kg/m^3), ρ_{pl} is the bulk density of the product lime (Kg/m^3).

There is an apparent loss of volatile content of coal in the preheating zone of the coal fired kilns (Macedo, 1958). Thus a modified value of stone to fuel ratio by weight (x_r') is employed while computing the height of the burning zone to which the feed enters from the preheating zone

$$\text{Thus } X_r' = X_r / (1 - X_{fv}) \quad (3.16)$$

where x_{fv} is the fractional volatile matter in the sample of coal.

For a closely graded feed of limestone and fuel particles, the bulk density of the mixture is given by the equation :

$$\rho_{mf} = \rho_s \rho_f (1 + X_r) / (\rho_s + X_r \rho_f) \quad (3.17)$$

where ρ_s and ρ_f are the average bulk densities of limestone and fuel, respectively. Similarly, the modified value of the bulk density of the feed entering the burning zone, ρ_{mf} can be computed based on the modified value of x_r' .

Computer Programme for State-of-the-Art Process Engineering design computation is given in Appendix-B and the results for average conditions for a coal-fired lime shaft kiln of 10 tpd capacity are reported in Table-3.18.

3.4.5 Semi-Continuous Operation

The low capacity mixed-feed kilns in the building and small scale chemical industries are generally operated manually in one or

two shifts per day subject to the limitations of fuel, availability of labour and market demand fluctuations. The intermittent charging of raw materials and discharging of product tends to enhance the retention time which in turn leads to lowering down the productivity of the kiln.

In view of the operational practices being followed in a typical kiln, the retention time $\theta_{r/z}$ (in hours) for the same could be correlated by the expression :

$$\theta_{r/z} = 24 \theta_{t/c} (1 + A_{l/c}) (N_d \theta_d N_s)^{-1} \quad (3.18)$$

where $\theta_{t/c}$ is the retention time for the continuous operation of the moving bed calciner (hrs.), $A_{l/c}$ is the fractional time lag allowance for manual operation over mechanized operation usually about 0.16 as reported by Azbe (1941), N_d is the number of discharges per shift, N_s is the number of working shifts per day, and θ_d is the average time of each discharge (hrs).

The retention times for several running kilns were determined from the field operation studies and the same were compared with those computed from equation (3.18). The results are presented in Table-3.17.

3.4.6 Wall Thickness of Masonry Shaft

The minimum wall thickness of the masonry kiln for design purpose should be based on the worst conditions prevailing in the burning zone of the kiln. Let R_i and R_o represent the average inner radius and outer radius of the shaft kiln so that the wall thickness, W_t , is:

$$W_t = R_o - R_i$$

Let T_i , T_o and T be the temperature in $^{\circ}\text{C}$ for the maximum inner wall surface, minimum desired outerwall surface and surroundings, respectively.

Under steady state conditions, the expression for heat conducted through the wall, Q_{wc} (Chapman, 1960) is given by the equation:

$$Q_{wc} = 2\pi L k_w (T_i - T_o) / \ln (R_o/R_i) \quad (3.19)$$

and the heat loss from the external surface of the wall to the ambient air, Q_{wa} is given by the expression :

$$Q_{wa} = h_c 2\pi R_o L (T_2 - T_{\infty}) \quad (3.20)$$

TABLE-3.17

Comparison of Retention Times for Field Operating Kilns

Kiln No.	Identification of Kiln (Plant, site)	Retention Time Estimated from Field Data (hrs)	Retention Time Computed from Equation (3.18)	Deviation %
1.	KVIC, DDN	53.9	62.6	+16.1
2	KVIC, DDN	64.1	78.0	+21.7
3	CBRI, RKE	32.0	36.0	+12.5
4	PSLW, MRT	81.3	76.4	- 6.0
5	M&C, DDN	100.2	89.5	-10.7
6	VP , DDN	110.7	89.5	-19.2
7	HML, NRNL	111.1	84.0	-24.2
8	GHLI, RPR	83.0	77.4	- 6.7
9	TLI, MZFNR	68.2	75.0	+10.0
10	HC, PNTSB	63.9	72.1	+12.6
11	RC, KLMB	84.0	79.5	- 5.4
12	PC, MDDN	71.0	75.2	+ 5.9

TABLE-3.18

PROCESS ENGINEERING DESIGN OF COAL-FIRED LIME SHAFT KILNS

AVERAGE INPUT DATA

			2		
0.2500	2.2500	0.2250	10.0000	0.1000	0.0000
400.0000	1500.0000	6000.0000	300.0000	800.0000	0.4500
2.0000		2.0000	0.4000		4.0000
			0.1600		

RESULTS OF COMPUTATIONS

NOMINAL DESIGN CAPACITY OF LIME KILN = 10.00 TPD

LIMESTONE-TO-FUEL RATIO BY WEIGHT IN FEED INPUT AT TOP OF LIME KILN =

AVERAGE INNER DIAMETER OF THE LIME SHAFT KILN = 2.379 M

RETENTION TIMES (IN HOURS) FOR CONTINUOUS OPERATION :

PREHEATING	BURNING	COOLING	OVERALL
32.137	23.384	22.862	

HEIGHTS OF THE VARIOUS ZONES (IN METERS) FOR CONTINUOUS OPERATION

PREHEATING ZONE	BURNING ZONE	COOLING ZONE	EFFECTIVE
4.701	0.237	2.880	

Now under steady state conditions

$$Q_{wc} = Q_{wa}$$

Thus

$$k_w (T_i - T_o) / \ln (R_o/R_i) = h_c R_o (T_2 - T_\infty) \quad (3.21)$$

In the above equations L is the height of the kiln, k_w is the effective thermal conductivity of the wall insulation, h_c is the heat transfer coefficient due to natural convection from the outer wall to air.

The parameters were estimated using the data from Chapman (1960), Bird, et.al (1960), and Perry and Chilton (1968) for maximum inner wall temperature of 1200°C , the outer wall temperature of 40°C and the ambient temperature of 25°C . Keeping in view the thermal and functional requirements of lime kilns a masonry wall thickness of about 0.90 - 1.00 m was considered appropriate as assessed from a trial and error solution of equation (3.21).

3.5 INFERENCES

- (i) Field survey indicated wide variations in superficial lime output rates, product qualities and thermal performances of the low capacity

mixed-feed lime shaft kilns. Investigations in the field and laboratory revealed poor thermal performance of these kilns.

(ii) The existing knowledge and available data on process engineering design were partially modified and working correlations were evolved for computation of dimensional specifications of the coal fired lime shaft kilns.

(iii) The state-of-the-art on process engineering correlations, however, left much to be desired as, although, the equations could be used for computing the preliminary design specifications fairly well for average conditions of operation, yet the effect of the influencing design and operational parameters on the performance of the kiln could not be properly assessed.

(iv) On account of the close proximity of constituents in mixed firing the individual temperature profiles for limestone, fuel and the bulk gas phases along the height of the kiln could neither be experimentally determined nor theoretically predicted.

(v) The degrees of calcination of limestone and combustion of coal particles along the height of the burning zone also could not be determined.

(vi) The need was thus established to develop a mechanistic model for the steady state simulation of coal-fired lime shaft kilns with

a view to predicting the effect of various design and operational parameters on their performance and evolve appropriate conditions for optimal design.





CHAPTER-4

MODELLING OF COAL
FIRED LIME SHAFT KILN

Chapter-4

MODELLING OF COAL-FIRED LIME SHAFT KILN

4.1 PREAMBLE

Simulation of the mixed-feed lime shaft kiln requires a detailed analysis of the design and operating parameters. The important design parameters are :

(i) Superficial product output rate based on cross-sectional area of kiln $t/(m^2)$ (day)

(ii) Kiln height-to-diameter ratio

(iii) Wall insulation

Operating parameters of significance are :

(i) Limestone properties

a) Size of particles

b) Quality (composition, lattice structure, etc.)

(ii) Fuel properties

a) Size of particles

b) Quality (proximate and ultimate analyses)

(iii) Limestone-to-fuel ratio in feed input

(iv) Excess air

The quality of limestone determines its specific heat, density, calcination temperature and endothermic heat of decomposition. The quality of fuel determines its volatile and fixed carbon fractions, and its heating value.

Performance criteria could be based on :

- (i) Superficial lime output rate, $t/(m)^2$ (day), consistent in product lime quality with respect to underburning or overburning.
- (ii) Specific energy consumption per unit mass of product lime or thermal efficiency.

4.2 ANALYSIS OF THE PREHEATING ZONE

4.2.1 Definition and Assumptions

Preheating zone is located at the upper portion of the vertical shaft kiln. Mixed charge of limestone and coal particles is fed at the top of the kiln and gets heated to required temperatures as it moves down by exchanging heat from the upward flowing hot gases.

The preheating section is basically a direct contact solid-gas counter-current heat exchanger. This zone is assumed to extend till fuel particle temperature reaches auto-ignition temperature of volatile matter or when the temperature of limestone particles reaches the calcination temperature (about 1173 K) whichever occurs earlier. No changes in composition of limestone particles are effected till the attainment of calcination temperature. However, the demolsturization of coal particles starts in the temperature range of 373-383 K. The volatile matter is assumed to evolve when the fuel temperature lies in the range of about 673-1173 K. Instantaneous combustion of volatile matter in the boundary layer over the surface of the coal particle is assumed when the fuel temperature becomes equal to or greater than the auto-ignition temperature. The auto-ignition of volatile matter is assumed to occur at 948 K. The volatile matter released in the fuel temperature range of 673 to 948 K is assumed to be linear in temperature and it remains unburnt. This results in the partial loss of thermal efficiency. The burning of residual volatileionally combustion of fixed carbon may be essential before limestone attains calcination temperature, and this situation is treated as a part of the burning zone. The release of moisture is assumed to occur during prespecified number of kiln length intervals (number of discrete ΔZ steps) in view of the possible mass transfer limitation during its release through fuel particles.

The basic assumptions made in the analysis of the preheating zone are : (i) Flow patterns of solids and gas are characterized by

plug flow behaviour. Therefore, temperatures of solids and gas vary only along the axis of the kiln and variations in radial direction are ignored, (ii) Thermal conductivities, viscosities and solid volumes are constant in the zone, (iii) Heat loss from the kiln wall is assumed to result only from the exchange of heat between the gas and inside of kiln wall in view of the rapid mixing of gas in radial direction and point contacts of solid particles with kiln wall, (iv) At a given cross-section, the rate of heat transfer within the limestone and fuel particles is very fast as compared to the overall rate of heat transfer from gas to the particles. Consequently, the temperature gradients within the limestone and fuel particles are insignificant. This assumption is corroborated by the investigations of Hills (1968) for limestone particles, and Chung and Yun (1985) for coal particles.

The above assumptions are quite realistic and at the same time simplify the problem to some extent. The bulk movement of gaseous components from one phase to another at appropriate temperatures and their contribution in energy balances is an important feature of the proposed model for the preheating zone. Profiles of temperatures of gas, limestone and fuel particles, and fractional reduction in fuel quantity are obtained along the kiln axis by simultaneous solution of the set of three one dimensional steady state equations.

4.2.2 Differential Energy Balances

Over a differential volume elements, $\pi R_i^2 \Delta Z$ corresponding to width ΔZ in the axial direction at a given location Z (Fig. 4.1) in the zone along the length of the kiln, with Z being taken as zero at the top of the kiln and having an increasing positive value towards the bottom of the kiln, the balances have been written in the finite difference form, where R_i is the internal radius of the kiln. Appropriate modes of heat exchange are considered for interphase heat transfer between limestone and fuel particles, and gas.

4.2.2.1 Heat Balance For Limestones :

Heat is exchanged between the stone particles and the fuel particles by conduction and radiation. Heat is also exchanged between the stone particles and the bulk gas largely by convection and partially by radiation. The net heat received by the limestone particles is utilized in raising the sensible heat content of limestone by increasing its temperature. Thus the heat balance for limestones becomes

$$\begin{aligned} & (h_c + h_r)_{fs} (T_f - T_s) a_f \pi R_i^2 - (h_c + h_r)_{sg} (T_s - T_g) a_s \pi R_i^2 \Delta Z \\ & = \Delta (\dot{m}_s c_s T_s) \end{aligned} \quad (4.2.2.1.1)$$

- where T_g , T_f , T_s are the temperatures of bulk gas, fuel and stone particles, respectively in K; a_f and a_s are the interfacial areas of

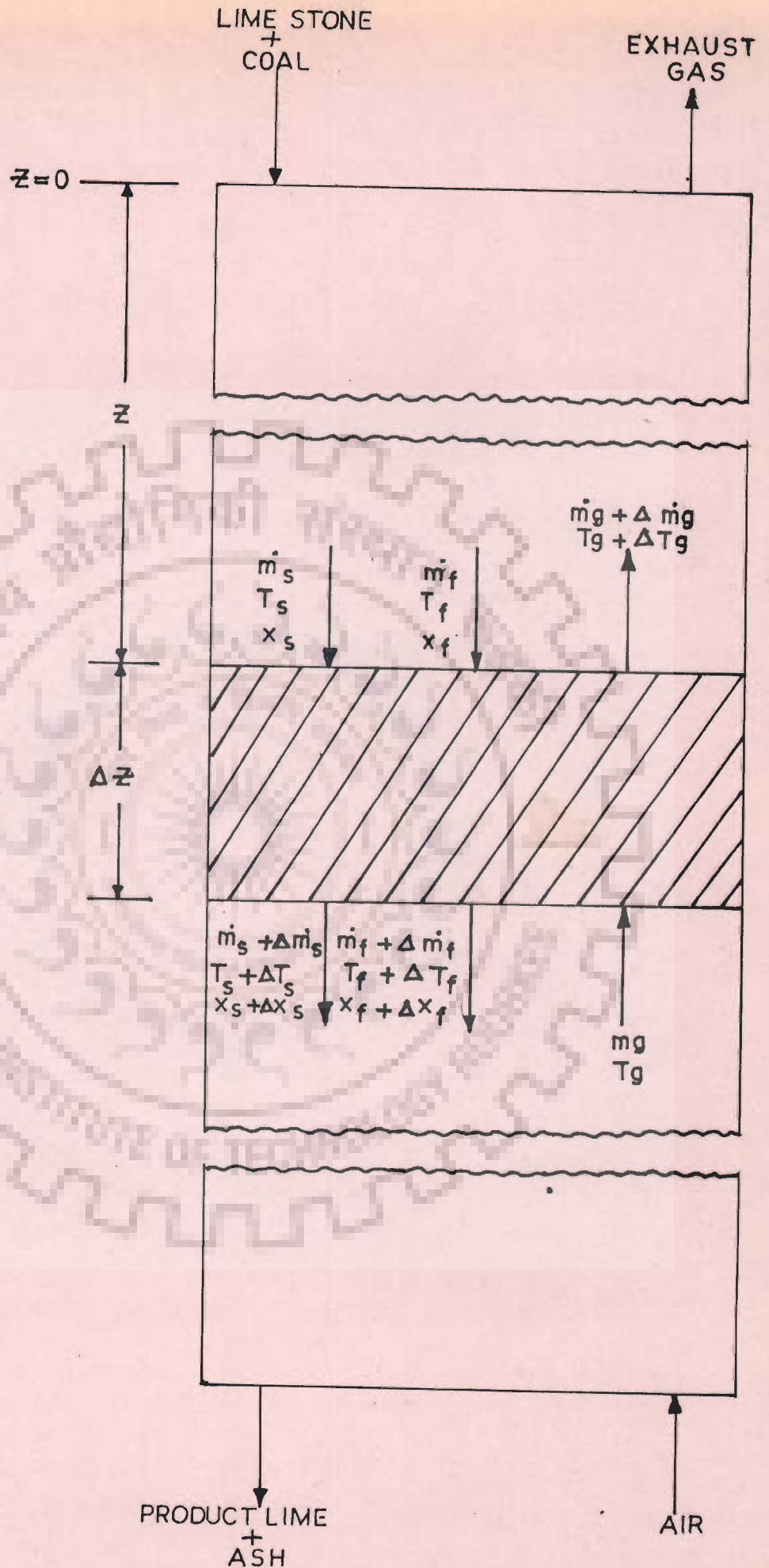


FIG. 41- DIFFERENTIAL VOLUME ELEMENT IN A GENERAL SECTION OF LIME SHAFT KILN

fuel and stone particles, m^2/m^3 of bed volume; \dot{m}_s is the mass flow rate of limestone, Kg/hr; C_s is the specific heat of limestone particles, Kcal/(Kg)(K); h_c is the heat transfer coefficient due to conduction between fuel and stone particles in Kcal/(hr)(m²)(K), and it is heat transfer coefficient due to convection between the gas and stone particles; and h_r is the heat transfer coefficient due to radiation. The subscript fs denotes from fuel to stone, and sg from stone to gas.

The first term on left hand side of the above equation indicates the heat received by the limestone particles from the fuel particles and the second term with negative sign indicates the transfer of heat from limestone particles to gas.

4.2.2.2 Heat Balance For Fuel :

(i) For simple preheating, the fuel particles exchange heat with the bulk gas by convection and radiation. Heat is also exchanged between limestone and fuel particles by conduction and radiation. Thus this balance could be written as:

$$\begin{aligned} & (h_c + h_r)_{gf} (T_g - T_f) a_f \kappa R_i^2 \Delta Z - (h_c + h_r)_{fs} (T_f - T_s) a_f \kappa R_i^2 \Delta Z \\ & = \Delta (\dot{m}_f C_f T_f) \end{aligned} \quad (4.2.2.2.1)$$

where \dot{m}_f is the mass flow rate of the fuel particles in Kg/hr and C_f is the specific heat of fuel particles. The subscript gf denotes from gas to fuel.

The first term on the left hand side of the above equation indicates the heat received by the fuel particles from the gas and the second term with negative sign shows the heat transfer from fuel particles to stone particles.

(ii) For preheating with demoiaturization, the endothermic heat of desorption-cum-vaporization of water has to be accounted for.

Thus,

$$\begin{aligned} & (h_c + h_r)_{gf} (T_g - T_f) a_f \tau R_i^2 \Delta Z - (h_c + h_r)_{fs} (T_f - T_s) a_f \tau R_i^2 \Delta Z \\ & - \dot{m}_f \Delta x_f (\lambda_w + C_w T_f) = \Delta (\dot{m}_f C_f T_f) \end{aligned} \quad (4.2.2.2)$$

where x_f is the fractional devolatization of fuel based on unit mass of fuel input, λ_w is the endothermic heat of desorption of water in Kcal/Kg, and C_w is the specific heat of water vapour. The third term with negative sign on the left hand side of the above equation indicates the amount of heat required for demoiaturization and raising the moisture evolved to fuel temperature.

(iii) For preheating with devolatilization without volatile matter combustion, the endothermic heat of devolatilization and for raising the volatile matter evolved to fuel temperature has been similarly accounted in the heat balance as indicated below (Third term on the left hand side):

$$\begin{aligned} & (h_c + h_r)_{gf} (T_g - T_f) a_f \pi R_i^2 \Delta Z - (h_c + h_r)_{fs} (T_f - T_s) a_f \pi R_i^2 \Delta Z \\ & - \dot{m}_f \Delta x_f (\lambda_{vm} + C_{vm} T_f) = \Delta (\dot{m}_f C_f T_f) \end{aligned} \quad (4.2.2.2.3)$$

where λ_{vm} is the heat of devolatilization in Kcal/hr and C_{vm} is the specific heat of the volatile matter.

4.2.2.3 Gas Phase Heat Balance :

The upward flow of gas (negative Z direction) is counter-current to the downflow (positive Z direction) of limestone and fuel particles. On account of the assumption of good radial mixing for the gas phase and negligible heat exchange between solid phases and wall due to point contacts, the wall heat losses have been accounted for in the heat balance for the gas phase.

(i) For the case of simple preheating, the gas heat balance could be written as :

$$(h_c + h_r)_{gf} (T_g - T_f)_{af} \pi R_i^2 \Delta Z + (h_c + h_r)_{gs} (T_g - T_s)_{as} \pi R_i^2 \Delta Z + \Delta H_1 = \Delta(\dot{m}_g C_g T_g) \quad (4.2.2.3.1)$$

where ΔH_1 is the heat loss through the kiln wall in Kcal/hr. The left hand side terms indicate the total amount of sensible heat loss and is positive. Thus T_g will increase in positive Z - direction.

(ii) For preheating with demosturization, the bulk transport of water vapour at a temperature T_f from the fuel to the gas phase takes place. The fourth term with negative sign accounts for this sensible heat receipt by the gas phase in the following heat balance equation :

$$(h_c + h_r)_{gf} (T_g - T_f)_{af} \pi R_i^2 \Delta Z + (h_c + h_r)_{gs} (T_g - T_s)_{as} \pi R_i^2 \Delta Z + \Delta H_1 - \dot{m}_f \Delta x_f C_{vm} T_f = \Delta(\dot{m}_g C_g T_g) \quad (4.2.2.3.3)$$

4.2.2.4 Devolatilization of Coal :

For the case of devolatilization, the fraction of volatile matter evolved from the fuel has been assumed linear to rise in the fuel

temperature for the range of devolatilization temperatures (673 - 1173 K). Thus,

$$\Delta x_f = X_{vm} \Delta T_f / (1173 - 673) \quad (4.2.2.4.1)$$

$$\text{for } 673 \leq T_f \leq 1173 \text{ K}$$

where X_{vm} is the fractional content of volatile matter in coal.

4.3 MODEL FOR COMBUSTION BEHAVIOUR OF A COAL PARTICLE

The proximate analysis of coal provides necessary information for describing its combustion behaviour in a mixed-feed lime shaft kiln. The volatile matter is assumed to evolve when the temperature lies usually in the range of 673-1173 K. The temperature range can be varied, if desired. Instantaneous combustion of volatile matter in the boundary layer over the surface of the coal particle is generally assumed when the fuel temperature becomes equal to or greater than auto-ignition temperature of the volatile matter at conditions prevailing in the kiln at that point. Auto-ignition temperature is assumed as 948 K, but other values can also be assigned if considered necessary. The volatile matter evolved in the fuel temperature range of 673 to 948 K has already been assumed to escape unburnt in the analysis of the preheating zone resulting in partial loss of thermal efficiency.

Instantaneous combustion of volatile matter evolved at fuel temperatures above the auto-ignition temperature of the volatile matter, and oxidation of the fixed carbon content of coal are sufficient to describe the combustion behaviour of the fuel. The release of the volatile matter from the incipient point of its instantaneous combustion is assumed to occur in prespecified discrete ΔZ steps, which can be assigned any desired value, of kilns length intervals in view of the possible mass transfer limitations during its evolution and instantaneous combustion at the surface of the fuel particles resulting in rapid increase in their temperatures. Burning is assumed to be uniform at the exposed surface of coal.

The ignition of the fixed carbon content of the coal particle has been assumed to commence only after the completion of devolatilization. Possibility exists that the ignition of fixed carbon content of fuel may at times occur before the entire volatile matter has been evolved. However, the probability of oxygen reaching the fuel particle surface, so as to cause combustion of the fixed carbon, when the volatile matter is being evolved and getting burnt around the coal particle is extremely small. Therefore, a simplified approach is used whereby ignition of the fixed carbon is assumed to occur after complete burning of the volatile matter evolved beyond the auto-ignition temperature attained by the fuel. This assumption is also corroborated by Lowe, et. al (1977), Conglidis and Geogarkis (1981), and Thring (1962).

The kinetics of shrinking particle size model has been assumed for combustion of the fixed carbon content of coal alongwith the simultaneous removal of ash from the fuel particle. This model is also referred as ash segregation model. The rate of reaction, mass of fixed carbon consumed/(external surface) (time), for combustion of the fixed carbon to carbon dioxide is a first order reaction with respect to the concentration or partial pressure of oxygen in the gas phase. For combustion kinetics, fixed carbon is treated as pure carbon. Two resistances, namely, surface reaction and diffusion of oxygen through the gas film around shrinking coal particle play a dominant roles and these, in turn, determine the effective rate constant for combustion of the fixed carbon. The possibility of formation of carbon monoxide through incomplete combustion of the fixed carbon has been ignored for conditions obtaining in the kiln.

The reaction for combustion of carbon (fixed carbon) to carbon dioxide is described by the equation :



The rate of combustion of carbon (Levensprel, 1975) is defined as

$$\text{rate} = - (1/s_{ex}) \, dm_c/dt, \text{ Kg}/(m^2) \text{ (hr)} \quad (4.3.2)$$

where s_{ex} is the external surface of the particles, m^2 ; m_c is the

mass of carbon, Kg; and t is the time, hr. For the case of a spherical particle, the rate expression is written as :

$$\begin{aligned} \text{rate} &= - (1/4 \pi r^2) \frac{d}{dt} (4 \pi r^3 \rho_c/3) \\ &= - \rho_c \frac{dr}{dt} \end{aligned} \quad (4.3.3)$$

where ρ_c is the density of carbon (Kg/m^3) and r is the radius of the particle (m) at any given instant. It is a first order reaction with respect to the concentration or partial pressure of oxygen in the gas phase. Using appropriate units, the rate is written in terms of partial pressure of oxygen in the gas phase surrounding the particle as :

$$- \rho_c \frac{dr}{dt} = \bar{k}_s p_{O_2} \quad (4.3.4)$$

where \bar{k}_s is the overall rate constant due to combined effect of surface reaction as well as gas film diffusional resistances, $\text{Kg}/(\text{m}^2) (\text{hr}) (\text{atm})$, and p_{O_2} is the partial pressure of oxygen in the gas phase, atm.

The fractional conversion, x_c , of the fixed carbon component of coal is given as :

$$x_c = 1 - (r/r_p)^3 \quad (4.3.5)$$

where r_{p_f} is the original radius of carbon particle (fuel particle).

Differentiating equation (4.3.5)

$$dx_c = -3 r^2 dr / r_{p_f}^3 \quad (4.3.6)$$

and rearranging

$$dr = -dx_c r_{p_f}^3 / 3 r^2 \quad (4.3.7)$$

Equation (4.3.5) can be rearranged to give :

$$r^2 = r_{p_f}^2 (1-x_c)^{2/3} \quad (4.3.8)$$

Substituting for r^2

$$\begin{aligned} dr &= -dx_c r_{p_f}^3 / 3 r_{p_f}^2 (1-x_c)^{2/3} \\ &= -dx_c r_{p_f} / 3(1-x_c)^{2/3} \end{aligned} \quad (4.3.9)$$

Substituting for dr in equation (4.3.4), we get

$$\ell_c r_{p_f} dx_c / 3(1-x_c)^{2/3} = \bar{k}_s p_{O_2} dt \quad (4.3.10)$$

For the conditions obtaining in lime shaft kiln, the interval in real time can be expressed as space time interval if solids move in plug flow at an apparent velocity $v_{sf}/\pi R_i^2 (1-\epsilon_b)$, that is

$$dt = dz / \left[\frac{v_{sf}}{\pi R_i^2 (1-\epsilon_b)} \right] \quad (4.3.11)$$

where ϵ_b is the bed porosity and v_{sf} is volumetric flow rate of solids, fuel and limestone-lime particles.

Substitution in equation (7.3.10) gives

$$\begin{aligned} \epsilon_c r_{pf} dx_c v_{sf} / (1-x_c)^{2/3} \\ = 3 \bar{k}_s p_{O_2} \pi R_i^2 (1-\epsilon_b) dZ \end{aligned} \quad (4.3.12)$$

In the finite difference form, this equation for fixed carbon combustion is written as :

$$\begin{aligned} \Delta x_c = \frac{3 \pi R_i^2 \bar{k}_s p_{O_2} (1-\epsilon_b) \Delta Z (1-x_{c_{av}})^{2/3}}{\epsilon_c r_{pf} v_{sf}} \end{aligned} \quad (4.3.13)$$

The density of fixed carbon in fuel particles after completion of devolatilization can be related to the initial density of fuel particles as :

$$e_c = \xi X_{fc}$$

where X_{fc} is the mass fraction of fixed carbon in fuel. Therefore,

$$\Delta x_c = \frac{3\pi R_i^2 \bar{k}_s p_{O_2} \Delta Z (1 - \epsilon_b)(1 - x_{c_{av}})^{2/3}}{\xi X_{fc} r_{pf} v_{sf}} \quad (4.3.14)$$

By definition :

$$1/\bar{k}_s = 1/k_s + 1/k_d \quad (4.3.15)$$

where k_s is the surface rate constant and k_d is the mass transfer coefficient for diffusion of oxygen. Thus,

$$\bar{k}_s = k_s k_d / (k_s + k_d) \quad (4.3.16)$$

Using appropriate conversion factors, the expression defined by Parker and Hottel (1936) for computation of surface reaction rate constant becomes :

$$k_s = 3.44 \times 10^{11} T_f^{-1/2} e^{-44000/RT_f} \quad (4.3.17)$$

where R is the gas constant and T_f is the temperature of the fuel particle.

The diffusion rate constant for oxygen through gas film consisting largely of carbon dioxide as the main product of combustion is given by Field (1969) as

$$k_d = 0.2304 (T_f/1600)^{0.75} / d_{p_f} \quad (4.3.18)$$

where T_f is the fuel film temperature and d_{p_f} is the diameter of the fuel particle.

The equations (4.3.14) through (4.3.18) are used for the computation of fractional degree of combustion of fixed carbon content of fuel. The effective rate constant \bar{k}_s is computed at each axial position based on the conditions prevailing at that point in the kiln.

When the fuel temperature reaches 1573 K (assumed ash fusion temperature) and above, the fusion of ash particle will result in the formation of a porous ash layer around the shrinking core of

fixed carbon interspersed with fine ash particles. Combustion of fixed carbon is then assumed to occur at the interface of the porous ash layer and fixed carbon core. Mass transfer resistance to oxygen diffusion through ash layer is considered insignificant because complete melting of ash with formation of glassy impervious layer is not visualized as this will result in total loss of unburnt fixed carbon in fuel particles. Shrinking of ash layer resulting in the increase of its density is related to the temperature of fuel particle. This is discussed in detail in Chapter-5. The temperature gradient within the fuel particle consisting of ash layer and fixed carbon core is assumed negligible because of rapid heat conduction.

4.4 HEAT CONDUCTION THROUGH LIME LAYER OF A CALCINING LIMESTONE PARTICLE

The shrinking core model (Fig. 2.1) has been assumed for the decomposition of a limestone sphere undergoing calcination with no change in its size. The decomposition starts at the surface of the particle and proceeds inwards towards the centre. At a given instant there is a central core of undecomposed calcium carbonate surrounded by a shell of calcium oxide with reaction carbonate occurring at the interface between the core and the shell. It has further been assumed that the calcination rate controlling mechanism

is the rate of conduction of heat through the lime layer to the limestone-core boundary. The surface of stone exchanges heat with fuel and gases by conduction convection, and radiation mechanisms. The undecomposed limestone core is assumed to remain at the calcination temperature which is considered as constant irrespective of the core size. A part of the heat received by the stone surface is used for the heating up of the lime layer. The net amount of heat received at the lime-limestone interface is used for the dissociation of CaCO_3 . The heat conduction through the porous lime layer can be analysed as a quasi-steady state process because the rate of heat conduction through the outer shell of lime is very fast as compared to the rate of change of temperature at the surface of lime-limestone particles or the rate of reduction of the limestone core radius. This assumption is similar to that used for the analysis of diffusion of gaseous reactant through the layer of solid product to the surface of unreacted core (Levenspiel, 1975). It may be noted that, in general, intraparticle heat conduction is much faster as compared to interparticle mass transfer (Smith, 1970) and therefore quasi-steady state conduction through lime layer is very much justified.

The stone particle conduction equation is solved using the usual quasi-steady state assumption for any specified surface temperature and limestone conversion. The surface temperature and fractional conversion change with axial position which, in turn, affects the sensible heat accumulation in lime layer.

The use of quasi-steady state assumption for heat conduction through product lime layer for computation of instantaneous radial temperature profile in outer lime shell can be obtained by neglecting heat accumulation in the lime layer. Thus, the intraparticle conduction equation for spherical particles can be written in the form :

$$d^2 T/dr^2 + (2/r) dT/dr = 0 \quad (4.4.1)$$

with boundary conditions :

$$(i) \text{ at } r = r_{p_s}, T = T_s$$

$$(ii) \text{ at } r = r_c, T = T_d$$

where T is the temperature in the outer lime layer of calcining limestone particle, r is the general radial position in the lime layer, r_c is the radius of the calcium carbonate core, r_{p_s} is the size of the limestone particle, T_s is the temperature at the surface of the limestone-lime particle, and T_d is the temperature of decomposition of limestone.

The solution of the above equation is :

$$T = -C_1/r + C_2 \quad (4.4.2)$$

where C_1 and C_2 are the constants of integration. The values of the same obtained from the given boundary conditions are :

$$C_1 = r_c r_{p_s} (T_s - T_d) / (r_{p_s} - r_c)$$

$$C_2 = T_d + r_{p_s} (T_s - T_d) / (r_{p_s} - r_c) -$$

$$r_c r_{p_s} (T_s - T_d) / r (r_{p_s} - r_c)$$

The substitution for C_1 and C_2 in equation (4.4.2) and simplification gives the desired temperature profile in the lime layer :

$$T = T_d + r_{p_s} (T_s - T_d) (1 - r_c/r) / (r_{p_s} - r_c) \quad (4.4.3)$$

The instantaneous temperature profile in product lime layer predicted by equation (4.4.3) is valid for lime-limestone particles at any given axial position in the kiln. It may be noted that as the limestone particles move through the burning zone, not only the surface temperature (T_s) changes, but the core radius (r_c) also changes from r_{p_s} to zero. However, for any given values of T_s and r_c , the equation (4.4.3) will remain valid due to the quasi-steady state assumption.

In order to calculate the rate of calcination as lime-limestone

particles move down the burning zone, appropriate consideration to the heating up of the lime layer will have to be given in the heat balance for a calcining limestone particle. The overall sensible heat requirement in heating up of lime layer above calcination temperature may account for nearly 5 to 10 percent of the heat of calcination. Thus,

Heat conducted inward from the external surface of the limestone - lime particle = Heat utilized for calcination of limestone
+ sensible heat change of the lime layer of the particle.

or

$$k_1 4\pi r_{ps}^2 \left. \frac{dT}{dr} \right|_{r=r_{ps}} = -E_s \rho_s 4\pi r_c^2 \frac{dr_c}{dt} + \frac{d(S_{hl})}{dt} \quad (4.4.4)$$

where k_1 is the thermal conductivity of the lime layer, Kcal/(hr)(m)(k); E_s is the endothermic heat of dissociation, Kcal/Kg of limestone; ρ_s is the density of limestone, Kg/m³; and S_{hl} is the sensible heat content of the lime layer, Kcal. From the generalized nature of temperature profile as indicated by equation (4.4.3), on rearrangement we get

$$\left. \frac{dT}{dr} \right|_{r=r_{p_s}} = \frac{(T_s - T_d) (r_c / r_{p_s})}{r_{p_s} (1 - r_c / r_{p_s})}$$

Noting that the shrinking unreacted core of radius r_c can be correlated with the fractional conversion of limestone (x_s) by the expression :

$$\left(\frac{r_c}{r_{p_s}} \right)^3 = 1 - x_s \quad (4.4.5)$$

the temperature gradient at lime-limestone particle surface in terms of T_s and x_s can be given as :

$$\left. \frac{dT}{dr} \right|_{r=r_{p_s}} = \frac{(T_s - T_d)(1 - x_s)^{1/3}}{r_{p_s} \left[1 - (1 - x_s)^{1/3} \right]} \quad (4.4.6)$$

Differentiation of equation (4.4.5) and rearrangement gives

$$r_c^2 dr_c = r_{p_s}^3 dx_s / 3 \quad (4.4.7)$$

Knowing the temperature profile in lime layer, its sensible heat content, S_{hl} , can be obtained by the expression :

$$S_{hl} = \int_{r_c}^{r_{p_s}} 4\pi r^2 dr \ell_1 C_1 \left[T_d + \frac{r_{p_s} (T_s - T_d) (1 - r_c/r)}{(r_{p_s} - r_c)} \right] \quad (4.4.8)$$

Integration of the above equation gives :

$$S_{hl} = 4\pi \ell_1 C_1 \left[T_d (r_{p_s}^3 - r_c^3) / 3 + (T_s - T_d) \left\{ \frac{(r_{p_s}^3 - r_c^3)}{3} - \frac{r_c (r_{p_s}^2 - r_c^2)}{2} \right\} / (1 - r_c/r_{p_s}) \right] \quad (4.4.9)$$

which can be simplified to give:

$$S_{hl} = 2\pi r_{p_s}^3 \ell_1 C_1 / 3 \left\{ 1 - (1 - x_s)^{1/3} \right\} \left[2 x_s \left\{ T_s - T_d (1 - x_s)^{1/3} \right\} - 3(1 - x_s)^{1/3} \left\{ 1 - (1 - x_s)^{2/3} \right\} (T_s - T_d) \right] \quad (4.4.10)$$

Substitution of equations (4.4.6), (4.4.7) and (4.4.10) in equation (4.4.4) leads to:

$$k_1 4\pi r_{p_s} (T_s - T_d) (1 - x_s)^{1/3} / \left\{ 1 - (1 - x_s)^{1/3} \right\}$$

$$\begin{aligned}
 &= E_s \epsilon_s 4\pi r_p^3 dx_s / 3 dt \\
 &+ d/dt \left\{ \frac{\frac{4}{3}\pi r_p^3 \epsilon_s c_e}{1 - (1-x_s)^{1/3}} \left[x_s \{T_s - T_d (1-x_s)^{1/3}\} - \frac{3}{2} (1-x_s)^{1/3} \right. \right. \\
 &\quad \left. \left. - (1-x_s)^{2/3} \right] (T_s - T_d) \right\}
 \end{aligned}$$

(4.4.11)

which is rearranged to give :

$$\begin{aligned}
 \frac{k_e (T_s - T_d) dt}{\{(1-x_s)^{-1/3} - 1\}} &= \frac{E_s \epsilon_s r_p^2 dx_s}{3} + \frac{\epsilon_s c_e r_p^2}{3} d \left\{ \right. \\
 &\quad \frac{x_s T_s}{\{1 - (1-x_s)^{1/3}\}} - \frac{x_s T_d (1-x_s)^{1/3}}{\{1 - (1-x_s)^{1/3}\}} - 1.5 (T_s - T_d) (1-x_s)^{1/3} \left[\right. \\
 &\quad \left. \left. 1 + (1-x_s)^{1/3} \right] \right\}
 \end{aligned}$$

(4.4.12)

Now for the conditions obtaining in shaft kiln, dt is related with dz as per equation (4.3.11). Substitution and simplification in equation (4.4.12), the conduction equation in finite difference form becomes

$$\begin{aligned}
 \frac{3 k_e \pi R_i^2 (1-\epsilon_b) (T_s - T_d) \Delta z}{r_p^2 v_{st} \{(1-x_{s,w})^{-1/3} - 1\}} &= E_s \epsilon_s \Delta x_s + \epsilon_s c_e \Delta \left\{ \frac{x_s T_s}{1 - (1-x_s)^{1/3}} - \right. \\
 &\quad \left. \frac{x_s T_d (1-x_s)^{1/3}}{1 - (1-x_s)^{1/3}} - 1.5 (T_s - T_d) (1-x_s)^{1/3} [1 + (1-x_s)^{1/3}] \right\}
 \end{aligned}$$

(4.4.13)

4.5 ANALYSIS OF THE BURNING ZONE

4.5.1 Complexities of the Zone and Some Simplifying Assumptions

The analysis and modelling of the burning zone of a mixed-feed lime shaft kiln is extremely complex. A realistic kiln model will have to account for the complicated heat and mass transfer processes alongwith chemical conversion reactions. The main variables to be solved for are : the degree of calcination of limestone, extent of combustion of volatile matter and fixed carbon content of coal, surface temperature of limestone, fuel temperature and bulk gas temperature. Furthermore, it is necessary to account for the release of ash on combustion of the fixed carbon as well, as the fusion of ash after the fuel attains ash fusion temperature, variations in particle surface areas, changes in packed bed densities, heating up of the product quick lime layer after properly accounting for its changing temperature profile, modes of heat exchange between solids and gases, changes in heat transfer coefficients, effectiveness factors for estimating active heat exchange surface areas, variations in specific heat with temperature and composition, the changes in surface reaction rate and diffusional transport rate constants for the combustion of the fixed carbon content of the fuel particles, variations in gas emissivities for gas-solid radiant heat exchange, etc.

In view of the highly complicated nature of the burning zone, some simplifying assumptions have to be made to facilitate the solution

of this otherwise intractable problem without sacrificing the reality of the situation at the same time. In the normal operation of a shaft kiln the radial temperature variations of the gas phase and solids may be neglected and may be treated to change only with the axial position (Z) of the kiln.

Based on the generalized assumptions enumerated earlier for the analysis of the preheating zone, and the assumption of quasi-steady state heat conduction for calcining limestone particles, implying that the rate of heat transfer through the product lime layer is fast compared to the rate of shrinkage of the core resulting in the rapid establishment of the temperature profile for any given lime layer surface temperature and unreacted limestone core radius, the following balances are written at a given axial position for a differential element of kiln length:

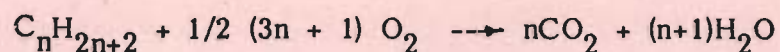
- (i) Heat balance for limestone particles
- (ii) Heat balance for fuel particles
- (iii) Heat balance for the gas phase

The bulk movement of oxygen at gas temperature from gas phase to burning fuel particle and the gaseous combustion products from fuel at fuel temperature and carbon dioxide produced as a result of calcination of limestone at the product lime layer surface temperature are to be properly accounted for in the heat and mass balances. The above three balances alongwith the appropriate equations

for the calcining behaviour of limestone and the combustion behaviour of the volatile matter and fixed carbon contents of coal particles should suffice to predict the conversion profiles of limestone and fuel particles, and temperature profile of the gas, fuel and surface temperature of lime-limestone particles. The temperature profile for the lime layer was also computed for any lime surface temperature and fractional conversion of limestone. This profile is used to estimate the changes in sensible heat of lime layer which is expected to become important as limestone conversion and surface temperature of lime layer increase.

Although the volatile matter in coal consists of saturated and unsaturated hydrocarbons, tarry vapours, hydrogen, carbon monoxide and other minor constituents (Himus, 1958; and Smith and Stinson, 1952), yet a composition, such as, C_nH_{2n+2} can be assumed for the volatile matter as a reasonable assumption for the simplification of analysis and computation. An average molecular weight of 20 for the decomposed volatile matter has been assumed (Fuchs and Sandhoff, 1942).

The volatile matter is assumed to burn instantaneously and completely resulting in the formation of carbon dioxide and water according to the following chemical reaction :



(4.5.1.1)

4.5.2 Differential Material and Energy Balances

The heat conduction equation in lime shell with calcination reaction at lime-limestone interface, the instantaneous combustion of the volatile matter or fixed carbon combustion equations for the fuel have to be used together with material balances and interphase heat balances for obtaining unique solution for each differential kiln volume in the burning zone.

4.5.2.1 Heat Balance for Limestones

No ash is released during the combustion of volatile matter. Ash released during combustion of the fixed carbon at the fuel temperature, when fuel temperature is less than the assumed ash fusion temperature, is assumed to spread over the surface of limestone particles and in the process attains the temperature of the stone surface. The stone particles also receive heat by conduction and radiation from the burning fuel particles. Some of the heat from the fuel is transferred to gas by convection and radiation, if the gas temperature is less than that of the stone.

The net heat received by the lime-limestone particles is utilized mainly for the endothermic calcination process, but some of the heat is also used for the heating up of the quick lime layer formed. The carbon dioxide released at the temperature of calcination

from the reaction interface also gets heated to lime-limestone surface temperature while passing through the lime layer. The transport of carbon dioxide produced from limestone calcination and fuel combustion processes to the gas phase also takes place and needs to be accounted for in the material and energy balances.

Over a differential volume element, $\pi R_i^2 \Delta Z$, of width ΔZ in the axial direction at a given location (Z being taken as positive from top towards lower end of the zone), the heat balance for the limestone particles could be written as :

$$\begin{aligned}
 & (h_c + h_{rfs}) (T_f - T_s) a_f \pi R_i^2 \Delta Z - (h_c + h_{rsg}) (T_s - T_g) a_s \pi \\
 & R_i^2 \Delta Z + m_{f_o} (\Delta x_a) C_a T_f = \dot{m}_{s_o} \Delta x_s E_s + \dot{m}_{s_o} \Delta x_s \\
 & (44/100) C_{CO_2} T_s + \dot{m}_{s_o} \Delta x_s (44/100) C_{CO_2} (T_s - T_d) + \\
 & \Delta (\dot{m}_a C_a T_s) + .56 \dot{m}_{s_o} C_1 \Delta \left[x_s T_s / \{ 1 - (1-x_s)^{1/3} \} - \right. \\
 & \left. x_s T_s (1-x_s)^{1/3} / \{ 1 - (1-x_s) \} - \right. \\
 & \left. 1.5 (T_s - T_d) (1-x_s)^{1/3} \{ 1 + (1-x_s)^{1/3} \} \right] \quad (4.5.2.1)
 \end{aligned}$$

where x_s is the conversion based on original mass flow rate of limestone at kiln top, x_a is the fraction of ash released based on

original mass flow rate of fuel at kiln top, \dot{m}_a is the mass flow rate (Kg/hr) of the ash released, \dot{m}_{s_o} is the mass flow rate of limestone and \dot{m}_{f_o} is the mass flow rate of fuel at kiln top (Kg/hr), C_a is the specific heat of ash, Kcal/(Kg)(K); and T_d is the decomposition temperature of limestone (K).

The first and second terms on the left hand side of the above equations are already explained and the third term indicates the sensible heat received by the stone associated with the ash released from the coal during fixed carbon combustion. The first, second, third, fourth and fifth terms on the right hand side of the above equation indicate the calcination heat requirement, sensible heat associated with CO_2 released from stone at T_s , sensible heat required for heating the CO_2 from T_d to T_s while passing through lime layer, sensible heat accumulation in ash spread on stone particles and sensible heat accumulation in lime layer due to changes in its temperature, respectively.

4.5.2.2 Heat Balance for Gas Phase

The bulk of gas phase receives heat from fuel as well as stone particles by convection and radiation alongwith the bulk transport of carbon dioxide from the calcining limestone particles and burning fuel particles at the appropriate temperatures. The transport of water vapour formed during volatile matter burning also needs to be taken into account.

For the case of volatile matter combustion, the gas phase

heat balance can be written as :

$$\begin{aligned}
 & (h_c + h_r)_{fg} (T_f - T_g) a_f \pi R_i^2 \Delta Z + (h_c + h_r)_{sg} (T_s - T_g) \\
 & a_s \pi R_i^2 \Delta Z + \dot{m}_{f_o} \Delta x_f (56.5/20) C_{CO_2} T_f + \dot{m}_{f_o} \Delta x_f \\
 & (41/20) C_w T_f + \dot{m}_{s_o} \Delta x_s (44/100) C_{CO_2} T_s - \\
 & \dot{m}_{f_o} \Delta x_f (77.5/20) C_{O_2} T_g - \Delta H_1 = - \Delta (\dot{m}_g C_g T_g)
 \end{aligned}$$

(4.5.2.2.1)

where C_w is the specific heat of water vapour. The first, second and seventh terms on the left hand side of the above equation are already explained, the third and fourth terms indicate sensible heat of CO_2 and water produced due to volatile matter combustion at T_f , and sixth and seventh terms are the sensible heat of CO_2 at T_s received by gas from calcination of stone and the sensible heat of oxygen supplied by gas at T_g to fuel for volatile matter combustion. It may be noted that one kmol of volatile matter (molecular weight taken is 20) requires 77.5 Kg of O_2 and produces 56.5 Kg of CO_2 and 41 Kg of water during combustion as per the stoichiometric equation (4.5.1.1). Right hand side term with negative sign indicates the heat accumulation by the gas in negative z direction, that is, in its direction of flow.

$$(h_c + h_{rfg}) (T_f - T_g) a_f \pi R_1^2 \Delta Z + (h_c + h_{rsg}) (T_s - T_g) a_s$$

$$\pi R_1^2 \Delta Z + \dot{m}_{f_o} \Delta x_f (44/12) C_{CO_2} T_f + \dot{m}_{s_o} \Delta x_s (44/100)$$

$$C_{CO_2} T_s - \dot{m}_{f_o} \Delta x_f (32/12) C_{O_2} T_g = - \Delta(\dot{m}_g C_g T_g)$$

(4.5.2.2.2)

The terms in the above equation are self explanatory in view of the fact that one kmol of fixed carbon (molecular weight 12) requires 32 Kg of Oxygen and produces 44 Kg of CO₂ during its combustion.

4.5.2.3 Heat Balance for Fuel

The net heat released from the combustion of volatile matter or fixed carbon content of fuel is supplied to the stone and gas phases. Bulk transport of combustion products at fuel temperature also carry sensible heat alongwith them to the gas phase. Oxygen needed for combustion is received from the gas phase at the temperature of the gas.

For volatile matter combustion, the endothermic heat required for the devolatilization process is also to be accounted for. The differential heat balance for the fuel for the combustion of volatile matter can be written as :

$$\begin{aligned}
& \dot{m}_{f_o} \Delta x_f H_{vm} - \dot{m}_{f_o} \Delta x_f \lambda_{vm} + \dot{m}_{f_o} \Delta x_f (77.5/20) C_{O_2} T_g \\
& = (h_c + h_{r'fs}) (T_f - T_s) a_f \pi R_i^2 \Delta Z + (h_c + h_{r'fg}) (T_f - T_g) \\
& a_f \pi R_i^2 \Delta Z + \Delta(\dot{m}_f C_f T_f) + \dot{m}_{f_o} \Delta x_f (56.5/20) C_{CO_2} \\
& T_f + \dot{m}_{f_o} \Delta x_f (41/20) C_w T_f \quad (4.5.2.3.1)
\end{aligned}$$

where H_{vm} is the heat of combustion of the volatile matter. The first term and second term with negative sign on the left hand side of the above equation indicate exothermic heat of combustion of gaseous volatile matter and endothermic heat of devolatilization, respectively. The third term on the right hand side of the above equation indicates the sensible heat accumulation of fuel particles. All other terms in the above equations are explained earlier. For the case of fixed carbon combustion, the fuel heat balance becomes

$$\begin{aligned}
& \dot{m}_{f_o} \Delta x_f H_{fc} + \dot{m}_{f_o} \Delta x_f (32/12) C_{O_2} T_g = (h_c + h_{r'fs}) \\
& (T_f - T_s) a_f \pi R_i^2 \Delta Z + (h_c + h_{r'fg}) (T_f - T_g) a_f \pi R_i^2 \Delta Z \\
& + \Delta(\dot{m}_f C_f T_f) + \dot{m}_{f_o} \Delta x_f (44/12) C_{CO_2} T_f + \dot{m}_{f_o} \Delta x_f C_a T_f \\
& \quad (4.5.2.3.2)
\end{aligned}$$

where H_{fc} is the heat of combustion of the fixed carbon (Kcal/Kg). The first term in the above equation indicates the exothermic heat of combustion of the fixed carbon.

4.5.2.4 Material Balance for Limestones

The mass flow rate of limestones decreases along the axis of the kiln in the positive Z - direction on account of the release of carbon dioxide. Thus,

$$\Delta \dot{m}_s = - \dot{m}_{s_0} (44/100) \Delta x_s \quad (4.5.2.4.1)$$

4.5.2.5 Material Balance for Fuel

The mass flow rate of fuel decreases along the positive Z - direction during the volatile matter release from the fuel. Thus,

$$\Delta \dot{m}_f = - \dot{m}_{f_0} \Delta x_f \quad (4.5.2.5.1)$$

$$\text{for } x_f \leq x_{fm} + x_{fv}$$

It may be noted that the above equation is also applicable to the preheating zone where demosturization and devolatization without combustion of volatile matter take place.

For fixed carbon combustion with ash release, the mass flow rate of fuel changes as :

$$\Delta \dot{m}_f = - \dot{m}_{f_0} (\Delta x_f + \Delta x_a) \quad (4.5.2.5.2)$$

$$\text{for } x_{fm} + x_{fv} \leq x_f \leq x_{ff}$$

No ash is released during fixed combustion with ash fusion. Thus the material balance for this case becomes :

$$\Delta \dot{m}_f = - \dot{m}_{f_0} \Delta x_f \quad (4.5.2.5.3)$$

$$\text{for } x_{ff} \leq x_f \leq x_{f \max}$$

$$\text{where } x_{f \max} = x_{fm} + x_{fv} + x_{fc}$$

4.5.2.6 Material Balance for Gas Phase

The changes in mass flow rates of limestone particles and fuel particles account for the change in mass flow rate of gas. Thus,

$$\Delta \dot{m}_g = - \dot{m}_{s_0} \Delta x_s (44/100) - \dot{m}_{f_0} \Delta x_f \quad (4.5.2.6.1)$$

The first and second terms with negative signs indicate the increase in the mass of gas due to bulk transfer of CO_2 from the calcining limestone particles and the combustion of fuel. It may be noted that the above equation without the first term on the right hand side is also applicable to the preheating zone where only demosturization or devolatilization without combustion of volatile matter takes place.

4.5.2.7 Material Balance for Ash Release

Ash is assumed to be distributed uniformly alongwith the fixed carbon in the entire volume of the fuel particles. Thus, ash release has a linear relationship with the fixed carbon content of the fuel before fuel attains the ash fusion temperature, that is, $x_{fm} + x_{fv} \leq x_f \leq x_{ff}$ as per the equation :

$$x_a = m x_f + C \quad (4.5.2.7.1)$$

where m and C are the constants to be determined from the limiting conditions :

$$\text{for } x_f = x_{fm} + x_{fv}, \quad x_a = 0$$

$$\text{for } x_f = x_{fm} + x_{fv} + x_{fc}, \quad x_a = x_{fa} \quad (4.5.2.7.2)$$

Solving the above equations, we get

$$x_a = x_{fa} (x_f - x_{fm} - x_{fv}/x_{fc}) \quad (4.5.2.7.3)$$

Differentiating the above equation and writing in the finite difference form, the following relationship is obtained :

$$\Delta x_a = x_{fa} \Delta x_f / x_{fc} \quad (4.5.2.7.4)$$

which is valid for $(x_{fm} + x_{fv}) \leq x_f \leq (x_{fm} + x_{fv} + x_{fc})$.

If ash fusion occurs then the applicability of equation (4.5.2.7.4) will be restricted only upto x_{ff} . The mass flow rate of ash released at any given time in the burning zone is given as :

$$\dot{m}_a = \dot{m}_{f_0} x_a \quad (4.5.2.7.4)$$

and therefore,

$$\dot{m}_a = \dot{m}_{f_0} \Delta x_a \quad (4.5.2.7.5)$$

4.5.2.8 Relationship between x_f and x_c

The fractional conversion of fixed carbon in fuel x_c used in equation 4.3.14 is related linearly to the fractional conversion of fuel x_f by an equation similar to equation (4.5.2.7.1) but the limiting conditions are :

$$\text{for } x_f = x_{fm} + x_{fv}, \quad x_c = 0$$

$$\text{and for } x_f = x_{fm} + x_{fv} + x_{fc}, \quad x_c = 1 \quad (4.5.2.7.6)$$

Solution of linear equation with limiting conditions,

we get

$$x_c = (1/x_{fc}) (x_f - x_{fm} - x_{fv}) \quad (4.5.2.7.7)$$

and therefore,

$$\Delta x_c = \Delta x_f / x_{fc} \quad (4.5.2.7.8)$$

4.5.3 Computation of the Average Temperature of Solid Mass at the end of Burning Zone

The solid mass at the end of the burning zone consists of quick lime particles with or without limestone core, fuel ash and cinders/ash clinkers. The fuel ash has already been assumed to be spread over the surface of the limestone-lime particles. The size and amount of the cinders/ash clinkers at the end of the burning zone is also quite small. Thus the entire lot of solid mass could be assumed to possess uniform average temperature once the combustion of fuel or calcination of limestone is complete.

The average temperature could be computed on the basis of the weighted mean of the different constituents of the solid particles as :

$$T_{\text{solid}} = \left\{ \dot{m}_{s_o} x_{s_{av}} (56/100) C_l T_{ll_{av}} + \dot{m}_{s_o} (1-x_{s_{av}}) C_s T_d \right. \\ \left. + \dot{m}_{f_o} x_{a_{av}} C_a T_{s_{av}} + \dot{m}_{f_o} (1-x_{f_{av}} - x_{a_{av}}) C_f T_{f_{av}} \right\} /$$

$$\left[\dot{m}_{s_o} x_{s_{av}} (56/100) C_l + \dot{m}_{s_o} (1-x_{s_{av}}) C_s + \right. \\ \left. \dot{m}_{f_o} x_{a_{av}} C_{fa} + \dot{m}_{f_o} (1 - x_{f_{av}} - x_{a_{av}}) C_f \right]$$

(4.5.3.1)

where $x_{s_{av}}$ is the fractional conversion of limestone at the end

of the burning zone and $T_{ll_{av}}$ is the average temperature of the lime particles. The $T_{ll_{av}}$ is computed from the sensible heat balance using the lime layer temperature profile at the completion of calcination ($x_{sav} = 1.0$) or at the end of burning zone ($x_f = x_{fm} + x_{fv} + x_{fc}$) whichever occurs earlier as per the following equation :

$$T_{ll_{av}} = T_{s_{av}} / \{1 - (1-x_s)^{1/3}\} - T_d(1-x_{s_{av}}) / \{1-(1-x_{s_{av}})\} - 1.5 (T_{s_{av}} - T_d) (1-x_{s_{av}})^{1/3} \{1+(1-x_{s_{av}})^{1/3}\} / x_{s_{av}} \quad (4.5.3.2)$$

The average temperature of the solid mass computed from equation (4.5.3.1) is used in the analysis of the cooling zone in which the heat exchange takes place from the solid mass to the gas phase.

4.6 ANALYSIS OF THE COOLING ZONE

The cooling zone is located at the lower most part of the kiln. In this zone, the down flowing hot quick lime and coal ash particles exchange heat with the upflowing air. Air is introduced at the bottom of the kiln to supply enough oxygen for the combustion of fuel. Theoretical air requirement is calculated assuming complete

combustion of the volatile matter and fixed carbon in the fuel. The cooling zone is assumed to commence after the attainment of the uniform temperature of lime layer alongwith the unburnt limestone core, if any. The basic assumptions made for the formulation of a mathematical model for this zone are similar to those made for the modelling of the preheating zone. Since no combustion of coal takes place in this zone, all solid materials, including quick lime or lime-limestone particles, ash and clinkers/cinders, are assumed to be at the same temperature, therefore, the analysis of this zone becomes simpler than that of the preheating zone.

The temperature profiles of solids and gas along the axis of the kiln for this zone are obtained by simultaneous solution of the one dimensional steady state heat balance equations for solids and gas. The solids entering the cooling zone from the burning section for the mixed feed kiln comprise of partially or fully calcined particles of stones, fuel ash and cinders/clinkers. This solid mass is assumed to have uniform average temperature as discussed earlier in section (4.5.3).

The heat is assumed to be transferred from the solids to air largely by the mechanism of convection. Thus the model equation for the sensible heat loss of solids due to heat transfer to upflowing air in this zone is (with Z being taken positive towards bottom


of the kiln) :

$$\dot{m}_{s_{av}} C_{s_{av}} (-\Delta T_s) = (h_{c_{sg}}) (T_s - T_g) a_s \pi R_i^2 \Delta Z \quad (4.6.1)$$

Similarly the net sensible heat gain by the gas in negative z direction, that is, direction of gas flow, is equal to heat received from solids minus heat loss to the wall :

$$-\Delta(\dot{m}_g C_g T_g) = (h_{c_{sg}}) (T_s - T_g) a_s \pi R_i^2 \Delta Z - \Delta H_l \quad (4.6.2)$$

where $\dot{m}_{s_{av}}$ is the average mass flow rate of the solid mass (Kg/hr) in the cooling zone.



CHAPTER-5
DEVELOPMENT OF SIMULATION
PROGRAMME

Chapter-5

DEVELOPMENT OF SIMULATION PROGRAMME

The development of simulation programme invariably requires the estimation of system parameters and properties as a first step. This was also considered necessary for the solution of model equations for mixed-feed lime shaft kiln as discussed in the previous chapter. This chapter presents the correlations used for system parameters and properties estimation, correlation used to estimate heat losses through kiln wall, and the salient features of computer programmes for the three zones of the lime kiln alongwith the information flow diagrams.

5.1 SYSTEM PARAMETERS AND PROPERTIES ESTIMATION

5.1.1 Specific Heats of Components

The correlations for specific heats as functions of temperature for various components were largely taken from Perry and Chilton (1968), but other sources, such as Murray (1947), and Knibbs and Gee (1959) were also used. If more than one correlation were available, the same were checked for different temperatures. The correlations for specific heats in Kcal/(Kg)(K) used finally in the simulation programme with the temperature range over which they are reported to be accurate are given below:

$$(i) C_{CaCO_3} = 0.1968 + 0.1189 \times 10^{-3} T - 0.3076 \times 10^4 / T^2$$

(Temperature range 273-1033 K)

(5.1.1.1)

$$(ii) C_{CaO} = 0.1786 + 0.0864 \times 10^{-3} T - 0.1928 \times 10^4 / T^2$$

(Temperature range 273-1173 K)

(5.1.1.2)

$$(iii) C_{O_2} = 0.2584 + 0.8063 \times 10^{-5} T - 5865.6 / T^2$$

(Temperature range 300-5000 K)

(5.1.1.3)

$$(iv) C_{CO_2} = 0.1441 + 0.2305 \times 10^{-3} T - 0.0776 \times 10^{-6} / T^2$$

(Temperature range 273-1200 K)

(5.1.1.4)

$$(v) C_{air} = 0.2372 + 0.2900 \times 10^{-4} T - 1360 / T^2$$

(Temperature range not specified)

(5.1.1.5)

$$(vi) C_w = 0.4567 + 0.8333 \times 10^{-5} T + 0.7444 \times 10^{-7} T^2$$

(Temperature range 300 - 2500 K)

(5.1.1.6)

$$(vii) C_{CH_4} = 0.2138 + 0.6194 \times 10^{-3} T - 0.08 \times 10^{-6} T^2$$

(Temperature range 283-1033 K)

(5.1.1.7)

$$(viii) C_{coke} = -0.1640 + 0.1136 \times 10^{-2} T - 0.49 \times 10^{-6} T^2$$

(Temperature range 294 - 1573 K)

(5.1.1.8)

Methane has been assumed to be a close approximation for estimating the specific heat of volatile matter. The specific heat for coke was estimated from a knowledge of its three mean values given for three different temperature ranges as given by Hougen et.al (1956).

5.1.2 Heat Transfer Coefficients

The correlation proposed by Zuideveld and Vandenberg (1971) for computation of gas-solid heat transfer coefficient in $\text{Kcal}/(\text{hr}) \cdot (\text{m}^2)(\text{K})$ was used in the present work. The equation given below is applicable for the range $30 < \text{Re} < 3,000$:

$$\text{Nu} = 1.9 \text{Re}^{0.50} \text{Pr}^{0.33} \quad (5.1.2.1)$$

where $\text{Nu} = (h_{cgs}) d_p / k_g$

$$\text{Re} = d_p G / \mu_g$$

$$\text{Pr} = C_{pg} / \mu_g \cdot k_g$$

The heat transfer coefficient due to radiation from fuel to stone particles was computed from the well known equation :

$$(h_r)_{fs} = \epsilon \sigma_r (T_f^4 - T_s^4) / (T_f - T_s) \quad (5.1.2.2)$$

where

$$\sigma_r = 4.96 \times 10^{-8} \text{ Kcal} / (\text{m}^2) (\text{hr}) (\text{K}^4)$$

Heat transfer coefficient due to radiation between the combustion gases and solid particles was estimated from the equation used by Zuideveld and Vandenberg (1971). The equation is :

$$(h_r)_{sg} = 4.5 + 1.33 d_p \epsilon_b \quad (5.1.2.3)$$

where d_p is the average size of particle and ϵ_b is the bed porosity.

The heat transfer coefficient due to conduction between the fuel and solid particles has been calculated based on an estimated value of effective thermal conductivity of the fuel and solid particles and centre to centre distance between the contacting particles :

$$(h_c)_{fs} = 2 k_e / (d_{p_s} + d_{p_f}) \quad (5.1.2.4)$$

$$\text{where } 1/k_e = 1/k_s + 1/k_f \quad (5.1.2.5)$$

is used to compute the effective thermal conductivity for fuel-stone particle heat transfer and is based on the concept of resistances in series on account of the close proximity of the fuel and stone contacting particles.

For computation of wall to fluid heat transfer coefficients for packed beds, the following correlations proposed by Leva et. al (1948) and Smith (1970) were used:

For cooling of hot gases in fixed beds:

$$h_{wg} = 3.50 (k_g/D_t)^{0.7} e^{-4.6 d_p/D_t} (d_p G/\mu)^{0.7}$$

$$(5.1.2.6)$$

(valid for $d_p/D_t = 0.08 - 0.27$ and $d_p G/\mu = 250 - 3,000$) (5.1.2.6)

For the heating of cool gases in packed beds :

$$h_{wg} = 0.813 (k_g/D_t) e^{-6 d_p/D_t} (d_p G/\mu)^{0.9}$$

(valid for $d_p/D_t < 0.35$) (5.1.2.7)

The free convection equation proposed by Chapman (1960) used for the estimation of heat transfer coefficient from external wall surface of kiln to still air in appropriately revised units is:

$$h_c = 1.22 (\Delta T/L)^{1/4}, \text{ Kcal/(hr)(m}^2\text{)(K)} \quad (5.1.2.8)$$

where $\Delta T = T_{w_o} - T_{\infty}$, K

L = Height of surface, m

Heat transfer coefficients have been computed at each bed position from the function subprograms as a part of the main executive computer programme.

5.1.3 Heat of Combustion of Volatile Matter

Various correlations have been proposed by investigators for estimation of the calorific value of coal from a knowledge of its

proximate analysis (Lowry, 1945; Majumdar, 1954; and Brame and King, 1955). The heating values of coals of different volatile matter were calculated on dry ash free basis using Gumz's formula (Lowry, 1945) which was found to predict fairly accurate value of heating value for the entire range of coal compositions:

$$H_f = 8,150 + 6,543 V - 17,308 V^2, \text{ Kcal/Kg} \quad (5.1.3.1)$$

where V is the fractional volatile matter content of dry ash-free coal.

The heating value of volatile matter was then computed by subtracting the heating value of fixed carbon from the computed calorific value of the dry ash free coal (Lowe et. al, 1977 and Majumdar, 1954). The heating value of fixed carbon was taken as 8,200 Kcal/Kg of fixed carbon (Brame and King, 1955). The heating value of volatile matter (Kcal/Kg volatile matter) computed by the above mentioned procedure showed variations in these values with fractional volatile matter content of coal. This conclusion was found to be valid for the Indian coals also (Brame and King, 1955).

5.1.4 Interfacial Areas of Solid Particles

For a packed bed of solids the particle surface area per unit bed volume is given by the following equation (Perry and Chilton, 1968) :

$$a = 6(1 - \epsilon_b) / \phi d_p \quad (5.1.4.1)$$

where a is the specific surface or area of particle surface per unit bed volume; ϵ_b is the bed porosity; ϕ is the sphericity of particle, and d_p is the average particle diameter.

Equation (5.1.4.1) may be written as

$$a = a_o(1 - \epsilon_b) \quad (5.1.4.2)$$

where a_o is the particle surface per unit volume of solids and is equal to $6/\phi d_p$.

For granular solids of mixed sizes, as applicable in the case of limestone and fuel particles the average particles diameter may be computed from the equation :

$$1/d_p = \sum x/d_{p,x} \quad (5.1.4.3)$$

where x is the weight fraction of particle diameter, $d_{p,x}$

The surface area a_o of particles in mixed-feed lime kiln computed by equations given above will give total surface area of limestone and fuel particles present in packed bed. Therefore, a_o can be expressed as the sum of limestone and fuel surface areas:

$$a_o = a_{s_o} + a_{f_o} \quad (5.1.4.4)$$

In mixed-feed lime kilns the fuel particle size is kept, in general, nearly one-half of that of limestone particles. Thus, some fuel particles can quite easily be incorporated within the interstitial space created by the limestone particles matrix. Let α be the fraction of fuel particles that occupies independent volume in the mixed bed of limestone and coal particles and, therefore, $(1-\alpha)$ is the fraction which is held up within the limestone particles matrix. The α can have a value between zero and unity and it can be correlated as:

$$\begin{aligned} \alpha &= (n_f/n_s - \beta) / (n_f/n_s) \\ &= 1 - \beta(n_s / n_f) \end{aligned} \quad (5.1.4.5)$$

where n_f and n_s are the number of fuel and stone particles, respectively, and β is a constant that takes into account the number of fuel particles held within the limestone particles matrix.

The ratio n_f/n_s can be quite easily calculated from the following relationship:

$$\begin{aligned} n_f/n_s &= \left[V_{f_o} / (\pi/6) d_{p_f}^3 \right] / \left[V_{s_o} / (\pi/6) d_{p_s}^3 \right] \\ &= V_{f_o} d_{p_s}^3 / V_{s_o} d_{p_f}^3 \end{aligned} \quad (5.1.4.6)$$

The subscript 'o' indicates conditions at the top of the kiln, that is, at the inlet of kiln. It is quite clear that

$$\begin{aligned} V_{f_o} / V_{s_o} &= \dot{m}_{f_o} \ell_{s_o} / \dot{m}_{s_o} \ell_{f_o} \\ &= \ell_{s_o} / X_r \ell_{f_o} \end{aligned}$$

Thus

$$n_f/n_s = (1/X_r) (\ell_{s_o} / \ell_{f_o}) (d_{p_s} / d_{p_f})^3 \quad (5.1.4.7)$$

Substituting for (n_f/n_s) in equation (5.1.4.7), α becomes:

$$\alpha = 1 - \beta X_r (\ell_{f_o} / \ell_{s_o}) (d_{p_f} / d_{p_s})^3 \quad (5.1.4.8)$$

If we assume that limestone particles form a cubic matrix and one fuel particle is at the body centre of this cube, then each limestone particle of a unit cell will hold one fuel particle. Therefore, β will become equal to unity and this value of β has been used in the computation. But the value of β other than unity can also be used, if considered desirable.

Using the definition of α as discussed above, the effective surface areas per unit volume of the bed can be expressed as:

$$a_{s_0} = 6 V_s / \phi_s d_p (V_s + \alpha V_f) \quad (5.1.4.9)$$

$$a_{f_0} = 6 V_f / \phi_f d_p (V_s + \alpha V_f) \quad (5.1.4.10)$$

where V_s and V_f are the individual volumes of limestone and fuel particles.

Thus the surface area of limestone and fuel particles per unit volume of kiln bed can be given as:

$$a_s = 6 (1 - \epsilon_b) / \phi_s d_p (1 + \alpha V_f / V_s) \quad (5.1.4.11)$$

$$a_f = 6 (1 - \epsilon_b) (V_f / V_s) / \phi_f d_p (1 + \alpha V_f / V_s) \quad (5.1.4.12)$$

Computations of specific surface areas for limestone and fuel particles are carried out using the above equations in the main executive computer programme for the kiln zone in which the reduction in volume of fuel particles due to burning of fixed carbon does not occur. The variations on account of changing particle size of fuel due to fixed carbon combustion and density changes after ash fusion are also taken into account in the programme for the burning zone. The phenomenological reasoning behind the development of modified equations for surface area computations during fixed carbon burning of fuel without and with ash fusion is discussed below.

For the case of fixed carbon combustion, size of the fuel particles keeps on decreasing. The fuel particles held up within the unit cells of limestone particles on size reduction will not affect the total bed volume, but may result only in increase in the bed porosity. But the volume of fuel particles present outside the unit cell of limestone particles will be reduced on size reduction. This, in effect, will lead to an increase in the surface area of limestone per unit bed volume since the ratio of limestone particles to total bed volume will increase. In the present case, the limestone particles volume is not assumed to change in the kiln, the decrease in the independent volume of fuel particles relative to limestone volume can be expressed for $x_f \geq (x_{fm} + x_{fv})$ as :

$$\text{Independent volume of fuel particles} / \text{Volume of limestone particles} = \propto V_f (1 - x_{fa} - x_f) / V_s (1 - x_{fa} - x_{fm} - x_{fv})$$

(5.1.4.13)

and increasing limestone surface area per unit bed volume a'_s in this zone, assuming constant bed porosity, will become :

$$a'_s = a_s (1 + \propto V_f / V_s) / \left\{ 1 + \propto V_f (1 - x_{fa} - x_f) / V_s (1 - x_{fa} - x_{fm} - x_{fv}) \right\} \quad (5.1.4.14)$$

The numerical value of the terms in bracket for $x_f \geq (x_{fm} + x_{fv})$ is greater than unity and increases with increase in x_f after the evolution of moisture and volatile matter. The value of limestone surface area per unit bed volume before the commencement of fixed carbon combustion, a_s , has already been defined earlier by equation (5.1.4.11).

The fuel surface area will, however, decrease due to combustion of fixed carbon and consequent reduction in particle size. Since the surface area is proportional to square of diameter and volume is proportional to cube of diameter of fuel particles, the reduction in surface area due to fixed carbon burning for $x_f \geq (x_{fm} + x_{fv})$ can be expressed as:

Change in surface area per unit volume change

$$= (V_f/V_s) \left[\frac{(1 - x_{fa} - x_f)}{(1 - x_{fa} - x_{fm} - x_{fv})} \right]^{2/3} \quad (5.1.4.15)$$

and changing fuel surface area per unit bed volume a'_f in this zone, assuming constant bed porosity, will become:

$$a'_f = a_f \left(\frac{1 - x_{fa} - x_f}{1 - x_{fa} - x_{fm} - x_{fv}} \right)^{2/3} \left\{ \frac{1 + \alpha \frac{V_f}{V_s}}{1 + \alpha \frac{V_f}{V_s} \left(\frac{1 - x_{fa} - x_f}{1 - x_{fa} - x_{fm} - x_{fv}} \right)} \right\} \quad (5.1.4.16)$$

The value of fuel surface area per unit bed volume before the commencement of fixed carbon combustion, a_f , has already been defined earlier by equation (5.1.4.12).

In the derivation of the above equations it is assumed that ash formed on burning of fixed carbon is not retained by the fuel particle and is held inside the interstitial space of limestone particle matrix without requiring independent bed volume. The presence of ash in interstitial space will reduce the porosity of bed. The assumption of constant bed porosity is, therefore, reasonable because decrease in porosity due to presence of ash is compensated by the reduction in the volume of fuel particles held up within the interstitial space of limestone particles.

At the point of ash fusion corresponding to an assumed temperature (T_{ff}) of 1573 K, the conditions are :

$$x_f = x_{ff}$$

$$r_f = r_{ff}$$

If the temperature of fuel particles exceed T_{ff} , ash formed due to

combustion of fixed carbon will not be released and it forms a porous layer around the unburnt core.

During ash fusion (for $x_{ff} \leq x_f \leq 1 - x_{fa}$) the ash layer around unburnt core of the fuel particles will tend to fuse more and more with increase in fuel temperature. The increase in ash layer density due to progressive fusion is related to fuel temperature according to the relation:

$$e_f = e_{ff} (T_f/T_{ff})^a \quad (5.1.4.17)$$

where a is a constant to account for the extent of density variation of ash with fuel temperature. The constituents of fuel during ash fusion are: core having unburnt fixed carbon with associated ash and outer shell of fused ash.

The independent volume of fuel particles relative to limestone volume, assumed constant, for $x_f \geq x_{ff}$ can be expressed as:

Independent volume of fuel particles / Volume of limestone particles =

$$\propto \frac{V_f}{V_s} \left[\left(\frac{1 - x_{fa} - x_f}{1 - x_{fa} - x_{fv} - x_{fv}} \right) + \frac{(x_f - x_{ff}) x_{fa} (T_f/T_{fa})^a}{(1 - x_{fa} - x_{fv} - x_{fv})} \right] \quad (5.1.4.18)$$

The first term within parenthesis inside large bracket of the above equation indicates the normal reduction in fuel core on account of fixed carbon combustion and the second term inside large bracket takes into account the additional volume of fused ash sticking on to the outer surface of the burning fuel particle after properly accounting for the density variation of the outer shell of fused ash. Therefore, increase in limestone surface area per unit bed volume after commencement of ash fusion, a_s'' , assuming constant bed porosity, will become:

$$a_s'' = a_s \left\{ \frac{1 + \alpha \frac{V_f}{V_s}}{1 + \alpha \frac{V_f}{V_s} \left[\left(\frac{1 - x_{fa} - x_f}{1 - x_{fa} - x_{fm} - x_{fu}} \right) + \frac{(x_f - x_{ff}) x_{fa}}{(1 - x_{fa} - x_{fu} - x_{fa})} \left(\frac{T_{ff}}{T_f} \right)^a \frac{\rho_f}{\rho_{ff}} \right]} \right\} \quad (5.1.4.19)$$

The reduction in surface area of fuel particles on account of reduction in volume due to fixed carbon burning and ash fusion for $x_f > x_{ff}$ has now to be accounted for. Since the surface area is proportioned to square of diameter and volume is proportional to cube of diameter, the reduction in surface area of fuel unit volume change is given by:

$$= \frac{V_f}{V_s} \left\{ \frac{1 - x_{fa} - x_{ff}}{(1 - x_{fa} - x_{fm} - x_{fu})} \right\}^{2/3} \left[\left(\frac{1 - x_{fa} - x_f}{1 - x_{fa} - x_{ff}} \right) + \frac{(x_f - x_{ff}) x_{fa}}{1 - x_{fa} - x_{ff}} \left(\frac{T_{ff}}{T_f} \right)^a \frac{\rho_f}{\rho_{ff}} \right]^{2/3} \quad (5.1.4.20)$$

and change in fuel surface area per unit bed volume with commencement of ash fusion, a_f'' , assuming constant bed porosity, will become:

$$a_f'' = a_f \left\{ \frac{\left(1 + \alpha \frac{V_f}{V_s}\right) \left(\frac{1 - x_{fa} - x_{ff}}{1 - x_a - x_m - x_{fv}}\right)^{3/2} \left[\left(\frac{1 - x_a - x_f}{1 - x_a - x_{ff}}\right) + \frac{(x_f - x_{ff}) x_{fa}}{1 - x_a - x_{ff}} \left(\frac{T_{ff}}{T_f}\right)^a \frac{e}{e_{ash}} \right]}{1 + \alpha \frac{V_f}{V_s} \left[\left(\frac{1 - x_{fa} - x_f}{1 - x_{fa} - x_m - x_{fv}}\right) + \frac{(x_f - x_{ff}) x_{fa}}{(1 - x_m - x_{fv} - x_{fa})} \left(\frac{T_{ff}}{T_f}\right)^a \left(\frac{e_s}{e_{ash}}\right) \right]} \right\} \quad (5.1.4.21)$$

5.2 HEAT LOSS THROUGH KILN WALL

The kiln wall consists of ordinary bricks masonry lined inside with firebricks.

Let R_i = inner radius of kiln, m

W_{fb} = fire bricks lining thickness, m

The kiln radius upto the level of fire bricks is:

$$R_{fb} = R_i + W_{fb}, \text{ m}$$

R_o = outer radius of kiln, m

$$= R_{fb} + W_{rb}$$

T_{gi} = bulk gas temperature, K

T_{wi} = average inner wall temperature, K

T_{wo} = outer wall temperature, K

T_{fb} = temperature at the interface of firebricks and clay bricks, K

Over a differential element of width ΔZ in the axial direction of kiln, heat is assumed to be transferred from the bulk gas to the inner wall of kiln by convective and radiative exchanges:

$$Q_{gw} = 2\pi R_i \Delta Z (h_c + h_r)_{gw} (T_{gi} - T_{wi}) \quad (5.2.1)$$

Heat conducted through firebricks insulation is given by the equation (Chapman, 1960):

$$Q_{fb} = \frac{2\pi \Delta Z k_{fb} (T_{wi} - T_{fb})}{\ln(R_{fb}/R_i)} \quad (5.2.2)$$

Similarly, heat conducted through burnt clay (red) bricks is:

$$Q_{rb} = 2\pi \Delta Z k_{rb} (T_{fb} - T_{wo}) / \ln(R_o/R_{fb}) \quad (5.2.3)$$

Heat is lost from the external kiln wall to ambient largely by natural convection:

$$Q_{wa} = (h_c)_{wa} 2\pi R_o \Delta Z (T_{wo} - T_{\infty}) \quad (5.2.4)$$

where T represents the ambient air temperature.

Under steady state conditions, all heat transfer rates involving transfer steps in series must be equal:

$$Q_{gw} = Q_{fb} = Q_{rb} = Q_{wa} = \Delta H_1 \quad (5.2.5)$$

Defining overall (effective) heat transfer coefficient, $(U_i)_{\text{eff}}$ on the basis of inner wall area of kiln, the heat exchange from the bulk gas phase to the ambient air may be represented as :

$$\Delta H_1 = (U_i)_{\text{eff}} \cdot 2\pi R_i \Delta Z (T_{gi} - T_{\infty}) \quad (5.2.6)$$

The combination of equation (5.2.1) through (5.2.6) leads to

$$(U_i)_{\text{eff}} = R_i^{-1} \left\{ \frac{1}{R_i} (h_c)_{gw} + \frac{\ln(R_{fb}/R_i)}{k_{fb}} + \frac{\ln(R_o/R_{fb})}{k_{rb}} + \frac{1}{r_o} (h_c + h_r)_{wa} \right\}^{-1} \quad (5.2.7)$$

The main executive programmes first estimate the overall heat transfer coefficient using equation (5.2.7) through function subprograms for the individual heat transfer coefficients and then compute wall heat losses from equation (5.2.6) for all the three zones of the lime kiln.

5.3 SALIENT FEATURES OF COMPUTER PROGRAMMES

The sets of differential equations derived for the analysis of the preheating and burning zones are highly non-linear in nature, particularly those used to predict the behaviour of the burning zone. These equations were solved by using appropriate numerical techniques.

The system equations of the preheating, burning and cooling zones are written in the forward finite difference form and they are solved over the differential element along the axis of the kiln for the $(i + 1)$ th grid point knowing the set of values of the i th grid point. The solutions are converged within the prespecified tolerance limits. This methodology of computations is continued starting with the input parameters for a given zone until final conditions defining the end of that zone are attained. In this manner dependent variables of temperature and fractional conversion are computed for these zones. The problem of convergence is quite troublesome for the burning zone in view of many complexities and highly non-linear behaviour. Enormous difficulties were encountered in the estimation of system parameters for obtaining a unique and realistic solution. Many strategies of ordering of system equations were tried to achieve rapid convergence within the acceptable limits of accuracy. The choice of appropriate equations for estimating heat and mass transport and reaction rate coefficients was limited in view of the lack of published information appropriate to this system.

The computer programmes were written in FORTRAN IV. Salient features for the same are discussed as follows:

5.3.1 The Preheating Zone

Fig. 5.1 represents the information flow diagram for the analysis of the preheating zone. Programme for the same is given in the Appendix-C. It analyses the cases of simple preheating, preheating with desorption of water from coal particles, and preheating with devolatilization without combustion of the volatile matter. For a given set of input conditions at top of the lime kiln and relevant data, the cross-sectional area and inner diameter of the kiln are computed for a nominal lime production rate prespecified as 10 tonnes per day and the chosen value of the design variable - superficial lime output rate based on cross-sectional area of kiln (tonnes) / (sqm) (day). The flow rates of limestone and coal particles at top of kiln and required air flow rates (induced at the bottom of the kiln) are computed. Provision has been made for computation of the heating value of coal and heat of combustion of volatile matter (though not required for the analysis of the preheating zone).

The specific heats of various components as functions of temperature and the interfacial packing surfaces for limestone (ASPZ) and coal particles (AFPZ) are computed. The energy and material

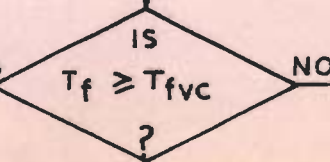
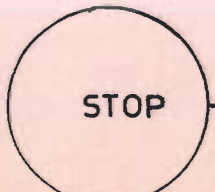
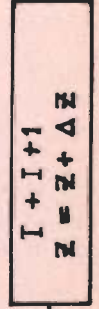
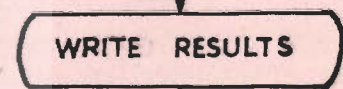
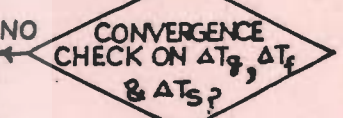
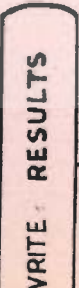
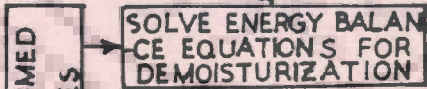
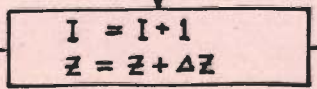
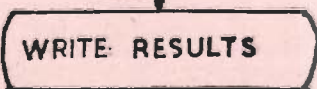
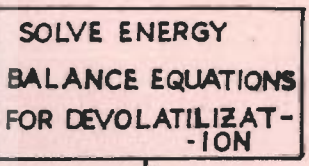
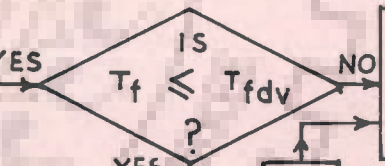
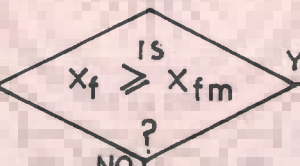
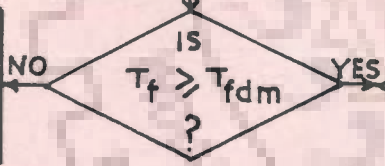
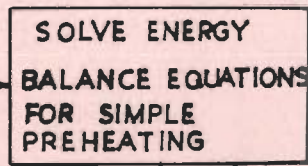
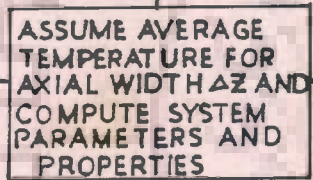
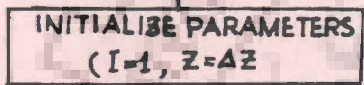
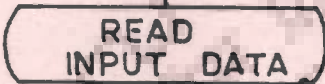
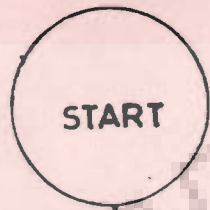


FIG. 5-1 - INFORMATION FLOW DIAGRAM FOR ANALYSIS OF THE PREHEATING ZONE

balances are then computed for conditions prevailing in a differential zone of the preheating section. Function subprograms are given at the end of the main executive programme for computation of the heat transfer coefficients from fuel to stone (HFS), fuel to bulk gas (HFG), stone to bulk gas (HSG), bulk gas to kiln wall (HGW), and external wall surface to ambient air (HWA) at any axial position (Z) measured from top of the kiln.

The system equations are linearized, put in difference form and for assumed average temperatures of limestone (TSAVG), fuel (TFAVG) and bulk gas phase (TGAVG), the new values of the same are computed for stone, fuel and gas from the respective heat balances. The fractional degrees of demolsturization and devolatillization are computed by making use of the assumptions already discussed in Chapter-4.

The new computed values are compared with the old values (assumed or previously computed) and if the desired tolerance levels on the three temperatures are not achieved, the computations are repeated by using the new computed values of temperatures as revised initial values for the next iteration. This iterative procedure is continued till convergence for a differential width ΔZ is obtained.

The computation then moves to the next axial location and the procedure is continued till the end of the preheating zone. The end of the preheating zone is defined when the fuel achieves the

prespecified autoignition temperature at which instantaneous combustion of the volatile matter is assumed to occur. In this region gas temperatures are always higher than those of limestone and fuel particles and heat transfer takes place from gas to solids. The three temperatures, therefore, increase as we move from kiln inlet to the end of the preheating zone.

5.2.3 The Burning Zone

The analysis of this zone was observed to be highly complex due to combustion reactions of volatile matter and fixed carbon and calcination of limestone, and also due to changes in surface areas of limestone-lime and fuel particles per unit bed volume as well as due to radial temperature gradients in limestone lime particles.

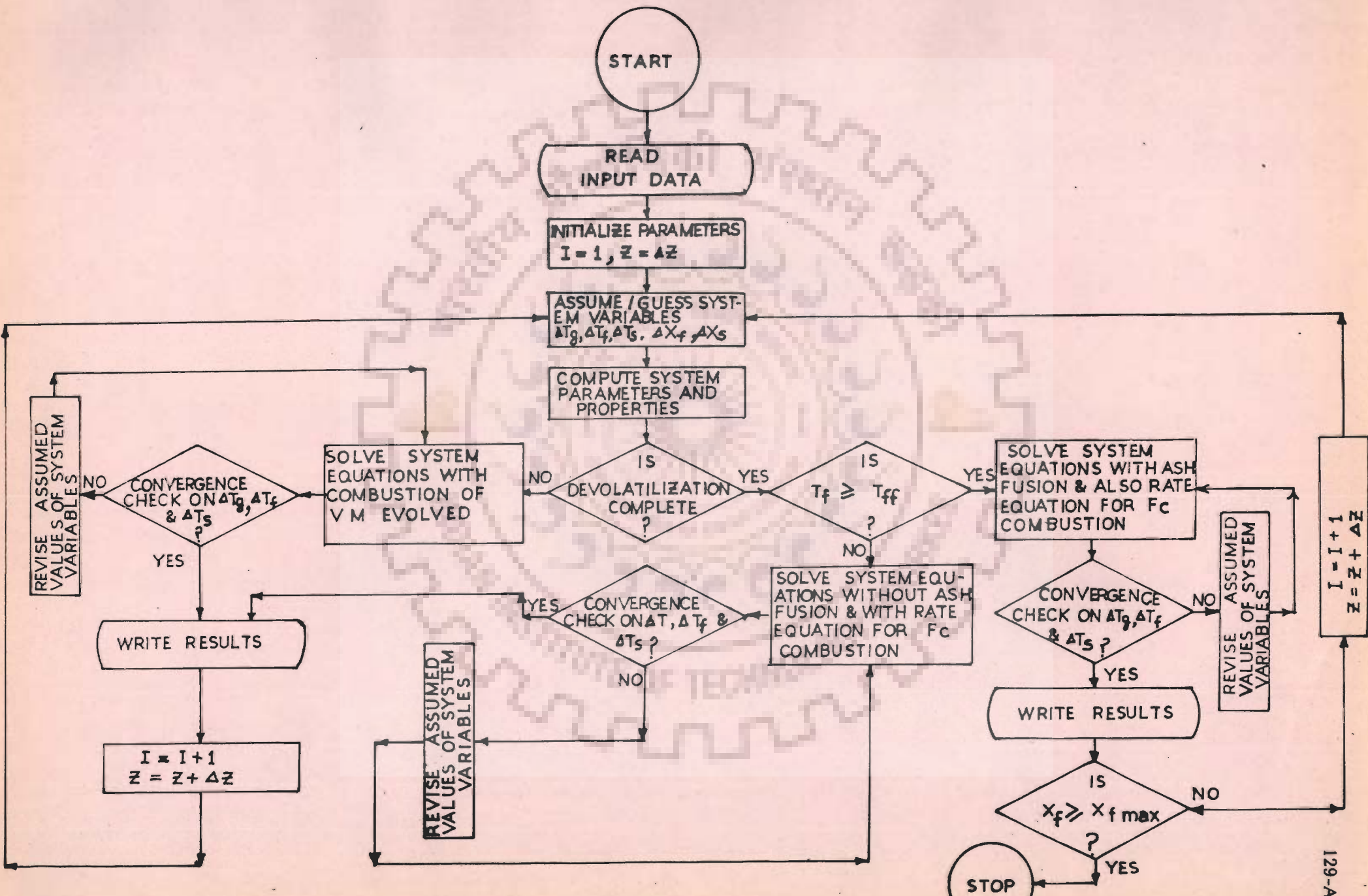
The auto-ignition of volatile matter at the surface of fuel particles raises their temperature quickly above that of gas and limestone-lime particles. Heat is then transferred from fuel to gas and also to limestone-lime particles. Since the surface temperatures of limestone-lime particles is expected to keep on rising in most of the burning zone to meet the heat conduction requirements for calcination, heat transfer will also occur from these particles to gas. Thus gas temperatures will be expected to fall very rapidly in the burning zone. In the burning zone combustion of fixed carbon is assumed to occur only after all the volatile matter is evolved as

discussed in Chapter-4.

The results of computations indicated the existence of the following subzones of the burning zone :

- (i) Buffer Zone : incorporating volatile matter combustion, but only preheating of limestone upto the calcination temperature. No intraparticle temperature gradients are assumed to exist in limestone particles.
- (ii) Calcination Zone : incorporating combustion of residual volatile matter, if any, and fixed carbon alongwith calcination of limestone. Limestone core is at dissociation temperature and temperature gradients exist in the outer shell of lime.
- (iii) Finising Zone : incorporating combustion of the remaining part of the fixed carbon content of coal, if any, after complete calcination. No intraparticle temperature gradients are assumed to exist in lime particles.

An information flow diagram for analysis of the burning zone is given in Fig. 5.2 and the computer programme for the same is given in Appendix-D. The values of the system variables and properties alongwith the relevant output data obtained from the computed results



of the preheating zone are fed as input data to the main executive programme for burning zone. The heat of combustion of the volatile matter is computed from the knowledge of the proximate analysis of coal using equation (5.1.3.1).

The heat transfer coefficients, the effectiveness factors for heat exchange among the phases, variations in interfacial areas, specific heats of components at different temperatures, the material balances to compute flow rates, compositions, etc. are then estimated by the computations in this zone.

The model equations for dissociation of limestone, combustion of coal particles, and heat balances for the stone, fuel and gas phases are utilized in the programme to compute the temperature changes of limestone-lime particles, fuel particles and gas alongwith degree of calcination of limestone and combustion of coal over a differential volume element of width ΔZ at a location (Z) along the axis of the kiln from a knowledge of the initial guessed values of the five system dependent variables, that is, T_s , T_f , T_g , x_s and x_f . Initial guess value for each of the dependent parameter is obtained from second order polynomial utilizing the converged values for three previous Z steps as soon as they become available to reduce computation time by achieving faster convergence.

Attempts have been made to solve the highly non-linear system

equations within the stipulated ranges of tolerance levels. During the computations it was observed that one hundred iterations were, in general, sufficient for achieving convergence. For a prespecified ΔZ value, in some cases computed values showed either oscillations or divergence. Therefore, if the desired convergence was not achieved in the maximum specified iterations, the provision was made in the programme to reduce the step size ΔZ by one-tenth of the prespecified ΔZ value and continue the reduction in the ΔZ value till desired convergence was achieved within one hundred iterations. This value of ΔZ was used in subsequent computations for a given set till further reduction in step size was found necessary due to non-attainment of convergence in one hundred iterations.

The burning zone programme solves all the three subzones, that is, upto the point of complete combustion of the fixed carbon in fuel particles. Ash fusion temperature of 1573 K has been assumed, this can be varied if desired, beyond which the fusion and non-removal of ash from fuel particles was assumed not to hinder the fixed carbon combustion process in view of very small size of fuel particles at this stage.

It may be noted that the average lime particle temperature is computed at the beginning of the finishing zone by sensible heat balance of lime particle. Similarly, average solid mass, consisting

of limestone-lime particles, free ash and cinders/ash clinkers, temperature is computed at the end of the finishing zone by appropriate sensible heat balance.

Function subprograms are given at the end of the main executive programme for computation of various interphase heat transfer coefficients, fuel to gas, lime-limestone particles to gas, fuel to lime-limestone particles, kiln wall to ambient air, and for overall rate constant for combustion of fixed carbon content of coal due to combined effect of surface combustion reaction rate constant and mass transfer resistance for oxygen transport for combustion of fixed carbon to carbon-dioxide.

5.3.3 The Cooling Zone

An information flow diagram for the analysis of the cooling zone is given in Fig. 5.3. The computer programme for the analysis of the same is given in the Appendix-E. It is basically analogous to that of the simple preheating zone with signs reversed as the heat is transferred from the solid mass consisting of stone particles (quick lime lumps) free ash and cinders/ash clinkers to the bulk of the gas phase. The system properties and relevant output data from the burning zone is taken as input data in this programme and the desired computations are done to obtain the temperature profile for the gas

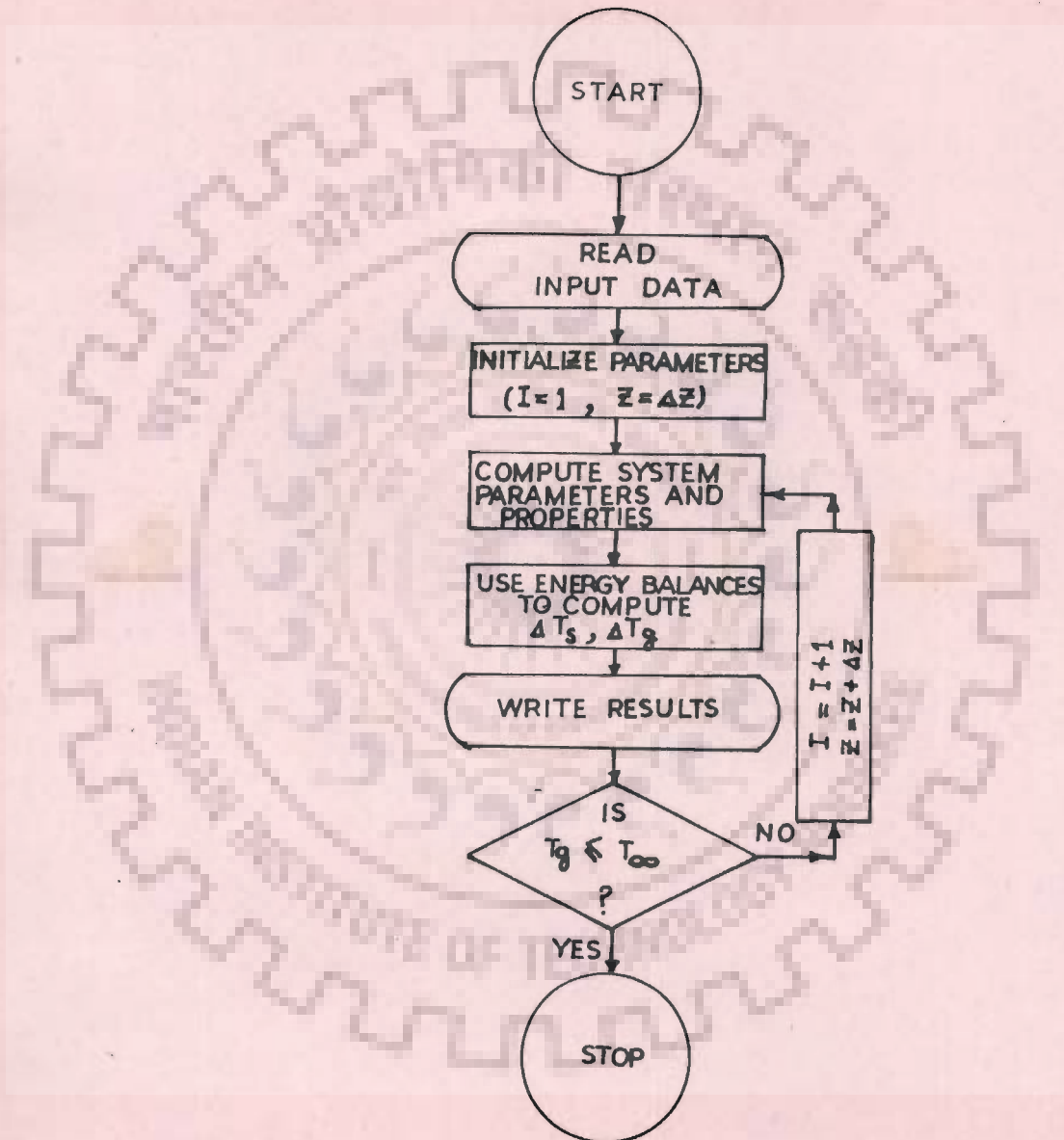
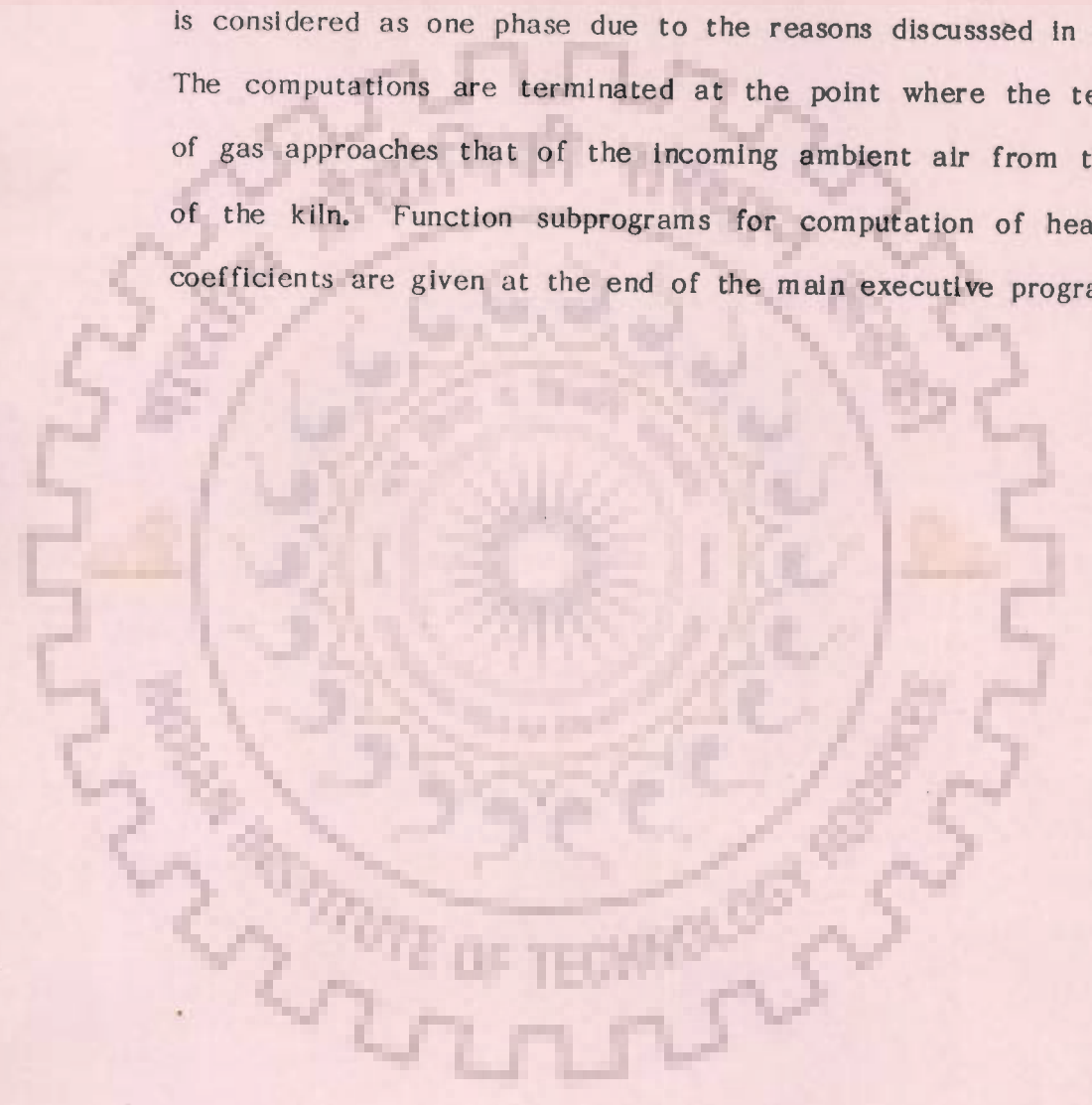
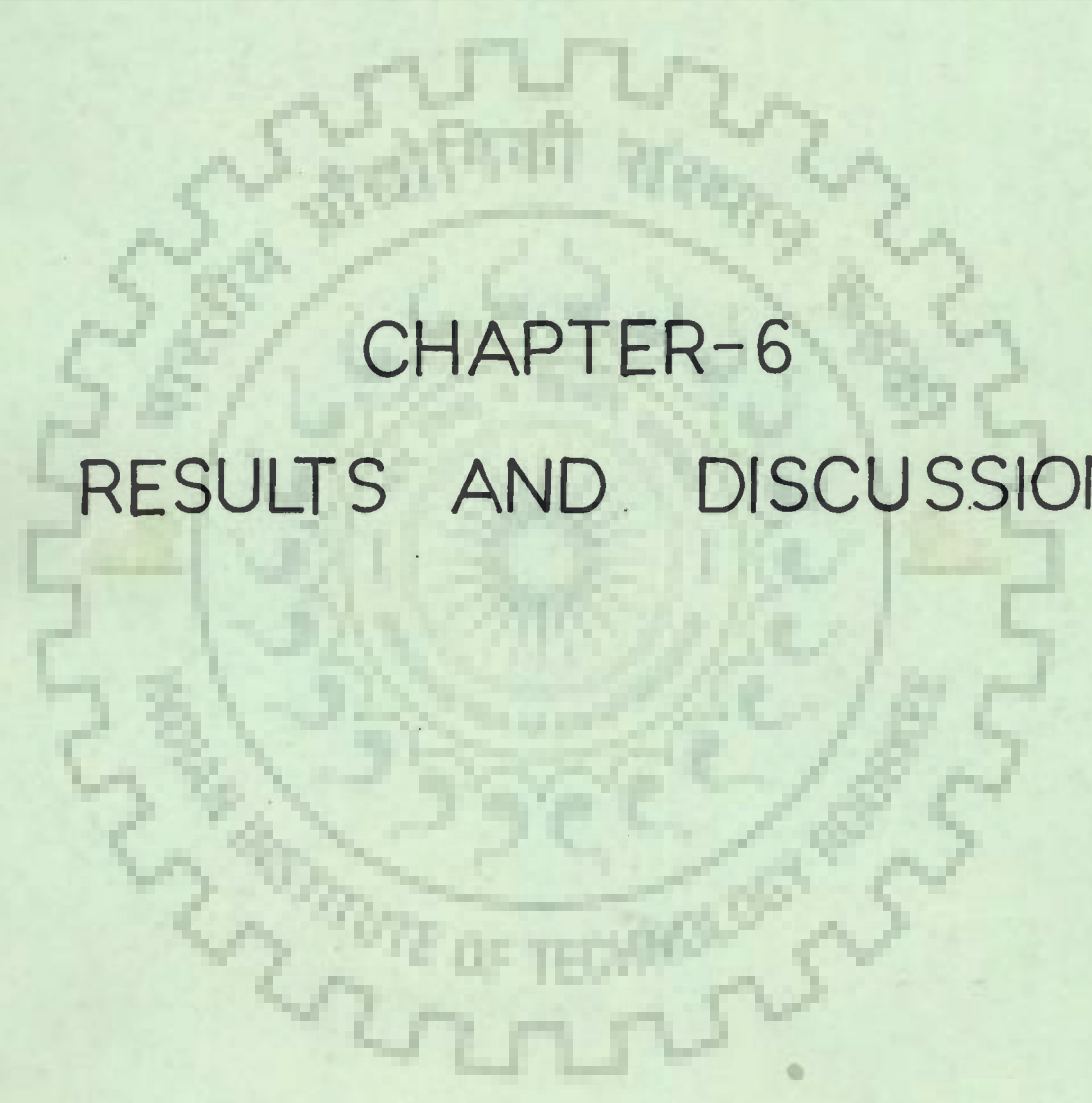


FIG. 5-3 - INFORMATION FLOW DIAGRAM FOR ANALYSIS OF COOLING ZONE

phase and solid particles from the gas and solid energy balances. In these computations it may be noted that the entire solid mass is considered as one phase due to the reasons discussed in Chapter-4. The computations are terminated at the point where the temperature of gas approaches that of the incoming ambient air from the bottom of the kiln. Function subprograms for computation of heat transfer coefficients are given at the end of the main executive programme.





CHAPTER-6
RESULTS AND DISCUSSION

Chapter-6

RESULTS AND DISCUSSION

6.1 CHOICE OF PARAMETERS FOR SIMULATION STUDIES

The values of important design, operation and system parameters were carefully chosen keeping in view the general industrial practice and published literature. Some design and operating parameters were varied within the ranges commonly encountered for mixed-feed lime shaft kilns. Some system parameters had to be varied in different kiln zones to obtain acceptable results. This section briefly discusses these parameters.

The values of important parameters corresponding to average design and operating conditions and their ranges investigated are given in Table-6.1.

Lime shaft kilns with a nominal lime production rate of 10 tonnes/day are generally considered optimum for natural draft operation and are abundantly used in building lime industry in India. The Central Building Research Institute, Roorkee, and the Khadi and Village Industries Commission, Bombay have also advocated the use of lime shaft kilns with a lime production rate of 10 tonnes/day for natural draft operation in the small scale sector.

TABLE-6.1

Important Design & Operating Conditions : Average Values & Ranges

<u>Sl.No.</u>			<u>Investigated</u>		
	<u>Parameter</u>	<u>Symbol</u>	<u>Units</u>	<u>Average Value</u>	<u>Range</u>
<u>Design</u>					
1.	Nominal lime production rate	P_n	t/day	10	Not varied
2.	Superficial lime output rate	P_s	$t/(m^2)(day)$	2.25	2.0 - 2.5
3.	Inner lining thickness of fire bricks	W_{fb}	m	0.23	Fixed
4.	Wall thickness of burnt clay (red) bricks	W_{rb}	m	0.69	0.46 - 0.92
5.	Kiln exhaust gas temperature	T_{g_o}	K	748	698 - 798
<u>Operating</u>					
6.	Limestone-to-fuel ratio by weight in feed input	X_r	t/t	5.5	5.0 - 6.0
7.	Particle size of limestone	d_{p_s}	m	0.100	0.088 - 0.112
8.	Particle size of fuel	d_{p_f}	m	0.050	0.044 - 0.056
9.	Fractional content of volatile matter in fuel	X_{fv}	-	0.225	0.150 - 0.300
10.	Excess air fraction	X_{ea}	-	0.125	0.000 - 0.250

The average values (base conditions) and the ranges of parameter values specified for different design and operating parameters are also based on the field studies of Indian building lime industry. In order to have a general purpose simulation programme all design and operating conditions are to be specified as input data.

It is important to note that the kiln exhaust temperature (T_{g_o}) has been given the status of a design variable while the effective kiln height L_e is not included as a design variable in Table-6.1. For any new design situation L_e needs to be computed and it depends greatly on T_{g_o} in addition to other operating and design parameters. However, for an existing kiln, L_e will have to be specified as a design parameter and the value of T_{g_o} will have to be assumed for starting the computations from the top of the kiln for computing L_e . If the computed value of L_e does not agree with the design value, then iteration over T_{g_o} needs to be carried out by treating it as a recycle variable till the convergence on L_e is achieved. If no value of T_{g_o} is able to give convergence on L_e , some other operating parameter may have to be suitably modified for achieving convergence.

The values of the important system parameters used in the simulation are given in Table-6.2. The values of these parameters

TABLE-6.2

Values of Major System Parameters

<u>Sl. No.</u>	<u>Parameter</u>	<u>Symbol</u>	<u>Units</u>	<u>Value</u>	<u>Remarks</u>
1	2	3	4	5	6
1.	Ambient air/ room temperature	T_a	K	300	
2.	Temperature for start of demoi- sturation from fuel	T_{dm}	K	373-383	Total moisture release is assumed uniform in 8 intervals of ΔZ of 0.05 m each corresponding to an approximate residence time of 1.4 hours.
3.	Temperature for initiation of devola- tilization of fuel	T_{dvm}	K	673	Release of volatile matter in the temperature range of 673 to 1173 K is assumed to be linear with respect to increase in fuel temperature
4.	Auto-ignition tempra- ture of volatile matter	T_{vmc}	K	948	Volatile matter remaining at 948 K is assumed to release uniformly in 10 intervals of ΔZ of 0.05 m each corresponding to an approximate residence time of 1.8 hours
5.	Ash fusion temperature of fuel	T_{ff}	K	1,573	-
6.	Moisture fraction in fuel	X_{fm}	Kg/Kg	0.05	-
7.	Ash content in fuel	X_{fa}	Kg/Kg	0.25	-

1	2	3	4	5	6
8.	Heat of demoi- strization	H_{dm}	Kcal/Kg	875	-
9.	Heat of devolati- lization	H_{dv}	Kcal/Kg	650	-
10.	Heat of combustion of volatile matter	H_{vm}	Kcal/Kg	9,024	Computed from equation (5.1.3.1) for average fuel proximate analysis
11.	Heat of combustion of volatile matter	H_{fc}	Kcal/Kg	8,200	-
12.	Chemical formula for volatile matter	$C_n H_{2n+2}$	-	$n = 1.29$	Molecular weight is taken as 20 based on apprxi- mate composition of the volatile matter obtained during coal carbonization
13.	Effectiveness factors for heat exchange from:				The values and their variations are discussed in the text
(a)	Stone-to-gas	η_{sg}	-	0.0125-0.0250	
(b)	Fuel-to-stone	η_{fs}	-	0.150-0.200	
(c)	Fuel-to-gas	η_{fg}	-	0.0150-0.0500	
(d)	Gas-to-kiln wall	η_{gw}	-	0.100 (fixed)	

have been kept the same for all the sets of design and operating conditions. However, the nature of the simulation programme remains of general purpose only, since all these system parameters are to be basically read as input data.

A brief justification is given below for some of the system parameter values given in Table-6.2. In standard procedure for proximate analysis of fuel (Brame and King, 1955), finely ground powdered coal sample is kept at 373 to 383 K for about one hour to determine moisture content. In the present study as the size of coal particles is substantial and varies from 44 to 56 mm, time requirement for complete demosturization will be much greater and, therefore, the passage of fuel through 0.4 m kiln length corresponding to a mean residence time of about 1.4 hours has been assumed.

The volatile matter is usually released in the temperature range of 400 to 900°C (Fuchs and Sandhoff; Himus, 1958, and Lowry, 1945) and it is assumed to be evolved linearly with temperature in this range. However, this linear behaviour of volatile matter evolution with the temperature continues till the fuel achieves autoignition temperature for the volatile matter. The standard procedure for volatile matter determination requires keeping the finely ground powdered fuel in a muffle furnace at 1173 ± 15 K for seven minutes. For fuel particles size range used in this investigation, time requirement for the evolution of the residual volatile matter after

the commencement of its combustion will be much greater, and, therefore, a mean residence time of about 1.8 hours is provided.

The auto-ignition temperatures in air for the important constituents in the volatile matter evolved from coal are generally in the range of 537 to 750°C (Brame and King, 1955; Himus, 1958; Lees, 1980; and Shaw 1974). Presence of inerts enhances the ignition temperature and it can also suppress the combustion. For the purpose of estimation of system properties, methane (molecular weight 16) may be taken as a close approximation of the volatile matter (assumed molecular weight 20). Reported values for the ignition temperature of methane are from 556 to 700°C in the oxygen environment and from 650-750°C in the ambient air (Brame and King, 1955). The oxygen content in the kiln gas at a position where combustion of the volatile matter is likely to occur will be much lower due to the combustion of the fixed carbon and a part of the volatile matter in the burning zone. Furthermore, the carbon dioxide content will be much higher due to the calcination of limestone, combustion of fixed carbon and a part of the volatile matter. This will also reduce the partial pressure of oxygen in the kiln gas and will increase the spontaneous ignition temperature for the volatile matter. Accordingly, the assumed value of 948 K (675°C) for the spontaneous auto-ignition temperature is quite reasonable. However, this value can also be varied, if considered desirable.

The ash fusion temperature is reported usually in the range of 1493 to 1613 K for different types of ashes produced as a result of combustion of coal (Brame and King, 1955; Himus, 1958; and Lowry, 1945). Basically ash fusion temperature depends upon the ash composition. Ash fusion temperature T_{ff} is assumed as 1573 K in the present work. The same can be varied, if considered desirable, depending upon the actual nature of ash.

The endothermic heat of demosturization from the fuel particles has been estimated as the sum of the normal values of latent heat and heat of desorption of water vapour. The volatile matter is evolved due to thermal decomposition of coal and requires the endothermic heat for the breakage of relevant bonds. Since no published information could be found regarding the endothermic heat of devolatilization, the same was estimated from a knowledge of the heats of thermal decomposition for heavy petroleum residues (Nelson, 1958). The values used are given in Table-6.2 and some other values can be substituted if more precise information about them is available.

Heat of combustion of fixed carbon (H_{fc}) is chosen as 8200 Kcal/Kg as per the Gautal's formula for estimation of heating value of fuel from the knowledge of its proximate analysis (Brame and King, 1955).

The inclusion of effectiveness factors for interphase heat or mass transfer accounts for the fact that the entire solid surface is not active for the interphase exchanges in packed beds (Perry and Chilton, 1968; Smith, 1970). For a mixed feed lime shaft kiln, pronounced decrease in heat exchange rates can be expected due to dead spaces for flow at the places of contact between particles of mixed sizes. Since exact estimates were not available, different values for effectiveness factors were tried so as to achieve realistic temperature and conversion profiles and to obtain proper calcination at a reasonable superficial lime output rate with a kiln of proper height. The following values of effectiveness factors for various interphase heat exchanges are used in different zones for all sets of design and operating conditions:

	Pre-heating zone	Bur ning zone from to	Cooling zone
Stone to gas, η_{sg}	0.0250	0.0250 - 0.0125	0.0125
Fuel to gas, η_{fg}	0.050	0.050 - 0.015	-
Fuel to stone, η_{fs}	0.200	0.200 - 0.150	-
Gas to kiln wall, η_{gw}	0.100	0.100	0.100

The values of effectiveness factors are not allowed to change in the preheating and cooling zones because no changes occur in packed

bed conditions for these zones. However, the values of effectiveness factors are assumed to decrease linearly with increase in fixed carbon combustion as particles of lime-limestone and fuel move down in the burning zone because the packed bed characteristics change significantly due to the release of ash and reduction in fuel particles size. For obvious reasons the values of effectiveness factors at the beginning and end of the burning zone are identical to those used in preheating zone and cooling zone, respectively.

The ash released on account of burning of the fixed carbon spreads on the stone particles. Reduction in the fuel volume may lead to some increase in the bed porosity. But ash may also cause plugging of the bed at some places which will result in gas channeling and poor gas solid contact. The tendency towards plugging will increase with increase in ash quantity and, therefore, η_{sg} is allowed to decrease from 0.0250 to 0.0125 as fixed carbon burns progressively till it is completely consumed.

The ash released on account of fixed carbon burning of coal particles is assumed to attain stone temperature instantaneously due to the high contact area. The shrinking fuel particles are likely to be trapped in ash layer over lime-limestone particles more and more as ash quantity grows and fuel particles size reduces. The existence

of product ash layer after ash fusion over burning fuel particles will also hinder the heat exchange rate from fuel to gas. Thus η_{fg} is allowed to decrease more sharply than η_{sg} , i.e. from 0.050 to 0.015 as fixed carbon burns progressively till it is completely consumed.

The possibility of the existence of powdered ash layer in between lime-limestone and fuel particles with increase in ash quantity is quite high and this will hinder the heat exchange rate from fuel to limestone particles. Further, product ash layer after ash fusion on burning fuel particles will create additional reduction in fuel to stone heat exchange. Therefore, η_{fs} is allowed to decrease from 0.20 to 0.15 as fixed carbon burns progressively till it is consumed completely.

Table-6.3 lists the important parameters related to kiln design, operation and energy efficiencies. In addition to these some other computed parameters, such as, particle surface areas, interphase heat transfer coefficients and rates and cumulative wall heat loss are also given in the Tables of results F.1 to F.9, Appendix-F. These were not important as far as the overall design and performance of the kiln is concerned but they give a deeper insight into actual phenomenological behaviour inside the kiln as lime-limestone and fuel particles and gas pass through different axial positions of the kiln.

TABLE-6.3

Computed Parameters of Significance

<u>Sl.</u>	<u>Parameter</u>	<u>Symbol</u>	<u>Units</u>
1.	Effective kiln height	L_e	m
1.1	Height of preheating zone	H_{pz}	m
1.2	Height of burning zone	H_{bz}	m
1.3	Height of cooling zone	H_{cz}	m
2.	Limestone-lime surface temperature	T_s	K
3.	Fuel temperature	T_f	K
4.	Gas temperature	T_g	K
5.	Fractional limestone calcination	x_s	Kg/Kg
6.	Fractional fuel conversion	x_f	%
7.	Input heat accounted	IHA	%
8.	Thermal efficiency	η_e	%
9.	Sensible heat loss in kiln exhaust gas	SHLKEG	%
10.	Sensible heat loss in product lime and fuel residues	SHLPL	%
11.	Combustion heat loss in unburnt volatile matter	CHLUVM	%
12.	Heat loss through kiln wall	HLKW	%

First six computed parameters listed in Table-6.3 are already explained earlier. Input heat accounted (IHA) is the ratio of all output heat terms to all input heat terms, both sensible and latent. IHA gives an idea of the overall heat balance achieved for the kiln as a whole. From energy efficiency point of view, the thermal efficiency appears to be the most important and widely used term and is defined (Boynton, 1967) as:

$$\text{Thermal efficiency} = \frac{\text{Theoretical heat required for calcination}}{\text{total heat of combustion of fuel supplied}} \quad (6.1.1)$$

Some investigators might prefer to include the sensible heat required to preheat limestone to calcination temperature in the numerator of right hand side of the above defining equation. But this is not very proper because a significant fraction of the total sensible heat of product lime and carbon dioxide is recovered in the cooling and preheating zones, respectively. The remaining terms in Table-6.3 specify the various specific heat loss terms and give an idea of the individual contributions to the overall heat loss.

It may be noted again that the effective kiln height (L_e) is treated as an output-design parameter and its value is computed by the simulation system. However, if the computed value of the effective kiln height becomes very large, natural draft operation may not be feasible. The field survey indicates that the kiln heights vary from 5 to 12 m for lime production rates of 5 to 15 tonnes per day (Table-3.1). However, one kiln was observed to have an effective height of 14.5 m with nominal lime production of 20 tonnes per day with a provision for forced draft. This kiln was observed by the author to give lime production rate of only about 14 tonnes per day with natural draft. Thus, it may be quite realistic to impose a maximum limit of 14 m for the effective kiln height for which natural draft operation may be considered feasible. Furthermore, for small capacity low investment kilns with lime production rates of approximately 10 tonnes per day, the maximum limit of 14 m for L_e may also be justified from operational convenience also.

6.2 SIMULATION RESULTS FOR THE BASE CONDITIONS

6.2.1 General

The computer programmes written in Fortran IV were run on the digital computer SN-73 manufactured by ESSEN (Indian Version

of PDP-11/73 of DEC, USA) and installed at the Central Building Research Institute, Roorkee. Unique solutions were obtained for all the cases. Execution time for each set of conditions for the three zones varied, in general, from 50 to 100, 150 to 300 and 30-50 seconds for preheating, burning and cooling zones, respectively.

Results obtained in respect of temperature and conversion profiles alongwith interfacial areas of solid particles, interphase heat transfer coefficients, interphase heat exchange rates and cumulative wall heat losses for the base conditions corresponding to average values of design and operating parameters are reported in Tables F.1 (A-1) through F.1 (A-3) for the preheating-cum-devolatilization zone (without volatile matter combustion), the burning zone (incorporating the combustion of volatile matter and fixed carbon contents of fuel), and the cooling zone, respectively. Results for burning zone also include the ratio of sensible heat accumulation in lime layer to the total heat (sensible heat plus heat of calcination) received by limestone-lime particles in the axial width ΔZ , lime layer sensible heat above the dissociation temperature T_d , and partial pressures of oxygen and carbon dioxide.

The relevant profiles for the three zones of the lime kiln are given in Figs. 6.1 through 6.3. The curves were plotted using HP 7475 A Colour Graphics Plotter manufactured by Hewlett-Packard

of USA and installed at the Central Building Research Institute, Roorkee.

6.2.2 Temperature Profiles and Fuel Behaviour

in the preheating zone

Fig. 6.1 shows the temperature profiles of gas, fuel and limestone particles as well as the fractional weight loss (x_f) of fuel in the preheating zone of the lime kiln. The fuel temperature initially rises at a sharp rate upto a temperature of 373 K, incipient demoisturization temperature, for the case of simple preheating. As no moisture is evolved, the fuel weight loss remains zero as indicated by a straight line on the abscissa of the graph. Thereafter, the process of demoisturization starts and the rate of rise of fuel temperature along the axial direction during its downward movement in the kiln falls for next eight intervals of ΔZ of 0.05 m during which the total moisture (weight percent of fuel) was assumed to release at a uniform rate. Thus x_f shows a linear change in its value 0 to 0.05. Since the fuel attained a temperature of 379.3 K at the completion of demoisturization, and devolatilization is not assumed to commence until T_f becomes 673 K, its temperature again shows a sharper rise and x_f value remains constant at 0.05. As the difference between gas temperature (T_g) and fuel temperature (T_f)

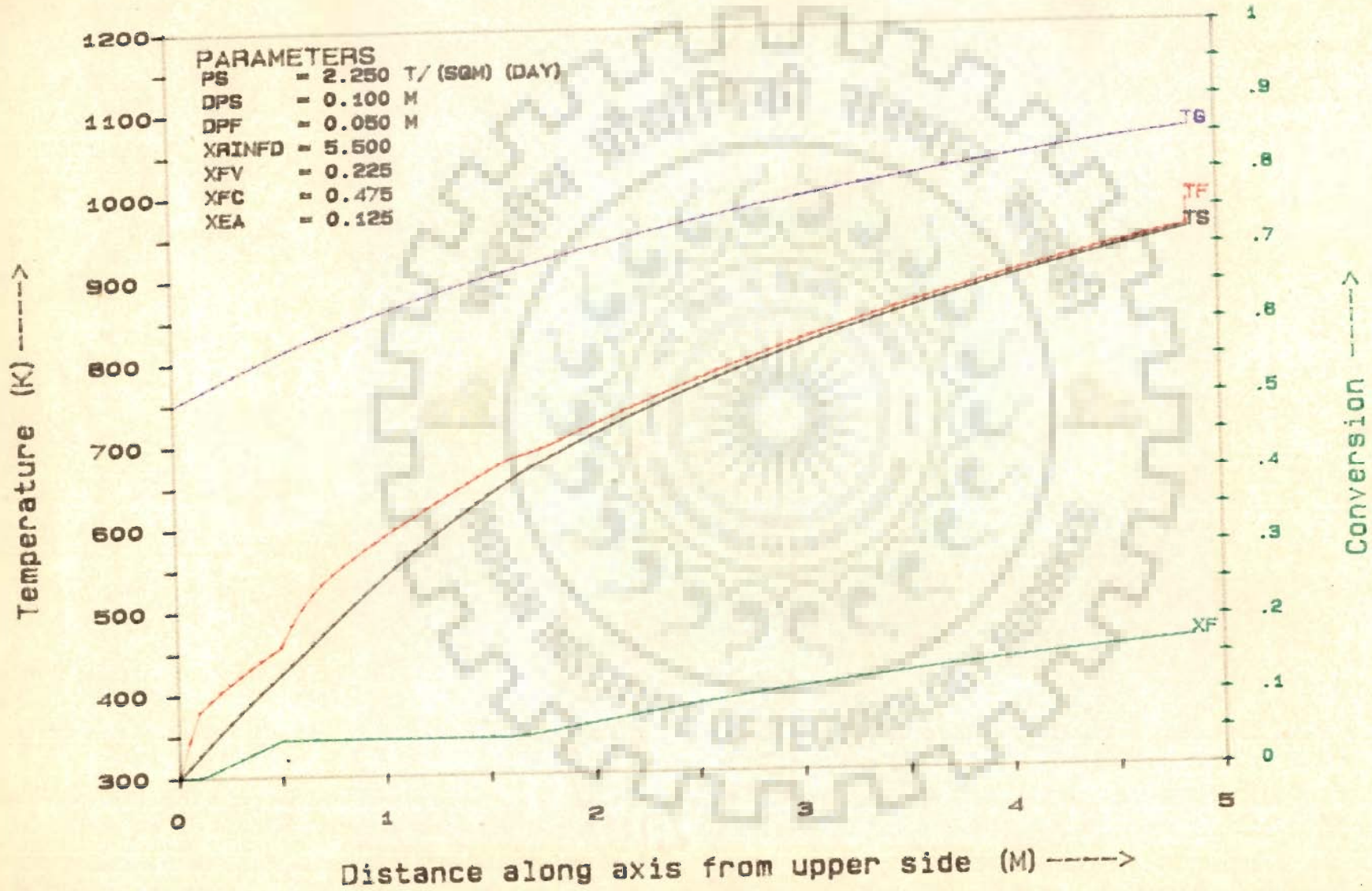


FIG.6.1 - TEMPERATURE PROFILES & FUEL BEHAVIOUR IN PREHEATING ZONE

becomes smaller, the rate of heat transfer from gas to fuel ($-Q_{fg}$) decreases and the rate of rise of T_f also decreases.

As the fuel attains a temperature of 673 K, the release of volatile matter requires latent heat of devolatilization, and hence the rate of rise in T_f with distance along the axis of the kiln shows a further decline. Since the rate of devolatilization is proportional to the rate of change in T_f , the fuel conversion values show a proportional increase with T_f till the fuel attains auto-ignition temperature for the volatile matter, that is, 948 K or a slightly higher value achieved for the first time by the fuel. Temperature at which auto-ignition occurred was observed to lie always within 948 and 951 K for all the conditions investigated. This also indicates the end of the preheating-cum-devolatilization zone without involving combustion of the volatile matter.

In the preheating zone the limestone temperature (T_s) shows a gradual increase as it moves downward along the axis of the kiln without attaining the calcination temperature (T_d) of 1173 K. Thus variation in limestone temperature is uniform and only the rate of increase of T_s shows a decrease with increase in T_s because of declining rate of heat transfer from gas to limestone ($-Q_{sg}$) as a result of decrease in $(T_g - T_s)$. In this zone the gas temperature (T_g) also shows a similar behaviour as that of T_s except that its rate

of rise is much smaller in comparison to that of T_s because total thermal inertia of the gas ($\dot{m}_g C_g$) is much higher than that of the stone ($\dot{m}_s C_s$). This will also indicate that the kiln exhaust gases can never be cooled by heat exchange to the limestone and fuel to the ambient temperature even for an infinitely long preheating zone, since temperature pinch-in between hot and cold stream will have to occur at the end of the preheating zone. Under these conditions of infinite preheating zone length, the following conditions will have to be satisfied for the kiln to be functional, that is, to have limestone calcination in the burning zone:

$$T_g = T_s = T_f = 948 \text{ K (Auto-ignition temperature)}$$

At this condition, the kiln exhaust gas temperature T_{g_o} will be close to 620 K.

6.2.3 Temperature and Conversion Profiles in the Burning Zone

Table F.1 (A-2) and Fig. 6.2 depicts the temperature and conversion profiles obtained for the base conditions in the burning zone.

6.2.3.1 Fuel Temperature

Initially, the temperature rise of the fuel is very sharp on account of the volatile matter evolved since the fuel attains the assumed auto-ignition temperature for the volatile matter (948 K)

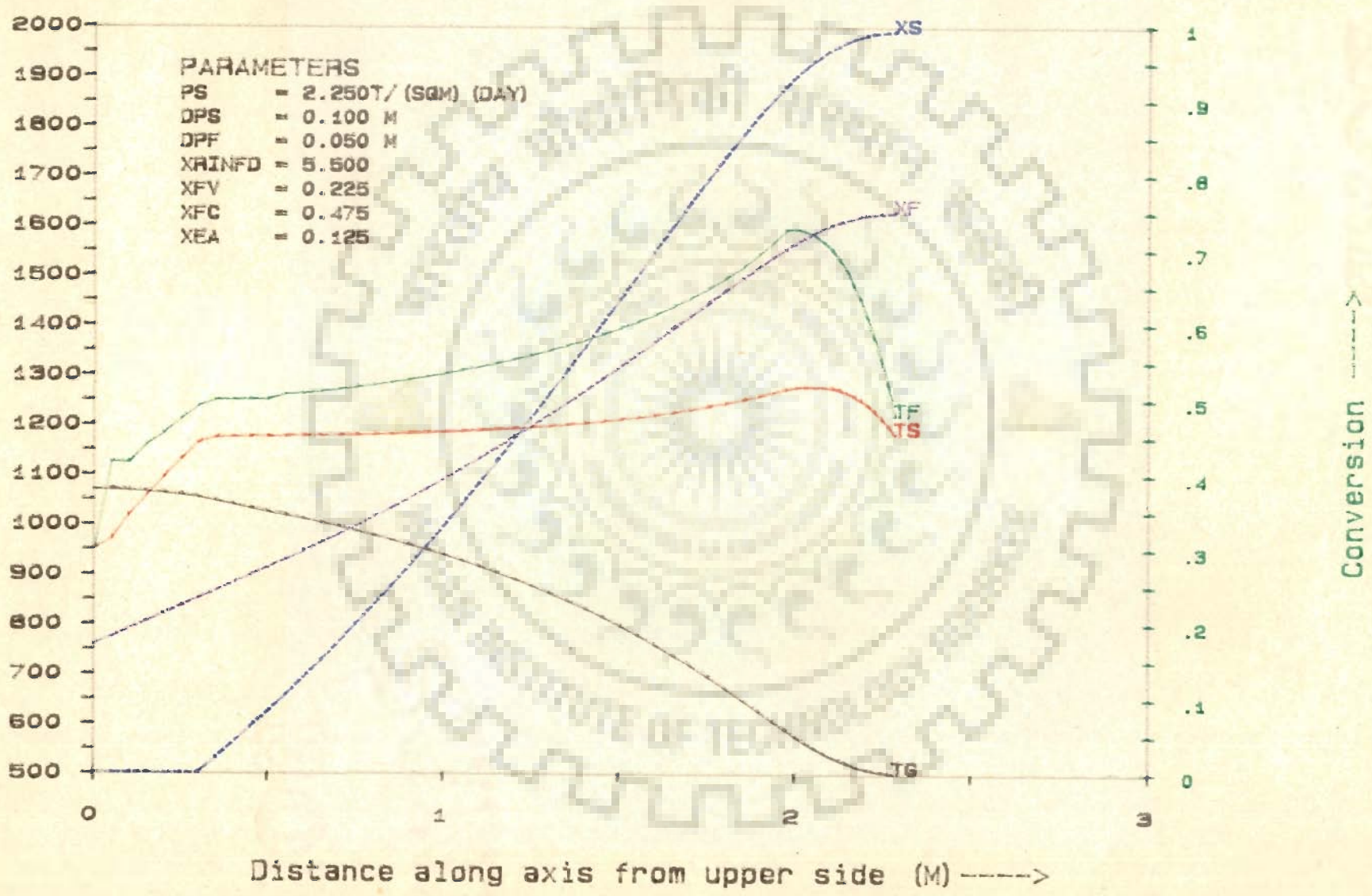


FIG.6.2 - TEMPERATURE & CONVERSION PROFILES IN BURNING ZONE

or higher. T_f shows a decline in the next ΔZ interval and then increases with increase in Z . In the actual situation, this discontinuity in the fuel temperature should not occur. At the inlet of the burning zone, it may be noted that T_g was greater than T_f , while T_f and T_s were very close to each other. ($T_g = 1069.7$ K, $T_f = 949.7$ K and $T_s = 947.4$ K). In one ΔZ interval T_f rose by 176.2 K and becomes very much higher than T_s and also higher than T_g ($T_f = 1125.9$ K, $T_s = 970.1$ K and $T_g = 1069.5$ K). The interphase heat transfer rates Q_{fs} , Q_{fg} and Q_{sg} are computed at the average converged temperatures at the two grid points for the ΔZ interval. The heat transfer rate from fuel to stone (Q_{fs}) has very high radiant heat transfer contribution which depends on the difference of fourth power of the respective temperatures ($T_f^4 - T_s^4$). In view of the foregoing reasons, the Q_{fs} value for the first ΔZ interval is only 135 Kcal/hr and this shoots to an extremely high value of 12426 Kcal/hr for the next ΔZ interval (Table 6.1, A-21). The corresponding values for heat transfer rates from fuel to gas (Q_{fg}) in the first and second ΔZ intervals are - 408 and + 191 Kcal/hr, respectively. Thus the total heat transferred from fuel in the second ΔZ interval is 12617 Kcal/hr. The heat generated in fuel by the combustion of volatile matter in second Z interval is only 12611 Kcal/hr ($\dot{m}_{f_0} \Delta x_f H_{vm}$) and is slightly lesser than that transferred from the fuel. It is, therefore, clear that the fuel temperature will show a fall at the end of second interval ($T_f = 1122.4$ K) because the heat generated in fuel is lower than the heat

transferred from fuel to stone and gas. This discontinuity in T_f behaviour for the first two ΔZ intervals could be avoided by reducing the value of ΔZ interval to a lower value, say 0.01 m, for an initial kiln length of 0.10 to 0.15 m at the beginning of the burning zone. This will avoid such a large change in Q_{fs} and, therefore, in T_f . T_f will then show a more smooth behaviour at the beginning of the burning zone.

At the completion of the volatile matter evolution vis-a-vis its instantaneous combustion, the fuel attains a temperature of 1250.5 K which is sufficiently high to have an appreciable rate of combustion of the fixed carbon, as oxygen will now be able to reach the surface of the fuel particles. It may be noted that the size of the fuel particles (d_{pf}) and, therefore, its surface area (a_f) do not change till the completion of combustion of the volatile matter. But once the fixed carbon begins to burn, ash segregation from the fuel particles takes place leading to shrinkage of the fuel size and consequent reduction in its surface area. Reduction in a_f will also affect the rate of heat generation by combustion of the fixed carbon and also the rate of heat transfer from the fuel particles to gas and the limestone particles. The changes in fuel particles temperature T_f in burning zone depend upon the net rate of heat accumulation by the fuel particles, that is, the rate of generation of heat by combustion of the fixed carbon minus the heat transfer rates Q_{fs} and Q_{fg} .

It is clear from the tabulated results in Table F.1 (A-2) and Fig. 6.2 that T_f rises upto a maximum value of 1594.3 K as the fuel particles move downward in the burning zone. When T_f approaches the ash fusion temperature (T_{ff}) of 1573 K or higher for the first time, the fusion of ash checks its segregation from the fuel particles and further combustion of the fixed carbon will approach the shrinking core model, eventhough the particle size will change to some extent due to the assumption of density variations with T_f . The ash layer is assumed to be porous and quite thin so that the diffusion of oxygen to the surface of the fixed carbon core is assumed to take place without substantial hindrance. Further, the temperature gradients across the thin ash layer are neglected so that the entire fuel particle consisting of the ash layer and the fixed carbon core is assumed to be at a uniform temperature. With the commencement of ash fusion, reduction in external surface area of fuel particles (a_f) is very small, but the reduction in surface area of the core on account of combustion of the fixed carbon is effected rather rapidly with increasing x_f . Thus, soon after initiation of the process of ash fusion, that is, for x_f greater than x_{ff} Q_{fs} and Q_{fg} exceed the rate of heat generation due to the fixed carbon combustion and hence the fuel temperature (T_f) starts falling. It may be noted from the Table F.1 (A-2) that $T_{f_{max}}$ occurs at an axial distance Z of 2.0 m from the commencement of the burning zone and T_f is 1218.9 K at the end of the burning zone with the burning zone height (H_{bz}) of 2.28 m.

6.2.3.2 Surface Temperature of Limestone-Lime Particles

Table F.1 (A-2) and Fig. 6.2 also show the variations in the stone surface temperature T_s with axial position from the start of the burning zone, Z . At the start of the burning zone T_s is 947.4 K and it rises rapidly to its decomposition temperature (T_d) of 1173 K. The slow rise in T_s in the first ΔZ interval of the burning zone may be attributed partly to the error due to the choice of $Z = 0.05$ m as per the explanation given earlier and partly to the fact that T_f is extremely close to T_s ($T_f = 949.7$ K and $T_s = 947.4$ K) and, therefore, Q_{fs} will be very small at the start of the burning zone. After the limestone particles traverse a distance of 0.35 m in the burning zone, T_s reaches the calcination temperature ($T_s = 1173.2$ K) and further increase in T_s is greatly reduced since most of the net heat received by heat exchange ($Q_{fs} - Q_{sg}$) is consumed in the calcination of the limestone particles. This is obvious from the extremely low values of RSHLHD in Table F.1 (A-2). RSHLHD is the ratio of the sensible heat accumulation in the lime layer to the net heat (sensible plus calcination) received by the lime-limestone particles. It may also be noted that only upto an axial distance of 0.15 m in the burning zone, T_g is greater than T_s . After that T_s becomes much larger than T_g and the heat transfer rate from the stones to gas (Q_{sg}) tends to increase for most of the burning

zone in the downward direction. With increase in T_f , T_s also increases to meet the heat conduction requirements through the growing thickness of the lime layer. T_s attains a maximum value of 1277.0 K at $Z = 2.025$ m soon after the maximum value of T_f at $Z = 2.000$ m. The ratio RSHLHD also increases to a maximum value of 0.1166 at $Z = 2.180$ m. It may also be noted that the net heat received by the limestone-lime particles by heat exchange ($Q_{fs} - Q_{sg}$) also increases with increase in downward axial distance Z , attains a maximum value at $Z = 1.600$ m and then starts decreasing with further increase in Z . ($Q_{fs} - Q_{sg}$) is found to be always positive (upto $Z = 2.260$ m). For the last Z interval at the end of the burning zone x_f , x_s , T_f , T_s and T_g were obtained by second order polynomial equations using sets of the previous three converged values for each of the variables to ensure complete combustion of the fuel ($x_f = x_{f_{\max}} = 1 - x_{fa}$) at the end of the burning zone since it was found to be virtually impossible to obtain their values by solving the model equations due to various constraints.

6.2.3.3 Bulk Gas Temperature

Table F.1 (A-2) and Fig. 6.2 show the variation in gas temperatures (T_g) with axial position (Z) from the start of the burning zone. At the end of the preheating zone T_g was higher than T_f as

well as T_s . But after the very first ΔZ interval of 0.05 m, T_f becomes appreciably higher than T_g and after four ΔZ intervals of 0.05 m each, T_s also becomes higher than T_g . Thus the net heat received by the gas from the heat exchange ($Q_{fg} + Q_{sg}$) becomes positive at $Z = 0.150$ m and remains positive thereafter with a maximum value at $Z = 1.500$ m. In addition, the gas also receives heat by convective transport of the hot combustion gaseous products at T_g and the product of calcination, carbon dioxide gas, at T_s . Convective transport to gas is always positive. Since the gas flows from the bottom to the top of the kiln, that is, in the negative Z direction, T_g falls in the positive Z direction and the rate of fall of T_g will increase with increase in the rate of total heat ($Q_{fg} + Q_{sg} + \text{Convective transport}$) received by the gas. Thus, T_g drops from the beginning to the end of the burning zone with steepest fall at $Z = 1.850$ m. T_g drops from 1069.7 K at the beginning to 500.6 K at the end of the burning zone.

6.2.3.4 Fuel Conversion

Table F.1 (A-2) and Fig. 6.2 also show the variation in fractional fuel conversion (x_f) with axial position (Z) from the start of the burning zone. During the volatile matter combustion x_f is linearly increasing with increase in Z as a sequel to the assumption that the residual volatile matter at the auto-ignition temperature

is released uniformly in ten intervals of Z of 0.05 m each due to the mass transport limitations as pointed out earlier in Table-6.2. After the completion of the volatile matter combustion at $Z = 0.5$ m, the fixed carbon combustion rate will depend upon the overall rate constant per unit area of the fixed carbon core surface due to the combined effect of surface reaction and mass transfer resistances (\bar{k}_s), area of the fixed carbon core surface which is related to the two third power of the fixed carbon remaining unburnt and T_g . Increase in \bar{k}_s is rapid with increase in T_f initially, but at very high values of T_f , \bar{k}_s tends to approach an asymptotic value. Thus x_f increases rapidly with Z upto the ash fusion temperature and then its further increase is relatively slow. However, it may be noted that x_f rises monotonically with Z till the entire fixed carbon is burnt, that is, $x_f = 1 - x_{fa} = 0.75$.

6.2.3.5 Limestone Conversion

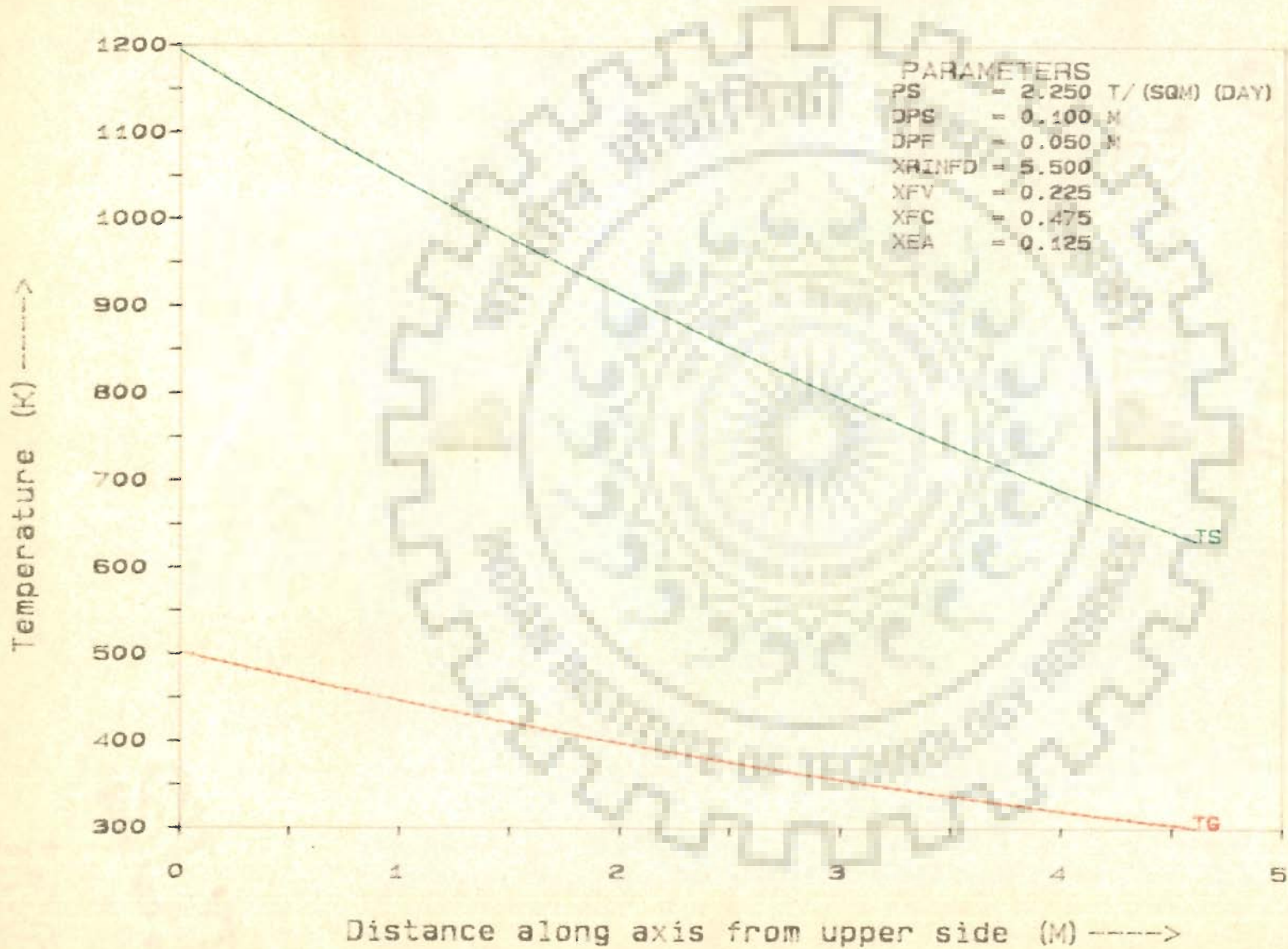
Table F.1 (A-2) and Fig. 6.2 indicate the variation in fractional limestone conversion (x_s) with axial distance (Z). No limestone calcination occurs ($x_s = 0$) till T_s is less than the calcination temperature (T_d) of 1173 K upto $Z = 0.35$ m. Thence, the rate of x_s increase is closely related to the rate of net heat received by the limestone - lime particles ($Q_{fs} - Q_{sg}$). Thus, the rate of x_s increase is maximum at $Z = 1.6$ m, corresponding

to the maximum $(Q_{fs} - Q_{sg})$ value, and then it slows down till the end of the burning zone. It is observed that 99.3 percent calcination of limestone occurs till the end of the burning zone in this case.

6.2.4 Temperature Profiles in the Cooling Zone

Table F.I (A-3) and Fig. 6.3 depict the solids and gas temperature profiles in the cooling zone for the base conditions. The weighted mass temperature of all solids at the end of the burning zone was calculated using the equation (4.5.3.1). The calcination of unconverted limestone remaining at the end of the burning zone, if any is considered insignificant in the cooling zone in view of the extremely rapid drop in solid mass temperature below the calcination temperature of 1173 K, even though T_s at the end of the burning zone may be somewhat higher than 1173 K. The weighted solid mass temperature and the gas temperature at the beginning of the cooling zone are 1194.7 and 500.6 K, respectively. The corresponding temperatures at the end of the cooling zone are 632.2 and 299.6 K. It may be noted that the cooling zone is assumed to end when the gas temperature for the first time becomes equal to or less than the ambient temperature T_∞ (300 K).

Fig. 6.3 indicates that the rate of drop of T_s is faster as compared to T_g because of the thermal inertia of the solids is lesser



6.3 - TEMPERATURE PROFILES IN COOLING ZONE

than that of the gas as already explained in section 6.2.2. It is quite clear from the Fig. 6.3 that the complete recovery of sensible heat from the solids will not be possible even with an infinitely large cooling zone. For the assumed pinch-in of temperatures T_g and T_s at the end of the cooling zone with $T_g = T_\infty = 300$ K for an infinite cooling zone will occur only if the weighted mass temperature of all the solids at the beginning of the cooling zone is equal to 862 K. Thus, the lime-limestone particles temperature (T_s) at the end of the burning zone will be lower than 862 K. Such a low T_s value at the end of the burning zone is undesirable for proper calcination in the burning zone. Such a situation will mean unrealistically high limestone to fuel ratio (X_r) and correspondingly extremely low fractional degree of calcination, x_s . It, therefore, appears that for the most optimal operation, the following conditions must occur at the end of the burning zone :

$$T_s = 1173 \text{ K and } x_s = 1.00.$$

Under these conditions the product lime temperature at the end of the cooling zone is expected to be close to 625 K for this case of average design and operating parameter values.

6.2.5 Important Design and Performance Results from Simulation

In sections 6.2.2 to 6.2.4 the temperature and conversion profiles have been discussed in detail to provide phenomenological

understanding of the changes in limestone, fuel and gas in the preheating, burning and cooling zones of the kiln. Table 6.4 gives the important design and performance results obtained from simulation. For the base conditions (Set No. 1) and for the variations in the parameter values. The tabulated results give effective kiln height (L_e), fractional degree of calcination (x_s), product lime exit temperature, product quality and thermal efficiency. These results are of greatest interest to a designer or an operator of a lime shaft kiln. Table 6.5 gives the details of heights for the three zones, namely, the preheating, burning, and cooling, and the values of maximum limestone-lime surface temperature ($T_{s_{max}}$) and fuel temperature ($T_{f_{max}}$) alongwith their positions from the top of the kiln. $T_{s_{max}}$ and x_s are used to characterize product quality in the following manner :

Product Quality

Defining Conditions

Wellburnt

$$x_s \geq 0.95 \text{ and } T_{s_{max}} < 1573\text{K}$$

Underburnt

$$x_s < 0.95 \text{ and } T_{s_{max}} < 1573\text{K}$$

Overburnt

$$x_s \text{ is not specified and } 1573\text{K} \leq T_{s_{max}} < 1773\text{K}$$

Deadburnt

$$x_s \text{ is not specified and } T_{s_{max}} \geq 1773\text{K}$$

$T_{s_{max}}$ specifications for burning quality are based only on extremely limited published information, but the values used appear to be reasonable and are in general agreement with the lime manufacturing practices (Boynton, 1967).

For the base conditions excellent design and performance results are predicted by the simulation. Table-6.6 gives details of the energy balance and important heat losses as input heat accounted (IHA) defined in section 6.1, fraction of the volatile matter in fuel escaping unburnt (FVMU), sensible heat loss in kiln exhaust gas (SHLKEG), combustion heat loss in unburnt volatile matter (CHLUVM), sensible heat loss in product lime (SHLPL) and heat loss through kiln wall (HLKW). Thermal efficiency (η_t) and energy loss terms FVMU, SHLKEG, CHLUVM, SHLPL and HLKW are based on heat of combustion of the total volatile matter and the fixed carbon. The value of IHA indicates the extent to which total input heat terms (sensible plus heats of combustion) are accounted for in the output heat terms for the kiln. In view of the complexities involved in computations, IHA values in the range of 93.18 to 100.1 percent are considered excellent. The thermal efficiency is 36.9 percent and the major sources of heat losses are : SHLKEG = 28.9 percent, CHLUVM = 18.5 percent and SHLPL = 4.4 percent. The possibility of improving thermal efficiency by reducing heat losses is discussed in subsequent sections in which the results for variations in parameters are discussed. But

TABLE-6.4

Design and Performance Results Obtained from the Simulation System

Set No.	Parameter Varied	Value of Parameter	Effective Kiln Ht. (m)	Fractional Degree of Calcination	Exit Lime Temperature (K)	Product(Lime) Quality	Thermal Efficiency (Percent)
1	2	3	4	5	6	7	8
1(A)	Nil	The Base Conditions	11.7	0.9929	632.2	Wellburnt	36.87
2(A)	Particle size of limestone	0.088	9.6	0.9874	683.2	Wellburnt	36.66
2(B)	-do- (d_{p_s})	0.112	13.5	0.9916	607.4	Wellburnt	36.82
3(A)	Particle size of fuel (d_{p_f})	0.044	11.2	0.9884	627.3	Wellburnt	36.70
3(B)	-do-	0.056	11.9	0.9894	662.5	Wellburnt	36.73
4(A)	Superficial lime output rate (P_s)	2.00	10.9	0.9956	633.6	Wellburnt	36.96
4(B)	-do-	2.50	12.4	1.0000	624.0	Wellburnt	37.13
5(A)	Limestone to fuel ratio (X_r)	5.0	8.9	1.0000	1234.2	Overburnt	33.75
5(B)	-do-	6.0	14.7	0.9370	503.6	Underburnt	37.95

Table Contd. .../

1	2	3	4	5	6	7	8
6(A)	Volatile matter content (X_{fv})	0.150	8.4	1.0000	1374.2	Overburnt	35.89
6(B)	-do-	0.300	19.4	0.8741	418.8	Underburnt	35.33
7(A)	Excess Air Fraction (X_{ea})	0.00	10.30	1.0000	791.1	Wellburnt	37.13
7(B)	-do-	0.25	13.9	0.9847	491.8	Wellburnt	36.56
8(A)	Wall thickness of brick masonry (W_{rb})	0.46	11.7	0.9937	634.3	Wellburnt	36.89
8(B)	-do-	0.92	11.5	0.9921	646.6	Wellburnt	36.84
9(A)	Exhaust gas temperature	698.0	10.4	0.9680	907.9	Wellburnt	35.94
9(B)	-do- (T_{g_o})	798.0	13.6	1.0000	533.8	Wellburnt	37.13

Note: The base conditions are; $d_{p_s} = 0.100$ m; $d_{p_f} = 0.050$ m; $P_s = 2.25$ t/(m²) (day); $X_T = 5.5$ t/t; $X_{fv} = 0.225$; $X_{ea} = 0.125$, $W_{rb} = 0.69$ m and $T_{g_o} = 748$ K.

The values of the parameters varied are in the same units as those used for the base conditions.

TABLE-6.5
DETAILS of Kiln Zonal Heights and Maximum Temperature Locations

Set No.	Heights of the zones (m)			Maximum Temperatures(K) and Their Axial Location (m) from top of Kiln			
	Preheating	Burning	Cooling	Stone Surface $T_{s\max}$	Z for $T_{s\max}$	Fuel $T_{f\max}$	Z for $T_{f\max}$
	1(A)	4.85	2.28	4.60	1277.0	6.88	1594.3
2(A)	4.10	2.29	3.25	1251.5	6.15	1576.7	6.13
2(B)	5.50	2.28	5.75	1294.1	7.53	1581.8	7.50
3(A)	4.75	1.88	4.55	1290.8	6.42	1608.6	6.34
3(B)	4.85	2.73	4.35	1258.7	7.35	1586.1	7.32
4(A)	4.50	2.06	4.30	1341.7	6.38	1579.7	6.67
4(B)	5.15	2.49	4.75	1270.4	7.34	1581.7	7.31
5(A)	5.00	2.27	1.60	1608.6	7.23	1710.1	7.15
5(B)	4.75	2.27	7.70	1240.8	6.75	1580.5	6.72
6(A)	4.65	2.77	1.00	1607.1	7.39	1676.7	7.37
6(B)	5.05	1.89	12.45	1231.6	6.69	1576.7	6.69
7(A)	4.60	2.40	3.25	1286.9	6.82	1585.9	6.71
7(B)	5.10	2.19	6.65	1267.7	7.03	1581.4	7.00
8(A)	4.80	2.28	4.60	1277.7	6.83	1594.9	6.80
8(B)	4.85	2.28	4.40	1276.0	6.88	1593.4	6.85
9(A)	6.35	2.29	1.75	1256.5	8.35	1574.8	8.32
9(B)	3.95	2.27	7.40	1399.0	6.20	1593.3	5.92

TABLE-6.6
Details of Energy Balances and Significant Heat Losses

Set No.	<u>IHA</u> (Percent)	<u>FVMU</u> (Fraction)	<u>SHLKEG</u> (Percent)	<u>CHLUVM</u> (Percent)	<u>SHLPL</u> (Percent)	<u>HLKW</u> (Percent)
1(A)	93.98	0.5409	28.91	18.53	4.35	1.59
2(A)	94.25	0.5373	28.91	18.41	5.18	1.36
2(B)	93.98	0.5474	28.91	18.76	3.98	1.79
3(A)	93.81	0.5448	28.91	18.67	4.29	1.50
3(B)	94.41	0.5419	28.91	18.57	4.84	1.65
4(A)	93.78	0.5350	28.91	18.33	4.36	1.50
4(B)	94.60	0.5537	28.91	18.97	4.20	1.66
5(A)	100.07	0.5472	28.39	15.71	13.99	1.42
5(B)	94.52	0.5503	29.44	18.86	2.82	1.71
6(A)	99.29	0.5462	26.99	14.44	17.54	1.51
6(B)	96.31	0.5549	32.56	22.05	1.64	1.95
7(A)	94.60	0.5430	26.68	18.61	6.89	1.53
7(B)	94.25	0.5498	31.15	18.84	2.33	1.66
8(A)	93.99	0.5371	28.91	18.40	4.38	1.71
8(B)	94.00	0.5393	28.91	18.48	4.58	1.47
9(A)	94.44	0.5463	25.39	18.53	9.23	1.76
9(B)	96.76	0.5477	32.54	18.77	2.87	1.55

the tabulated values of the thermal efficiency for all the sets of conditions show that by adjusting the effective kiln height (L_e), the thermal efficiency in the range of 36.9 ± 1.5 percent is possible. L_e value of 11.7 m obtained from the base conditions is quite reasonable and the natural draft may very well meet the combustion air flow requirements.

6.3 EFFECT OF VARIATIONS IN THE DESIGN AND OPERATIONAL PARAMETERS

The average conditions for the design and operation of a lime shaft kiln are given in Table-6.1. For studying the effect of variations in the design and operational parameters, it was considered desirable to vary only one parameter at a time in the specified range given in Table 6.1 keeping all the other parameters corresponding to the average values. Furthermore, the values of the important system parameters were not changed and the same were maintained as given in Table-6.2. The two additional values of the varying parameters, namely, at the minimum and the maximum of the ranges, were used for obtaining simulation results. These two computed results along with the same obtained for the base conditions form a set for each parameter variation. Each of the eight parameters, which were permitted to vary, is treated as an independently varying parameter

in order to study the effect of the same. The results of this sensitivity analysis can be very useful in the evolution of optimal conditions for design and operation of such types of the low capacity mixed-feed kilns. The detailed computed results are given in the Appendix-F, tables F.2 to F.9 with A-1 to A-3 and B-1 to B-3 being subclassifications for the minimum and maximum values of parameters varied in the analysis of the three zones of the kiln. The computed values of the important design and performance results of simulation are also given in tables 6.4 to 6.6.

The general trends for changes in temperatures and conversions in the preheating, burning and cooling zones were similar to those obtained for the base conditions. Thus, further discussion on the same is not considered essential. The effect of the variations in the design and operating variables can be discussed properly with the help of the tabulated results as given in tables 6.4 to 6.6.

6.3.1 Particle Size of Limestone (d_{p_s})

The effective height of the kiln (L_e) shows a considerable change with variation in particle size of limestone as per set numbers 1 and 2 in Tables-6.4 through 6.6. For d_{p_s} increase by 1.27 times, the increase in L_e is 1.40 times. Therefore, assuming power law variation L_e appears to be proportional to $(d_{p_s})^{1.4}$. The state-of-the-art correlations for the preheating, burning and cooling

times appear to depend upon 0.5, 1.0 to 2.0 and 0.5 power of d_{p_s} , respectively, as per equations 3.10 through 3.12 discussed earlier in Chapter-3. The effect of variations in d_{p_s} on fractional degree of calcination is less than 0.6 percent and on thermal efficiency is less than 0.2 percent. The quality of the product lime as well as the thermal efficiency are, therefore, insignificantly affected by changes in d_{p_s} in the selected range of investigation.

The slight reduction in the fractional conversion of limestone (x_s) for smaller size of the particle may be attributable to the uniformity of the effectiveness factors (η_{sg}) used for the different d_{p_s} values. In a practical situation, it is well known that the η_{sg} values may decrease for smaller sizes of limestones. This, in turn, will reduce the heat exchange rate from limestones to gas, and thereby will increase the rate of net heat received by the limestone particles in the burning zone ($Q_{fs} - Q_{sg}$); and, therefore, x_s .

6.3.2 Particle Size of Fuel (d_{p_f})

Set numbers 1 and 3 in Tables-6.4 to 6.6 do not indicate any significant variations in the effective kiln height, fractional degree of calcination and thermal efficiency on account of the changes in the particle size of the fuel. For d_{p_f} increase by 1.27 times, the increase in L_e is only 1.07 times, the change in x_s is only 0.5 percent

and the thermal efficiency changes by only 0.2 percent. The product lime remains well burnt in all the three cases. However, the results show that the d_{P_s}/d_{P_f} ratio of approximately 2 appears to be the most satisfactory. This conclusion is in conformity with the thumb rule prescribed earlier in the Indian Standards on the design of the mixed-feed lime shaft kilns (I.S. 1849, 1967 and I.S. 1861, 1961).

6.3.3 Superficial Lime Output Rate (P_s)

The results obtained for variation in superficial lime output rate are given in the set numbers 1 and 4, and in Tables-6.4 through 6.6. It is seen that the effective height of the kiln (L_e) increases by about 15 percent when P_s is increased from 2.0 to 2.5 tonnes/(m² day). The change in x_s is nearly 0.7 percent and the same in thermal efficiency is about 0.3 percent. Product lime is well burnt in all the three cases. The power law assumption indicates that L_e is proportional to $(P_s)^{0.6}$. This agrees very well with variations in height as a function of $(P_s)^{0.5}$, as suggested by the state-of-the-art correlations (equations 3.10 through 3.15). The construction cost of the kiln is expected to be proportional to the kiln wall area ($\pi D_i L_e$) where D_i is the internal diameter of the kiln. For a specified nominal lime production rate, D_i is proportional to $(P_s)^{-0.5}$. Thus, the cost of the kiln is approximately proportional to $(P_s)^{0.1}$, that is, a very small dependence on P_s . However, larger diameter and smaller height kilns may not be preferable, even though the initial

cost may be slightly less, because of the possibility of non-uniformity of feeding vis-a-vis product withdrawal and also significant non-uniformity in the gas flow over the entire inner cross-section of the kiln for a lower P_s value. Slightly higher x_s and thermal efficiency values and lower value of $T_{s\max}$ may tilt the balance in favour of higher P_s value of 2.5 tonnes/(m²)(day). This value of P_s is in conformity with the recommendations of the Indian Standards Institution (ISI, 1961 and 1967). With increase in P_s the gas velocity increases which tends to improve the gas-solid heat transfer coefficients resulting in improved heat exchange rates. The thermal performance of a coal fired kiln can, therefore, be enhanced slightly by increasing P_s , say to about 3.0 t/(m²)(day), and correspondingly the effective kiln height upto a maximum limit of 14 m for the natural draft.

6.3.4 Limestone-to-Fuel-Ratio in Feed Input (X_r)

Set numbers of 1 and 5 in Tables-6.4 to 6.6 describe the effect of changes in limestone-to-fuel-ratio (by weight) in the feed input at the top of the shaft kiln. The X_r value has a pronounced effect on the height of the kiln. Increase in X_r from 5.0 to 6.0 increases L_e from 8.9 to 14.7 m and thermal efficiency by 4.2 percent, decreases product lime exit temperature from 1234.2 to 503.6 K and changes the product lime characteristics from the overburnt to the

underburnt conditions. In view of the lower thermal efficiency and the overburnt quality of lime X_r below 5.5 is undesirable. X_r value of 6.0 is also unacceptable because L_e exceeds the limiting value of 14.0 m imposed for the low capacity natural draft kiln and also due to the underburnt quality of the product lime. However, X_r value of about 5.8 may give well burnt product lime, satisfy the restriction on L_e and may improve thermal efficiency by nearly 0.5 percent. From the Table-6.6, it is clear that at a higher value of X_r reduction in the sensible heat loss in the product lime is so significant that it not only compensates for the increases in other sources of heat losses, but also improves the overall thermal efficiency. The lower product lime exit temperature will also facilitate its handling.

6.3.5 Volatile Matter Content in Fuel (X_{fv})

The effect of the volatile matter in fuel X_{fv} can be assessed from the set numbers 1 and 6 in Tables-6.4 through 6.6. The effective height of kiln increases with increase in X_{fv} . The use of a fuel with X_{fv} of 0.15 also results in the overburnt lime product with L_e as low as 8.5 m. The overburning can be avoided by increasing P_s and/or limestone-to-fuel ratio X_r which, in turn, will require additional kiln height and may also improve the thermal efficiency. It is, thus, obvious that a fuel with a low volatile matter content, say coke, can be effectively used at high P_s and X_r to produce well burnt lime at good thermal efficiency. Probably this explains the choice of the

coke fired lime shaft kilns for the large scale manufacture of lime for use in the chemical and allied industries. The tabulated values for the set number 6 (B) corresponding to X_{fv} of 0.30 are correct only if air is available at the bottom of the kiln not at ambient temperature of 300 K, but at a temperature considerably higher than 313 K. An approximate energy balance shows that the cooling zone height becomes infinite when $T_s = T_g = 312.5$ K. Thus, for natural draft operation a fuel with X_{fv} values higher than 0.25 may not be very successful unless someone is willing to operate at low limestone-to-fuel-ratio of about 5.0. Another problem with a high X_{fv} fuel is the underburnt nature of the product lime. This can also be solved to a large extent by using X_r close to 5.0.

6.3.6 Excess Air (X_{ea})

Data obtained for variations in excess air used for combustion are given as set numbers 1 and 7 and Tables-6.4 to 6.6. Tabulated results indicate that increasing the amount of excess air has unsuitable effect since the kiln height L_e is increased, fractional degree of calcination is reduced and the thermal efficiency is also reduced. Thus use of excess air must be as low as possible so long as it does not affect the inherent combustion characteristics of fuel.

Table-6.6 indicates that for all the cases studied, fraction of the volatile matter in the fuel that remains unburnt varies from 53.7 to 55.5% with a mean value of 54.5%. It is, therefore, clear

that even for 0 percent excess here (calculated on the basis of complete combustion of fixed carbon and total volatile matter) case substantial quantity of excess oxygen remains in the exhaust gas at the top of the kiln. Because of the intrinsic characteristics of the shaft kilns, nearly 54.5 percent of the volatile matter is bound to remain unburnt. Even for zero percent theoretical air case, calculations show that actually it amounts to using 28.4 percent excess air, if the same is computed on the basis of that required for the combustion of the fixed carbon and the fraction of volatile matter actually being burnt. Thus, the supply of air can be significantly reduced to lower than what is computed even for the so called zero percent excess air case.

6.3.7 Wall Thickness of Masonry Shaft (W_{rb})

For the range of wall thicknesses investigated in this study, set numbers 1 and 8 in Tables-6.4 to 6.6 indicate totally insignificant changes in the kiln height (L_e), fractional degree of calcination (x_s) and thermal efficiency. This is also clear from Table-6.6, since increase in burnt clay brick thickness from 0.46 to 0.92 m has hardly reduced the wall heat loss from 1.7 to 1.5 percent, a totally insignificant change. Wall heat loss values in masonry kilns, in general, have lower heat losses by conduction through wall than those reported for steel shell coke fired kilns. Boynton (1967) reports kiln wall heat loss for steel shell coke fired kilns in the range of 2 to 3 percent and therefore, kiln wall losses for the masonry kilns in the range

of 1.4 to 1.8 percent appear to be quite reasonable.

6.3.8 Exhaust Gas Temperature (T_{g_o})

The effect of exhaust gas temperature (T_{g_o}) when used as an input parameter is given in set numbers 1 and 9 in Tables-6.4 to 6.6. Increase in T_{g_o} from 698 to 798 K increases the effective kiln length (L_e) by 1.31 times, fractional degree of calcination by 3.2 percent and thermal efficiency by 2.2 percent. The product lime is well burnt in all the three cases. Table-6.5 indicates that use of T_{g_o} of 798 K requires smaller preheating zone, but considerably longer cooling zone. While T_{g_o} of 690 K requires larger preheating zone, but considerably smaller cooling zone. Consequently preheating of air by cooling of the product lime for T_{g_o} of 798 K is considerably larger as compared to that for T_{g_o} of 698 K.

Table 6.6 indicates that for T_{g_o} of 798 K, eventhough sensible heat loss in kiln exhaust gas (SHLKEG) is increased by 7.1 percent, but this is well compensated by decrease in sensible heat loss in product lime (SHLPL) by 6.3 percent as compared to that for T_{g_o} of 698 K. In section 6.2.2 it has been indicated that use of T_{g_o} close to 620 K may require an infinite length of the cooling zone, because in that case the condition at the end of the preheating zone would be : $T_g = T_s = T_f = 948$ K (auto-ignition temperature for the volatile matter). Due to higher thermal efficiency and x_s ,

use of T_{g_0} close to 798 K for designing a coal-fired lime shaft kiln appears to be quite appropriate.

6.4 CONDITIONS FOR OPTIMAL DESIGN AND OPERATION

In view of the discussions in the foregoing sections, it is expected that some thought be given to identify the optimal conditions for the mixed-feed lime shaft kilns having natural draft operation, even though the aim of the present investigation was largely to develop a uniquely stable and efficient simulation system for these kilns, a stupendous task in itself, and not to carry out rigorous optimization studies for such kilns. The parametric sensitivity analysis provides a sound basis for predicting the effect of individual variation in an input design or operating parameter on the output design and/or performance parameters. A realistic objective function for optimization may be to minimize specific energy consumption subject to two constraints, namely, wellburnt lime product and a maximum of 14 m kiln height for the natural draft operation. Occasionally, we may like to maximise productivity of an existing kiln by sacrificing, to a limited extent either specific energy consumption or lime product quality. From a kiln owner's point of view, the net profit may be the sole criterion for an optimal kiln. Thus, for rigorous optimization studies, it becomes necessary to clearly define the objective function and constraints on the system.

Since optimization was not the aim of this investigation,

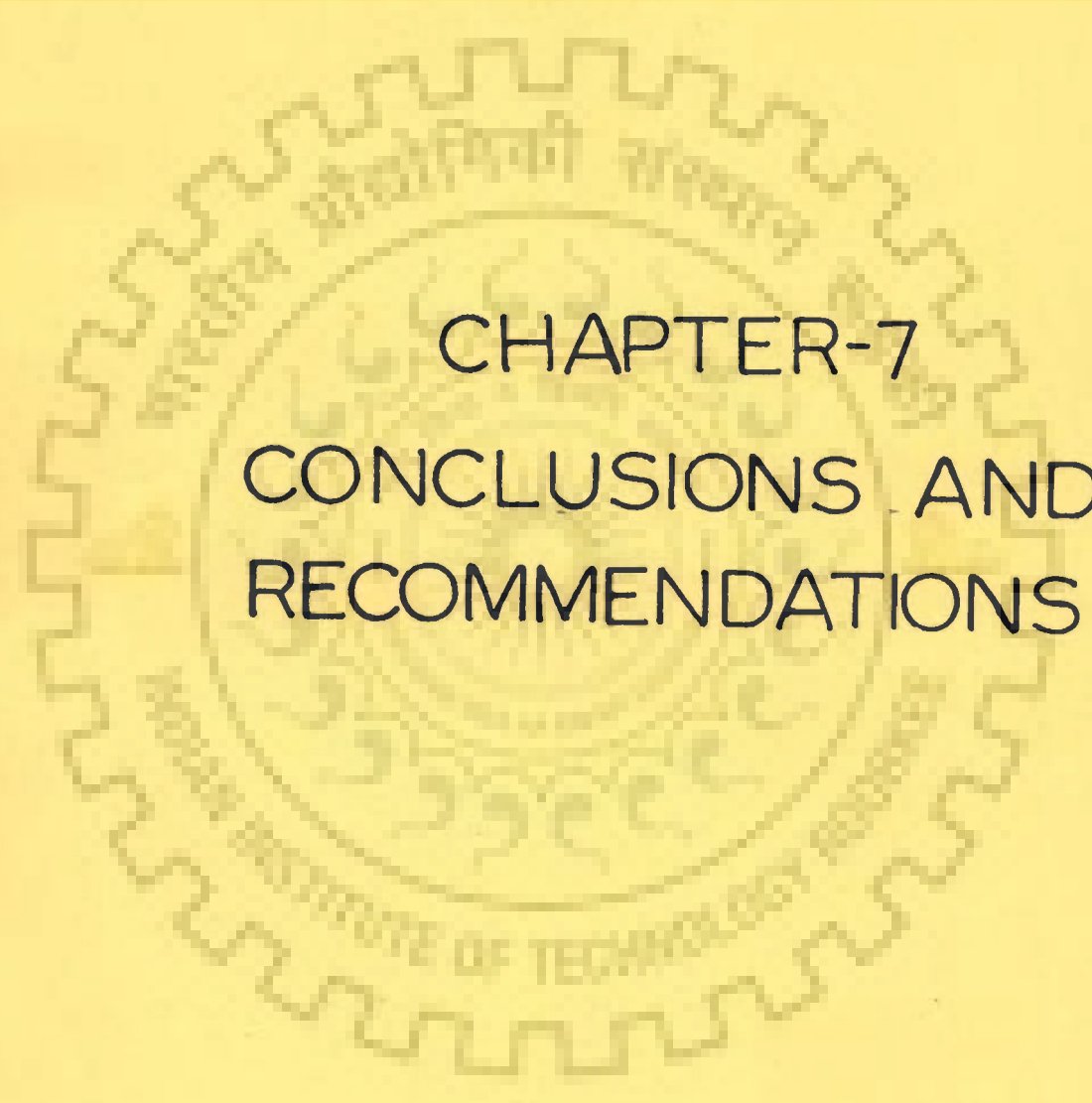
no effort has been made in that direction. However, on the basis of discussions given earlier, the following design and operating conditions may be the most appropriate from the thermal efficiency point of view for a nominal lime production rate (P_n) of 10 tpd:

- (i) Particle size of limestone (d_{P_s}) = 0.100 m
- (ii) Ratio of particle size of fuel to size of limestone (d_{P_f}/d_{P_s}) = 0.5
- (iii) Superficial lime output rate (P_s) = 3.0 t/(m²) (day)
- (iv) Limestone to fuel ratio (X_r) = 5.8
- (v) Fractional content of volatile matter in fuel (X_{fV}) = as low as possible, but not exceeding 0.25
- (vi) Excess air based on total combustion of fixed carbon and total volatile matter (X_{ea}) = - 10 percent
- (vii) Wall thickness of masonry shaft (W_{rb}) excluding lining thickness of fire bricks = 0.46 m
- (viii) Exhaust gas temperature (T_{g_o}) = 813 K

These conditions will meet the requirements of well burnt lime quality

and maximum effective kiln height restriction to 14 m and at the same time may give thermal efficiency better than 38.5 percent. Use of higher T_{g_0} is recommended for two other reasons. Firstly, it will result in a desirable product lime temperature of nearly 498 K which will facilitate its quick handling. Secondly effort can also be made to use these higher temperature kiln exhaust gases with or without combustion of the unburnt volatile matter for some other heating application.

For the above conditions, effective kiln height (L_e) to its internal diameter (D_1) ratio is nearly 6.5. This ratio is expected to vary widely for kilns with different nominal lime production rates. However, from the construction point of view, it may be desirable to have a suitable ratio of L_e/D_1 . It is suggested that the design value of L_e/D_1 may be kept close to 6.5 by suitably adjusting the superficial lime output rates in the range of 2.5 to 3.0 and d_{p_s} between 0.075 to 0.125 m for P_n in the range of 5 to 20 tpd subject to the maximum L_e value of 14 m.



CHAPTER-7
CONCLUSIONS AND
RECOMMENDATIONS

Chapter-7

CONCLUSIONS AND RECOMMENDATIONS

7.1 CONCLUSIONS

7.1.1 Field surveys indicate wide variations in the design and operating practices of the mixed-feed lime shaft kilns resulting in many cases one or more of the following :

- (i) Low thermal efficiencies
- (ii) Poor lime quality
- (iii) Low lime productivity

7.1.2 Thumb rules and/or the state-of-the-art correlations provide a reasonable but crude base for the design or operation of these kilns. However, they do not lead to the optimal design or operation of such kilns.

7.1.3 No attempt has been made so far to scientifically simulate the mixed-feed lime shaft kilns. The only reported effort relates to gas fired kilns with many unrealistic simplifying assumptions. Thus, the major contribution of the present investigation is the development

of a simulation system for the mixed-feed lime shaft kilns using realistic and, in general, rigorous description of the phenomenological behaviour. This simulation system is uniquely stable and efficient for widely varying design and operating conditions.

7.1.4 With the help of this simulation system, parametric sensitivity analysis for all the major design and operating parameters has been carried out; and the important findings are summarized in Tables-6.4 to 6.6.

7.1.5 The sensitivity analysis led to the identification of the following optimal design and/or operating conditions:

- (i) Particle size of limestone (d_{P_s}) = 0.100 m
- (ii) Ratio of particle size of fuel to size of limestone
(d_{P_f} / d_{P_s}) = 0.5
- (iii) Superficial lime output rate (P_s) = 3.0 t/(m²) (day)
- (iv) Limestone to fuel ratio (X_r) = 5.8
- (v) Fractional content of volatile matter in
fuel (X_{fv}) = as low as possible, but not exceeding 0.25

- (vi) Excess air based on total combustion of fixed carbon and total volatile matter (X_{ea}) = - 10 percent
- (vii) Wall thickness of masonry shaft (W_{rb}) excluding fire bricks = 0.46 m
- (viii) Exhaust gas temperature (T_{g_o}) = 813 K
 subject to the constraint of well burnt lime product, the maximum kiln height of 14 m for the natural draft operation and the best possible thermal efficiency.

7.1.6 It appears that the thermal efficiencies better than 40 percent are improbable to achieve in these kilns. However, the same in the range of 38 to 39 percent can be easily achieved by optimizing the design and operation of the mixed-feed lime shaft kiln for each specific application.

7.2 RECOMMENDATIONS

7.2.1 Effort should be made to experimentally measure the temperature profiles of the gas, lime-limestone particles and the fuel particles as a function of axial position in a mixed-feed lime shaft kiln.

7.2.2 Possibility of the mass transfer limitations for diffusion of the product carbon dioxide through the quick lime layer, and its effect on the validity of the heat conduction controlled lime-limestone calcination model needs to be investigated for the large sized limestone particles.

7.2.3 It is necessary to find a method to effectively use the large amount of the sensible heat and the heat of combustion of the unburnt volatile matter in the exhaust gas of the lime shaft kiln. This combined heat loss through the kiln exhaust gas varied from 41.4 to 54.6 percent with a mean value of 47.4 percent of the total heat of combustion of coal.

7.2.4 The simulation system developed in the present investigation must be subjected to a more rigorous optimization of design and operation of the lime shaft kilns. It may be extended on the suggested lines for optimization of the existing kiln of prespecified height and diameter for achieving optimal operation in terms of the lime quality, productivity and the thermal efficiency.

REFERENCES

- Adhia, J.D., 'Nomograph Determines Lime Kiln Performance', *Rock Products*, 55 (12), 115 (1952).
- Azbe, V.J., 'Burning Spalls Efficiently', *Rock Products*, 44 (5), 55 (1941).
- Azbe, V.J., 'Increasing the Capacity of Lime Kilns With Induced Draft Fans', *Rock Products*, 44 (11), 34 (1941).
- Azbe, V.J., 'Lime Experimentation', *Rock Products*, 45 (2-4), 72, 62 & 49 (1942).
- Azbe, V.J., 'A series of papers on Lime', 47 (3, 7 & 9), 58, 53 & 68 (1944).
- Azbe, V.J., 'Economical Manufacture of Quality Lime', 48 (8-10), 92, 81 & 102 (1945).
- Azbe, V.J., 'Instrumentation and Control of the Vertical Kiln', *Rock Products*, 49 (11), 90 (1946).
- Azbe, V.J., 'Efficient Methods of Manufacturing Chemical Lime', *Rock Products*, 50 (9), 86 (1947).
- Azbe, V.J., 'Theory and Practice of Lime Manufacture', *Rock Products*, 56 (2-5, 7, 9 & 12) 100, 102, 138, 84, 80, 100 & 111 (1953); 57, 89 (1954).
- Balazsovics, G., 'Theoretical Investigation of Heat and Mass Transfer in Lime Burning', *Radex Rundschau*, No.1, 434 (1959).
- Balazsovics, G., 'Effect of Heat Transfer on Efficiency of Burning Zone of Lime Shaft Kiln', *Zement Kalk Gips*, 12 (10), 466 (1959).

Balazsovics, G., 'Effect of the Calcining Losses of Burnt Lime on the Dimensions and Designing of the Lime Kilns', Radex Rundschau, No. 5, 324 (1970).

Balazsovics, G., 'Supplements to the Theory of Lime Calcination', Chem. Abstracts, 82 (8), Abst. No. 47193 (1975).

Bangham, D.H., Progress in Coal Science, Butterworths Scientific Publications, London (1950).

Bapat, J.D., 'Engineering Aspects of Lime Manufacture For Building Materials', Proc. Natl. Seminar on Building Materials - Their Science and Technology, New Delhi, April 1982.

Beckenbach, K., 'Annular Shaft Kiln Saves Fuel Costs', Rock Products, 74 (7), 68 (1971).

Bennett, C.O. and Myers, J.E., Momentum, Heat and Mass Transfer, McGraw Hill Book Company, Inc., New York (1962).

Bijawat, H.C., 'Rates and Activation Energy for the Decomposition of Limestone', Chem. and Industry, 331 (1957).

Bird, R.B., Stewart, W.E. and Lightfoot, E.N., Transport Phenomena, Wiley and Sons, Inc., New York (1960).

Boynton, R.S., Chemistry and Technology of Lime and Limestone, Interscience Publishers, New York (1967).

Boyer, A.E., 'Controlled Oxidation of Coal', Chemical Engineering in the Coal Industry by F.W. Sharpley, Pergamon Press, London, 3 (1956).

Brame, J.S.S. and King, J.G., Fuel - Solid Liquid and Gaseous, Edward Arnold (Publishers) Ltd., London (1955).

Brzakovic, P., 'Problems of Determining Lime Kiln Thermal Efficiency', Chem. Abstracts, 82 (8), Abst. No. 47191 (1975).

Bukur, D.B. and Amundson, N.R., 'Fluidized Bed Char Combustion Diffusion Limited Models', Chem. Engng. Sci., 36 (7), 1239 (1981).

Campbell, I.E., High Temperature Technology, John Willey and Sons, Inc., New York (1956).

Chapman, A.J., Heat Transfer, The Macmillan Company, New York (1960).

Chopra, S.K., 'Large Scale Manufacture of Lime', Proc. National Consultation on Development of Lime and Lime Pozzolana Industries and Practices', New Delhi (1985).

Chung, Y.C. and Yun, C.K., 'Detection of Two Moving Boundaries in a Burning Pellet of Coal', Chem. Engng. Sci., 40 (7), 1239 (1985).

Congalidis, J.P. and Georgakis, C., 'Multiplicity Patterns in Atmospheric Fluidized Bed Coal Combustors', Chem. Engng. Sci. 31, 1529 (1981).

Cremer, H.W. and Davies, T., Chemical Engineering Practice, Vol. 2, Butterworths Scientific Publications, London (1956).

Dandois, C.E. and Smithwick, W.J., 'New Shaft Kiln for Lime Production', J. Mining Engineering, 25 (4), 64 (1973).

Das, M.C., 'Modern Gas Fired Vertical Shaft Lime Kiln', Chem. Engng. World, 9 (11), 83 (1974).

Dave, N.G., et.al, 'Some Recent Investigations on Design and Performance of Indian Lime Kilns', Proc. Consultation : Lime-Pozzolana, N.B.O., New Delhi (1977).

- Dave, N.G. and Masood, I., 'Studies of the Existing Lime Kilns in India', Proc. Seminar on Lime : Manufacture and Uses, New Delhi, 98 (1972).
- Eigen, H., 'Increasing Output of Coke Fired Lime Shaft Kiln', 10 (3), 99 (1957).
- Eigen, H., 'Burning of Small Sized Limestone in the Cross-Current Shaft Kiln', Zement Kalk Gips, 10 (9), 346 (1957).
- Eigen, H., 'Problems of Coke Fired Lime Shaft Kiln', Zement Kalk Gips, 10 (12), 504 (1957).
- Eigen, H., 'Technical Limits of Heat Consumption of Coke Fired Lime Shaft Kilns', Zement Kalk Gips, 11 (6) 258 (1958).
- Eigen, H., 'Fresh Knowledge on Coke Fired Lime Shaft Kilns', Zement Kalk Gips, 12 (11), 509 (1959).
- Eigen, H., 'Continuous Operation of Lime Shaft Kilns as Prerequisite for Uniform Quality of Quick Lime', Zement Kalk Gips, 15 (2), 57 (1962).
- Fay, G.C., 'Kiln Design for Fuel Economy', American Ceram. Soc. Bulletin, 60 (5), 561 (1981).
- Fiedler, U., 'Development Trends in Shaft Kilns for Lime Burning', Chem. Abstracts, 84 (3), Abst. No. 33285 (1976).
- Field, M.A., 'Rate of Combustion of Graded Fraction of Char From a Low Rank Coal Between 1200^oK and 2,000^oK', Combustion and Flame, 13, 237 (1969).

Fishwick, J.H., 'Limestone Calcination in Various Atmospheres', *Rock Products*, 73(7), 84(1970).

Flachsenberg, P., 'German Lime Kiln Developments Meet Quality Demands', *Rock Products*, 73 (7), 75 (1970).

Foust, A.S. et.al., *Principles of Unit Operations*, John Wiley and Sons, Inc. N.Y.(1960).

Fuchs, W. and Sandhoff, A.G., 'Theory of Coal Pyrolysis', *Industrial Engineering Chemistry*, 34, 567 (1942).

Furnas, C.C., 'Heat Transfer from a Gas Stream to a Bed of Solids', *Ind. and Engng. Chem.*, 22, 721 (1930) and 'The Rate of Calcination of Limestone', 23, 537 (1931).

Garret, H.M., 'Improving Kiln Thermal Efficiency', *Rock Products*, 77 (5 and 6), 77 and 78 (1974).

Gibbs, R., 'Calcining Rates of Limestone', *Rock Products*, 45 (5), 66 (1942).

Govindakrishnayya, P., 'Oil Firing of Lime Kilns', *Proc. Symposium on Manufacture and Use of Building Lime in India*, Rewa, M.P., 47 (1958).

Gribbin, W., 'Vertical Shaft Kilns-Present and Future', *Rock Products*, 73 (12), 68 (1970).

Griswold, J., *Fuels, Combustion and Furnaces*, McGraw Hill Co. Inc., London (1946).

Henglein, F.A., *Chemical Technology*, Pergamon Press, London (1969).

Hills, A.W.D., 'The Mechanism of Thermal Decomposition of Calcium Carbonate', Chem. Engng. Sci., 23 (4), 297 (1968).

Himus, G.W., 'The Elements of Fuel Technology', Leonard Hills (Books) Ltd., London (1958).

Hoffman, F., 'Present State of Oil Firing Technique for Lime Shaft Kilns', Zement Kalk Gips, 16 (6), 227 (1963).

Holman, L., 'Kiln Draft Control', Pit and Quarry, 42 (11), 115 (1950).

Hottel, H.C. and Stewart, I.M., 'Space Requirements for Combustion of Pulverized Coal', Ind. and Engng. Chem., 32 (5), 719 (1940).

Hougen, O.A., Watson, K.M. and Ragatz, R.A., Chemical process Principles (Part I), John Wiley and Sons, Inc., New York, 255 (1956).

Hussain, A., Chemical Process Simulation, Wiley Eastern Ltd., New Delhi (1986).

I.S.I., Code of Practice for Manufacture of Lime in Vertical Mixed-Feed Type Kilns, I.S.No. 1861, Indian Standards Institution, New Delhi (1961).

I.S.I., Code of Practice for Design and Installation of Lime Kilns, I.S. No. 1849, Indian Standards Institution, New Delhi (1967).

I.S.I., Building Limes, I.S. No. 712, Indian Standards Institution, New Delhi (1973).

Jeschar, R., 'Process Engineering Problems of Lime Shaft Kilns', Zement Kalk Gips, 24 (1), 1 (1971).

Johnson, A.J. and Auth, G.H., Fuels and Combustion Handbook, McGraw Hill Book Company, Inc. (1951).

Jussen, R. and Schwarze, W., 'Coal and Natural Gas Firing in a Lime Shaft Kiln', Zement Kalk Gips, 27 (4), 190 (1974).

Kitaev, B.I., et. al., Heat Exchange in Shaft Furnaces, Pergamon Press, London (1967).

Knibbs, N.V.S. and Gee, B.J., Lime and Limestone', Salem Engineering Ltd. (1959).

Koloberdin, V.I., Blinichev, V.N. and Streltsov, V.V., 'Kinetics of Thermal Decomposition of Carbonates', Intl. Chem. Engng., 12 (2 and 1), 276 and 101 (1972 and 1975).

Koloberdin, V.I., Trefonov, I.I. and Putnikov, N.A., 'Study of the Effect of Shape of Limestone Particles on Their Rate of Calcination', Chem. Abstracts, 85 (4), Abst. No. 48851 (1976).

Kunii, D. and Levenspiel, O., Fluidization Engineering, John Wiley and Sons, Inc., 433 (1962).

Lapidus, L. and Amundson, N.R., Chemical Reactor Theory, Prentice Hall inc., New Jersey (1977).

Lees, F.P., Loss Prevention in the Process Industries, Butterworths, London (1980).

Levenspiel, O., Chemical Reaction Engineering, Second Edition, Wiley Eastern Ltd., New Delhi (1975).

Li, J.B., et. al, 'Theoretical Decomposition of Limestone', Chem. Abstracts, 85 (2), Abst. No. 24885 (1976).

Libby, P.A. and Blake, T.R., 'Theoretical Study of Burning Carbon Particles', Combustion and Flame, 36 (2), 139 (1979).

Lowe, A., Wall, T.F. and Stewart, I.M.C., 'Combustion Kinetics in the Modeling of Large Pulverized Fuel Furnaces', A.I.Ch.E. Journal, 23 (4), 440 (1977).

Lowry, H.H., Chemistry of Coal Utilization, Vol. I, Chapman and Hall Ltd., London (1945).

Macedo, N., 'Factors in the Design and Economic Operation of a Lime Kiln', Proc. Symposium on Manufacture and Use of Building Lime in India, Rewa, M.P., 47 (1958).

Macedo, N., 'Current Practices of Lime Burning in Shaft Kilns and Scope for Improvement', Seminar on Building Limes, Problems of Raw Materials, Burning, Hydration and New Uses, New Delhi (1967).

Macrae, J.C., An Introduction to the Study of Fuel, Elsevier Publishing Company, Amsterdam, London, New York (1966).

Majumdar, B.K., 'Coal Systematics : Deductions From Proximate Analysis', J.S.I.R., 13 (12), 857 (1954).

Middlemas, J.W., 'New Oil Fired Lime Shaft Kiln', Zement Kalk Gips, 17 (6), 263 (1964).

Middlemas, J.W., 'Lime Burning and Development of Oil Fired Lime Kilns', Inst. Fuel Journal, 36 (269), 244 (1963).

Munrow, W.D. and Amundson, N.R., 'Solid Fluid Heat Exchange in Moving Beds', Ind. Eng. Chem. 42 (8), 1481 (1950).

Murray, J.A., 'Specific Heat Data for Evaluation of Lime Kiln Performance', *Rock Products*, 50 (8), 148 (1947).

Murray, J.A. et. al, 'Shrinkage of High Calcium Limestones During Burning', *J. Amer. ceram. Soc.*, 37 (7), 323 (1954).

Narsimhan, G., 'Theoretical Decomposition of Calcium Carbonate', *Chem. Engng. Sci.*, 16 (1-2), 7(1961).

Nelson, W.L., *Petroleum Refinery Engineering*, McGraw-Hill Book Company, Inc., New York (1958).

Parker, A.S. and Hottel, H.C., 'Rate of Combustion of Carbon', *Ind. & Engng. Chem.*, 28 (8), 1334 (1936).

Parson, M.F., 'New Approach to Vertical Shaft Kiln', *Pit and Quarry*, 57 (2), 124 (1964).

Perry, R.H. and Chilton, C.H., *Chemical Engineers Hand Book*, Fourth Edition, McGraw Hill Book Co. Inc., N.Y. (1968).

Rai, M. and Sharma, C.S., 'A study of Lime Industry in Dehradun', *Indian Bullder*, 14 (11), 20 (1966).

Ross, I.B. and Davidson, J.F., 'The Comustion of Carbon Particles in a Fluidized Bed', *Chem. Engng. Res. & Design : Transactions of the Institution of Chem. Engrs.*, 60 (2), 108 (1982).

Ruch, H., 'Measurement and Control Engineering in Lime Burning', *Zement Kalk Gips*, 26 (6), 257 (1973).

Ruch, H., 'The Theoretical Limits of Heat Consumption in Lime Burning Considered on the Basis of Physico-Chemical Relationships', *Zement Kalk Gips*, 34 (1), 20 (1981).

Satterfield, C.N. and Feakes, F., 'Kinetics of the Thermal Decomposition of Calcium Carbonate', A.I.Ch.E. Journal, 5 (1), 115 (1959).

Schwarzkopf, F., 'Comparison of Modern Lime Calcining Systems', Rock Products, 73 (7), 68 (1970).

Shafer, R.R., 'Lime Calcining Options', Rock Products, 84 (10), 60 (1981).

Sharpley, F.W., Chemical Engineering in the Coal Industry, Pergamon Press, London, New York (1956).

Shaw, A.K., Combustion Engineering and Fuel Technology, Oxford and I.B.H. Publishing Company, New Delhi, Bombay, Calcutta (1974).

Shiele, E. and Berens, L.W., 'Effect of Shaft Kiln Design on the Properties of Quick Lime, Zement Kalk Gips, 27 (1) (1974).

Smith, J.M., Chemical Engineering Kinetics, 2nd Edition, McGraw Hill Book Company, Inc., New York (1970).

Smith, M.L. and Stinson, K.W., Fuels and Combustion, McGraw Hill Book Company, Inc., New York (1952).

Sobek, F., 'Comparison Between Flameless Burning Process and Traditional Burning Methods, Masalah Bangunan, 22 (2), 8 (1977).

Spence, R., 'Lime and Surkhi Manufacture in India', Appropriate Technology, 1 (4), 6 (1974-75).

Szep, A. et.al., 'Determination of Specific Coal Consumption During Limestone and Dolomite Decomposition', Chem. Abstracts, 98 (7), Abst. No. 109810, 139 (1983).

- Tanski, E.S., 'Kiln Efficiencies', Pit and Quarry, 54 (8), 97 (1962).
- Thring, M.W., Science of Flames and Furnaces, Chapman and Hall Ltd., London (1962).
- Transtel, S. and Ulrich, W., 'The Mechanism of Limestone Calcination', Cement Lime and Gravel, No. 11, 388 (1965).
- Tu, C.M., Davis, H. and Hottel, H.C., 'Combustion on Rate of Carbon', Ind. & Engng. Chem., 26, 749 (1934).
- Vankrevelin, D.W., Coal Science, Elsevier Publishing Company, New York, London (1957).
- Verma, C.L. and Dave N.G., 'Design of Mixed Feed Lime Shaft Kilns', Proc. Natl. Seminar on Building Materials - Their Science and Technology, New Delhi (1982).
- Verma, C.L. and Saxena, N.B., 'Trends in the Design and Development of Lime Shaft Kilns', Chem. Concepts, 5 (9), 23 (1978).
- Verma, C.L. and Saxena, N.B., 'A Performance Study of Some Low Capacity Mixed-Feed Lime Kilns With Special Reference to Conical Kilns', Chemical Age of India, 29 (7), 575 (1978).
- Verma, S.K., Majumdar, S.N. and Sen, M.M., 'The Manufacture of Lime and its Fuel Utilization Pattern and Problems', Proc. National Consultation on Development of Lime and Lime Pozzolana Industries and Practices, New Delhi (1985).
- Walas, S.M., Reaction Kinetics for Chemical Engineers, McGraw Hill Book Company, Inc., New York (1959).
- Weisz, W.H., 'Kiln Performance Chartered from Studies of Gas Analysis', Rock Products, 55 (3), 88 (1952).

Wuhrer, J., 'Theory of Burning of Small Sized Limestone', Zement Kalk Gips, 16 (6), 219 (1963).

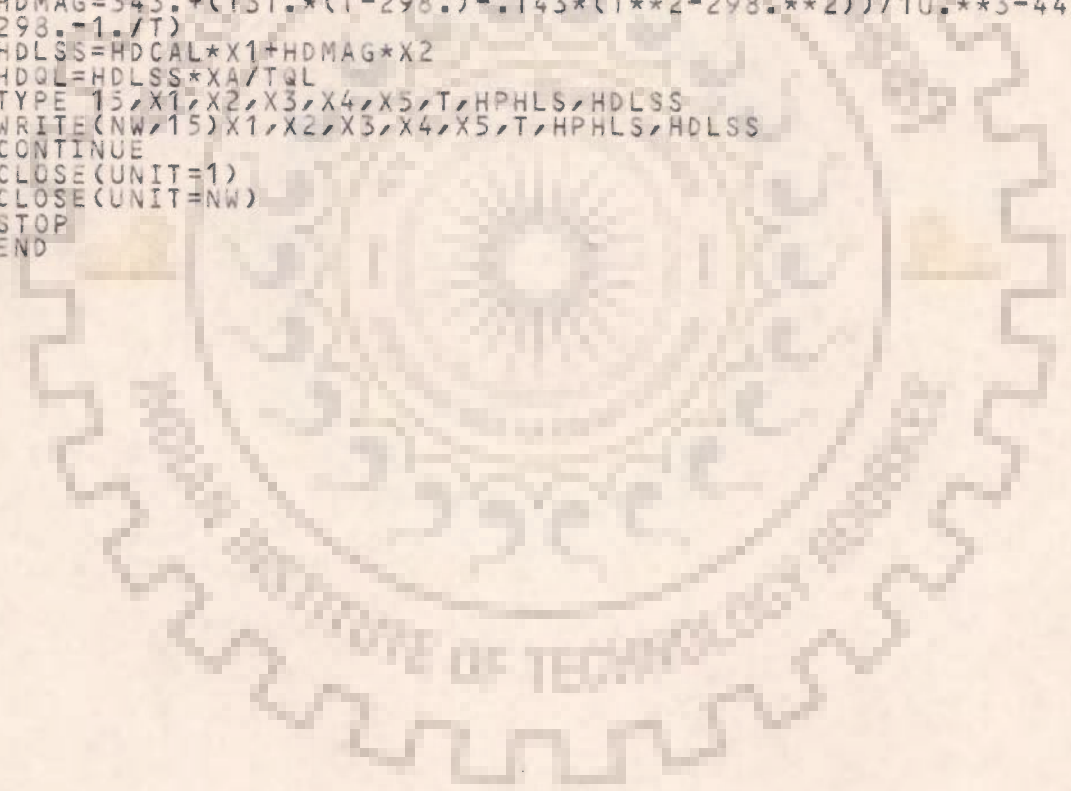
Zuideveld, P.L. and Vandenberg, P.J., 'Design of Lime Shaft Kilns', Chem. Engng. Sci., 26 (6), 875 (1971).



```

C *****
C ***** ENERGY REQUIREMENTS IN LIME BURNING *****
C *****
OPEN(UNIT=1,NAME='ELB.DAT',TYPE='OLD')
READ(1,*)NW,N
OPEN(UNIT=NW,NAME='ELBRES.OUT',TYPE='NEW')
WRITE(NW,5)
WRITE(NW,10)
5  FORMAT(22X,'ENERGY REQUIREMENTS IN LIME BURNING'//)
10  FORMAT(/,          X1          X2          X3          X4          X5
1  T(K)          HPHLS          HDLSS'//)
15  FORMAT(5F10.3,F10.1,2F10.2)
DO20J=1,N
READ(1,*)X1,X2,X3,X4,X5,T
CAO=0.560*X1*XA
OMG=0.476*X2*XA
TQL=CAO+OMG
C PREHEATING ENERGY PER KG OF LIMESTONE SAMPLE (HPHLS)
ALPHA=0.1968*X1+0.1216*X2+0.1312*X3+0.2165*X4+0.1543*X5
BETA=(0.1189*X1+0.333*X2+0.1452*X3+0.0879*X4+.1*X5)/10.**3
GAMMA=(0.3076*X1+0.0379*X2+0.4020*X3+0.5125*X4+0.2650*X5)*10.**4
HPHLS=ALPHA*(T-298.)+(BETA/2.)*(T**2-298.**2)-GAMMA*(1./298.-1./T)
C HPHQL=HPHLS/TQL
C HEAT OF DISSOCIATION PER KG OF LIMESTONE (HDLSS)
1  HDCAL=425.+(6.6*(T-298.)-.02155*(T**2-298.**2))/10.**3+41.*(1./
1  298.-1./T)
HDMAG=343.+(131.*(T-298.)-.143*(T**2-298.**2))/10.**3-4430.*(1./
HDLSS=HDCAL*X1+HDMAG*X2
HDQL=HDLSS*XA/TQL
C TYPE 15,X1,X2,X3,X4,X5,T,HPHLS,HDLSS
20 WRITE(NW,15)X1,X2,X3,X4,X5,T,HPHLS,HDLSS
CONTINUE
CLOSE(UNIT=1)
CLOSE(UNIT=NW)
STOP
END

```



```

*****
STATE-OF-THE-ART PROCESS ENGINEERING COMPUTATIONS FOR THE
DESIGN OF COAL-FIRED LIME SHAFT KILNS
*****
OPEN(UNIT=1,FILE='LKD.DAT',TYPE='OLD')
READ(1,*) NW
OPEN(UNIT=NW,FILE='LKDRES.OUT',TYPE='NEW')
READ(1,*) PS,TPD,DPS
READ(1,*) XFA,XFV,XP,XS
READ(1,*) RHOBFO,RHOBFO,RHOBFO
READ(1,*) ES,HF,ETAL,FAS
READ(1,*) ANS,AND,ALC,THETAD
WRITE(NW,20)
WRITE(NW,25)
WRITE(NW,05) NW
WRITE(NW,10) PS,TPD,DPS
WRITE(NW,15) XFA,XFV,XP,XU
WRITE(NW,10) RHOBFO,RHOBFO,RHOBFO
WRITE(NW,15) ES,HF,ETAL,FAS
WRITE(NW,15) ANS,AND,ALC,THETAD
WRITE(NW,30)
5  FORMAT(38X,I4)
10  FORMAT(24X,3F12.4)
15  FORMAT(16X,4F12.4)
20  FORMAT(11X,'PROCESS ENGINEERING DESIGN OF COAL-FIRED
25  1 LIME SHAFT KILNS')
30  FORMAT(7/31X,'AVERAGE INPUT DATA')
35  FORMAT(7/28X,23HRESULTS OF COMPUTATIONS)
40  FORMAT(7/2X,69HLIMESTONE-TO-FUEL RATIO BY WEIGHT IN FEED
45  1 INPUT AT TOP OF LIME KILN =,F6.3)
50  FORMAT(7/14X,'RETENTION TIMES (IN HOURS) FOR CONTINUOUS
55  1 OPERATION :')
60  FORMAT(10X,'PREHEATING',13X,'BURNING',13X,'COOLING
65  1',4X,'OVERALL FOR KILN')
70  FORMAT(4F20.3)
75  FORMAT(7X,'HEIGHTS OF THE VARIOUS ZONES (IN METERS) FOR
1 CONTINUOUS OPERATION :')
2  FORMAT(7/12X,47HAVERAGE INNER DIAMETER OF THE LIME SHAFT KILN =,
3  1F6.3,' M')
4  FORMAT(5X,'PREHEATING ZONE',8X,'BURNING ZONE',8X,'COOLING
5  1 ZONE',4X,'EFFECTIVE HEIGHT')
6  FORMAT(7/16X,38HNOMINAL DESIGN CAPACITY OF LIME KILN =,
7  1F5.2,' TPD')
8  AREA=TPD/PS
9  RI=SQRT(AREA/3.14)
10 DI=2.*RI
11 XU=1.-XS
12 XR=HF*ETAL/(ES*(1.-XU))
13 THETAP=(686.*DPS**1.5)/(FAS*SQRT(PS))
14 THETAB=6350.*DPS*(0.052*DPS+1./((20.25+180.*DPS+6.75*SQRT(
15  1PS/DPS))*FAS))
16 THETAC=(488.*DPS**1.5)/(FAS*SQRT(PS))
17 THETAT=THETAP+THETAB+THETAC
18 RHOBM=RHOBFO*RHOBFO*(1.+XR)/(RHOBFO+XR*RHOBFO)
19 XRDASH=XR/(1.-XFV)
20 RHOBMD=RHOBFO*RHOBFO*(1.+XRDASH)/(RHOBFO+XRDASH*RHOBFO)
21 HPZ=74.3*(1.+XR)*PS*THETAP/(XP*XS*XR*RHOBM)
22 HBZ=74.3*(1.+XRDASH)*PS*THETAB/(XP*XS*XRDASH*RHOBMD)
23 HCZ=(41.7+74.3*XFA/(XS*XR)+74.3*(1.-XS)/XS)*PS*THETAC/
24 1(XP*RHOBFO)
25 HOVRAL=HPZ+HBZ+HCZ
26 WRITE(NW,75) TPD
27 WRITE(NW,35) XR
28 WRITE(NW,65) DI
29 WRITE(NW,40)
30 WRITE(NW,45)
31 WRITE(NW,50) THETAP,THETAB,THETAC,THETAT
32 WRITE(NW,55)
33 WRITE(NW,70)
34 WRITE(NW,50) HPZ,HBZ,HCZ,HOVRAL
35 CLOSE(UNIT=1)
36 CLOSE(UNIT=NW)
37 STOP
38 END

```

```

*****
PROGRAMME FOR SIMULATION OF LIME SHAFT KILN :
STARTING FROM TOP OF THE KILN
*****
DIMENSION TG(400),TF(400),TS(400)
DIMENSION TGGG(400),TFFF(400),TSSS(400)
DIMENSION MG(400),MF(400),XR(400),XF(400)
DIMENSION TITLE(80),STITLE(80),DATAIN(80),RESTAB(80)
REAL KG,MUG,MG,MF,MSF
OPEN(UNIT=1,FILE='PDV.DAT',TYPE='OLD')
READ(1,15) TITLE
READ(1,15) STITLE
READ(1,15) DATAIN
READ(1,15) RESTAB
READ(1,*) NP,NW,NPRINT
OPEN(UNIT=NW,FILE='PDVRES.OUT',TYPE='NEW')
OPEN(UNIT=NP,FILE='PDVPLT.OUT',TYPE='NEW')
*****
THE FORTRAN VARIABLES USED IN THE FOLLOWING INPUT STATEMENTS
ARE DEFINED SUBSEQUENT TO EACH STATEMENT GENERALLY IN ORDER
OF THEIR APPEARANCE
*****
READ(1,*) TG(1),TF(1),TS(1)
(BULK GAS TEMPERATURE,FUEL TEMPERATURE AND STONE
SURFACE TEMPERATURE)
READ(1,*) PS,XRINF,TPD
(SUPERFICIAL PRODUCT OUTPUT RATE BASED ON EMPTY KILN
CROSS-SECTION,LIMESTONE-TO-FUEL-RATIO IN FEED MIX,
NOMINAL PRODUCTION RATE OF LIME SHAFT KILN)
READ(1,*) DPS,DPF,PHIS,PHIF,EBED,DZ
(PARTICLE SIZE OF LIMESTONE,PARTICLE SIZE OF FUEL,
SPHERICITY OF STONE PARTICLE,SPHERICITY OF FUEL
PARTICLE,BED POROSITY,AXIAL WIDTH OF DIFFERENTIAL
ELEMENT)
READ(1,*) XFM,XFV,XFC,XFA,XEA
(FRACTIONAL MOISTURE CONTENT,VOLATILE MATTER,FIXED
CARBON,ASH CONTENT AND FRACTIONAL EXCESS AIR)
READ(1,*) RHOFO,RHOSO,CFO,HLTWTR,HLTDVM
(DENSITY OF FUEL,STONE PARTICLES,SPECIFIC HEAT OF
FUEL,HEAT OF DESORPTION-CUM-DEMOISTURIZATION FROM
FUEL,LATENT HEAT OF DEVOLATILIZATION)
READ(1,*) ETASG,ETAFG,ETAFS,ETAFC,ETAGW
(EFFECTIVENESS FACTORS FOR HEAT EXCHANGE FROM STONE
TO GAS,FUEL TO GAS,FUEL TO STONE,ETC.)
READ(1,*) ALPHA,GAMMA,UNTDZ,UNTDVZ
(CONSTANTS TO ACCOUNT FOR GAS EMISSIVITIES,DEMOISTUR-
IZATION AND DEVOLATILIZATION PROCESSES)
READ(1,*) FBCTY,RBCTY,FBTHK,RBTHK,REMSY,TAMB,TWOPDV
(THERMAL CONDUCTIVITY OF FIRE BRICKS,RED BURNT CLAY
BRICKS,THICKNESS OF FIRE BRICKS INSULATION,BURNT
CLAY BRICKS,EMISSIVITY OF RED BRICKS SURFACE,AMBIENT
TEMPERATURE AND EXTERNAL WALL TEMPERATURE)
READ(1,*) KG,MUG,TKS,RGAS,SIGMAR,EMSVTY,VIEWFO
(GAS THERMAL CONDUCTIVITY,VISCOSITY,THERMAL CONDUCTI-
VITY OF COAL,VIEW FACTOR)
READ(1,*) TPHZ,TPHDVZ,TPHCVM,TOLER1,TCLER2
(TEMPERATURES FOR ONSET OF DEVOLATILIZATION PROCESS,
COMBUSTION OF VOLATILE MATTER,COMPLETION OF VM EVOLU-
TION AND TOLERANCES)
READ(1,*) IMAX,ITMAX,IRANDM,MINLMT,MAXLMT
(CONSTANTS,MAXIMUM/MINIMUM VALUES)
WRITE(NW,85) TITLE
WRITE(NW,85) STITLE
WRITE(NW,90) DATAIN
WRITE(NW,23) NP,NW,NPRINT
WRITE(NW,30) TG(1),TF(1),TS(1)
WRITE(NW,30) PS,XRINF,TPD
WRITE(NW,50) DPS,DPF,PHIS,PHIF,EBED,DZ
WRITE(NW,45) XFM,XFV,XFC,XFA,XEA
WRITE(NW,45) RHOFO,RHOSO,CFO,HLTWTR,HLTDVM
WRITE(NW,45) ETASG,ETAFG,ETAFS,ETAFC,ETAGW
WRITE(NW,10) ALPHA,GAMMA,UNTDZ,UNTDVZ
WRITE(NW,40) FBCTY,RBCTY,FBTHK,RBTHK,REMSY,TAMB,TWOPDV
WRITE(NW,35) KG,MUG,TKS,RGAS,SIGMAR,EMSVTY,VIEWFO
WRITE(NW,45) TPHZ,TPHDVZ,TPHCVM,TOLER1,TCLER2
WRITE(NW,55) IMAX,ITMAX,IRANDM,MINLMT,MAXLMT

```



```

RO=RFB+RBTHIK
DO=2.*RO
CSTKLN=(ALOG(RFB/RI)/FBCDTY)+(ALOG(RO/RFB)/RBCDTY)
BETA=XFM+XFV*(TPHDVZ-TPHZ)/(TPHCVM-TPHZ)
I=1
XF(1)=0.0
MG(1)=WA+WF*(1.-XFA)+WS*0.44
MF(1)=WF*(1.0-XF(1))
XR(1)=WS/MF(1)
MSF=WS+MF(1)
WGN2T=WA*0.768
WGO2T=WA*.232-WF*((XFC*32./12.)-(XFMAX-BETA)*(77.77/20.))
WGCO2T=WS*0.44+WF*XFC*(44./12.)+WF*(XFMAX-BETA)*(56.58/20.)
WGH2OT=WF*(XFM+(XFMAX-BETA)*(41.15/20.))
WGVMT=WF*(BETA-XFM)
WGTTLT=WGN2T+WGO2T+WGCO2T+WGH2OT+WGVMT
TWO=TWOPDV

```

2

```

TGAVG=TG(I)
TFAVG=TF(I)
TSAVG=TS(I)
TSOLD=TSAVG
TFOLD=TFAVG
TGOLD=TGAVG
XFAVG=XF(I)
WGAVG=MG(I)
WFAVG=MF(I)
WSAVG=WS
WAVGTL=WGAVG+WFAVG+WSAVG
XWG=WGAVG/WAVGTL
XWF=WFAVG/WAVGTL
XWS=WSAVG/WAVGTL
TEOPRG=TGAVG*XWG+TFAVG*XWF+TSAVG*XWS

```

C
C
C

```

*****
SPECIFIC HEATS OF VARIOUS CONSTITUENTS
*****
CPO2=0.2584+(0.3063*TGAVG*10.**-5)-5865.6/(TGAVG**2)
CPCO2=0.1441+(0.2305*TGAVG*10.**-3)-(0.0776*10.**-6)/(TGAVG**2)
CPCO2F=0.1441+(0.2305*TFAVG*10.**-3)-(0.0776*10.**-6)/(TFAVG**2)
CPAIR=0.2372+(0.2900*TGAVG*10.**-4)-1360./(TGAVG**2)
CPWTRG=.4567+(0.3333*TGAVG*10.**-5)+(0.7444*TGAVG*TGAVG*10.**-7)
CPWTRF=.4567+(0.3333*TFAVG*10.**-5)+(0.7444*TFAVG*TFAVG*10.**-7)
CPVMG=0.2138+(0.6194*TGAVG*10.**-3)+(0.0800*TGAVG*TGAVG*10.**-6)
CPVMF=0.2138+(0.6194*TFAVG*10.**-3)+(0.0800*TFAVG*TFAVG*10.**-6)
CS=0.1968+(0.1189*TSAVG*10.**-3)-(0.3076*10.**4)/(TSAVG**2)
CF=CFO+(XFAVG/XFMAX)*(CFMAX-CFO)

```

C

```

*****
DPAVG=(DPS*WSAVG+DPF*WFAVG)/(WSAVG+WFAVG)
XRAVG=WSAVG/WFAVG
TGI=TGAVG
TKF=((TKEMAX-TKFMIN)*XFAVG+(TKFMIN*XFMAX-TKFMAX*XFMIN))/
1*(XFMAX-XFMIN)
EFFKS=TKS*TKF/(TKS+TKF)
WGNZZ=WGN2T
IF(XFAVG.LE.BETA) WGOZZ=WGO2T
IF(XFAVG.GT.BETA) WGOZZ=WGO2T+WF*(XFAVG-BETA)*(77.77/20.)
IF(XFAVG.LE.BETA) WGCOZZ=WGCO2T
IF(XFAVG.GT.BETA) WGCOZZ=WGCO2T-WF*(XFAVG-BETA)*(56.58/20.)
IF(XFAVG.EQ.XFMIN) WGH2OZ=WGH2OT
IF(XFAVG.GT.XFMIN.AND.XFAVG.LE.XFM) WGH2OZ=WGH2OT-
1*WF*(XFAVG-XFMIN)
IF(XFAVG.GE.XFM.AND.XFAVG.LE.BETA) WGH2OZ=WGH2OT-WF*(XFM-XFMIN)
IF(XFAVG.GT.BETA) WGH2OZ=WGH2OT-WF*(XFM-XFMIN)-WF*
1*(XFAVG-BETA)*(41.15/20.)
IF(XFAVG.LE.BETA) WGVMZ=WGVMT
IF(XFAVG.GT.BETA) WGVMZ=0.0
WGAIRZ=WGNZZ+WGOZZ
WGTTLZ=WGAIRZ+WGCOZZ+WGH2OZ+WGVMZ
XGAIRZ=WGAIRZ/WGTTLZ
XGCOZZ=WGCOZZ/WGTTLZ
XGH2OZ=WGH2OZ/WGTTLZ
XGVMZ=WGVMZ/WGTTLZ
CG=CPAIR*XGAIRZ+CPCO2*XGCOZZ+CPWTRG*XGH2OZ+CPVMG*XGVMZ
IF(I.GT.1) GO TO 23
CGTOP=CG
RHOF=RHOFC*(1.-XFAVG)
ASSPZ=ETASG
ASFPZ=ETAFG
ASFRPZ=ETAFFS
G=WGAVG/AREA
CORFAC=1.-(ALPHA*(XFAVG-XFMIN)/(BETA-XFMIN))

```

23

```

IF(TF(I).LT.TPHDVZ) GO TO 16
IF(BETACV.GT.C.) GO TO 13
BETACV=XF(I)
HEIGHT=(FLOAT(I)-1.)*DZ
13 CONTINUE
ASSPZ=ETASG
ASFPZ=ETAFG
ASFRPZ=ETAFSC
KG=0.044C
MUG=0.1296
CORFAC=(1.-ALPHA)-((GAMMA-ALPHA)*(XFAVG-BETACV)/(1.-XFA-BETACV))
C *****
C HEAT TRANSFER COEFFICIENTS
C *****
16 HCHRFS=HFS(EFFKS,DPS,DPF,EMSVTY,SIGMAR,VIEWF,TFAVG,TSAVG)
HCHRSG=HSG(EBED,DPS,KG,MUG,CG,G,CORFAC)
HCHRFG=HFG(EBED,DPF,KG,MUG,CG,G,CORFAC)
C *****
IF(I.EQ.1) GO TO 36
QFS=HCHRFS*(TFAVG-TSAVG)*AFPZ*ASFRPZ*AREA*DZ
QFG=HCHRFG*(TFAVG-TGAVG)*AFPZ*ASFPZ*AREA*DZ
QSG=HCHRSG*(TSAVG-TGAVG)*ASPZ*ASSPZ*AREA*DZ
GO TO 37
36 ENGASI=MG(I)*CG*(TG(I)-273.0)
ENSTNI=WS*CS*(TS(I)-273.0)
ENFULI=MF(I)*CF*(TF(I)-273.0)
37 Z=(FLOAT(I)-1.)*DZ
Y=(I/NPRINT)-FLOAT(I)/FLCAT(NPRINT)
IF(Y.NE.0) GO TO 3
C WRITE(NW,55)Z,XF(I),TG(I),TF(I),TS(I)
TYPE 95,Z,XF(I),TG(I),TF(I),TS(I)
WRITE(NP,120)Z,XF(I),TG(I),TF(I),TS(I)
WRITE(NW,75)I,Z,XF(I),TG(I),TF(I),TS(I),TWO,
3 1HCHRFS,HCHRFG,HCHRSG,ASPZ,AFPZ,QFS,QFG,QSG,DELHTL
IF((TS(I).LT.TS(I-1)).OR.(XF(I).LT.XF(I-1))) GO TO 21
IF(TF(I).GE.TPHCVM.AND.HVM.EQ.D.) GO TO 21
IF(XF(I).GE.XFMAX.AND.HVM.GT.C.) GO TO 21
IF(XF(I).GE.XFMAX.AND.TF(I).GE.TPHCVM) GO TO 21
IF(TS(I).GE.TPHCVM) GO TO 21
IF(TF(I).GE.TPHDVZ) GO TO 21
I=I+1
IF(I.GT.IMAX) GO TO 21
ITER=1
IF(TF(I-1).GT.TPHZ.AND.TF(I-1).LT.TPHDVZ) GO TO 33
TGGG(ITER)=TG(I-1)
TFFF(ITER)=TF(I-1)
TSSS(ITER)=TS(I-1)
GO TO 34
33 IF(XF(I-4).LE.XFMIN) GO TO 28
XFASNM=(2.*XF(I-1)-3.*XF(I-2)+XF(I-3))*(XF(I-1)-XF(I-2))
XFASDN=2.*XF(I-2)-3.*XF(I-3)+XF(I-4)
IF(XFASDN.EQ.C.) GO TO 28
XF(I)=XF(I-1)+XFASNM/XFASDN
GO TO 29
28 XF(I)=3.*XF(I-1)-3.*XF(I-2)+XF(I-3)
29 TG(I)=3.*TG(I-1)-3.*TG(I-2)+TG(I-3)
TF(I)=3.*TF(I-1)-3.*TF(I-2)+TF(I-3)
TS(I)=3.*TS(I-1)-3.*TS(I-2)+TS(I-3)
DELTG=TG(I)-TG(I-1)
DELTF=TF(I)-TF(I-1)
DELTS=TS(I)-TS(I-1)
DLTGIP=DELTG
DLTFIP=DELTF
DLTSIP=DELTS
TGIP=TG(I)
TFIP=TF(I)
TSIP=TS(I)
TGGG(ITER)=TGIP
TFFF(ITER)=TFIP
TSSS(ITER)=TSIP
C *****
C ESTIMATION OF WALL HEAT LOSSES
C *****
34 DELTWO=TWOPDV-TAMB
AHWA=HWA(DZ,REEMSY,SIGMAR,TWOPDV,TAMB,DELTWO)
AHGW=HGW(EBED,DPAVG,DI,KG,MUG,G,CORFAC,ETAGW)
IF(AHWA.EQ.0.) GO TO 9
UIEFFI=RI*(1./(RI*AHGW)+CSTKLN+1./(RO*AHWA))
UIEFF=1./UIEFFI
DELHL=UIEFF*2.*3.14*RI*DZ*(TGI-TAMB)

```

DELHTL=DELHTL+DELHL
TWI=TGI-DELHL/(3.14*DI*DZ*AHGW)
TWO=TAMB+DELHL/(3.14*DO*DZ*AHWA)
TWOPDV=TW

C *****
9 IF(TF(I-1)-373.0) 1,1,4
1 XF(I)=XF(I-1)
DELXF=0.0
XFAVG=XF(I)
HVM=0.0
GO TO 7

C *****
4 IF(TF(I-1)-TPHZ) 5,5,6
C DEGREE OF DEMOISTURIZATION OF FUEL
C *****
5 DELXF=(0.99999*XFM-XFMIN)/UNDMZ
XF(I)=XF(I-1)+DELXF
IF(XF(I).GE.(0.99999*XFM)) XF(I)=0.99999*XFM
DELXF=XF(I)-XF(I-1)
XFAVG=(XF(I-1)+XF(I))/2.0
HVM=0.0
GO TO 7

6 IF(XF(I-1).EQ.BETACV) GO TO 11
IF(XF(I-1).EQ.XFMAX) GO TO 21
IF(BETACV.GT.0.) GO TO 11
IF(TF(I-1)-TPHDVZ) 8,8,11

C *****
C DEGREE OF DEVOLATILIZATION WITHOUT COMBUSTION OF VM
C *****
8 DELXF=(XFV/(TPHCVM-TPHZ))*DELTF
XF(I)=XF(I-1)+DELXF
IF(XF(I).GE.(0.99999*XFMAX)) XF(I)=XFMAX
XFAVG=(XF(I-1)+XF(I))/2.0
HVM=0.0
GO TO 7

C *****
C PROVISION FOR COMPUTATION OF DEGREE OF DEVOLATILIZATION WITH
C COMBUSTION OF VM
C *****

11 DELXF=(XFMAX-BETACV)/UNTDVZ
IF(XFV.EQ.0.) DELXF=0.0
XF(I)=XF(I-1)+DELXF
IF(XF(I).GE.(0.99999*XFMAX)) XF(I)=XFMAX
XFAVG=(XF(I-1)+XF(I))/2.0
HVM=HFVM

7 IF(XFV.EQ.0.) HVM=0.0
DELMF=-WF*DELXF
MF(I)=MF(I-1)+DELMF
DELMG=-WF*DELXF
MG(I)=MG(I-1)+DELMG
WFAVG=(MF(I-1)+MF(I))/2.0
MSF=WS+WFAVG
WGAVG=(MG(I-1)+MG(I))/2.0
XR(I)=WS/MF(I)

C *****
C HEAT BALANCE FOR LIMESTONES
C *****

ALSB1=HCHRES*(TFAVG-TSAVG)*AFPZ*ASFRPZ*AREA*DZ
ALSB2=HCHRSG*(TSAVG-TGAVG)*ASPZ*ASSPZ*AREA*DZ
ALSBT=ALSB1-ALSB2
DELTS=ALSBT/(WS*CS)
IF(TF(I-1).GT.TPHZ.AND.TF(I-1).LT.TPHDVZ) DELTS=
1(DELTS+DLTSIP)/2.0
TS(I)=TS(I-1)+DELTS
TSAVG=(TS(I-1)+TS(I))/2.0

C *****
C GAS PHASE HEAT BALANCE
C *****

ALGB1=HCHFRFG*(TFAVG-TGAVG)*AFPZ*ASFRPZ*AREA*DZ
ALGB2=HCHRSG*(TSAVG-TGAVG)*ASPZ*ASSPZ*AREA*DZ
IF(TF(I-1).LT.373.0) ALGB3=0.0
IF(TF(I-1).GT.373.0.AND.XF(I-1).LT.XFM) ALGB3=
1WF*DELXF*CPWTRF*(TFAVG-273.0)
IF(XF(I-1).GE.(0.99999*XFM).AND.TF(I-1).LT.TPHZ) ALGB3=0.0
IF(TF(I-1).GT.TPHZ.AND.HVM.EQ.0.) ALGB3=
1WF*DELXF*CPVMF*(TFAVG-273.0)
IF(HVM.EQ.0.) GO TO 24
ALGB3=0.0
ALGB4=-WF*DELXF*(77.77/20.)*CPO2*(TGAVG-273.0)
ALGB5=WF*DELXF*(56.58/20.)*CPCO2F*(TFAVG-273.0)


```

24 ALGB6=WF*DELXF*(41.15/20.)*CPWTRF*(TFAVG-273.0)
ALGBT=ALGB1+ALGB2+ALGB3+ALGB4+ALGB5+ALGB6
ALGBT=ALGBT-DELHL
ALGBN=ALGBT+CG*(TGAVG-273.0)*DELMG
DELTG=-ALGBN/(CG*WGAVG)
IF(TF(I-1).GT.TPHZ.AND.TF(I-1).LT.TPHDVZ) DELTG=
1(DELTG+DLTGIP)/2.0
TG(I)=TG(I-1)+DELTG
TGAVG=(TG(I-1)+TG(I))/2.0
C *****
27 IF(TF(I-1).LT.373.0)ALFBT=0.0
IF(TF(I-1).GT.373.0.AND.XF(I-1).LT.XFM)ALFBT=-WF*DELXF*HLTWTR
IF(XF(I-1).GE.(.99999*XFM).AND.TF(I-1).LE.TPHZ) ALFBT=0.0
IF(TF(I-1).GT.TPHZ.AND.TF(I-1).LT.TPHDVZ)ALFBT=-WF*DELXF*HLTDVM
IF(TF(I-1).GT.TPHDVZ.AND.HVM.GT.0.)ALFBT=WF*HVM*DELXF+
1WF*DELXF*(77.77/20.)*CPO2*(TGAVG-273.0)-WF*DELXF*HLTDVM
C *****
C HEAT BALANCE FOR FUEL
C *****
ARFB1=HCHRF*(TFAVG-TSAVG)*AFPZ*ASFRPZ*AREA*DZ
ARFB2=HCHRF*(TFAVG-TGAVG)*AFPZ*ASEPZ*AREA*DZ
ARFB3=-WF*CF*(TFAVG-273.0)*DELXF
IF(TF(I-1).LT.373.0) ARFB4=0.0
IF(TF(I-1).GT.373.0.AND.XF(I-1).LT.XFM) ARFB4=
1WF*DELXF*CPWTRF*(TFAVG-273.0)
IF(XF(I-1).LE.XFM.AND.TF(I-1).LT.TPHZ) ARFB4=0.0
IF(TF(I-1).GT.TPHZ.AND.HVM.EQ.0.) ARFB4=
1WF*DELXF*CPVMF*(TFAVG-273.0)
IF(HVM.EQ.0.) GO TO 12
ARFB4=0.0
ARFB5=WF*DELXF*(56.58/20.)*CPCO2F*(TFAVG-273.0)
ARFB6=WF*DELXF*(41.15/20.)*CPWTRF*(TFAVG-273.0)
12 ARFBT=ARFB1+ARFB2+ARFB3+ARFB4+ARFB5+ARFB6
ALFBN=ALFBT-ARFBT
DELTTF=ALFBN/(WF*CF*(1.0-XFAVG))
IF(TF(I-1).LT.TPHZ.OR.TF(I-1).GT.TPHDVZ) GO TO 26
IF(DELTF.GT.0.0.AND.DELXF.GT.0.0) GO TO 26
DELXF=0.999*DELXF
XF(I)=XF(I-1)+DELXF
XFAVG=(XF(I)+XF(I-1))/2.0
DELTTF=DELXF/(XFAVG*(TPHCVM-TPHZ))
TF(I)=TF(I-1)+DELTTF
TFAVG=(TF(I-1)+TF(I))/2.0
GO TO 27
C *****
26 IF(TF(I-1).GT.TPHZ.AND.TF(I-1).LT.TPHDVZ) DELTF=
1(DELTF+DLTFIP)/2.0
TF(I)=TF(I-1)+DELTTF
TFAVG=(TF(I-1)+TF(I))/2.0
THRCFL=WF*HVM*DELXF
HUHLS=WS*CS*(TS(I)-TS(I-1))
HUHBF=WF*CF*((TF(I)-273.0)*(1.-XF(I))-
1(TF(I-1)-273.0)*(1.-XF(I-1)))
HUHGAS=-CG*(MG(I)*(TG(I)-273.0)-MG(I-1)*(TG(I-1)-273.0))
THUSFG=HUHLS+HUHBF+HUHGAS
IF(1.LE.IRANM) GO TO 17
IF(ITER.GT.MINLMT.AND.ITER.LT.MAXLMT) GO TO 17
WRITE(NW,60)ITER,DELXF,DELTG,DELTTF,DELTS,DELMF,DELMG,UIEFF,
1G,CG,CORFAC
C *****
C CONVERGENCE CRITERIA ON AVERAGED VALUES OF TEMPERATURES
C *****
17 IF(TGAVG.EQ.TG(I-1)) GO TO 14
TGG=ABS((TGAVG-TGOLD)/(TGAVG-TG(I-1)))
14 IF(TSAVG.EQ.TS(I-1)) GO TO 19
TSS=ABS((TSAVG-TSOLD)/(TSAVG-TS(I-1)))
19 IF(TFAVG.EQ.TF(I-1)) GO TO 22
TFF=ABS((TFAVG-TFOLD)/(TFAVG-TF(I-1)))
22 IF(TSS.GT.TOLER1)GO TO 18
IF(TGG.GT.TOLER1)GO TO 18
C *****
IF(TFF.GT.TOLER2)GO TO 18
IF(TS(I).GE.(.999*TPHCVM)) TS(I)=TPHCVM
ENGASO=MG(I)*CG*(TG(I)-273.0)
ENSTNO=WS*CS*(TS(I)-273.0)
ENFULO=MF(I)*CF*(TF(I)-273.0)
GO TO 2
18 TFOLD=TFAVG
TSOLD=TSAVG
TGOLD=TGAVG

```

```

ITER=ITER+1
IF(ITER.GT.ITMAX) GO TO 21
TGGG(ITER)=TG(I)
TFFF(ITER)=TF(I)
TSSS(ITER)=TS(I)
DELTF=((TGGG(ITER)+TGGG(ITER-1))/2.0)-TG(I-1)
DELTF=((TFFF(ITER)+TFFF(ITER-1))/2.0)-TF(I-1)
DELTS=((TSSS(ITER)+TSSS(ITER-1))/2.0)-TS(I-1)
TG(I)=TG(I-1)+DELTF
TF(I)=TF(I-1)+DELTF
TS(I)=TS(I-1)+DELTS
TGAVG=(TG(I)+TG(I-1))/2.0
TFAVG=(TF(I)+TF(I-1))/2.0
TSAVG=(TS(I)+TS(I-1))/2.0
HCHRFHS=HFS(EFFKS,DPS,DPF,EMSVTY,SIGMAR,VIEWF,TFAVG,TSAVG)
HCHRSRG=HSG(EBED,DPS,KG,MUG,CG,G,CORFAC)
HCHRFRG=HFG(EBED,DPF,KG,MUG,CG,G,CORFAC)
TGOLD=TGAVG
TFOLD=TFAVG
TSOLD=TSAVG
IF(TF(I).GT.373.0.AND.XF(I).LT.XFM) GO TO 7
IF(HVM.EQ.0.) GO TO 9
GC TO 7
IF(I.GT.IMAX) I=I-1
THDMZN=WF*XF*HLTWTR
WRITE(NW,65) BETACV,HEIGHT
WRITE(NW,70) Z
WRITE(NW,105) ENGASI,ENSTNI,ENFULI
WRITE(NW,110) ENGASO,ENSTNO,ENFULO
WRITE(NW,135) DELHTL
WRITE(NW,140) THDMZN
WRITE(NP,125) I
CLOSE(UNIT=1)
CLOSE(UNIT=NP)
CLOSE(UNIT=NW)
STOP
END

```

21

```

C *****
C END OF MAIN PROGRAM
C *****
C *****
C FUNCTION SUBPROGRAMS ARE LISTED AS FOLLOWS
C *****

```

```

FUNCTION HFS(EFFKS,DPS,DPF,EMSVTY,SIGMAR,VIEWF,TFAVG,TSAVG)
HCFS=2.0*EFFKS/(DPS+DPF)
HRFS=EMSVTY*SIGMAR*VIEWF*(TFAVG**2+TSAVG**2)*(TFAVG+TSAVG)
HFS=HCFS+HRFS
RETURN
END

```

C *****

```

FUNCTION HFG(EBED,DPF,KG,MUG,CG,G,CORFAC)
REAL KG,MUG
RE=DPF*G/MUG
PR=CG*MUG/KG
HCFG=(1.9*KG/DPF)*(RE**0.5)*(PR**0.33)
HRFG=4.5+1.33*DPF*EBED
HFG=HCFG+HRFG
RETURN
END

```

C *****

```

FUNCTION HSG(EBED,DPS,KG,MUG,CG,G,CORFAC)
REAL KG,MUG
RE=DPS*G/MUG
PR=CG*MUG/KG
HCSG=(1.9*KG/DPS)*(RE**0.5)*(PR**0.33)
HRSG=4.5+1.33*DPS*EBED
HSG=HCSG+HRSG
RETURN
END

```

C *****

```

FUNCTION HWA(DZ, RBEMSY, SIGMAR, TWOPDV, TAMB, DELTWO)
HCWA=1.22*(DELTWC/DZ)**(1./4.)
HRWA=RBEMSY*SIGMAR*(TWOPDV**2+TAMB**2)*(TWOPDV+TAMB)*0.0
HWA=HCWA+HRWA
RETURN
END

```

C *****

```

FUNCTION HGW(EBED, DPAVG, DI, KG, MUG, G, CORFAC, ETAGW)
REAL KG, MUG
DPDTR=DPAVG/DI
RE=DPAVG*G/MUG
HCGW1=3.50*(KG/DI)*EXP(-4.6*DPDTR)*RE**0.7
HCGW2=0.813*(KG/DI)*EXP(-6.0*DPDTR)*RE**0.9
HCGW=(HCGW1+HCGW2)/2.0
HRGW=4.5+1.33*DPAVG*EBED
HRGW=HRGW*CORFAC
HGW=(HCGW+HRGW)*ETAGW
RETURN
END

```

C *****

C END OF FUNCTION SUBPROGRAMS

C *****



C
C
C
C

```

*****
SIMULATION OF LIME SHAFT KILN :
PROGRAM FOR THE ANALYSIS OF THE BURNING ZONE FROM UPPER SIDE
*****
DIMENSION TG(200),TF(200),TS(200)
DIMENSION MF(200),MS(200),MG(200)
DIMENSION TGDEL(125),TFDEL(125),TSDEL(125)
DIMENSION POG(200),DF(200),Z(200),DATAIN(80)
DIMENSION XA(200),XC(200),XF(200),XS(200),XR(200)
DIMENSION XADEL(125),XCDEL(125),XFDEL(125),XSDEL(125)
REAL KS,KD,KG,MUG,MG,MF,MS,MSF,N2MZ
OPEN(UNIT=1,FILE='BNG.DAT',TYPE='OLD')
READ(1,195) DATAIN
READ(1,*) NP,NW,NPRINT
OPEN(UNIT=NW,FILE='BNGRES.OUT',TYPE='NEW')
OPEN(UNIT=NP,FILE='BNGPLT.OUT',TYPE='NEW')

```

C
C
C

```

*****
FORTRAN VARIABLES USED IN THE INPUT STATEMENTS ARE DEFINED
AFTER EACH STATEMENT GENERALLY IN ORDER OF THEIR APPEARANCE
*****
READ(1,*) XF(1),XS(1),TG(1),TF(1),TS(1)

```

C
C
C

```

(DEGREES OF COMBUSTION OF FUEL,CALCINATION OF LIMESTONE
TEMPERATURES OF BULK GAS,FUEL AND STONE SURFACE)
READ(1,*) PS,XRINFD,TPD
(SUPERFICIAL PRODUCT OUTPUT RATE BASED ON EMPTY KILN
CROSS-SECTION,LIMESTONE-TO-FUEL-RATIO IN FEED MIX,
NOMINAL PRODUCTION RATE OF LIME SHAFT KILN)

```

C
C
C

```

READ(1,*) DPS,DPF,PHIS,PHIF,EBED,DELZ
(PARTICLE SIZES OF LIMESTONE,FUEL,SPHERICITIES OF
STONE,FUEL PARTICLES,BED POROSITY,AXIAL WIDTH OF
DIFFERENTIAL ELEMENT)

```

C
C
C

```

READ(1,*) XFM,XFV,XFC,XFA,XEA
(FRACTIONAL VALUES OF MOISTURE CONTENT,VOLATILE
MATTER,FIXED CARBON,ASH IN FUEL,EXCESS AIR)

```

C
C
C

```

READ(1,*) ETASG,ETAFG,ETAFS,ETASGF,ETAFGF,ETAFSF,ETAGW
(EFFECTIVENESS FACTORS FOR HEAT EXCHANGE BETWEEN
STONE,FUEL AND GASEOUS PHASES)

```

C
C
C

```

READ(1,*) ES,HFFC,ASHFAC,UNTDVZ,HLTDVM
(ENDOTHERMIC HEAT OF DECOMPOSITION OF LIMESTONE,HEATS
OF COMBUSTION OF VOLATILE MATTER,FIXED CARBON,FACTOR
FOR FUSION OF ASH,CONSTANT FOR DEVCLATILIZATION WITH
COMBUSTION,LATENT HEAT FOR DEVCLATILIZATION PROCESS)

```

C
C
C

```

READ(1,*) FBCDTY,RBCDTY,FBTHIK,RBTHIK,REMSY,TAMB,TWOBNG
(THERMAL CONDUCTIVITIES OF FIRE BRICKS,RED BURNT CLAY
BRICKS,THICKNESSES OF FIRE BRICKS INSULATION,RED CLAY
BRICKS,EMISSIVITY OF RED BRICKS,AMBIENT TEMPERATURE
AND EXTERNAL WALL TEMPERATURE)

```

C
C
C

```

READ(1,*) KG,MUG,TKL,RGAS,SIGMAR,EMSVTY,VIEWFO
(GAS THERMAL CONDUCTIVITY,VISCOSITY,THERMAL CONDUCTI-
VITY OF LIME LAYER,UNIVERSAL GAS CONSTANT,RADIATION
CONSTANT,EMISSIVITY OF COAL,VIEW FACTOR)

```

C
C
C

```

READ(1,*) RHOSC,RHOCFO,RHOASH,FACTOR,ALPHA,BETACV,GAMMA
(DENSITIES OF LIMESTONE,FUEL,ASH,CONSTANT TO ACCOUNT
FOR DIFFUSIONAL RESISTANCE FOR TRANSFER OF OXYGEN FROM
BULK GAS PHASE TO CARBON SURFACE,OTHER CONSTANTS TO
ACCOUNT FOR VARIATIONS IN GAS EMISSIVITY,TEMPERATURE
OF INCIPIENT COMBUSTION OF VOLATILE MATTER,ETC)

```

C
C
C

```

READ(1,*) TPHZ,TPHDVZ,TPHCVM,TD,TFASHE
(TEMPERATURES FOR ONSET OF DEVCLATILIZATION,COMBUSTI-
ONCF VOLATILE MATTER,COMPLETION OF VM EVOLUTION,DI-
SSOCIATION OF LIMESTONE,FUSION CF FUEL ASH)

```

C
C
C

```

READ(1,*) TOLER1,TOLER2,TOLER3,TOLER4,TOLERS
(TOLERANCE LEVELS FOR DIFFERENT VARIABLES)

```

```

READ(1,*) IMAX,ITERMX,IRANDM,MINLMT,MAXLMT
(CONSTANTS,MAXIMUM/MINIMUM VALUES)

WRITE(NW,60)
WRITE(NW,65)
WRITE(NW,70) DATAIN
WRITE(NW,25) NP,NW,NPRINT
WRITE(NW,85) XF(1),XS(1),TG(1),TF(1),TS(1)
WRITE(NW,30) PS,XRINFD,TPD
WRITE(NW,35) DPS,DPF,PHIS,PHIF,EBED,DELZ
WRITE(NW,45) XFM,XFV,XFC,XFA,XEA
WRITE(NW,40) ETASG,ETAFG,ETAFS,ETASGF,ETAFGF,ETAFSF,ETAGW
WRITE(NW,45) ES,HFFC,ASHFAC,UNTDVZ,HLTDVM
WRITE(NW,40) FBCDTY,RBCDTY,FBTHIK,RBTHIK,REMSY,TAMB,TWOBNG
WRITE(NW,80) KG,MUG,TKL,RGAS,SIGMAR,EMSVTY,VIEWFO
WRITE(NW,40) RHOSC,RHOCFO,RHOASH,FACTOR,ALPHA,BETACV,GAMMA

```

C
C
C
C
C
C
C
C
C

```

FCFADF=XFC/(XFV+XFC)
HFNDAF=8150.+6543.*VMFADF-17308.*(VMFADF**2)
CVFNET=HFNDAF*(XFV+XFC)
HFVM=(HFNDAF-8200.*FCFADF)/VMFADF
*****
WRITE(NW,45) DI,WS,Wf,WA,HFVM
WRITE(NP,180) PS,DPS,DPF,XRINFDF,XFV,XFC,XEA
WRITE(NW,155)
WRITE(NW,100)
XSMIN=0.0
XSMAX=1.0
XCMIN=0.0
XCMAx=1.0
XFMIN=XF(1)
XFMAX=(1.-XFA)
XAMIN=0.0
XAMAX=XFA
XFVMIN=0.999*(XFM+XFV)
XFVMAX=1.001*(XFM+XFV)
RPF=DPF/2.0
RPS=DPS/2.0
TKFMIN=0.15
TKFMAX=1.25
CFO=0.25
CFCMAX=0.40
CFAMAX=0.75*CFCMAX
CFMAX=(CFCMAX*XFC+CFAMAX*XFA)/(XFC+XFA)
VIEWF=VIEWFO
ALPHA1=(ETAFS/ETAFS-1.)/(1.-XFM-XFV-XFA)
BETA1=(ETAFGF/ETAFG-1.)/(1.-XFM-XFV-XFA)
GAMMA1=(ETASGF/ETASG-1.)/(1.-XFM-XFV-XFA)
XRAVG=WS/(WF*(1.-XFMIN))
RHOL=RHOsc*0.56
RHOS=RHOsc*(1.0-XS(1)*.44)
RHOF=RHOFC*(1.-XFMIN)
VR=XRAVG*RHOF/RHOS
XSTONE=WS/(WS+WF)
XFUEL=WF/(WS+WF)
DPSAVG=1./(XSTONE/DPS+XFUEL/DPF)
VFSRAT=RHOsc/(RHCFO*XRINFDF)
ALFA=1.-((DPF/DPS)**3)/VFSRAT
ASBZO=6.*(1.-EBED)/(PHIS*DP SAVG*(1.+ALFA*VFSRAT))
AFBZO=6.*(1.-EBED)*VFSRAT/(PHIF*DP SAVG*(1.+ALFA*VFSRAT))
RFB=RI+FBTHIK
RO=RFB+RETHIK
DC=2.*RO
CSTKLN=(ALOG(RFB/RI)/FBCDTY)+(ALOG(RO/RFB)/RECDTY)
BETA=XFM+XFV*(TPHDVZ-TPHZ)/(TPHCVM-TPHZ)
I=1
Z(I)=0.0
DZ=DELZ
DF(I)=DPF
TWO=TWOBNQ
XC(I)=XCMIN
MG(I)=WA+WF*(XFMAX-XFMIN)+WS*(XSMAX-XS(1))*0.44
WC2Z1=WA*.232-WF*(XFMAX-XFM-XFV)*(32./12.)
IF(XF(1).LE.(XFM+XFV)) WC2Z1=WC2Z1-WF*(XFM+XFV-XF(1))*
1(77.77/20.0)
WC0Z1=WS*(XSMAX-XS(1))*0.44+WF*(XFMAX-XFM-XFV)*44./12.
IF(XF(1).LE.(XFM+XFV)) WC0Z1=WC0Z1-WF*(XFM+XFV-XF(1))*
1(56.58/20.0)
IF(XF(1).LE.(XFM+XFV)) WH2OZ1=WF*(XFM+XFV-XF(1))*(41.15/20.)
IF(XF(1).GT.(XFM+XFV)) WH2OZ1=0.0
TGAvg=TG(I)
TFAvg=TF(I)
TSAvg=TS(I)
IF(XF(I).GE.XFVMIN.AND.XF(I).LE.XFVMAX) XF(I)=(XFM+XFV)
IF(XF(I).GT.(XFM+XFV)) GO TO 51
DF(I)=DPF
XC(I)=XCMIN
XA(I)=XAMIN
GO TO 52
51 IF(XFASHF.LE.C.) GO TO 48
XA(I)=XA(I-1)
GO TO 52
48 DF(I)=DPF*((XFMAX-XF(I))/(XFMAX-XFM-XFV))*1./3.))
XA(I)=XAMAX*((XF(I)-XFM-XFV)/(XFMAX-XFM-XFV))+XAMIN
52 G=MG(I)/AREA
MS(I)=WS*(1.0-XS(I)*.44)
MF(I)=WF*(1.0-XF(I)-XA(I))

```

49

```

IF(MF(I).EQ.0.) GO TO 49
XR(I)=MS(I)/MF(I)
WN2Z=WA*0.768
N2MZ=WN2Z/28.C
IF(XF(I).LT.(XFM+XFV)) W02Z=W02Z1+WF*(XF(I)-XF(1))*(77.77/20.)
IF(XF(I).GE.(XFM+XFV).AND.XF(1).LT.(XFM+XFV)) W02Z=W02Z1+
1WF*(XFM+XFV-XF(1))*(77.77/20.)+WF*(XF(I)-XFM-XFV)*(32./12.)
IF(XF(1).GE.(XFM+XFV)) W02Z=W02Z1+WF*(XF(I)-XFM-XFV)*(32./12.)
O2MZ=W02Z/32.C
IF(XF(I).LT.(XFM+XFV)) WCO2Z=WCO2Z1-WF*(XF(I)-XF(1))*
1(56.58/20.)-WS*(XS(I)-XS(1))*44
IF(XF(I).GE.(XFM+XFV).AND.XF(1).LT.(XFM+XFV)) WCO2Z=WCO2Z1-
1WF*(XFM+XFV-XF(1))*(56.58/20.)-WF*(XF(I)-XFM-XFV)*(44./12.)-
2WS*(XS(I)-XS(1))*44
IF(XF(1).GE.(XFM+XFV)) WCO2Z=WCO2Z1-WF*(XF(I)-XFM-XFV)*
1(44./12.)-WS*(XS(I)-XS(1))*44
CO2MZ=WCO2Z/44.O
IF(XF(I).LT.(XFM+XFV)) WH2OZ=WH2OZ1-WF*(XF(I)-XF(1))*
1(41.15/20.)
IF(XF(I).GE.(XFM+XFV)) WH2OZ=C.O
H2OMZ=WH2OZ/18.O
TMGZ=C2MZ+CO2MZ+N2MZ+H2OMZ
POG(I)=O2MZ/TMGZ
PCO2G=C02MZ/TMGZ

```

C
C
C

```

*****
SPECIFIC HEATS OF VARIOUS CONSTITUENTS
*****
CPO2=C.2584+(C.8063*TGAVG*10.**-5)-5865.6/(TGAVG**2)
CPCO2=C.1441+(C.2505*TFAVG*10.**-3)-(C.0776*10.**-6)/(TFAVG**2)
CPCO2F=C.1441+(C.2305*TFAVG*10.**-3)-(C.0776*10.**-6)/(TFAVG**2)
CPCO2S=C.1441+(C.2305*TSAVG*10.**-3)-(C.0776*10.**-6)/(TSAVG**2)
CPAIR=C.2372+(C.2900*TGAVG*10.**-4)-1360./(TGAVG**2)
CS=C.1988+(C.1189*TSAVG*10.**-3)-(C.3076*10.**-4)/(TSAVG**2)
CPWTRG=C.4567+(C.8333*TGAVG*10.**-5)+(C.7444*TGAVG*TGAVG*10.**-7)
CPWTRF=C.4567+(C.8333*TFAVG*10.**-5)+(C.7444*TFAVG*TFAVG*10.**-7)
IF(TF(I).GE.1573.O) GO TO 57
IF(XF(I).GT.(XFM+XFV)) GO TO 81
CF=CFO+(XF(I)/(XFM+XFV))*(CFMAX-CFO)
GO TO 57

```

81

```

IF(XFASHF.GT.C.) GO TO 57
CFCKE=-C.1640+(C.1136*TFAVG*10.**-2)-(C.49*TFAVG*TFAVG*10.**-6)
CFASH=C.75*CFCKE
CF=(CFCKE*XFC+CFASH*XFA)/(XFC+XFA)

```

C

57

```

*****
XRAVG=XR(I)
DFAVG=DF(I)
IF(XFASHF.GT.C.) DFAVG=(DF(I)+DFBZAF)/2.O
POGAVG=PCG(I)
XCAVG=XC(I)
XFAVG=XF(I)
XSAVG=XS(I)
XAAVG=XA(I)
WGAVG=MG(I)
WFAVG=MF(I)
WSAVG=MS(I)
WAAVG=WF*XAAVG
IF(XSAVG.LE.0.) GO TO 62

```

C
C
C

```

*****
AVERAGE TEMPERATURE OF CALCINED LIME LAYER
*****
SHBKLI=(1.-XSAVG)**(1./3.)
IF(SHBKLI.EQ.1.) GO TO 62
SHBKLI1=XSAVG*TSAVG/(1.-SHBKLI)
SHBKLI2=XSAVG*TD*SHBKLI/(1.-SHBKLI)
SHBKLI3=1.5*(TSAVG-TD)*SHBKLI*(1.+SHBKLI)
SHBBLI=SHBKLI1-SHBKLI2-SHBKLI3
TLLAVG=SHBBLI/XSAVG

```

62

```

*****
CL=C.1786+(C.0864*TLLAVG*10.**-3)-(C.1928*10.**-4)/(TLLAVG**2)
CPCO2L=C.1441+(C.2305*TLLAVG*10.**-3)-(C.0776*10.**-6)/(TLLAVG**2)
DPAVG=(DPS*WSAVG+DFAVG+WFAVG)/(WSAVG+WFAVG)
IF(HUDLSC.EQ.C.) GO TO 41

```

41

```

RSHLHD=DELSHS/(HUDLSC+DELSHS)
IF(XS(I-1).GE.XSMAX) GO TO 124
DELSHT=DELSHT+DELSHS
IF(XS(I-1).EQ.XSMAX.AND.XS(I-1).EQ.XSMAX) RSHLHD=1.O
WGAIRZ=WN2Z+WC2Z
WGCO2Z=WCO2Z
WGH2OZ=WH2OZ
CG=(WGAIRZ*CPAIR+WGCO2Z*CPCO2+WGH2OZ*CPWTRG)/

```

124

```

1(WGAI RZ+WGC02Z+WGH20Z)
TGI=TGAVG
CORFAC=(1.-ALPHA)-((GAMMA-ALPHA)*(XFAVG-BETA)/
1(1.-XFA-BETA))
MSF=WSAVG+WFAVG+WAAVG
ASNMR=ASBZO*(1.+ALFA*VFSRAT)
ASDNR=(1.+ALFA*VFSRAT*(1.-XFA-XFAVG)/(1.-XFM-XFV-XFA))
AFNMR1=AFBZO*(1.+ALFA*VFSRAT)
IF(XFASHF.GT.C.) GO TO 106
AFNMR2=((1.-XFA-XFAVG)/(1.-XFM-XFV-XFA))**(2./3.)
AFNMR=AFNMR1*AFNMR2
AFDNR=ASDNR
ASBZ=ASNMR/ASDNR
AFBZ=AFNMR/AFDNR
106 RHOS=RHOSC*(1.-XSAVG*0.44)
IF(XFASHF.GT.C.) RHOF=RHOFAF*((TFAVG/TFASHF)**ASHFAC)
IF(XF(I).GT.(XFM+XFV)) GO TO 71
RHOF=RHOFC*(1.-XFAVG)
ASBZ=ASBZC
AFBZ=AFBZC
71 TKF=((TKFMAX-TKFMIN)*XFAVG/(XFM+XFV))+TKFMIN
VSAVG=(WSAVG/RHOS)+(WFAVG/RHOF)+(WAAVG/RHOASH)
IF(TS(I).LE.TD) TKS=0.85
IF(TS(I).GT.TD) TKS=TKL
EFFKS=TKS*TKF/(TKS+TKF)
IF(XFAVG.GE.(C.999*XFMAX).OR.I.GE.IRANDB) GO TO 61
*****
OVERALL DIFFUSIONAL RESISTANCE AND HEAT TRANSFER COEFFICIENTS
*****
BARKS=DASHKS(CRGAS,TFAVG,TGAVG,DFAVG,FACTOR)
HCHRFS=HFS(EFFKS,DPS,DFAVG,EMSVTY,SIGMAR,VIEWF,TFAVG,TSAVG)
HCHRFG=HFG(EBED,DFAVG,KG,MUG,CG,G,CORFAC)
61 HCHRSG=HSC(EBED,DPS,KG,MUG,CG,G,CORFAC)
*****
IF(XFAVG.GT.(XFM+XFV)) GO TO 76
ASSBZ=ETASG
ASFBZ=ETAFG
ASFRBZ=ETAFS
GO TO 72
76 ASSBZ=ETASG*(1.+GAMMA1*(XFAVG-XFM-XFV))
ASFBZ=ETAFG*(1.+BETA1*(XFAVG-XFM-XFV))
ASFRBZ=ETAFS*(1.+ALPHA1*(XFAVG-XFM-XFV))
72 VR=XRAVG*RHOFC/RHOS
A=(1.+VR)*DPS/(6.*(1.-EBED)*VR)
FAF=A*AFBZ*ASFRBZ
FAS=A*ASBZ*ASSBZ
IF(TF(I).LT.TFASHF.AND.XFASHF.LE.0.) GO TO 54
IF(XFASHF.GT.C.) GO TO 59
XFASHF=XFC(I)
DFBZAF=DF(I)
AFBZAF=AFBZ
RHOFAF=RHOFC
CFFCAF=CFCOKE
CFASHF=CFASH
59 HEIGHT=Z(I)
ASNMR=ASNMR
ASDNR1=ASDNR
IF(TF(I).LT.TF(I-1)) GO TO 107
RHOFAF=(TFASHF/TFAVG)**ASHFAC
107 ASDNR2=(ALFA*VFSRAT*RHOFC*XFA*(XFAVG-XFASHF)/(RHOASH*
1(1.-XFM-XFV-XFA)))*RHOFAF
ASDNR=ASDNR1+ASDNR2
ASBZ=ASNMR/ASDNR
AFNMR1=AFNMR1
AFNMR2=((1.-XFA-XFASHF)/(1.-XFM-XFV-XFA))**(2./3.)
IF(TF(I).LT.TF(I-1)) GO TO 108
RHOFAF=(TFASHF/TFAVG)**ASHFAC
108 AFNMR3=((1.-XFA-XFAVG)/(1.-XFA-XFASHF)+RHOFC*XFA*(XFAVG-XFASHF
1)/(1.-XFA-XFASHF)*RHOASH)*RHOFAF)***(2./3.)
AFNMR=AFNMR1*AFNMR2*AFNMR3
AFDNR=ASDNR
AFBZ=AFNMR/AFDNR
CFNUM=(CFASHF*XFA*(XFMAX-XFASHF)/XFC)+CFFCAF*(XFMAX-XFAVG)
CFDNR=(XFA*(XFMAX-XFASHF)/XFC)+(XFMAX-XFAVG)
54 CF=CFNUM/CFDNR
QFS=HCHRFS*(TFAVG-TSAVG)*AFBZ*ASFRBZ*AREA*DZ
QFG=HCHRFG*(TFAVG-TGAVG)*AFBZ*ASFBZ*AREA*DZ
QSG=HCHRSG*(TSAVG-TGAVG)*ASBZ*ASSBZ*AREA*DZ
IF(I.NE.1) GO TO 101
ENGASI=MG(I)*CG*(TG(I)-273.0)

```

```

ENSTNI=MS(I)*CS*(TS(I)-273.0)
ENFULI=MF(I)*CF*(TF(I)-273.0)
IF(I.NE.IFANDM) GO TO 101
WRITE(NW,205)
101 Y=(I/NPRINT)-FLOAT(I)/FLOAT(NPRINT)
IF(Y.NE.C) GO TO 7
TYPE 55,Z(I),XF(I),XS(I),POG(I),TG(I),TF(I),TS(I),TLLAVG
WRITE(NW,145)I,Z(I),XF(I),XS(I),TG(I),TF(I),TS(I),TWO,
1RSHLHD,DELSHT,HCHRFS,HCHRFG,HCHRSG,ASBZ,AFBZ,QFS,QFG,QSG,
ZDELHTL,PCG(I),PCO2G
7 WRITE(NP,185)Z(I),XF(I),XS(I),TG(I),TF(I),TS(I)
IF(XF(I).GE.XFMAX.AND.TS(I).LE.(TD+10.)) GO TO 21
IF(XS(I).LT.XS(I-1).OR.XF(I).LT.XF(I-1)) GO TO 21
3 IF(XCAVG.GE.XCMAX.OR.XFAVG.GE.XFMAX) GO TO 21
I=I+1
IF(I.GT.IMAX) GO TO 21
Z(I)=Z(I-1)+DZ
IF(XF(I-1).LT.(XFM+XFV)) HF=HFVM
IF(XF(I-1).GE.(XFM+XFV).AND.XF(I-1).LT.XFMAX) HF=HFCC
C C C *****
ESTIMATION OF WALL HEAT LOSSES
C C C *****
DELTWO=TWCBNG-TAMB
AHWA=HWA(DZ,REMSY,SIGMAR,TWCBNG,TAMB,DELTWO)
AHGW=HGW(EBED,DPAVG,DI,KG,MUG,G,CORFAC,ETAGW)
IF(AHWA.EQ.0.) GO TO 33
UIEFFI=RI*(1./(RI*AHGW)+CSTKLN+1./(RO*AHWA))
UIEFF=1./UIEFFI
DELHL=UIEFF*3.14*DI*DZ*(TGI-TAMB)
DELHTL=DELHTL+DELHL
TWI=TGI-DELHL/(3.14*DI*DZ*AHGW)
TWO=TAMB+DELHL/(3.14*DO*DZ*AHWA)
TWOBNG=TWG
C C C *****
33 K=0
4 IF(TS(I-1)-TD) 1,4,4
IF(XS(I-1).EQ.XSMAX) GO TO 6
X1=(3.*AREA*RHO5M*DZ)
X2=-HCHRSG*(TSAVG-TGAVG)*FAS+HCHRFS*(TFAVG-TSAVG)*FAF
X3=(ES*RHO50*MSF*RPS)
DELXSP=X1*X2/X3
XS(I)=XS(I-1)+DELXSP
XSAVG=(XS(I-1)+XS(I))/2.0
1 ITER=1
9 IF(XSAVG.GT.XSMIN) GO TO 5
IF(XS(I-1).EQ.XSMIN.AND.TS(I-1).GE.TD) GO TO 5
XS(I)=XS(I-1)
DELXS=0.0
XSAVG=XS(I)
GO TO 6
5 IF(ITER.EQ.1.AND.XF(I-1).GE.(XFM+XFV)) GO TO 31
10 IF(XS(I-1).GE.(0.999*XSMAX)) GO TO 6
IF(XS(I).LT.XSMAX) GO TO 67
DELXS=XSMAX-XS(I-1)
GO TO 22
C C C *****
STONE HEAT BALANCE DURING CALCINATION OF LIMESTONE
C C C *****
67 J=0
IF(ITER.EQ.1) GO TO 104
DXSOLD=XSDEL(ITER-1)
GO TO 113
104 DXSOLD=DELXS
113 ALHSB1=HCHRFS*(TFAVG-TSAVG)*AFBZ*ASFREZ*AREA*DZ
ALHSB2=HCHRSG*(TSAVG-TGAVG)*ASBZ*ASSBZ*AREA*DZ
ALHSB3=WF*DELXA*CFASH*(TFAVG-273.0)
IF(XF(I-1).LT.(XFM+XFV)) ALHSB3=0.0
ALHSBT=ALHSB1-ALHSB2+ALHSB3
ARHSB1=WF*XAAVG*CFASH*DELTS
IF(XF(I-1).LT.(XFM+XFV)) ARHSB1=0.0
ARHSB2=WF*DELXA*CFASH*(TSAVG-273.0)
IF(XF(I-1).LT.(XFM+XFV)) ARHSB2=0.0
DELSHS=WS*0.56*CL*DELSH
ARHSB3=DELSHS
ARHSBT=ARHSB1+ARHSB2+ARHSB3
ALHSBN=ALHSBT-ARHSBT
DELXS=ALHSBN/(WS*(ES+(CPCO2L*(TSAVG-TD)+CPCO2S*
1(TSAVG-273.)))*44./100.))
DXSNEW=DELXS
IF(DXSNEW.EQ.0.) GO TO 19

```



```

19 IF(ABS((DXSNEW-DXSOLD)/DXSNEW).LE.TOLER4) GO TO 114
   J=J+1
   IF(J.GE.ITERMx) GO TO 114
   DXSOLD=(DXSOLD+DXSNEW)/2.0
   GO TO 113
114 IF(XS(I-3).LE.XSMIN.OR.DLXSIP.LE.0.) GO TO 22
   DXSLWR=(1.-TOLER1)*DLXSIP
   DXSUPR=(1.+TOLER1)*DLXSIP
   IF(DELXS.LT.DXSLWR.OR.DELXS.GT.DXSUPR)DELXS=(DELXS+DLXSIP)/2.0
22 IF(DELXS.LT.0.) DELXS=0.0
   IF(I.GE.IRANDM) DELXS=DLXSIP
   IF(ITER.EG.1) GO TO 86
   DELXS=(DELXS+XSDEL(ITER-1))/2.0
86 XSDEL(ITER)=DELXS
   IF(XS(I-1).GT.(0.999*XSMAX)) DELXS=0.0
   XS(I)=XS(I-1)+DELXS
   XSAVG=(XS(I-1)+XS(I))/2.0
C *****
   IF(XC(I-1).GT.(0.999*XCMAX)) GO TO 63
   IF(XCIP.LT.XCMAX) GO TO 66
   DELXC=XCMAX-XC(I-1)
   GO TO 29
66 IF(XF(I-1).GE.(XFM+XFV)) GO TO 73
C *****
C C C FRACTIONAL DEVOLATILIZATION OF FUEL FOR VM COMBUSTION
C *****
   DELXF=(XFM+XFV-BETACV)/UNTDVZ
   XF(I)=XF(I-1)+DELXF
   XFAVG=(XF(I-1)+XF(I))/2.0
   XFDEL(ITER)=DELXF
   GO TO 8
C *****
C C C DEGREE OF COMBUSTION OF FIXED CARBON CONTENT OF FUEL
C *****
73 DXCBKT=(1.-XCAVG)*(2./3.)
   DXCNUM=3.*AREA*(1.-EBED)*BARKS*POGAVG*DXCBKT*DZ
   DXCDNR=RHCFC*(XFM+XFV)*RPF*VSFAVG
   IF(DXCNUM.EG.0.) GO TO 126
   DELXC=DXCNUM/DXCNUM
126 IF(XC(I-3).LE.XCMIN.OR.DLXCIP.LE.0.) GO TO 29
   DXCLWR=(1.-TOLER1)*DLXCIP
   DXCUPR=(1.+TOLER1)*DLXCIP
   IF(DELXC.LT.DXCLWR.OR.DELXC.GT.DXCUPR)DELXC=(DELXC+DLXCIP)/2.0
29 IF(DELXC.LT.0.) DELXC=0.0
   IF((2.*XC(I-1)-XC(I-2)).GT.XCMAX) DELXC=XCMAX-XC(I-1)
   IF(I.GE.IRANDM) DELXC=DLXCIP
   IF(ITER.EG.1) GO TO 87
   DELXC=(DELXC+XCDEL(ITER-1))/2.0
87 XCDEL(ITER)=DELXC
   IF(XC(I-1).GT.(.999*XCMAx).OR.XF(I-1).GT.(.999*XFMAX))DELXC=0.0
   XC(I)=XC(I-1)+DELXC
   XCAVG=(XC(I)+XC(I-1))/2.0
   XF(I)=(XFM+XFV)*XC(I)+(XFM+XFV)
   DELXF=XF(I)-XF(I-1)
   XFDEL(ITER)=DELXF
   XFAVG=(XF(I-1)+XF(I))/2.0
C *****
   IF(XSIP.LT.XSMAX.OR.XFIP.LT.XFMAX) GO TO 8
   DELXF=XFMAX-XF(I-1)
   DELXS=XSMAX-XS(I-1)
   DELTG=DLTGIP
   DELTF=DLTFIP
   DELTS=DLTSIP
   XF(I)=XF(I-1)+DELXF
   XS(I)=XS(I-1)+DELXS
   TG(I)=TG(I-1)+DELTG
   TF(I)=TF(I-1)+DELTF
   TS(I)=TS(I-1)+DELTS
   GO TO 53
31 ZIP=Z(I-1)+DZ
C *****
C C C PREDICTIONS ON VALUES OF PARAMETERS
C *****
   AXS=((XS(I-1)-XS(I-2))/(Z(I-1)-Z(I-2))-(XS(I-2)-XS(I-3)))/
   1(Z(I-2)-Z(I-3)))/(Z(I-1)-Z(I-3))
   AXC=((XC(I-1)-XC(I-2))/(Z(I-1)-Z(I-2))-(XC(I-2)-XC(I-3)))/
   1(Z(I-2)-Z(I-3)))/(Z(I-1)-Z(I-3))
   ATG=((TG(I-1)-TG(I-2))/(Z(I-1)-Z(I-2))-(TG(I-2)-TG(I-3)))/
   1(Z(I-2)-Z(I-3)))/(Z(I-1)-Z(I-3))
   ATF=((TF(I-1)-TF(I-2))/(Z(I-1)-Z(I-2))-(TF(I-2)-TF(I-3)))/

```

```

1(Z(I-2)-Z(I-3))/(Z(I-1)-Z(I-3))
ATS=((TS(I-1)-TS(I-2))/(Z(I-1)-Z(I-2))-(TS(I-2)-TS(I-3)))/
1(Z(I-2)-Z(I-3))/(Z(I-1)-Z(I-3))
BXS=(XS(I-1)-XS(I-2))/(Z(I-1)-Z(I-2))-AXS*(Z(I-1)+Z(I-2))
BXC=(XC(I-1)-XC(I-2))/(Z(I-1)-Z(I-2))-AXC*(Z(I-1)+Z(I-2))
BTG=(TG(I-1)-TG(I-2))/(Z(I-1)-Z(I-2))-ATG*(Z(I-1)+Z(I-2))
BTF=(TF(I-1)-TF(I-2))/(Z(I-1)-Z(I-2))-ATF*(Z(I-1)+Z(I-2))
BTS=(TS(I-1)-TS(I-2))/(Z(I-1)-Z(I-2))-ATS*(Z(I-1)+Z(I-2))
CXSS=XS(I-3)-AXS*Z(I-3)*Z(I-3)-BXS*Z(I-3)
CXC=XC(I-3)-AXC*Z(I-3)*Z(I-3)-BXC*Z(I-3)
CTG=TG(I-3)-ATG*Z(I-3)*Z(I-3)-BTG*Z(I-3)
CTF=TF(I-3)-ATF*Z(I-3)*Z(I-3)-BTF*Z(I-3)
CTS=TS(I-3)-ATS*Z(I-3)*Z(I-3)-BTS*Z(I-3)
IF(XS(I-3).LE.XSMIN) GO TO 12
XS(I)=AXS*ZIP*ZIP+BXS*ZIP+CXSS
GO TO 13
12 XS(I)=XS(I-1)+DELXS
13 IF(XS(I).GE.XSMAX) XS(I)=XSMAX
IF(XC(I-3).LE.XCMIN) GO TO 77
XC(I)=AXC*ZIP*ZIP+BXC*ZIP+CXC
XF(I)=(XFMAX-XFM-XFV)*XC(I)+(XFM+XFV)
GO TO 79
77 XC(I)=XC(I-1)+DELXC
79 XF(I)=XF(I-1)+DELXF
IF(XC(I).GE.XCMAX) XC(I)=XCMAX
IF(XF(I).GE.XFMAX) XF(I)=XFMAX
TG(I)=ATG*ZIP*ZIP+BTG*ZIP+CTG
TF(I)=ATF*ZIP*ZIP+BTF*ZIP+CTF
TS(I)=ATS*ZIP*ZIP+BTS*ZIP+CTS
IF(XS(I).LT.XS(I-1)) XS(I)=XS(I-1)
IF(XC(I).LT.XC(I-1)) XC(I)=XC(I-1)
IF(XF(I).LT.XF(I-1)) XF(I)=XF(I-1)
DELXS=XS(I)-XS(I-1)
DELXC=XC(I)-XC(I-1)
DELXF=XF(I)-XF(I-1)
DELTF=TF(I)-TF(I-1)
DELTS=TS(I)-TS(I-1)
DELTG=TG(I)-TG(I-1)
102 DLXSIP=DELXS
DLXCIP=DELXC
DLXFIP=DELXF
DLTFIP=DELTF
DLTSIP=DELTS
DLTGIP=DELTG
XSDEL(ITER)=DELXS
XCDEL(ITER)=DELXC
XFDEL(ITER)=DELXF
TFDEL(ITER)=DELTF
TSDEL(ITER)=DELTS
TGDEL(ITER)=DELTG
XSAVG=(XS(I-1)+XS(I))/2.0
XCavg=(XC(I-1)+XC(I))/2.0
XFavg=(XF(I-1)+XF(I))/2.0
TFavg=(TF(I)+TF(I-1))/2.0
TSAVG=(TS(I)+TS(I-1))/2.0
TGavg=(TG(I)+TG(I-1))/2.0
XSIP=XS(I)
XCIP=XC(I)
XFIP=XF(I)
TGIP=TG(I)
TFIP=TF(I)
TSIP=TS(I)
IF(XFAVG.GE.(C.999*XFMAX).OR.I.GE.IRANDM) GO TO 83
BARKS=DASHKS(RGAS,TFavg,TGavg,DFavg,FACTOR)
HCHRFS=HFS(EFFKS,DPS,DFavg,EMSVTY,SIGMAR,VIEWF,TFavg,TSAVG)
HCHRFG=HFG(EBED,DFavg,KG,MUG,CG,G,CORFAC)
HCHRSG=HSG(EBED,DPS,KG,MUG,CG,G,CORFAC)
83 CC
78 IF(I.LT.IRANDM) GO TO 11
WRITE(NW,150)ITER,DLXFIP,DLXSIP,DLTGIP,DLTFIP,DLTSIP,DLXCIP,
TG,CORFAC,DFavg,BARKS,HCHRFS,DZ
11 ITER=ITER+1
GO TO 9
8 IF(XF(I-1).GE.(XFM+XFV)) GO TO 68
XA(I)=XA(I-1)
XC(I)=XC(I-1)
GO TO 69
68 XA(I)=XAMAX*((XF(I)-XFM-XFV)/(XFMAX-XFM-XFV))+XAMIN
69 IF(XFASHF.GT.C.) XA(I)=XA(I-1)
DELXA=XA(I)-XA(I-1)

```

```

XAAVG=(XA(I-1)+XA(I))/2.0
WAAVG=WF*XAAVG
DELMF=-WF*(DELF+DELXA)
MF(I)=MF(I-1)+DELMF
WFAVG=(MF(I-1)+MF(I))/2.0
DELMF=-WS*DELXS*0.44
MS(I)=MS(I-1)+DELMF
WSAVG=(MS(I)+MS(I-1))/2.0
MSF=WSAVG+WFAVG+WAAVG
DELMG=-WS*DELXS*0.44-WF*DELXF
MG(I)=MG(I-1)+DELMG
WGAVG=(MG(I-1)+MG(I))/2.0
IF(XS(I)-XSMIN) 14,14,15
*****
STONE HEAT BALANCE DURING NON-CALCINATION OF LIMESTONE
*****
14 ALHSB1=HCHRF*(TFAVG-TSAVG)*AFBZ*ASFRBZ*AREA*DZ
ALHSB2=HCHRS*(TSAVG-TGAVG)*ASBZ*ASSBZ*AREA*DZ
ALHSB3=WF*DELXA*CFASH*(TFAVG-273.)
IF(XF(I-1).LT.(XFM+XFV)) ALHSB3=0.0
ALHSBT=ALHSB1-ALHSB2+ALHSB3
ARHSBT=WF*DELXA*CFASH*(TSAVG-273.0)
IF(XF(I-1).LT.(XFM+XFV)) ARHSBT=0.0
ALHSBN=ALHSBT-ARHSBT
DELTS=ALHSBN/(WS*CS+WF*XAAVG*CFASH)
IF(XF(I-1).GE.(XFM+XFV)) GO TO 74
DELTS=ALHSBN/(WS*CS)
GO TO 58
74 IF(XS(I).EQ.XSMAX.AND.XS(I-1).LT.XSMAX) DELTS=(ALHSBN-WS*(XS(I)
1) -XS(I-1)))/(WS*XSAVG*.56*CL+WF*XAAVG*CFASH)
IF(XSAVG.GE.(0.999*XSMAX)) DELTS=ALHSBN/
1(WS*XSAVG*0.56*CL+WF*XAAVG*CFASH)
IF(XSAVG.GE.(0.999*XSMAX)) GO TO 58
IF(XF(I-1).LT.(XFM+XFV).OR.DLTSIP.LE.0.) GO TO 58
DTSLWR=(1.-TOLER2)*DLTSIP
DTSUPR=(1.+TOLER2)*DLTSIP
IF(DELTS.LT.DTSLWR.OR.DELTS.GT.DTSUPR)DELTS=(DELTS+DLTSIP)/2.0
IF(ITER.EQ.1) GO TO 88
58 DELTS=(DELTS+TDEL(ITER-1))/2.0
88 TDEL(ITER)=DELTS
IF(XS(I).EQ.XSMAX.AND.XS(I-1).LT.XSMAX) TS(I-1)=TLLAVG
TS(I)=TS(I-1)+DELTS
TSAVG=(TS(I-1)+TS(I))/2.0
*****
GO TO 16
15 IF(XS(I).EQ.XSMAX.AND.XS(I-1).LT.XSMAX) GO TO 14
IF(XSAVG.GE.(0.999*XSMAX)) GO TO 14
IF(XS(I-1).LE.XSMIN.AND.TS(I-1).LT.TD) GO TO 28
IF(XS(I-1).GE.(0.999*XSMAX)) GO TO 28
*****
HEAT CONDUCTION THROUGH LIME LAYER
*****
IF(XS(I-1).EQ.1.) GO TO 121
121 SHBKTP=(1.-XS(I-1))*(1./3.)
IF(SHBKTP.EQ.1.) GO TO 28
SHBK1=XS(I-1)*(TSAVG-1173.)/(1.-SHBKTP)
SHBK2=XS(I-1)*(TD-1173.)*SHBKTP/(1.-SHBKTP)
SHBK3=1.5*(TSAVG-TD)*SHBKTP*(1.+SHBKTP)
SHBBTP=SHBK1-SHBK2-SHBK3
28 CONTINUE
HCLDNR=3.*TKL*AREA*(1.-EBED)*DZ
HCLNUM=ES*RHOSO*VSFAVG*RPS*RPS
IF(XSAVG.EQ.1.) GO TO 123
123 ARHBKT=1./((1.-XSAVG)*(1./3.))
ARHBBT=(ARHBKT-1.)*DELXS
IF(HCLDNR.EQ.0.) GO TO 127
ARHSP1=ARHBBT*HCLNUM/HCLDNR
127 IF(XS(I).GE.1.) GO TO 122
122 SHBKTI=(1.-XS(I))*(1./3.)
IF(SHBKTI.EQ.1.) GO TO 27
SHBK1=XS(I)*(TSAVG-1173.)/(1.-SHBKTI)
SHBK2=XS(I)*(TD-1173.)*SHBKTI/(1.-SHBKTI)
SHBK3=1.5*(TSAVG-TD)*SHBKTI*(1.+SHBKTI)
SHBBTI=SHBK1-SHBK2-SHBK3
DELSH=SHBBTI-SHBETP
IF(HCLDNR.EQ.0.) GO TO 27
27 DELSHP=RHCL*CL*RPS*RPS*DELSH*(ARHBKT-1.)*VSFAVG/HCLDNR
ARHSP2=DELSHP
ARHSPT=ARHSP1+ARHSP2
TSINew=TD+ARHSPT

```

```

DELTS=TSINew-TS(I-1)
IF(XF(I-1).LT.(XFM+XFV).OR.DELTSIP.LE.C.) GO TO 36
DTSLWR=(1.-TOLER2)*DLTSIP
DTSUPR=(1.+TOLER2)*DLTSIP
36 IF(DELTS.LT.DTSLWR.OR.DELTS.GT.DTSUPR)DELTS=(DELTS+DLTSIP)/2.0
IF(I.GE.IRANDM) DELTS=DLTSIP
IF(ITER.EQ.1) GO TO 89
89 DELTS=(DELTS+TSDEL(ITER-1))/2.0
TSDEL(ITER)=DELTS
TS(I)=TS(I-1)+DELTS
TSAVG=(TS(I-1)+TS(I))/2.0
*****
HEAT BALANCE FOR GAS PHASE
*****
16 ALHGB1=HCHRFSG*(TFAVG-TGAVG)*AFBZ*ASFBZ*AREA*DZ
ALHGB2=HCHRFSG*(TSAVG-TGAVG)*ASBZ*ASSBZ*AREA*DZ
ALHGB3=WF*DELXF*(44./12.)*CPCO2F*(TFAVG-273.C)
IF(XF(I-1).LT.(XFM+XFV)) ALHGB3=WF*DELXF*(56.58/20.0)*
1CPCO2F*(TFAVG-273.0)
ALHGB4=WS*DELXS*(44./100.)*CPCO2B*(TSAVG-273.0)
ALHGB5=-WF*DELXF*(32./12.)*CPO2*(TGAVG-273.0)
IF(XF(I-1).LT.(XFM+XFV)) ALHGB5=-WF*DELXF*(77.77/20.0)*
1CPO2*(TGAVG-273.0)
ALHGB6=WF*DELXF*(41.15/20.0)*CPWTRF*(TFAVG-273.0)
IF(XF(I-1).GE.(XFM+XFV)) ALHGB6=0.0
ALHGBT=ALHGB1+ALHGB2+ALHGB3+ALHGB4+ALHGB5+ALHGB6
ALHGBT=ALHGBT-DELHL
ALHGBN=ALHGBT+CG*(TGAVG-273.0)*DELMG
DELTG=-ALHGBN/(CG*WGAVG)
IF(XF(I-1).LT.(XFM+XFV).OR.DLTGIP.GE.C.) GO TO 34
DTGLWR=(1.-TOLER2)*DLTGIP
DTGUPR=(1.+TOLER2)*DLTGIP
34 IF(DELTG.LT.DTGLWR.OR.DELTG.GT.DTGUPR)DELTG=(DELTG+DLTGIP)/2.0
IF(I.GE.IRANDM) DELTG=DLTGIP
IF(ITER.EQ.1) GO TO 91
91 DELTG=(DELTG+TGDEL(ITER-1))/2.0
TGDEL(ITER)=DELTG
TG(I)=TG(I-1)+DELTG
TGAVG=(TG(I-1)+TG(I))/2.0
*****
HEAT BALANCE FOR FUEL
*****
ALHFB1=WF*HF*DELXF
ALHFB2=WF*DELXF*(32./12.)*CPC2*(TGAVG-273.0)
IF(XF(I-1).LT.(XFM+XFV)) ALHFB2=WF*DELXF*(77.77/20.0)*
1CPCO2*(TGAVG-273.0)
ALHFB3=-WF*DELXF*HLTQVM
IF(XF(I-1).GE.(XFM+XFV)) ALHFB3=0.0
ALHFBT=ALHFB1+ALHFB2+ALHFB3
ARHFB1=HCHRFSG*(TFAVG-TSAVG)*AFBZ*ASFREZ*AREA*DZ
ARHFB2=HCHRFSG*(TFAVG-TGAVG)*AFBZ*ASFBZ*AREA*DZ
ARHFB3=-WF*CF*(TFAVG-273.0)*(DELXF+DELXA)
ARHFB4=WF*DELXF*(44./12.)*CPCO2F*(TFAVG-273.C)
IF(XF(I-1).LT.(XFM+XFV)) ARHFB4=WF*DELXF*(56.58/20.0)*
1CPCO2F*(TFAVG-273.0)
ARHFB5=WF*DELXF*(41.15/20.0)*CPWTRF*(TFAVG-273.0)
IF(XF(I-1).GE.(XFM+XFV)) ARHFB5=0.0
ARHFB6=WF*DELXA*CFASH*(TFAVG-273.0)
IF(XF(I-1).LT.(XFM+XFV)) ARHFB6=0.0
ARHFBT=ARHFB1+ARHFB2+ARHFB3+ARHFB4+ARHFB5+ARHFB6
ALHFBN=ALHFBT-ARHFBT
DELTF=ALHFBN/(WF*CF*(1.0-XFAVG-XAAVG))
IF(XF(I-1).LT.(XFM+XFV)) DELTF=ALHFBN/(WF*CF*(1.-XFAVG))
IF(XF(I-1).LT.(XFM+XFV).OR.DLTFIP.LE.C.) GO TO 37
DTFLWR=(1.-TOLER2)*DLTFIP
DTFUPR=(1.+TOLER2)*DLTFIP
37 IF(DELTF.LT.DTFLWR.OR.DELTF.GT.DTFUPR)DELTF=(DELTF+DLTFIP)/2.0
IF(I.GE.IRANDM) DELTF=DLTFIP
IF(ITER.EQ.1) GO TO 92
92 DELTF=(DELTF+TFDEL(ITER-1))/2.0
TFDEL(ITER)=DELTF
TF(I)=TF(I-1)+DELTF
TFAVG=(TF(I-1)+TF(I))/2.0
HUDLSC=WS*ES*DELXS
*****
IF(I.LT.IRANDM) GO TO 23
IF(ITER.GT.MINLMT.AND.ITER.LT.(1+ITERMX/2)) GO TO 23
IF(ITER.GT.(MINLMT+ITERMX/2).AND.ITER.LT.MAXLMT) GO TO 23
WRITE(NW,150)ITER,XFDEL(ITER),XSDEL(ITER),TGDEL(ITER),TFDEL(
1ITER),TSDEL(ITER),XCDEL(ITER),G,CORFAC,DFAVG,BARKS,HCHRFSG,DZ

```

```

*****
C CONVERGENCE CRITERIA
C *****
23 IF(ITER.EQ.1) GO TO 43
   IF(TFDEL(ITER).EQ.0.) GO TO 38
   TFFDEL=ABS((TFDEL(ITER)-TFDEL(ITER-1))/TFDEL(ITER))
38   IF(TFDEL(ITER).EQ.0.) TFFDEL=0.0
   IF(TSDEL(ITER).EQ.0.) GO TO 17
   TSSDEL=ABS((TSDEL(ITER)-TSDEL(ITER-1))/TSDEL(ITER))
17   IF(TSDEL(ITER).EQ.0.) TSSDEL=0.0
   IF(XSDEL(ITER).EQ.0.) GO TO 39
   XSSDEL=ABS((XSDEL(ITER)-XSDEL(ITER-1))/XSDEL(ITER))
39   IF(XSDEL(ITER).EQ.0.) XSSDEL=0.0
   IF(TGDEL(ITER).EQ.0.) GO TO 42
   TGGDEL=ABS((TGDEL(ITER)-TGDEL(ITER-1))/TGDEL(ITER))
42   IF(TGDEL(ITER).EQ.0.) TGGDEL=0.0
   IF(XS(I).GT.XSMIN) GO TO 26
   IF(TSSDEL.GT.TOLER5) GO TO 20
   GO TO 18
26   IF(XSSDEL.GT.TOLER4) GO TO 20
18   IF(TGGDEL.GT.TOLER5) GO TO 20
   IF(TFFDEL.GT.TOLER3) GO TO 20
*****
C IF(XS(I).EQ.XSMIN.AND.TS(I).GE.TD) GO TO 67
C IF(I.LT.IRANDM) GO TO 53
WRITE(NW,125)ITER,DELXF,DELXS,DELTG,DELTF,DELTS
53 IF(XF(I-1).LT.(XFM+XFV)) GO TO 93
   DLXCIC=DELXC
   DLXFIC=DELXF
   DLXSIC=DELXS
   DLTGIC=DELTG
   DLTFIC=DELTF
   DLTSIC=DELTS
   IF(DLXCIC.EQ.0.OR.DLXFIC.EQ.0.) GO TO 96
   IF(ABS((DLXCIC-DLXCIP)/DLXCIC).GT.TOLER3) GO TO 94
   IF(ABS((DLXFIC-DLXFIP)/DLXFIC).GT.TOLER3) GO TO 94
96   IF(DLXSIC.EQ.0.) GO TO 97
   IF(ABS((DLXSIC-DLXSIP)/DLXSIC).GT.TOLER3) GO TO 94
97   IF(DLTGIC.EQ.0.) GO TO 98
   IF(ABS((DLTGIC-DLTGIP)/DLTGIC).GT.TOLER3) GO TO 94
98   IF(DLTFIC.EQ.0.) GO TO 99
   IF(ABS((DLTFIC-DLTFIP)/DLTFIC).GT.TOLER3) GO TO 94
99   IF(DLTSIC.EQ.0.) GO TO 93
   IF(ABS((DLTSIC-DLTSIP)/DLTSIC).GT.TOLER3) GO TO 94
93   Z(I)=Z(I-1)+DZ
   IF(DELXS.GT.0.0.AND.TS(I).LT.TD) TS(I)=TD
   DELZ=DZ
   IF(XSAVG.GE.(.999*XSMAX)) TLLAVG=TSAVG
   IF(XFAVG.GE.(.999*XFMAX)) CF=CFASH
   TSOLID=(WS*XSAVG*.56*CL*TLLAVG+WS*(1.-XSAVG)*CS*TD+
1WF*XAAVG*CFASH*TSAVG+WF*(1.+XFAVG-XAAVG)*CF*TFAVG)/
2(WS*XSAVG*.56*CL+WS*(1.-XSAVG)*CS+WF*XAAVG*CFASH+
3WF*(1.-XFAVG-XAAVG)*CF)
   ENGASO=MG(I)*CG*(TG(I)-273.0)
   ENSTNC=WS*XSAVG*.56*CL*(TLLAVG-273.)+WS*(1.-XSAVG)*
1CS*(TD-273.)
   ENFULO=MF(I)*CF*(TF(I)-273.0)
   ENASHO=WA AVG*CFASH*(TS(I)-273.0)
56   IF(XS(I).GE.(.999*XSMAX)) XS(I)=XSMAX
   IF(XC(I).GE.(.999*XCMAX)) XC(I)=XCMAX
   IF(XF(I).GE.(.999*XFMAX)) XF(I)=XFMAX
   L=0
   GO TO 2
94   NZMZ=WN2Z/28.C
   IF(XF(I).LT.(XFM+XFV)) W02Z=W02Z1+WF*(XF(I)-XF(1))*(77.77/20.)
   IF(XF(I).GE.(XFM+XFV).AND.XF(1).LT.(XFM+XFV)) W02Z=W02Z1+
1WF*(XFM+XFV-XF(1))*(77.77/20.)+WF*(XF(I)-XFM-XFV)*(32./12.)
   IF(XF(1).GE.(XFM+XFV)) W02Z=W02Z1+WF*(XF(I)-XFM-XFV)*(32./12.)
   O2MZ=W02Z/32.C
   IF(XF(I).LT.(XFM+XFV)) WCO2Z=WCO2Z1-WF*(XF(I)-XF(1))*
1(56.58/20.0)-WS*(XS(I)-XS(1))*44
   IF(XF(I).GE.(XFM+XFV).AND.XF(1).LT.(XFM+XFV)) WCO2Z=WCO2Z1-
1WF*(XFM+XFV-XF(1))*(56.58/20.)-WF*(XF(I)-XFM-XFV)*(44./12.)-
2WS*(XS(I)-XS(1))*44
   IF(XF(1).GE.(XFM+XFV)) WCO2Z=WCO2Z1-WF*(XF(I)-XFM-XFV)*
1(44./12.)-WS*(XS(I)-XS(1))*44
   CO2MZ=WCO2Z/44.0
   IF(XF(I).LT.(XFM+XFV)) WH2OZ=WH2OZ1-WF*(XF(I)-XF(1))*
1(41.15/20.)
   IF(XF(I).GE.(XFM+XFV)) WH2OZ=0.0

```

```

H20MZ=WH2CZ/18.0
TMGZ=O2MZ+CO2MZ+N2MZ+H20MZ
POG(I)=O2MZ/TMGZ
POGAVG=(POG(I)+POG(I-1))/2.0
IF(XF(I).EQ.XFMAX) GO TO 129
129 DF(I)=DPF*((XFMAX-XF(I))/(XFMAX-XFM-XFV))*(.1/3.)
IF(XFASHF.GT.C.) DF(I)=(DF(I)+DFBZAF)/2.0
DFAVG=(DF(I)+DF(I-1))/2.0
G=WGAVG/AREA
ASNMR=ASBZO*(1.+ALFA*VFSRAT)
ASDNR=(1.+ALFA*VFSRAT*(1.-XFA-XFAVG))/(1.-XFM-XFV-XFA)
AFNMR1=AFBZO*(1.+ALFA*VFSRAT)
IF(XFASHF.GT.C.) GO TO 109
IF((XFA+XFAVG).EQ.1) GO TO 131
131 AFNMR2=((1.-XFA-XFAVG)/(1.-XFM-XFV-XFA))*(.2/3.)
AFNMR=AFNMR1*AFNMR2
AFDNR=ASDNR
ASBZ=ASNMR/ASDNR
AFBZ=AFNMR/AFDNR
109 RHOS=RHOSC*(1.-XSAVG*.44)
IF(XFASHF.GT.C.) RHOF=RHOFAF*((TFAVG/TFASHF))*ASHFAC
VSAVG=(WSAVG/RHOS)+(WFAVG/RHOF)+(WAAVG/RHOASH)
IF(XFASHF.LE.C.) GO TO 103
ASNMR=ASNMR
ASDNR1=ASDNR
IF(TF(I).LT.TF(I-1)) GO TO 111
111 RHOFAC=(TFASHF/TFAVG)*ASHFAC
ASDNR2=(ALFA*VFSRAT*RHOFC*XFA*(XFAVG-XFASHF))/(RHCASH*
1(1.-XFM-XFV-XFA))*RHOFAC
ASDNR=ASDNR1+ASDNR2
ASBZ=ASNMR/ASDNR
AFNMR1=AFNMR1
AFNMR2=((1.-XFA-XFASHF)/(1.-XFM-XFV-XFA))*(.2/3.)
IF(TF(I).LT.TF(I-1)) GO TO 112
112 RHOFAC=(TFASHF/TFAVG)*ASHFAC
IF((XFA+XFAVG).EQ.1.) GO TO 132
AFNMR3=((1.-XFA-XFAVG)/(1.-XFA-XFASHF)+RHOFO*XFA*(XFAVG-XFASHF
1)/((1.-XFA-XFASHF)*RHOASH)*RHOFAC))*(.2/3.)
132 AFNMR=AFNMR1*AFNMR2*AFNMR3
AFDNR=ASDNR
AFBZ=AFNMR/AFDNR
103 ITER=1
L=L+1
IF(L.EQ.5) GO TO 93
GO TO 102
20 IF(ITER.EQ.1) GO TO 43
XCAVG=XC(I-1)+(XCDEL(ITER)+XCDEL(ITER-1))/4.0
XFAVG=XF(I-1)+(XFDEL(ITER)+XFDEL(ITER-1))/4.0
XSAVG=XS(I-1)+(XSDEL(ITER)+XSDEL(ITER-1))/4.0
TFAVG=TF(I-1)+(TFDEL(ITER)+TFDEL(ITER-1))/4.0
TSAVG=TS(I-1)+(TSDEL(ITER)+TSDEL(ITER-1))/4.0
TGAVG=TG(I-1)+(TGDEL(ITER)+TGDEL(ITER-1))/4.0
43 ITER=ITER+1
IF(ITER.NE.ITERMX) GO TO 82
IF(XF(I-1).LT.(XFM+XFV)) GO TO 82
DZ=DZ+.005
IF(DZ.LE.C*.010) DZ=.010
K=K+1
IF(K.LE.5.OR.DZ.NE.C*.010) GO TO 1
IRANDM=I
GO TO 1
82 IF(ITER.GT.ITERMX) GO TO 21
GO TO 9
21 IF(I.GT.IMAX.OR.ITER.GT.ITERMX) I=I-1
ASCZ=ASBZ+AFBZ
DPAVG=(DPS*WSAVG+DFAVG+(WFAVG+WAAVG))/(WSAVG+WFAVG+WAAVG)
THCMVM=WF*XFV*HFVM
THCMFC=WF*XFC*HFFC
OHVMFC=THCMVM+THCMFC
HLUFVM=WF*(BETACV-XFM)*HFVM
THDVZN=WF*XFV*HLTDVM
ENHCAL=WS*XSAVG*ES
WRITE(NW,140) XFASHF,HEIGHT
WRITE(NW,160) Z(I)
WRITE(NW,115) TSCLID,ASCZ
WRITE(NW,200) DPAVG,XSAVG
WRITE(NW,170) ENGASI,ENSTNI,ENFULI
WRITE(NW,175) ENGASO,ENSTNO,ENFULO,ENASHO
WRITE(NW,210) DELHTL
WRITE(NW,215) THCMVM

```

```

WRITE(NW,220) THCMFC
WRITE(NW,225) OHVMFC
WRITE(NW,230) HLUFVM
WRITE(NW,235) THDVZN
WRITE(NW,240) ENHCAL
WRITE(NP,190) I
CLOSE(UNIT=NP)
CLOSE(UNIT=NW)
STOP
END
C *****
C END OF MAIN PROGRAM
C *****
C FUNCTION SUBPROGRAMS
C *****
C FUNCTION HFS(EFFKS,DPS,DFAVG,EMSVTY,SIGMAR,VIEWF,TFAVG,TSAVG)
HCFS=2.0*EFFKS/(DPS+DFAVG)
HRFS=EMSVTY*SIGMAR*VIEWF*(TFAVG**2+TSAVG**2)*(TFAVG+TSAVG)
HFS=HCFS+HRFS
RETURN
END
C *****
C FUNCTION HFG(EBED,DFAVG,KG,MUG,CG,G,CORFAC)
REAL KG,MUG
RE=DFAVG*G/MUG
PR=CG*MUG/KG
IF(RE.EQ.0.) GO TO 1
HCFG=(1.9*KG/DFAVG)*(RE**0.5)*(PR**0.33)
HRFG=4.5+1.33*DFAVG*EBED
HFG=HCFG+HRFG
RETURN
END
C *****
C FUNCTION HSG(EBED,DPS,KG,MUG,CG,G,CORFAC)
REAL KG,MUG
RE=DPS*G/MUG
PR=CG*MUG/KG
HSGS=(1.9*KG/DPS)*(RE**0.5)*(PR**0.33)
HRGS=4.5+1.33*DPS*EBED
HSG=HSGS+HRGS
RETURN
END
C *****
C FUNCTION DASHKS(RGAS,TFAVG,TGAVG,DFAVG,FACTOR)
REAL KS,KD
KS=3.44E+11*EXP(-44000./(RGAS*TFAVG))/SQRT(TFAVG)
KD=(0.2304*FACTOR*(TFAVG/1500.0)**0.75)/DFAVG
DASHKS=1./(1./KS+1./KD)
RETURN
END
C *****
C FUNCTION HWA(DZ,REEMSY,SIGMAR,TWOBNG,TAMB,DELTWO)
HCWA=1.22*(DELTWO/DZ)**(1./4.)
HRWA=REEMSY*SIGMAR*(TWOBNG**2+TAMB**2)*(TWOBNG+TAMB)*0.0
HWA=HCWA+HRWA
RETURN
END
C *****
C FUNCTION HGW(EBED,DPAVG,DI,KG,MUG,G,CORFAC,ETAGW)
REAL KG,MUG
DPDTR=DPAVG/DI
RE=DPAVG*G/MUG
HCGW1=3.50*(KG/DI)*EXP(-4.60*DPDTR)*RE**0.7
HCGW2=0.813*(KG/DI)*EXP(-6.0*DPDTR)*RE**0.9
HCGW=(HCGW1+HCGW2)/2.0
HRGW=4.5+1.33*DPAVG*EBED
HGW=(HCGW+HRGW)*ETAGW
RETURN
END
C *****
C END OF FUNCTION SUBPROGRAMS
C *****

```

```

WRITE(NW,45) TPHZ,TPHDVZ,TPHCVM,TD,TFASHF
WRITE(NW,85) TOLER1,TOLER2,TOLER3,TOLER4,TOLERS
WRITE(NW,50) IMAX,ITERMX,IRANDM,MINLMT,MAXLMT
25  FORMAT(25X,3I10)
30  FORMAT(22X,3F12.4)
35  FORMAT(4X,6F12.4)
40  FORMAT(1X,7F11.4)
45  FORMAT(10X,5F12.4)
50  FORMAT(15X,5I10)
55  FCRMAT(1X,7F10.6,4F12.4,4F10.3)
60  FCRMAT(25X,'SIMULATION OF LIME SHAFT KILN')
65  FCRMAT(26X,'ANALYSIS OF THE BURNING ZONE')
70  FCRMAT(/ /80A1/)
75  FCRMAT(8F10.4)
80  FCRMAT(1X,4F11.4,E12.4,2F11.4)
85  FCRMAT(10X,5F12.5)
90  FCRMAT(16X,4F12.4)
95  FCRMAT(15,8F8.1,F10.4)
100 FCRMAT(/3X,'I',2X,'Z(M)',6X,'XF',6X,'XS',2X,'TG(K)',2X,
1  'TF(K)',2X,'TS(K)',1X,'TW(K)',1X,'RSHLHD',1X,'DELSHT',3X,
2  'HFS',2X,'HFG',2X,'HSG',1X,'ASBZ',1X,'AFBZ',4X,'QFS',3X,
3  'QFG',2X,'QSG',1X,'DELHTL',2X,'POZG',1X,'PCO2G'/)
105 FCRMAT(15,6F10.1,F15.4)
110 FCRMAT(5F12.4,2F10.6)
115 FCRMAT(/2X,67HTEMPERATURE OF SOLIDS FROM BURNING ZONE AS INPUT
1  FOR COOLING ZONE =,F7.1,' K'/3X,41HAND SPECIFIC SURFACE
2  OF SOLID PARTICLES =,F5.2,' SQM PER CUM OF KILN VOLUME')
120 FCRMAT(15,5F12.1,F15.9)
125 FCRMAT(5X,15,2F15.9,3F12.4)
130 FCRMAT(18,5F12.4)
135 FCRMAT(18,5F10.4,2F11.6)
140 FCRMAT(/1X,25FASH FUSION STARTS AT XF =,F7.4,39H AT
1  HEIGHT-(FROM TOP OF BURNING ZONE) =,F6.3,' M')
145 FCRMAT(1X,13,F6.3,2F8.5,3F7.1,F6.1,F7.4,F7.0,F6.1,4F5.1,F7.0,
13F6.0,2F6.3)
150 FCRMAT(18,2F9.6,3F9.3,7F11.4)
155 FCRMAT(/ /30X,19HRESULTS OF ANALYSIS/)
160 FCRMAT(/22X,28HHEIGHT OF THE BURNING ZONE =,F6.3,' M')
165 FCRMAT(1F10.4,2F14.4,3F14.2)
170 FCRMAT(/2X,41HENTHALPIES OF GAS,STONE AND FUEL AT TOP =,
1F8.1,' ',F8.1,' ',F8.1,' ',F8.1,' ',KCAL/HR')
175 FCRMAT(/15X,48HENTHALPIES OF GAS,STONE,FUEL AND ASH AT BOTTOM
1 =/18X,F8.1,' ',F8.1,' ',F7.1,' ',F8.1,' ',KCAL/HR')
180 FCRMAT(F5.3,' ',F5.3,' ',F5.3,' ',F5.3,' ',F5.3,' ',F5.3,' ',
1,F5.3)
185 FCRMAT(F6.4,' ',F6.4,' ',F6.4,' ',F7.2,' ',F7.2,' ',F7.2)
190 FCRMAT(1X,14)
195 FCRMAT(8CA1)
200 FCRMAT(/1X,33FAVERAGE SIZE OF SOLID PARTICLES =,F6.3,' M',28H
1 AND DEGREE OF CALCINATION =,F7.4)
205 FCRMAT(/)
210 FCRMAT(/10X,43HHEAT LOSS THROUGH WALL OF BURNING SECTION =,
1F9.1,' ',KCAL/HR')
215 FCRMAT(/8X,45HTOTAL HEAT OF COMBUSTION OF VOLATILE MATTER =,
1F10.1,' ',KCAL/HR')
220 FCRMAT(/10X,42HTOTAL HEAT OF COMBUSTION OF FIXED CARBON =,
1F10.1,' ',KCAL/HR')
225 FCRMAT(/6X,50HOVERALL HEAT OF VOLATILE MATTER AND FIXED CARBON
1 =,F10.1,' ',KCAL/HR')
230 FCRMAT(/6X,50HHEAT LOSS IN UNBURNT FRACTION OF VOLATILE MATTER
1 =,F10.1,' ',KCAL/HR')
235 FCRMAT(/11X,4CHTOTAL LATENT HEAT FOR DEVCLATILIZATION =,
1F10.1,' ',KCAL/HR')
240 FCRMAT(/4X,53HTOTAL ENDOTHERMIC HEAT FOR CALCINATION OF LIME
1STONE =,F10.1,' ',KCAL/HR')
AREA=TPD/PS
RI=SQRT(AREA/3.14)
DI=2.*RI
WS=PS*AREA*1000.*100./(24.*56.)
WF=WS/XRINF D
*****
THEORETICAL AIR REQUIREMENT AND HEAT OF CCOMBUSTION OF VM
*****
THO2VM=(77.77/20.)*XFV
THO2FC=(32./12.)*XFC
TCTLO2=THO2VM+THO2FC
TOTLN2=TCTLO2/0.305
THAIR=TOTLO2+TOTLN2
WA=WF*THAIR*(1.+XEA)
VMFDAF=XFV/(XFV+XFC)

```



```

C *****
C SIMULATION OF LIME SHAFT KILN :
C PROGRAMME FOR THE ANALYSIS OF COOLING ZONE STARTING FROM UPPER SIDE
C *****
C DIMENSION TS(400),TF(400),TG(400),DATAIN(80)
C REAL KG,MUG
C OPEN(UNIT=1,FILE='CLG.DAT',TYPE='OLD')
C READ(1,95) DATAIN
C READ(1,*) NP,NW,NPRINT,IMAX
C OPEN(UNIT=NW,FILE='CLGRES.OUT',TYPE='NEW')
C OPEN(UNIT=NP,FILE='CLGPLT.OUT',TYPE='NEW')
C *****
C THE FORTRAN VARIABLES USED IN THE FOLLOWING ARE DEFINED AFTER
C EACH STATEMENT GENERALLY IN ORDER OF THEIR APPEARANCE
C *****
C READ(1,*) TG(1),TF(1),TS(1)
C (TEMPERATURES OF BULK GAS,FUEL AND STONE SURFACE)
C READ(1,*) PS,XRINFD,TPD,DPS,DPF,DZ
C (SUPERFICIAL PRODUCT OUTPUT RATE BASED ON EMPTY KILN CROSS-
C SECTION,STONE-TO-FUEL-RATIO IN KILN FEED INPUT,NOMINAL
C PRODUCTION RATE OF LIME SHAFT KILN,PARTICLE SIZE OF LIMESTONE,
C COAL IN KILN FEED,AXIAL WIDTH OF DIFFERENTIAL ELEMENT)
C READ(1,*) DPAVG,XSAVG,ASCZ,EBED,GAMMA,ETASG,ETAGW
C (AVERAGE SIZE OF SOLIDS,DEGREE OF CALCINATION OF LIMESTONE,
C INTERFACIAL PACKING SURFACE OF SOLIDS,BED POROSITY,
C CONSTANT FOR EMISSIVITY,EFFECTIVENESS FACTOR FOR HEAT EXCHANGE)
C READ(1,*) XFM,XFV,XFC,XFA,XEA
C (FRACTIONAL VALUES OF MOISTURE CONTENT,VOLATILE MATTER,FIXED
C CARBON,ASH CONTENT OF FUEL AND EXCESS AIR)
C READ(1,*) KG,MUG,TAMB,TWOCLG
C THERMAL CONDUCTIVITY OF GAS,VISCOSITY OF GAS,AMBIENT TEMPERATU-
C RE,EXTERNAL WALL TEMPERATURE)
C READ(1,*) FBCDTY,RBCDTY,FBTHIK,RBTHIK,RBEMSY,SIGMAR
C (THERMAL CONDUCTIVITIES OF FIRE BRICKS,RED BURNT CLAY BRICKS,
C THICKNESSES OF FIRE BRICKS INSULATION,RED BRICKS,EMISSIVITY OF
C RED BRICKS SURFACE,RADIATION CONSTANT)
C WRITE(NW,25)
C WRITE(NW,30)
C WRITE(NW,35) DATAIN
C WRITE(NW,05) NP,NW,NPRINT,IMAX
C WRITE(NW,10) TG(1),TF(1),TS(1)
C WRITE(NW,50) PS,XRINFD,TPD,DPS,DPF,DZ
C WRITE(NW,45) DPAVG,XSAVG,ASCZ,EBED,GAMMA,ETASG,ETAGW
C WRITE(NW,15) XFM,XFV,XFC,XFA,XEA
C WRITE(NW,60) KG,MUG,TAMB,TWOCLG
C WRITE(NW,20) FBCDTY,RBCDTY,FBTHIK,RBTHIK,RBEMSY,SIGMAR
5 FORMAT(20X,4I10)
10 FORMAT(22X,3F12.4)
15 FORMAT(10X,5F12.4)
20 FORMAT(4X,5F12.4,E12.4)
25 FORMAT(25X,'SIMULATION OF LIME SHAFT KILN')
30 FORMAT(26X,'ANALYSIS OF THE COOLING ZONE')
35 FORMAT(/80A1/)
40 FORMAT(/30X,19HRESULTS OF ANALYSIS/)
45 FORMAT(1X,7F11.4)
50 FORMAT(4X,6F12.4)
55 FORMAT(/24X,27HHEIGHT OF THE COOLING ZONE=,F5.3,'M')
60 FORMAT(16X,4F12.4)
65 FORMAT(1X,I4,F11.3,3F10.2,2F7.1,2F9.1)
70 FORMAT(/1X,62HENTHALPIES OF PRODUCT LIME AND ASH/CINDERS AT

```

```

1 BOTTOM OF KILN =,F8.1,' KCAL/HR')
75 FORMAT(16X,F16.4,2F16.2)
80 FORMAT(F5.3,' ','F5.3',' ','F5.3',' ','F5.3',' ','F5.3',' ','
1,F5.3)
85 FORMAT(F6.4,' ','F7.2',' ','F7.2)
90 FORMAT(1X,I4)
95 FORMAT(80A1)
100 FORMAT(/4X,'I',7X,'Z(M)',5X,'TG(K)',5X,'TS(K)',5X,'TW(K)',4X,
1'HSG',3X,'ASCZ',6X,'QSG',3X,'DELHTL'/)
105 FORMAT(/11X,42HENTHALPY OF AIR INTO LIME KILN AT BOTTOM =,
1F8.1,' KCAL/HR')
110 FORMAT(/10X,43HHEAT LOSS THROUGH WALL OF COOLING SECTION =,
1F9.1,' KCAL/HR')
AREA=TPD/PS
RI=SQRT(AREA/3.14)
DI=2.*RI
WS=PS*AREA*1000.*100./(24.*56.)
WF=WS/XRINF D
*****
C THEORETICAL AIR REQUIREMENT
C *****
C THO2VM=(77.77/20.)*XFV
C THO2FC=(32./12.)*XFC
C TOTLO2=THO2VM+THO2FC
C TOTLN2=TOTLO2/0.305
C THAIR=TOTLO2+TOTLN2
C WA=WF*THAIR*(1.+XEA)
C *****
WRITE(NW,15) AREA,DI,WS,WF,WA
WRITE(NW,40)
WRITE(NP,80) PS,DPS,DPF,XRINF D,XFV,XFC,XEA
WRITE(NW,100)
RFB=RI+FBTHIK
RO=RFB+RBTHIK
DO=2.*RO
CSTKLN=(ALOG(RFB/RI)/FBCDTY)+(ALOG(RO/RFB)/RBCDTY)
CORFAC=1.-GAMMA
ASSCLZ=ETASG
WSCLZ=WS*XSAVG*0.56+WS*(1.-XSAVG)+WF*XEA
WGCLZ=WA
DV=AREA*DZ
DAS=ASCZ*ASSCLZ*DV
G=WGCLZ/AREA
WGAVG=WA
WSAVG=WSCLZ
WAVGTL=WGAVG+WSAVG
XWG=WGAVG/WAVGTL
XWS=WSAVG/WAVGTL
TWO=TWOCLG
I=1
1 TGAVG=TG(I)
TSAVG=TS(I)
TFAVG=TSAVG
TBOPRG=TGAVG*XWG+TSAVG*XWS
C *****
C SPECIFIC HEATS OF DIFFERENT CONSTITUENTS
C *****
CS=0.1968+(0.1189*TSAVG*10.**-3)-(0.3076*10.**4)/(TSAVG**2)
CL=0.1786+(0.0864*TSAVG*10.**-3)-(0.1928*10.**4)/(TSAVG**2)
CFASH=(-0.1640+(0.1136*TFAVG*10.**-2)-(0.49*TFAVG*TFAVG*10.**

```

```

1-6))*0.75
CSAVG=(WS*XSAVG*0.56*CL+WS*(1.-XSAVG)*CS+WF*XFA*CFASH)/WSCLZ
CG=0.2372+(0.2900*TGAVG*10.**-4)-(1360./TGAVG**2)
*****
C AHSG=HSG(EBED,DPAVG,KG,MUG,CG,G,CORFAC)
TGI=TGAVG
2 Z=(FLOAT(I)-1.)*DZ
QSG=AHSG*(TS(I)-TG(I))
X=(I/NPRINT)-FLOAT(I)/FLOAT(NPRINT)
IF(X.NE.0) GO TO 7
TYPE 60,Z,TG(I),TF(I),TS(I)
WRITE(NP,85)Z,TG(I),TS(I)
WRITE(NW,65)I,Z,TG(I),TS(I),TWO,AHSG,ASCZ,QSG,DELHTL
IF(TG(I).LE.TAMB) GO TO 21
7 I=I+1
IF(I.GT.IMAX) GO TO 21
*****
C ESTIMATION OF WALL HEAT LOSSES
C *****
C DELTWO=TWOCLG-TAMB
AHWA=HWA(DZ,RBEMSY,SIGMAR,TWOCLG,TAMB,DELTWO)
AHGW=HGW(EBED,DPAVG,DI,KG,MUG,G,CORFAC,ETAGW)
IF(AHWA.EG.0.) GO TO 3
UIEFFI=RI*(1./(RI*AHGW)+CSTKLN+1./(RO*AHWA))
UIEFF=1./UIEFFI
DELHL=UIEFF*2.*3.14*DZ*RI*(TGI-TAMB)
DELHTL=DELHTL+DELHL
TWI=TGI-DELHL/(3.14*DI*DZ*AHGW)
TWO=TAMB+DELHL/(3.14*DO*DZ*AHWA)
TWOCLG=TWO
C *****
3 TS(I)=TS(I-1)-AHSG*(TS(I-1)-TG(I-1))*DAS/(WSCLZ*CSAVG)
TF(I)=TS(I)
DELHS=WSCLZ*CSAVG*(TS(I)-TS(I-1))
TG(I)=TG(I-1)+(DELHS-DELHL)/(WGCLZ*CG)
DELTG=TG(I)-TG(I-1)
DELTF=TF(I)-TF(I-1)
DELTS=TS(I)-TS(I-1)
GO TO 1
21 IF(I.GT.IMAX) I=I-1
HCLZ=Z
SHLPLM=WSCLZ*CSAVG*(TS(I)-273.0)
ENAIRI=WA*CG*(TG(I)-273.0)
WRITE(NW,55)HCLZ
WRITE(NW,70)SHLPLM
WRITE(NW,105)ENAIRI
WRITE(NW,110)DELHTL
WRITE(NP,90)I
CLOSE(UNIT=1)
CLOSE(UNIT=NP)
CLOSE(UNIT=NW)
STOP
END
*****
C END OF MAIN PROGRAM
C *****

```

C *****
C FUNCTION SUBPROGRAMS
C *****

```
FUNCTION HSG(EBED, DPAVG, KG, MUG, CG, G, CORFAC)
REAL KG, MUG
RE=DPAVG*G/MUG
PR=CG*MUG/KG
HCSG=(1.9*KG/DPAVG)*(RE**0.5)*(PR**0.33)
HRSG=4.5+1.33*DPAVG*EBED
HRSG=HRSG*CORFAC
HSG=HCSG+HRSG
RETURN
END
```

C *****

```
FUNCTION HWA(DZ, RBEMSY, SIGMAR, TWOCLG, TAMB, DELTWO)
HCWA=1.22*(DELTWO/DZ)**(1./4.)
HRWA=RBEMSY*SIGMAR*(TWOCLG**2+TAMB**2)*(TWOCLG+TAMB)*0.0
HWA=HCWA+HRWA
RETURN
END
```

C *****

```
FUNCTION HGW(EBED, DPAVG, DI, KG, MUG, G, CORFAC, ETAGW)
REAL KG, MUG
DPDTR=DPAVG/DI
RE=DPAVG*G/MUG
HCGW1=3.50*(KG/DI)*EXP(-4.6*DPDTR)*RE**0.7
HCGW2=0.813*(KG/DI)*EXP(-6.0*DPDTR)*RE**0.9
HCGW=(HCGW1+HCGW2)/2.0
HRGW=HRGW*CORFAC
HGW=(HCGW+HRGW)*ETAGW
RETURN
END
```

C *****
C END OF FUNCTION SUBPROGRAMS
C *****

NOMENCLATURE AND TABLES OF SIMULATION RESULTS

AFBZ	Interfacial area of fuel particles in burning zone, m^2/m^3 of bed volume
AFPZ	Interfacial area of fuel particles in preheating zone, m^2/m^3 of bed volume
ASBZ	Interfacial area of lime-limestone particles in burning zone, m^2/m^3 of bed volume
ASCZ	Interfacial area of solid mass in cooling zone, m^2/m^3 of bed volume
ASPZ	Interfacial area of limestone particles in preheating zone
DELHTL	Cumulative wall heat loss upto a given axial location Z (ith grid point) in a zone, Kcal/hr
DELSHT	Sensible heat accumulation in lime layer upto a given axial location (ith grid point) in burning zone, Kcal/hr
DPF	Particle size of fuel, m
DPS	Particle size of limestone, m
HFZ	Heat transfer coefficient from fuel particles to gas, Kcal/(hr $(m^2) (K)$)

HFS Heat transfer coefficient from fuel to stone particles, Kcal/(hr)
(m²)(K)

HSG Heat transfer coefficient from stone particles to gas phase,
Kcal/(hr) (m²) (K)

I Grid point in a zone (I = 1 at Z = 0)

PCO_{2G} Partial pressure of carbon dioxide, atm

PO_{2G} Partial pressure of oxygen, atm

PS Superficial product lime output rate, t/(m²) (day)

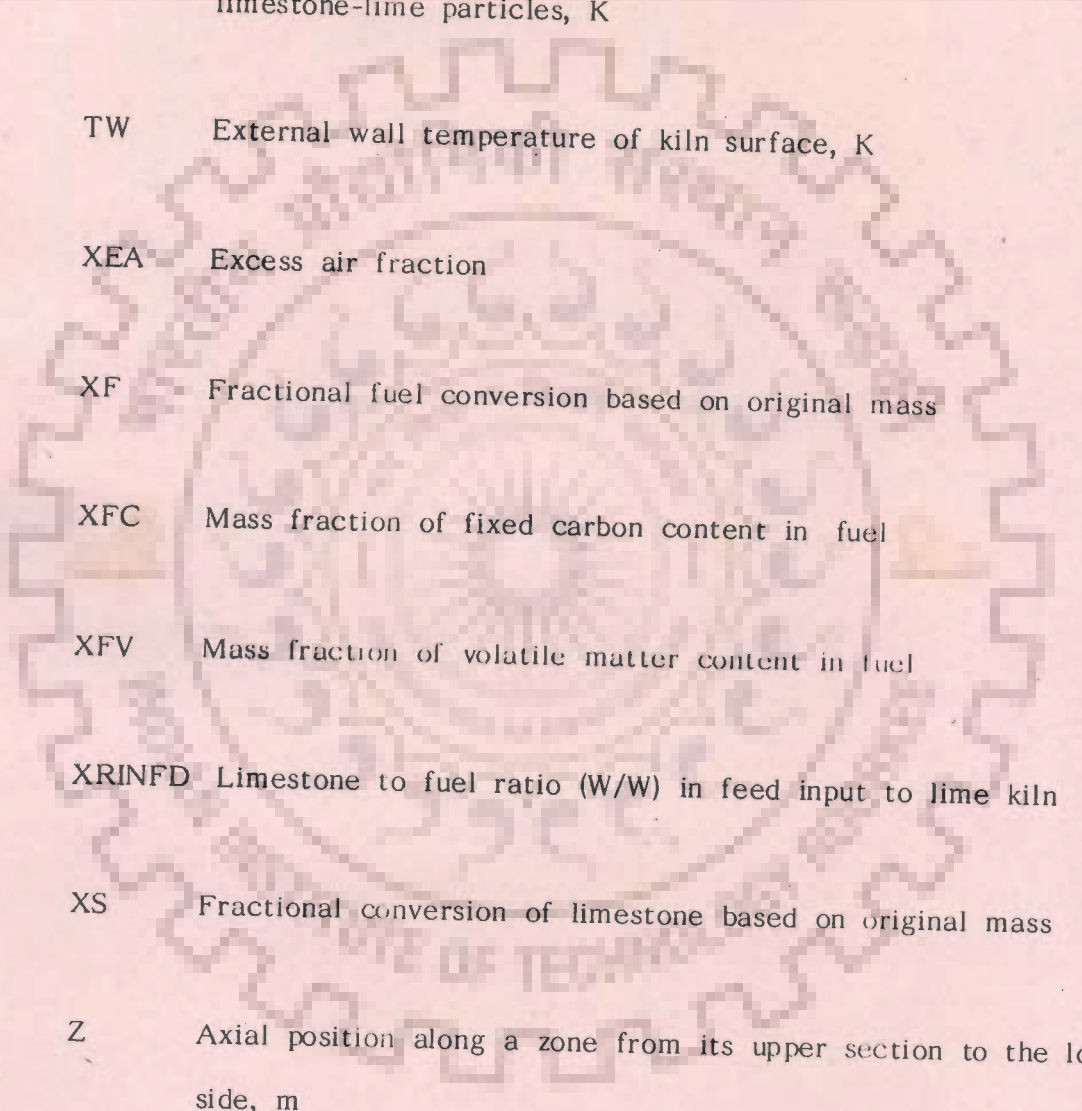
QFG Heat exchange rate from fuel to gas, Kcal/hr

QFS Heat exchange rate from fuel to stone particles, Kcal/hr

QSG Heat exchange rate from stone particles to gas, Kcal/hr

RSHLHDRatio of sensible heat change of the lime layer to total heat
received by limestone-lime particles in burning zone
(interval ΔZ)

TF Temperature of fuel particles, K



TG	Temperature of bulk gas phase, K
TS	Temperature of solid particles/mass, surface temperature of limestone-lime particles, K
TW	External wall temperature of kiln surface, K
XEA	Excess air fraction
XF	Fractional fuel conversion based on original mass
XFC	Mass fraction of fixed carbon content in fuel
XFV	Mass fraction of volatile matter content in fuel
XRINFD	Limestone to fuel ratio (W/W) in feed input to lime kiln
XS	Fractional conversion of limestone based on original mass
Z	Axial position along a zone from its upper section to the lower side, m

TABLE P.1 (A3)
 SIMULATION OF LIME SHAFT KILA
 ANALYSIS OF THE COOLING ZONE

INPUT DATA FOR SET NO. 1 (A)
 (AVERAGE CONDITIONS)

0.0940 2.2500 C.9929 5.5000 500.6000 1194.7000 1194.7000 250
 C.03500 0.0900 10.0000 0.4500 C.1000 0.0500 0.0500
 1.0100 C.0312 0.2250 0.4750 C.9000 0.0125 0.1000
 C.6000 0.0800 0.2300 304.7000 0.2500 0.1250
 4.4444 C.6000 2.3794 0.0800 0.0000 0.9000 0.4960E-07
 744.0477 135.2814 1394.5542

RESULTS OF ANALYSIS

I	Z(M)	TG(K)	TS(K)	TH(K)	HSG	ASCZ	BSG	DELHTL
1	0.0000	500.6000	1194.7000	1194.7000	250	0.0500	0.0500	0.1000
2	0.0000	499.9929	1179.4000	1179.4000	250	0.0500	0.0500	0.1000
3	0.0000	499.2500	1171.1111	1171.1111	250	0.0500	0.0500	0.1000
4	0.0000	498.5000	1163.3333	1163.3333	250	0.0500	0.0500	0.1000
5	0.0000	497.7500	1155.5556	1155.5556	250	0.0500	0.0500	0.1000
6	0.0000	497.0000	1147.7778	1147.7778	250	0.0500	0.0500	0.1000
7	0.0000	496.2500	1140.0000	1140.0000	250	0.0500	0.0500	0.1000
8	0.0000	495.5000	1132.2222	1132.2222	250	0.0500	0.0500	0.1000
9	0.0000	494.7500	1124.4444	1124.4444	250	0.0500	0.0500	0.1000
10	0.0000	494.0000	1116.6667	1116.6667	250	0.0500	0.0500	0.1000
11	0.0000	493.2500	1108.8889	1108.8889	250	0.0500	0.0500	0.1000
12	0.0000	492.5000	1101.1111	1101.1111	250	0.0500	0.0500	0.1000
13	0.0000	491.7500	1093.3333	1093.3333	250	0.0500	0.0500	0.1000
14	0.0000	491.0000	1085.5556	1085.5556	250	0.0500	0.0500	0.1000
15	0.0000	490.2500	1077.7778	1077.7778	250	0.0500	0.0500	0.1000
16	0.0000	489.5000	1070.0000	1070.0000	250	0.0500	0.0500	0.1000
17	0.0000	488.7500	1062.2222	1062.2222	250	0.0500	0.0500	0.1000
18	0.0000	488.0000	1054.4444	1054.4444	250	0.0500	0.0500	0.1000
19	0.0000	487.2500	1046.6667	1046.6667	250	0.0500	0.0500	0.1000
20	0.0000	486.5000	1038.8889	1038.8889	250	0.0500	0.0500	0.1000
21	0.0000	485.7500	1031.1111	1031.1111	250	0.0500	0.0500	0.1000
22	0.0000	485.0000	1023.3333	1023.3333	250	0.0500	0.0500	0.1000
23	0.0000	484.2500	1015.5556	1015.5556	250	0.0500	0.0500	0.1000
24	0.0000	483.5000	1007.7778	1007.7778	250	0.0500	0.0500	0.1000
25	0.0000	482.7500	1000.0000	1000.0000	250	0.0500	0.0500	0.1000
26	0.0000	482.0000	992.2222	992.2222	250	0.0500	0.0500	0.1000
27	0.0000	481.2500	984.4444	984.4444	250	0.0500	0.0500	0.1000
28	0.0000	480.5000	976.6667	976.6667	250	0.0500	0.0500	0.1000
29	0.0000	479.7500	968.8889	968.8889	250	0.0500	0.0500	0.1000
30	0.0000	479.0000	961.1111	961.1111	250	0.0500	0.0500	0.1000
31	0.0000	478.2500	953.3333	953.3333	250	0.0500	0.0500	0.1000
32	0.0000	477.5000	945.5556	945.5556	250	0.0500	0.0500	0.1000
33	0.0000	476.7500	937.7778	937.7778	250	0.0500	0.0500	0.1000
34	0.0000	476.0000	930.0000	930.0000	250	0.0500	0.0500	0.1000
35	0.0000	475.2500	922.2222	922.2222	250	0.0500	0.0500	0.1000
36	0.0000	474.5000	914.4444	914.4444	250	0.0500	0.0500	0.1000
37	0.0000	473.7500	906.6667	906.6667	250	0.0500	0.0500	0.1000
38	0.0000	473.0000	898.8889	898.8889	250	0.0500	0.0500	0.1000
39	0.0000	472.2500	891.1111	891.1111	250	0.0500	0.0500	0.1000
40	0.0000	471.5000	883.3333	883.3333	250	0.0500	0.0500	0.1000
41	0.0000	470.7500	875.5556	875.5556	250	0.0500	0.0500	0.1000
42	0.0000	470.0000	867.7778	867.7778	250	0.0500	0.0500	0.1000
43	0.0000	469.2500	860.0000	860.0000	250	0.0500	0.0500	0.1000
44	0.0000	468.5000	852.2222	852.2222	250	0.0500	0.0500	0.1000
45	0.0000	467.7500	844.4444	844.4444	250	0.0500	0.0500	0.1000
46	0.0000	467.0000	836.6667	836.6667	250	0.0500	0.0500	0.1000
47	0.0000	466.2500	828.8889	828.8889	250	0.0500	0.0500	0.1000
48	0.0000	465.5000	821.1111	821.1111	250	0.0500	0.0500	0.1000
49	0.0000	464.7500	813.3333	813.3333	250	0.0500	0.0500	0.1000
50	0.0000	464.0000	805.5556	805.5556	250	0.0500	0.0500	0.1000
51	0.0000	463.2500	797.7778	797.7778	250	0.0500	0.0500	0.1000
52	0.0000	462.5000	790.0000	790.0000	250	0.0500	0.0500	0.1000
53	0.0000	461.7500	782.2222	782.2222	250	0.0500	0.0500	0.1000
54	0.0000	461.0000	774.4444	774.4444	250	0.0500	0.0500	0.1000
55	0.0000	460.2500	766.6667	766.6667	250	0.0500	0.0500	0.1000
56	0.0000	459.5000	758.8889	758.8889	250	0.0500	0.0500	0.1000
57	0.0000	458.7500	751.1111	751.1111	250	0.0500	0.0500	0.1000
58	0.0000	458.0000	743.3333	743.3333	250	0.0500	0.0500	0.1000
59	0.0000	457.2500	735.5556	735.5556	250	0.0500	0.0500	0.1000
60	0.0000	456.5000	727.7778	727.7778	250	0.0500	0.0500	0.1000

TABLE F.2 (A3)
 SIMULATION OF LIME SHAFT KILN
 ANALYSIS OF THE COOLING ZONE

INPUT DATA FOR SET NO. 2 (A)
 (DPS=0.026 M)

F-12

RESULTS OF ANALYSIS

I

Z(M)	TE(K)	TS(K)	TW(K)	HSG	ASCZ	OSG	DELHTL
0.0	1116.0	1116.0	1116.0	11	N	77	0.0
0.5	1116.0	1116.0	1116.0	11	N	77	0.0
1.0	1116.0	1116.0	1116.0	11	N	77	0.0
1.5	1116.0	1116.0	1116.0	11	N	77	0.0
2.0	1116.0	1116.0	1116.0	11	N	77	0.0
2.5	1116.0	1116.0	1116.0	11	N	77	0.0
3.0	1116.0	1116.0	1116.0	11	N	77	0.0
3.5	1116.0	1116.0	1116.0	11	N	77	0.0
4.0	1116.0	1116.0	1116.0	11	N	77	0.0
4.5	1116.0	1116.0	1116.0	11	N	77	0.0
5.0	1116.0	1116.0	1116.0	11	N	77	0.0
5.5	1116.0	1116.0	1116.0	11	N	77	0.0
6.0	1116.0	1116.0	1116.0	11	N	77	0.0
6.5	1116.0	1116.0	1116.0	11	N	77	0.0
7.0	1116.0	1116.0	1116.0	11	N	77	0.0
7.5	1116.0	1116.0	1116.0	11	N	77	0.0
8.0	1116.0	1116.0	1116.0	11	N	77	0.0
8.5	1116.0	1116.0	1116.0	11	N	77	0.0
9.0	1116.0	1116.0	1116.0	11	N	77	0.0
9.5	1116.0	1116.0	1116.0	11	N	77	0.0
10.0	1116.0	1116.0	1116.0	11	N	77	0.0
10.5	1116.0	1116.0	1116.0	11	N	77	0.0
11.0	1116.0	1116.0	1116.0	11	N	77	0.0
11.5	1116.0	1116.0	1116.0	11	N	77	0.0
12.0	1116.0	1116.0	1116.0	11	N	77	0.0
12.5	1116.0	1116.0	1116.0	11	N	77	0.0
13.0	1116.0	1116.0	1116.0	11	N	77	0.0
13.5	1116.0	1116.0	1116.0	11	N	77	0.0
14.0	1116.0	1116.0	1116.0	11	N	77	0.0
14.5	1116.0	1116.0	1116.0	11	N	77	0.0
15.0	1116.0	1116.0	1116.0	11	N	77	0.0
15.5	1116.0	1116.0	1116.0	11	N	77	0.0
16.0	1116.0	1116.0	1116.0	11	N	77	0.0
16.5	1116.0	1116.0	1116.0	11	N	77	0.0
17.0	1116.0	1116.0	1116.0	11	N	77	0.0
17.5	1116.0	1116.0	1116.0	11	N	77	0.0
18.0	1116.0	1116.0	1116.0	11	N	77	0.0
18.5	1116.0	1116.0	1116.0	11	N	77	0.0
19.0	1116.0	1116.0	1116.0	11	N	77	0.0
19.5	1116.0	1116.0	1116.0	11	N	77	0.0
20.0	1116.0	1116.0	1116.0	11	N	77	0.0
20.5	1116.0	1116.0	1116.0	11	N	77	0.0
21.0	1116.0	1116.0	1116.0	11	N	77	0.0
21.5	1116.0	1116.0	1116.0	11	N	77	0.0
22.0	1116.0	1116.0	1116.0	11	N	77	0.0
22.5	1116.0	1116.0	1116.0	11	N	77	0.0
23.0	1116.0	1116.0	1116.0	11	N	77	0.0
23.5	1116.0	1116.0	1116.0	11	N	77	0.0
24.0	1116.0	1116.0	1116.0	11	N	77	0.0
24.5	1116.0	1116.0	1116.0	11	N	77	0.0
25.0	1116.0	1116.0	1116.0	11	N	77	0.0

HEIGHT OF THE COOLING ZONE=3.250M

TABLE P.2 (B1)

TITLE: SIMULATION OF LIME SHAFT KILN
 SUBTITLE: PREHEATING-CUM-DEVOLATILIZATION ZONE

INPUT DATA FOR SET NO. 2 (B)

(DPS=0.112 M)

RESULTS OF ANALYSIS

Z	Z (M)	XF	TS(1)	TF(1)	TS(2)	Ts(K)	HFS	HFG	HSG	ASPZ	APPZ	BFS	BFG	BSC	DELTA
11	0.000	0.000	1200.0	1200.0	1200.0	1200.0	0.000	0.000	0.000	0.000	0.000	0.000	0.000	0.000	0.000
10	0.100	0.000	1200.0	1200.0	1200.0	1200.0	0.000	0.000	0.000	0.000	0.000	0.000	0.000	0.000	0.000
9	0.200	0.000	1200.0	1200.0	1200.0	1200.0	0.000	0.000	0.000	0.000	0.000	0.000	0.000	0.000	0.000
8	0.300	0.000	1200.0	1200.0	1200.0	1200.0	0.000	0.000	0.000	0.000	0.000	0.000	0.000	0.000	0.000
7	0.400	0.000	1200.0	1200.0	1200.0	1200.0	0.000	0.000	0.000	0.000	0.000	0.000	0.000	0.000	0.000
6	0.500	0.000	1200.0	1200.0	1200.0	1200.0	0.000	0.000	0.000	0.000	0.000	0.000	0.000	0.000	0.000
5	0.600	0.000	1200.0	1200.0	1200.0	1200.0	0.000	0.000	0.000	0.000	0.000	0.000	0.000	0.000	0.000
4	0.700	0.000	1200.0	1200.0	1200.0	1200.0	0.000	0.000	0.000	0.000	0.000	0.000	0.000	0.000	0.000
3	0.800	0.000	1200.0	1200.0	1200.0	1200.0	0.000	0.000	0.000	0.000	0.000	0.000	0.000	0.000	0.000
2	0.900	0.000	1200.0	1200.0	1200.0	1200.0	0.000	0.000	0.000	0.000	0.000	0.000	0.000	0.000	0.000
1	1.000	0.000	1200.0	1200.0	1200.0	1200.0	0.000	0.000	0.000	0.000	0.000	0.000	0.000	0.000	0.000

VM COMBUSTION STARTS AT XF = 0.1732 AND AT HEIGHT (FROM TOP) = 5.500 M
 HEIGHT OF THE PREHEATING-CUM-DEVOLATILIZATION ZONE = 5.500 M

TABLE R2 (B3)

SIMULATION OF LIME SHAFT KILN
ANALYSIS OF THE COOLING ZONE

INPUT DATA FOR SET NO. 2 (B)

(DPS=0.112 M)

RESULTS OF ANALYSIS

I	Z (M)	T (K)	TS (K)	TR (K)	FSG	ASCZ	SSG	DELATL
1	0.000	1100.0	1100.0	1100.0	0.000	0.000	0.000	0.000
2	0.100	1095.0	1095.0	1095.0	0.000	0.000	0.000	0.000
3	0.200	1090.0	1090.0	1090.0	0.000	0.000	0.000	0.000
4	0.300	1085.0	1085.0	1085.0	0.000	0.000	0.000	0.000
5	0.400	1080.0	1080.0	1080.0	0.000	0.000	0.000	0.000
6	0.500	1075.0	1075.0	1075.0	0.000	0.000	0.000	0.000
7	0.600	1070.0	1070.0	1070.0	0.000	0.000	0.000	0.000
8	0.700	1065.0	1065.0	1065.0	0.000	0.000	0.000	0.000
9	0.800	1060.0	1060.0	1060.0	0.000	0.000	0.000	0.000
10	0.900	1055.0	1055.0	1055.0	0.000	0.000	0.000	0.000
11	1.000	1050.0	1050.0	1050.0	0.000	0.000	0.000	0.000
12	1.100	1045.0	1045.0	1045.0	0.000	0.000	0.000	0.000
13	1.200	1040.0	1040.0	1040.0	0.000	0.000	0.000	0.000
14	1.300	1035.0	1035.0	1035.0	0.000	0.000	0.000	0.000
15	1.400	1030.0	1030.0	1030.0	0.000	0.000	0.000	0.000
16	1.500	1025.0	1025.0	1025.0	0.000	0.000	0.000	0.000
17	1.600	1020.0	1020.0	1020.0	0.000	0.000	0.000	0.000
18	1.700	1015.0	1015.0	1015.0	0.000	0.000	0.000	0.000
19	1.800	1010.0	1010.0	1010.0	0.000	0.000	0.000	0.000
20	1.900	1005.0	1005.0	1005.0	0.000	0.000	0.000	0.000
21	2.000	1000.0	1000.0	1000.0	0.000	0.000	0.000	0.000
22	2.100	995.0	995.0	995.0	0.000	0.000	0.000	0.000
23	2.200	990.0	990.0	990.0	0.000	0.000	0.000	0.000
24	2.300	985.0	985.0	985.0	0.000	0.000	0.000	0.000
25	2.400	980.0	980.0	980.0	0.000	0.000	0.000	0.000
26	2.500	975.0	975.0	975.0	0.000	0.000	0.000	0.000
27	2.600	970.0	970.0	970.0	0.000	0.000	0.000	0.000
28	2.700	965.0	965.0	965.0	0.000	0.000	0.000	0.000
29	2.800	960.0	960.0	960.0	0.000	0.000	0.000	0.000
30	2.900	955.0	955.0	955.0	0.000	0.000	0.000	0.000
31	3.000	950.0	950.0	950.0	0.000	0.000	0.000	0.000
32	3.100	945.0	945.0	945.0	0.000	0.000	0.000	0.000
33	3.200	940.0	940.0	940.0	0.000	0.000	0.000	0.000
34	3.300	935.0	935.0	935.0	0.000	0.000	0.000	0.000
35	3.400	930.0	930.0	930.0	0.000	0.000	0.000	0.000
36	3.500	925.0	925.0	925.0	0.000	0.000	0.000	0.000
37	3.600	920.0	920.0	920.0	0.000	0.000	0.000	0.000
38	3.700	915.0	915.0	915.0	0.000	0.000	0.000	0.000
39	3.800	910.0	910.0	910.0	0.000	0.000	0.000	0.000
40	3.900	905.0	905.0	905.0	0.000	0.000	0.000	0.000
41	4.000	900.0	900.0	900.0	0.000	0.000	0.000	0.000
42	4.100	895.0	895.0	895.0	0.000	0.000	0.000	0.000
43	4.200	890.0	890.0	890.0	0.000	0.000	0.000	0.000
44	4.300	885.0	885.0	885.0	0.000	0.000	0.000	0.000
45	4.400	880.0	880.0	880.0	0.000	0.000	0.000	0.000
46	4.500	875.0	875.0	875.0	0.000	0.000	0.000	0.000
47	4.600	870.0	870.0	870.0	0.000	0.000	0.000	0.000
48	4.700	865.0	865.0	865.0	0.000	0.000	0.000	0.000
49	4.800	860.0	860.0	860.0	0.000	0.000	0.000	0.000
50	4.900	855.0	855.0	855.0	0.000	0.000	0.000	0.000
51	5.000	850.0	850.0	850.0	0.000	0.000	0.000	0.000
52	5.100	845.0	845.0	845.0	0.000	0.000	0.000	0.000
53	5.200	840.0	840.0	840.0	0.000	0.000	0.000	0.000
54	5.300	835.0	835.0	835.0	0.000	0.000	0.000	0.000
55	5.400	830.0	830.0	830.0	0.000	0.000	0.000	0.000
56	5.500	825.0	825.0	825.0	0.000	0.000	0.000	0.000
57	5.600	820.0	820.0	820.0	0.000	0.000	0.000	0.000
58	5.700	815.0	815.0	815.0	0.000	0.000	0.000	0.000
59	5.800	810.0	810.0	810.0	0.000	0.000	0.000	0.000
60	5.900	805.0	805.0	805.0	0.000	0.000	0.000	0.000
61	6.000	800.0	800.0	800.0	0.000	0.000	0.000	0.000
62	6.100	795.0	795.0	795.0	0.000	0.000	0.000	0.000
63	6.200	790.0	790.0	790.0	0.000	0.000	0.000	0.000
64	6.300	785.0	785.0	785.0	0.000	0.000	0.000	0.000
65	6.400	780.0	780.0	780.0	0.000	0.000	0.000	0.000
66	6.500	775.0	775.0	775.0	0.000	0.000	0.000	0.000
67	6.600	770.0	770.0	770.0	0.000	0.000	0.000	0.000
68	6.700	765.0	765.0	765.0	0.000	0.000	0.000	0.000
69	6.800	760.0	760.0	760.0	0.000	0.000	0.000	0.000
70	6.900	755.0	755.0	755.0	0.000	0.000	0.000	0.000
71	7.000	750.0	750.0	750.0	0.000	0.000	0.000	0.000

HEIGHT OF THE COOLING ZONE=5.750M

TABLE P.3 (A3)

SIMULATION OF LIFT SHAFT COOLING ZONE ANALYSIS OF THE

INPUT DATA FOR SET NO. 3 (A)

(DIFF. COEFF. = 4.0)

RESULTS OF ANALYSIS

Z (M)	T ₀ (K)	T _S (K)	T ₁ (K)	HSG	ASCZ	CSG	DELMT
1.0000	293.15	293.15	293.15	1.0000	1.0000	1.0000	0.0000
1.1000	293.15	293.15	293.15	1.0000	1.0000	1.0000	0.0000
1.2000	293.15	293.15	293.15	1.0000	1.0000	1.0000	0.0000
1.3000	293.15	293.15	293.15	1.0000	1.0000	1.0000	0.0000
1.4000	293.15	293.15	293.15	1.0000	1.0000	1.0000	0.0000
1.5000	293.15	293.15	293.15	1.0000	1.0000	1.0000	0.0000
1.6000	293.15	293.15	293.15	1.0000	1.0000	1.0000	0.0000
1.7000	293.15	293.15	293.15	1.0000	1.0000	1.0000	0.0000
1.8000	293.15	293.15	293.15	1.0000	1.0000	1.0000	0.0000
1.9000	293.15	293.15	293.15	1.0000	1.0000	1.0000	0.0000
2.0000	293.15	293.15	293.15	1.0000	1.0000	1.0000	0.0000
2.1000	293.15	293.15	293.15	1.0000	1.0000	1.0000	0.0000
2.2000	293.15	293.15	293.15	1.0000	1.0000	1.0000	0.0000
2.3000	293.15	293.15	293.15	1.0000	1.0000	1.0000	0.0000
2.4000	293.15	293.15	293.15	1.0000	1.0000	1.0000	0.0000
2.5000	293.15	293.15	293.15	1.0000	1.0000	1.0000	0.0000
2.6000	293.15	293.15	293.15	1.0000	1.0000	1.0000	0.0000
2.7000	293.15	293.15	293.15	1.0000	1.0000	1.0000	0.0000
2.8000	293.15	293.15	293.15	1.0000	1.0000	1.0000	0.0000
2.9000	293.15	293.15	293.15	1.0000	1.0000	1.0000	0.0000
3.0000	293.15	293.15	293.15	1.0000	1.0000	1.0000	0.0000
3.1000	293.15	293.15	293.15	1.0000	1.0000	1.0000	0.0000
3.2000	293.15	293.15	293.15	1.0000	1.0000	1.0000	0.0000
3.3000	293.15	293.15	293.15	1.0000	1.0000	1.0000	0.0000
3.4000	293.15	293.15	293.15	1.0000	1.0000	1.0000	0.0000
3.5000	293.15	293.15	293.15	1.0000	1.0000	1.0000	0.0000
3.6000	293.15	293.15	293.15	1.0000	1.0000	1.0000	0.0000
3.7000	293.15	293.15	293.15	1.0000	1.0000	1.0000	0.0000
3.8000	293.15	293.15	293.15	1.0000	1.0000	1.0000	0.0000
3.9000	293.15	293.15	293.15	1.0000	1.0000	1.0000	0.0000
4.0000	293.15	293.15	293.15	1.0000	1.0000	1.0000	0.0000
4.1000	293.15	293.15	293.15	1.0000	1.0000	1.0000	0.0000
4.2000	293.15	293.15	293.15	1.0000	1.0000	1.0000	0.0000
4.3000	293.15	293.15	293.15	1.0000	1.0000	1.0000	0.0000
4.4000	293.15	293.15	293.15	1.0000	1.0000	1.0000	0.0000
4.5000	293.15	293.15	293.15	1.0000	1.0000	1.0000	0.0000
4.6000	293.15	293.15	293.15	1.0000	1.0000	1.0000	0.0000
4.7000	293.15	293.15	293.15	1.0000	1.0000	1.0000	0.0000
4.8000	293.15	293.15	293.15	1.0000	1.0000	1.0000	0.0000
4.9000	293.15	293.15	293.15	1.0000	1.0000	1.0000	0.0000
5.0000	293.15	293.15	293.15	1.0000	1.0000	1.0000	0.0000

HEIGHT OF THE COOLING ZONE = 4.550M

TABLE E.3 (B1)

TITLE: SIMULATION OF LIME SHAFT KILN
STITLE: PREHEATING-CUM-DEVOLATILIZATION ZONE

INPUT DATA FOR SET NO. 3 (E)

(DFF=0.C56)

RESULTS OF ANALYSIS

I	Z(N)	XF	TE(I)	TF(I)	TS(I)	TL(K)	HFS	HFG	HSG	ASPZ	AFPZ	OFS	CF6	CS6	DELNTL
1	1	0.0000	1000.00	1000.00	1000.00	1000.00	0.0000	0.0000	0.0000	0.0000	0.0000	0.0000	0.0000	0.0000	0.0000
2	2	0.0000	1000.00	1000.00	1000.00	1000.00	0.0000	0.0000	0.0000	0.0000	0.0000	0.0000	0.0000	0.0000	0.0000
3	3	0.0000	1000.00	1000.00	1000.00	1000.00	0.0000	0.0000	0.0000	0.0000	0.0000	0.0000	0.0000	0.0000	0.0000
4	4	0.0000	1000.00	1000.00	1000.00	1000.00	0.0000	0.0000	0.0000	0.0000	0.0000	0.0000	0.0000	0.0000	0.0000
5	5	0.0000	1000.00	1000.00	1000.00	1000.00	0.0000	0.0000	0.0000	0.0000	0.0000	0.0000	0.0000	0.0000	0.0000
6	6	0.0000	1000.00	1000.00	1000.00	1000.00	0.0000	0.0000	0.0000	0.0000	0.0000	0.0000	0.0000	0.0000	0.0000
7	7	0.0000	1000.00	1000.00	1000.00	1000.00	0.0000	0.0000	0.0000	0.0000	0.0000	0.0000	0.0000	0.0000	0.0000
8	8	0.0000	1000.00	1000.00	1000.00	1000.00	0.0000	0.0000	0.0000	0.0000	0.0000	0.0000	0.0000	0.0000	0.0000
9	9	0.0000	1000.00	1000.00	1000.00	1000.00	0.0000	0.0000	0.0000	0.0000	0.0000	0.0000	0.0000	0.0000	0.0000
10	10	0.0000	1000.00	1000.00	1000.00	1000.00	0.0000	0.0000	0.0000	0.0000	0.0000	0.0000	0.0000	0.0000	0.0000
11	11	0.0000	1000.00	1000.00	1000.00	1000.00	0.0000	0.0000	0.0000	0.0000	0.0000	0.0000	0.0000	0.0000	0.0000
12	12	0.0000	1000.00	1000.00	1000.00	1000.00	0.0000	0.0000	0.0000	0.0000	0.0000	0.0000	0.0000	0.0000	0.0000
13	13	0.0000	1000.00	1000.00	1000.00	1000.00	0.0000	0.0000	0.0000	0.0000	0.0000	0.0000	0.0000	0.0000	0.0000
14	14	0.0000	1000.00	1000.00	1000.00	1000.00	0.0000	0.0000	0.0000	0.0000	0.0000	0.0000	0.0000	0.0000	0.0000
15	15	0.0000	1000.00	1000.00	1000.00	1000.00	0.0000	0.0000	0.0000	0.0000	0.0000	0.0000	0.0000	0.0000	0.0000
16	16	0.0000	1000.00	1000.00	1000.00	1000.00	0.0000	0.0000	0.0000	0.0000	0.0000	0.0000	0.0000	0.0000	0.0000
17	17	0.0000	1000.00	1000.00	1000.00	1000.00	0.0000	0.0000	0.0000	0.0000	0.0000	0.0000	0.0000	0.0000	0.0000
18	18	0.0000	1000.00	1000.00	1000.00	1000.00	0.0000	0.0000	0.0000	0.0000	0.0000	0.0000	0.0000	0.0000	0.0000
19	19	0.0000	1000.00	1000.00	1000.00	1000.00	0.0000	0.0000	0.0000	0.0000	0.0000	0.0000	0.0000	0.0000	0.0000
20	20	0.0000	1000.00	1000.00	1000.00	1000.00	0.0000	0.0000	0.0000	0.0000	0.0000	0.0000	0.0000	0.0000	0.0000

VM COMBUSTION STARTS AT XF = 0.1719 AND AT HEIGHT (FROM TOP) = 4.850 P
 WEIGHT OF THE PREHEATING-CUM-DEVOLATILIZATION ZONE = 4.850 P

TABLE #.3 (B2)

SIMULATION OF LIPE SHAFT KILA ANALYSIS OF THE BURNING ZONE

INPUT DATA FOR SET NO. 3 (P)

(DPF=0.056 M)

RESULTS OF ANALYSIS

I	Z (M)	XF	XS	TE (K)	TF (K)	TS (K)	TL (K)	RS	LH	DELS	T	HFS	HFG	HSG	ASBZ	AFBZ	QF5	QF6	Q56	DEL4TL	PC26	PC026
0.00000000000000000000	0.00000000000000000000	0.00000000000000000000	0.00000000000000000000	0.00000000000000000000	0.00000000000000000000	0.00000000000000000000	0.00000000000000000000	0.00000000000000000000	0.00000000000000000000	0.00000000000000000000	0.00000000000000000000	0.00000000000000000000	0.00000000000000000000	0.00000000000000000000	0.00000000000000000000	0.00000000000000000000	0.00000000000000000000	0.00000000000000000000	0.00000000000000000000	0.00000000000000000000	0.00000000000000000000	0.00000000000000000000
0.00000000000000000000	0.00000000000000000000	0.00000000000000000000	0.00000000000000000000	0.00000000000000000000	0.00000000000000000000	0.00000000000000000000	0.00000000000000000000	0.00000000000000000000	0.00000000000000000000	0.00000000000000000000	0.00000000000000000000	0.00000000000000000000	0.00000000000000000000	0.00000000000000000000	0.00000000000000000000	0.00000000000000000000	0.00000000000000000000	0.00000000000000000000	0.00000000000000000000	0.00000000000000000000	0.00000000000000000000	0.00000000000000000000

ASH FUSION STARTS AT XF = 0.7204 AT HEIGHT (FROM TOP OF BURNING ZONE) = 2.470 M
 HEIGHT OF THE BURNING ZONE = 2.725 M

TABLE P.4 (A2)
 SIMULATION OF LIME SHAFT KILN
 ANALYSIS OF THE BURNING ZONE

INPUT DATA FOR SET NO. 4 (A)
 [PS=2.0T/(SAM)(DAY)]
 RESULTS OF ANALYSIS

I	Z(M)	XF	XS	TE(K)	TF(K)	TS(K)	TK(K)	REHLHD	DELSHT	HFS	HFG	HSG	ASBZ	AFBZ	GFS	GFG	GSG	DELNLT	PC26	PC26
1	2.500	0.000	0.000	1000	1000	1000	1000													
2	2.400	0.000	0.000	1000	1000	1000	1000													
3	2.300	0.000	0.000	1000	1000	1000	1000													
4	2.200	0.000	0.000	1000	1000	1000	1000													
5	2.100	0.000	0.000	1000	1000	1000	1000													
6	2.000	0.000	0.000	1000	1000	1000	1000													
7	1.900	0.000	0.000	1000	1000	1000	1000													
8	1.800	0.000	0.000	1000	1000	1000	1000													
9	1.700	0.000	0.000	1000	1000	1000	1000													
10	1.600	0.000	0.000	1000	1000	1000	1000													
11	1.500	0.000	0.000	1000	1000	1000	1000													
12	1.400	0.000	0.000	1000	1000	1000	1000													
13	1.300	0.000	0.000	1000	1000	1000	1000													
14	1.200	0.000	0.000	1000	1000	1000	1000													
15	1.100	0.000	0.000	1000	1000	1000	1000													
16	1.000	0.000	0.000	1000	1000	1000	1000													
17	0.900	0.000	0.000	1000	1000	1000	1000													
18	0.800	0.000	0.000	1000	1000	1000	1000													
19	0.700	0.000	0.000	1000	1000	1000	1000													
20	0.600	0.000	0.000	1000	1000	1000	1000													
21	0.500	0.000	0.000	1000	1000	1000	1000													
22	0.400	0.000	0.000	1000	1000	1000	1000													
23	0.300	0.000	0.000	1000	1000	1000	1000													
24	0.200	0.000	0.000	1000	1000	1000	1000													
25	0.100	0.000	0.000	1000	1000	1000	1000													
26	0.000	0.000	0.000	1000	1000	1000	1000													

26 FUSION STARTS AT XF = 0.694C AT HEIGHT (FROM TOP OF BURNING ZONE) = 1.785 M
 HEIGHT OF THE BURNING ZONE = 2.060 M

TABLE #.4 (A3)
 SIMULATION OF LINE SHAFT KILA
 ANALYSIS OF THE COOLING ZONE

INPUT DATA FOR SET NO. 4 (A)

P-24

[FPS=2.0T/(CSM)(DAY)]

RESULTS OF ANALYSIS

I	Z (M)	TC (K)	TS (K)	TA (K)	HSG	ASCZ	CSG	DELHTL
7	0.0	29.0	29.0	29.0	1.0	0.0	0.0	0.0
8	0.1	28.5	28.5	28.5	1.0	0.0	0.0	0.0
9	0.2	28.0	28.0	28.0	1.0	0.0	0.0	0.0
10	0.3	27.5	27.5	27.5	1.0	0.0	0.0	0.0
11	0.4	27.0	27.0	27.0	1.0	0.0	0.0	0.0
12	0.5	26.5	26.5	26.5	1.0	0.0	0.0	0.0
13	0.6	26.0	26.0	26.0	1.0	0.0	0.0	0.0
14	0.7	25.5	25.5	25.5	1.0	0.0	0.0	0.0
15	0.8	25.0	25.0	25.0	1.0	0.0	0.0	0.0
16	0.9	24.5	24.5	24.5	1.0	0.0	0.0	0.0
17	1.0	24.0	24.0	24.0	1.0	0.0	0.0	0.0
18	1.1	23.5	23.5	23.5	1.0	0.0	0.0	0.0
19	1.2	23.0	23.0	23.0	1.0	0.0	0.0	0.0
20	1.3	22.5	22.5	22.5	1.0	0.0	0.0	0.0
21	1.4	22.0	22.0	22.0	1.0	0.0	0.0	0.0
22	1.5	21.5	21.5	21.5	1.0	0.0	0.0	0.0
23	1.6	21.0	21.0	21.0	1.0	0.0	0.0	0.0
24	1.7	20.5	20.5	20.5	1.0	0.0	0.0	0.0
25	1.8	20.0	20.0	20.0	1.0	0.0	0.0	0.0
26	1.9	19.5	19.5	19.5	1.0	0.0	0.0	0.0
27	2.0	19.0	19.0	19.0	1.0	0.0	0.0	0.0
28	2.1	18.5	18.5	18.5	1.0	0.0	0.0	0.0
29	2.2	18.0	18.0	18.0	1.0	0.0	0.0	0.0
30	2.3	17.5	17.5	17.5	1.0	0.0	0.0	0.0
31	2.4	17.0	17.0	17.0	1.0	0.0	0.0	0.0
32	2.5	16.5	16.5	16.5	1.0	0.0	0.0	0.0
33	2.6	16.0	16.0	16.0	1.0	0.0	0.0	0.0
34	2.7	15.5	15.5	15.5	1.0	0.0	0.0	0.0
35	2.8	15.0	15.0	15.0	1.0	0.0	0.0	0.0
36	2.9	14.5	14.5	14.5	1.0	0.0	0.0	0.0
37	3.0	14.0	14.0	14.0	1.0	0.0	0.0	0.0
38	3.1	13.5	13.5	13.5	1.0	0.0	0.0	0.0
39	3.2	13.0	13.0	13.0	1.0	0.0	0.0	0.0
40	3.3	12.5	12.5	12.5	1.0	0.0	0.0	0.0
41	3.4	12.0	12.0	12.0	1.0	0.0	0.0	0.0
42	3.5	11.5	11.5	11.5	1.0	0.0	0.0	0.0
43	3.6	11.0	11.0	11.0	1.0	0.0	0.0	0.0
44	3.7	10.5	10.5	10.5	1.0	0.0	0.0	0.0
45	3.8	10.0	10.0	10.0	1.0	0.0	0.0	0.0
46	3.9	9.5	9.5	9.5	1.0	0.0	0.0	0.0
47	4.0	9.0	9.0	9.0	1.0	0.0	0.0	0.0
48	4.1	8.5	8.5	8.5	1.0	0.0	0.0	0.0
49	4.2	8.0	8.0	8.0	1.0	0.0	0.0	0.0
50	4.3	7.5	7.5	7.5	1.0	0.0	0.0	0.0

HEIGHT OF THE COOLING ZONE=4.30M

SIMULATION OF LIPE SHAFT KILN
ANALYSIS OF THE BURNING ZONE

INPUT DATA FOR SET NO. 4 (B)

[FPS=2.5T/(SGM)(DAY)]

RESULTS OF ANALYSIS

I	Z (M)	XF	XS	TE (K)	TF (K)	TS (K)	TT (K)	RS	LHD	DELS	T	HFS	HFG	HSG	ASBZ	AFBZ	GFS	GFE	QSG	DEL	MTL	PC26	PC026
1	0.000	0.000	0.000	293.15	293.15	293.15	293.15	0.000	0.000	0.000	0.000	0.000	0.000	0.000	0.000	0.000	0.000	0.000	0.000	0.000	0.000	0.000	0.000

ASH FUSION STARTS AT XF = 0.6970 AT HEIGHT (FROM TOP OF BURNING ZONE) = 2.120 M
HEIGHT OF THE BURNING ZONE = 2.490 M

TABLE P.4 (B3)

SIMULATION OF LIME SHAFT KILN
ANALYSIS OF THE COOLING ZONE

INPUT DATA FOR SET NO. 4 (B)

P-27

[PS=2.5T/(SGM)(DAY)]

RESULTS OF ANALYSIS

Z	Z (M)	TE (K)	TS (K)	TH (K)	HSG	ASCZ	QSG	DELHTL
1	0.000	4.4	1118.6	1118.6	11	5	77	11
2	0.000	4.4	1117.0	1117.0	11	5	75	11
3	0.000	4.4	1115.6	1115.6	11	5	74	11
4	0.000	4.4	1114.1	1114.1	11	5	73	11
5	0.000	4.4	1112.6	1112.6	11	5	72	11
6	0.000	4.4	1111.1	1111.1	11	5	71	11
7	0.000	4.4	1109.7	1109.7	11	5	70	11
8	0.000	4.4	1108.3	1108.3	11	5	69	11
9	0.000	4.4	1106.9	1106.9	11	5	68	11
10	0.000	4.4	1105.5	1105.5	11	5	67	11
11	0.000	4.4	1104.1	1104.1	11	5	66	11
12	0.000	4.4	1102.7	1102.7	11	5	65	11
13	0.000	4.4	1101.3	1101.3	11	5	64	11
14	0.000	4.4	1100.0	1100.0	11	5	63	11
15	0.000	4.4	1098.6	1098.6	11	5	62	11
16	0.000	4.4	1097.3	1097.3	11	5	61	11
17	0.000	4.4	1095.9	1095.9	11	5	60	11
18	0.000	4.4	1094.5	1094.5	11	5	59	11
19	0.000	4.4	1093.2	1093.2	11	5	58	11
20	0.000	4.4	1091.8	1091.8	11	5	57	11
21	0.000	4.4	1090.4	1090.4	11	5	56	11
22	0.000	4.4	1089.1	1089.1	11	5	55	11
23	0.000	4.4	1087.7	1087.7	11	5	54	11
24	0.000	4.4	1086.3	1086.3	11	5	53	11
25	0.000	4.4	1085.0	1085.0	11	5	52	11
26	0.000	4.4	1083.6	1083.6	11	5	51	11
27	0.000	4.4	1082.3	1082.3	11	5	50	11
28	0.000	4.4	1080.9	1080.9	11	5	49	11
29	0.000	4.4	1079.5	1079.5	11	5	48	11
30	0.000	4.4	1078.2	1078.2	11	5	47	11
31	0.000	4.4	1076.8	1076.8	11	5	46	11
32	0.000	4.4	1075.4	1075.4	11	5	45	11
33	0.000	4.4	1074.1	1074.1	11	5	44	11
34	0.000	4.4	1072.7	1072.7	11	5	43	11
35	0.000	4.4	1071.3	1071.3	11	5	42	11
36	0.000	4.4	1070.0	1070.0	11	5	41	11
37	0.000	4.4	1068.6	1068.6	11	5	40	11
38	0.000	4.4	1067.3	1067.3	11	5	39	11
39	0.000	4.4	1065.9	1065.9	11	5	38	11
40	0.000	4.4	1064.5	1064.5	11	5	37	11
41	0.000	4.4	1063.2	1063.2	11	5	36	11
42	0.000	4.4	1061.8	1061.8	11	5	35	11
43	0.000	4.4	1060.4	1060.4	11	5	34	11
44	0.000	4.4	1059.1	1059.1	11	5	33	11
45	0.000	4.4	1057.7	1057.7	11	5	32	11
46	0.000	4.4	1056.3	1056.3	11	5	31	11
47	0.000	4.4	1055.0	1055.0	11	5	30	11
48	0.000	4.4	1053.6	1053.6	11	5	29	11
49	0.000	4.4	1052.3	1052.3	11	5	28	11
50	0.000	4.4	1050.9	1050.9	11	5	27	11
51	0.000	4.4	1049.5	1049.5	11	5	26	11
52	0.000	4.4	1048.2	1048.2	11	5	25	11
53	0.000	4.4	1046.8	1046.8	11	5	24	11
54	0.000	4.4	1045.4	1045.4	11	5	23	11
55	0.000	4.4	1044.1	1044.1	11	5	22	11
56	0.000	4.4	1042.7	1042.7	11	5	21	11
57	0.000	4.4	1041.3	1041.3	11	5	20	11
58	0.000	4.4	1040.0	1040.0	11	5	19	11
59	0.000	4.4	1038.6	1038.6	11	5	18	11
60	0.000	4.4	1037.3	1037.3	11	5	17	11
61	0.000	4.4	1035.9	1035.9	11	5	16	11
62	0.000	4.4	1034.5	1034.5	11	5	15	11
63	0.000	4.4	1033.2	1033.2	11	5	14	11
64	0.000	4.4	1031.8	1031.8	11	5	13	11
65	0.000	4.4	1030.4	1030.4	11	5	12	11
66	0.000	4.4	1029.1	1029.1	11	5	11	11
67	0.000	4.4	1027.7	1027.7	11	5	10	11
68	0.000	4.4	1026.3	1026.3	11	5	9	11
69	0.000	4.4	1025.0	1025.0	11	5	8	11
70	0.000	4.4	1023.6	1023.6	11	5	7	11
71	0.000	4.4	1022.3	1022.3	11	5	6	11
72	0.000	4.4	1020.9	1020.9	11	5	5	11
73	0.000	4.4	1019.5	1019.5	11	5	4	11
74	0.000	4.4	1018.2	1018.2	11	5	3	11
75	0.000	4.4	1016.8	1016.8	11	5	2	11
76	0.000	4.4	1015.4	1015.4	11	5	1	11

HEIGHT OF THE COOLING ZONE=4.750M

TABLE #.6 (A7)
 TITLE: SIMULATION OF LIME SHAFT KILN
 TITLE: PREHEATING-CUM-DEVOLATILIZATION ZONE

INPUT DATA FOR SET NO. 6 (A)
 (XFM=0.15)

RESULTS OF ANALYSIS

Z(A)	KF	TG(I)	TF(I)	TS(Z)	TK(K)	HFS	HFG	HSG	ASPZ	AF#2	BFS	BG	B6	B86	BELN1
000000	000000	000000	000000	000000	000000	000000	000000	000000	000000	000000	000000	000000	000000	000000	000000
000000	000000	000000	000000	000000	000000	000000	000000	000000	000000	000000	000000	000000	000000	000000	000000
000000	000000	000000	000000	000000	000000	000000	000000	000000	000000	000000	000000	000000	000000	000000	000000
000000	000000	000000	000000	000000	000000	000000	000000	000000	000000	000000	000000	000000	000000	000000	000000

VM COMBUSTION STARTS AT KF = 0.1319 AND AT HEIGHT (FROM TOP) = 4.650 M
 HEIGHT OF THE PREHEATING-CUM-DEVOLATILIZATION ZONE = 4.650 M

TABLE 2.6 (A3)
 SIMULATION OF LINE SHAFT KILA
 ANALYSIS OF THE COOLING ZONE

P-36

INPUT DATA FOR SET NO. 6 (A)
 (XFM=0.15)

RESULTS OF ANALYSIS

I	Z (M)	TG (K)	TS (K)	TW (K)	MSG	ASCZ	SSG	DELHTL
1	0.000000	160.5	159.33	158.1	156.9	155.7	154.5	153.3
2	0.000000	158.1	156.9	155.7	154.5	153.3	152.1	150.9
3	0.000000	156.9	155.7	154.5	153.3	152.1	150.9	149.7
4	0.000000	155.7	154.5	153.3	152.1	150.9	149.7	148.5
5	0.000000	154.5	153.3	152.1	150.9	149.7	148.5	147.3
6	0.000000	153.3	152.1	150.9	149.7	148.5	147.3	146.1
7	0.000000	152.1	150.9	149.7	148.5	147.3	146.1	144.9
8	0.000000	150.9	149.7	148.5	147.3	146.1	144.9	143.7
9	0.000000	149.7	148.5	147.3	146.1	144.9	143.7	142.5
10	0.000000	148.5	147.3	146.1	144.9	143.7	142.5	141.3
11	0.000000	147.3	146.1	144.9	143.7	142.5	141.3	140.1
12	0.000000	146.1	144.9	143.7	142.5	141.3	140.1	138.9
13	0.000000	144.9	143.7	142.5	141.3	140.1	138.9	137.7
14	0.000000	143.7	142.5	141.3	140.1	138.9	137.7	136.5
15	0.000000	142.5	141.3	140.1	138.9	137.7	136.5	135.3
16	0.000000	141.3	140.1	138.9	137.7	136.5	135.3	134.1
17	0.000000	140.1	138.9	137.7	136.5	135.3	134.1	132.9
18	0.000000	138.9	137.7	136.5	135.3	134.1	132.9	131.7
19	0.000000	137.7	136.5	135.3	134.1	132.9	131.7	130.5
20	0.000000	136.5	135.3	134.1	132.9	131.7	130.5	129.3
21	0.000000	135.3	134.1	132.9	131.7	130.5	129.3	128.1

HEIGHT OF THE COOLING ZONE=1.000M

TABLE P.6 (B3)

SIMULATION OF LIME SHAFT KILN
ANALYSIS OF THE COOLING ZONE

INPUT DATA FOR SET NO. 6 (B)

(XFV=0.30)

RESULTS OF ANALYSIS

Z (M)	TE (K)	TS (K)	TM (K)	HSG	ASCZ	QSG	DELTL
0.0000	1117.0	700.0	317.0	111.0	49.0	0.0000	0.0000
0.1000	1117.0	700.0	317.0	111.0	49.0	0.0000	0.0000
0.2000	1117.0	700.0	317.0	111.0	49.0	0.0000	0.0000
0.3000	1117.0	700.0	317.0	111.0	49.0	0.0000	0.0000
0.4000	1117.0	700.0	317.0	111.0	49.0	0.0000	0.0000
0.5000	1117.0	700.0	317.0	111.0	49.0	0.0000	0.0000
0.6000	1117.0	700.0	317.0	111.0	49.0	0.0000	0.0000
0.7000	1117.0	700.0	317.0	111.0	49.0	0.0000	0.0000
0.8000	1117.0	700.0	317.0	111.0	49.0	0.0000	0.0000
0.9000	1117.0	700.0	317.0	111.0	49.0	0.0000	0.0000
1.0000	1117.0	700.0	317.0	111.0	49.0	0.0000	0.0000
1.1000	1117.0	700.0	317.0	111.0	49.0	0.0000	0.0000
1.2000	1117.0	700.0	317.0	111.0	49.0	0.0000	0.0000
1.3000	1117.0	700.0	317.0	111.0	49.0	0.0000	0.0000
1.4000	1117.0	700.0	317.0	111.0	49.0	0.0000	0.0000
1.5000	1117.0	700.0	317.0	111.0	49.0	0.0000	0.0000
1.6000	1117.0	700.0	317.0	111.0	49.0	0.0000	0.0000
1.7000	1117.0	700.0	317.0	111.0	49.0	0.0000	0.0000
1.8000	1117.0	700.0	317.0	111.0	49.0	0.0000	0.0000
1.9000	1117.0	700.0	317.0	111.0	49.0	0.0000	0.0000
2.0000	1117.0	700.0	317.0	111.0	49.0	0.0000	0.0000
2.1000	1117.0	700.0	317.0	111.0	49.0	0.0000	0.0000
2.2000	1117.0	700.0	317.0	111.0	49.0	0.0000	0.0000
2.3000	1117.0	700.0	317.0	111.0	49.0	0.0000	0.0000
2.4000	1117.0	700.0	317.0	111.0	49.0	0.0000	0.0000
2.5000	1117.0	700.0	317.0	111.0	49.0	0.0000	0.0000
2.6000	1117.0	700.0	317.0	111.0	49.0	0.0000	0.0000
2.7000	1117.0	700.0	317.0	111.0	49.0	0.0000	0.0000
2.8000	1117.0	700.0	317.0	111.0	49.0	0.0000	0.0000
2.9000	1117.0	700.0	317.0	111.0	49.0	0.0000	0.0000
3.0000	1117.0	700.0	317.0	111.0	49.0	0.0000	0.0000
3.1000	1117.0	700.0	317.0	111.0	49.0	0.0000	0.0000
3.2000	1117.0	700.0	317.0	111.0	49.0	0.0000	0.0000
3.3000	1117.0	700.0	317.0	111.0	49.0	0.0000	0.0000
3.4000	1117.0	700.0	317.0	111.0	49.0	0.0000	0.0000
3.5000	1117.0	700.0	317.0	111.0	49.0	0.0000	0.0000
3.6000	1117.0	700.0	317.0	111.0	49.0	0.0000	0.0000
3.7000	1117.0	700.0	317.0	111.0	49.0	0.0000	0.0000
3.8000	1117.0	700.0	317.0	111.0	49.0	0.0000	0.0000
3.9000	1117.0	700.0	317.0	111.0	49.0	0.0000	0.0000
4.0000	1117.0	700.0	317.0	111.0	49.0	0.0000	0.0000
4.1000	1117.0	700.0	317.0	111.0	49.0	0.0000	0.0000
4.2000	1117.0	700.0	317.0	111.0	49.0	0.0000	0.0000
4.3000	1117.0	700.0	317.0	111.0	49.0	0.0000	0.0000
4.4000	1117.0	700.0	317.0	111.0	49.0	0.0000	0.0000
4.5000	1117.0	700.0	317.0	111.0	49.0	0.0000	0.0000
4.6000	1117.0	700.0	317.0	111.0	49.0	0.0000	0.0000
4.7000	1117.0	700.0	317.0	111.0	49.0	0.0000	0.0000
4.8000	1117.0	700.0	317.0	111.0	49.0	0.0000	0.0000
4.9000	1117.0	700.0	317.0	111.0	49.0	0.0000	0.0000
5.0000	1117.0	700.0	317.0	111.0	49.0	0.0000	0.0000

HEIGHT OF THE COOLING ZONE*****M

EXPLORATION OF LIQUID SHOCK KINETICS
APPLYING THE TURNING POINT

INPUT DATA FOR SET NO. 7 (A)
(XEA=0.00)

RESULTS OF ANALYSIS

I	Z (CM)	XF	XS	TK(K)	TF(K)	TS(K)	TD(K)	RSHLD	DELSHT	HFS	HFG	HSG	ASBZ	AFBZ	OFS	OFS	OSG	DELTEL	PCO2	PCO2
1	0.0	0.0000	0.0000	0.0000	0.0000	0.0000	0.0000	0.0000	0.0000	0.0000	0.0000	0.0000	0.0000	0.0000	0.0000	0.0000	0.0000	0.0000	0.0000	0.0000
2	0.1	0.0000	0.0000	0.0000	0.0000	0.0000	0.0000	0.0000	0.0000	0.0000	0.0000	0.0000	0.0000	0.0000	0.0000	0.0000	0.0000	0.0000	0.0000	0.0000
...

ASH FUSION STARTS AT XF = 0.6964 AT HEIGHT (FROM TOP OF BURNING ZONE) = 2.080 #
WEIGHT OF THE BURNING ZONE = 2.400 #

TABLE B.7 (A3)

SIMULATION OF LIME SHAFT KILN
ANALYSIS OF THE COOLING ZONE

INPUT DATA FOR SET NO. 7 (A)

(XEA=C.00)

RESULTS OF ANALYSIS

Z (M)	TE (K)	TS (K)	TW (K)	HSG	ASCZ	QSG	DELMTL
0.000	1111.1	1111.1	1111.1	1111.1	4444.4	7777.7	110.0
0.005	1111.1	1111.1	1111.1	1111.1	4444.4	7777.7	110.0
0.010	1111.1	1111.1	1111.1	1111.1	4444.4	7777.7	110.0
0.015	1111.1	1111.1	1111.1	1111.1	4444.4	7777.7	110.0
0.020	1111.1	1111.1	1111.1	1111.1	4444.4	7777.7	110.0
0.025	1111.1	1111.1	1111.1	1111.1	4444.4	7777.7	110.0
0.030	1111.1	1111.1	1111.1	1111.1	4444.4	7777.7	110.0
0.035	1111.1	1111.1	1111.1	1111.1	4444.4	7777.7	110.0
0.040	1111.1	1111.1	1111.1	1111.1	4444.4	7777.7	110.0
0.045	1111.1	1111.1	1111.1	1111.1	4444.4	7777.7	110.0
0.050	1111.1	1111.1	1111.1	1111.1	4444.4	7777.7	110.0
0.055	1111.1	1111.1	1111.1	1111.1	4444.4	7777.7	110.0
0.060	1111.1	1111.1	1111.1	1111.1	4444.4	7777.7	110.0
0.065	1111.1	1111.1	1111.1	1111.1	4444.4	7777.7	110.0
0.070	1111.1	1111.1	1111.1	1111.1	4444.4	7777.7	110.0
0.075	1111.1	1111.1	1111.1	1111.1	4444.4	7777.7	110.0
0.080	1111.1	1111.1	1111.1	1111.1	4444.4	7777.7	110.0
0.085	1111.1	1111.1	1111.1	1111.1	4444.4	7777.7	110.0
0.090	1111.1	1111.1	1111.1	1111.1	4444.4	7777.7	110.0
0.095	1111.1	1111.1	1111.1	1111.1	4444.4	7777.7	110.0
0.100	1111.1	1111.1	1111.1	1111.1	4444.4	7777.7	110.0
0.105	1111.1	1111.1	1111.1	1111.1	4444.4	7777.7	110.0
0.110	1111.1	1111.1	1111.1	1111.1	4444.4	7777.7	110.0
0.115	1111.1	1111.1	1111.1	1111.1	4444.4	7777.7	110.0
0.120	1111.1	1111.1	1111.1	1111.1	4444.4	7777.7	110.0
0.125	1111.1	1111.1	1111.1	1111.1	4444.4	7777.7	110.0
0.130	1111.1	1111.1	1111.1	1111.1	4444.4	7777.7	110.0
0.135	1111.1	1111.1	1111.1	1111.1	4444.4	7777.7	110.0
0.140	1111.1	1111.1	1111.1	1111.1	4444.4	7777.7	110.0
0.145	1111.1	1111.1	1111.1	1111.1	4444.4	7777.7	110.0
0.150	1111.1	1111.1	1111.1	1111.1	4444.4	7777.7	110.0
0.155	1111.1	1111.1	1111.1	1111.1	4444.4	7777.7	110.0
0.160	1111.1	1111.1	1111.1	1111.1	4444.4	7777.7	110.0
0.165	1111.1	1111.1	1111.1	1111.1	4444.4	7777.7	110.0
0.170	1111.1	1111.1	1111.1	1111.1	4444.4	7777.7	110.0
0.175	1111.1	1111.1	1111.1	1111.1	4444.4	7777.7	110.0
0.180	1111.1	1111.1	1111.1	1111.1	4444.4	7777.7	110.0
0.185	1111.1	1111.1	1111.1	1111.1	4444.4	7777.7	110.0
0.190	1111.1	1111.1	1111.1	1111.1	4444.4	7777.7	110.0
0.195	1111.1	1111.1	1111.1	1111.1	4444.4	7777.7	110.0
0.200	1111.1	1111.1	1111.1	1111.1	4444.4	7777.7	110.0
0.205	1111.1	1111.1	1111.1	1111.1	4444.4	7777.7	110.0
0.210	1111.1	1111.1	1111.1	1111.1	4444.4	7777.7	110.0
0.215	1111.1	1111.1	1111.1	1111.1	4444.4	7777.7	110.0
0.220	1111.1	1111.1	1111.1	1111.1	4444.4	7777.7	110.0
0.225	1111.1	1111.1	1111.1	1111.1	4444.4	7777.7	110.0
0.230	1111.1	1111.1	1111.1	1111.1	4444.4	7777.7	110.0
0.235	1111.1	1111.1	1111.1	1111.1	4444.4	7777.7	110.0
0.240	1111.1	1111.1	1111.1	1111.1	4444.4	7777.7	110.0
0.245	1111.1	1111.1	1111.1	1111.1	4444.4	7777.7	110.0
0.250	1111.1	1111.1	1111.1	1111.1	4444.4	7777.7	110.0

HEIGHT OF THE COOLING ZONE=3.250M

P-42

TABLE P.7 (E1)

TITLE: SIMULATION OF LIME SHAFT KILN
TITLE: PREHEATING-CUM-DEVOLATILIZATION ZONE

INPUT DATA FOR SET NO. 7 (B)

(XEA=0.25)

RESULTS OF ANALYSIS

DELHTL

056

056

056

AFPZ

ASPZ

HSG

HFG

HFS

TK(K)

TS(I)

TF(I)

TG(I)

XF

2(P)

I

(The following table contains the data points from the simulation results, which appear to be a grid of numerical values. The values are faint and partially obscured by a large watermark in the background. The grid is organized into columns corresponding to the labels above.)

I	2(P)	XF	TG(I)	TF(I)	TS(I)	TK(K)	HFS	HFG	HSG	ASPZ	AFPZ	056	056	056	DELHTL
1
...
...
...
...
...
...
...

WM COMBUSTION STARTS AT XF = 0.1737 AND AT HEIGHT (FROM TOP) = 5.100 M

HEIGHT OF THE PREHEATING-CUM-DEVOLATILIZATION ZONE = 5.100 M

SIMULATION OF THE SHAFT KILN
ANALYSIS OF THE BURNING ZONE

INPUT DATA FOR SET NO. 7 (B)
(XEA=0.15)

RESULTS OF ANALYSIS

18

I	Z(M)	XF	XS	TD(K)	TF(K)	TS(K)	T(K)	RSHLHD	DELSHT	HFS	HFE	HS6	ASBZ	AFBZ	QFS	QF6	Q56	DELATL	PC26	PC026
0000	0000	0000	0000	0000	0000	0000	0000	0000	0000	0000	0000	0000	0000	0000	0000	0000	0000	0000	0000	0000

ASH FUSION STARTS AT XF = 0.6965 AT HEIGHT (FROM TOP OF BURNING ZONE) = 1.870 M
 HEIGHT OF THE BURNING ZONE = 2.190 M

TABLE #.7 (B3)
 SIMULATION OF LIPE SHAFT KILN
 ANALYSIS OF THE COOLING ZONE

INPUT DATA FOR SET NO. 7 (B)
 (XEA=C.25)

RESULTS OF ANALYSIS

Z (M)	TG (K)	TS (K)	Tg (K)	MSG	ASCZ	QSG	DELHTL
0.00	507.4	491.0	507.4	11.0	44.4	14.6	77.7
0.05	507.4	491.0	507.4	11.0	44.4	14.6	77.7
0.10	507.4	491.0	507.4	11.0	44.4	14.6	77.7
0.15	507.4	491.0	507.4	11.0	44.4	14.6	77.7
0.20	507.4	491.0	507.4	11.0	44.4	14.6	77.7
0.25	507.4	491.0	507.4	11.0	44.4	14.6	77.7
0.30	507.4	491.0	507.4	11.0	44.4	14.6	77.7
0.35	507.4	491.0	507.4	11.0	44.4	14.6	77.7
0.40	507.4	491.0	507.4	11.0	44.4	14.6	77.7
0.45	507.4	491.0	507.4	11.0	44.4	14.6	77.7
0.50	507.4	491.0	507.4	11.0	44.4	14.6	77.7
0.55	507.4	491.0	507.4	11.0	44.4	14.6	77.7
0.60	507.4	491.0	507.4	11.0	44.4	14.6	77.7
0.65	507.4	491.0	507.4	11.0	44.4	14.6	77.7
0.70	507.4	491.0	507.4	11.0	44.4	14.6	77.7
0.75	507.4	491.0	507.4	11.0	44.4	14.6	77.7
0.80	507.4	491.0	507.4	11.0	44.4	14.6	77.7
0.85	507.4	491.0	507.4	11.0	44.4	14.6	77.7
0.90	507.4	491.0	507.4	11.0	44.4	14.6	77.7
0.95	507.4	491.0	507.4	11.0	44.4	14.6	77.7
1.00	507.4	491.0	507.4	11.0	44.4	14.6	77.7
1.05	507.4	491.0	507.4	11.0	44.4	14.6	77.7
1.10	507.4	491.0	507.4	11.0	44.4	14.6	77.7
1.15	507.4	491.0	507.4	11.0	44.4	14.6	77.7
1.20	507.4	491.0	507.4	11.0	44.4	14.6	77.7
1.25	507.4	491.0	507.4	11.0	44.4	14.6	77.7
1.30	507.4	491.0	507.4	11.0	44.4	14.6	77.7
1.35	507.4	491.0	507.4	11.0	44.4	14.6	77.7
1.40	507.4	491.0	507.4	11.0	44.4	14.6	77.7
1.45	507.4	491.0	507.4	11.0	44.4	14.6	77.7
1.50	507.4	491.0	507.4	11.0	44.4	14.6	77.7
1.55	507.4	491.0	507.4	11.0	44.4	14.6	77.7
1.60	507.4	491.0	507.4	11.0	44.4	14.6	77.7
1.65	507.4	491.0	507.4	11.0	44.4	14.6	77.7
1.70	507.4	491.0	507.4	11.0	44.4	14.6	77.7
1.75	507.4	491.0	507.4	11.0	44.4	14.6	77.7
1.80	507.4	491.0	507.4	11.0	44.4	14.6	77.7
1.85	507.4	491.0	507.4	11.0	44.4	14.6	77.7
1.90	507.4	491.0	507.4	11.0	44.4	14.6	77.7
1.95	507.4	491.0	507.4	11.0	44.4	14.6	77.7
2.00	507.4	491.0	507.4	11.0	44.4	14.6	77.7
2.05	507.4	491.0	507.4	11.0	44.4	14.6	77.7
2.10	507.4	491.0	507.4	11.0	44.4	14.6	77.7
2.15	507.4	491.0	507.4	11.0	44.4	14.6	77.7
2.20	507.4	491.0	507.4	11.0	44.4	14.6	77.7
2.25	507.4	491.0	507.4	11.0	44.4	14.6	77.7
2.30	507.4	491.0	507.4	11.0	44.4	14.6	77.7
2.35	507.4	491.0	507.4	11.0	44.4	14.6	77.7
2.40	507.4	491.0	507.4	11.0	44.4	14.6	77.7
2.45	507.4	491.0	507.4	11.0	44.4	14.6	77.7
2.50	507.4	491.0	507.4	11.0	44.4	14.6	77.7
2.55	507.4	491.0	507.4	11.0	44.4	14.6	77.7
2.60	507.4	491.0	507.4	11.0	44.4	14.6	77.7
2.65	507.4	491.0	507.4	11.0	44.4	14.6	77.7
2.70	507.4	491.0	507.4	11.0	44.4	14.6	77.7
2.75	507.4	491.0	507.4	11.0	44.4	14.6	77.7
2.80	507.4	491.0	507.4	11.0	44.4	14.6	77.7
2.85	507.4	491.0	507.4	11.0	44.4	14.6	77.7
2.90	507.4	491.0	507.4	11.0	44.4	14.6	77.7
2.95	507.4	491.0	507.4	11.0	44.4	14.6	77.7
3.00	507.4	491.0	507.4	11.0	44.4	14.6	77.7

HEIGHT OF THE COOLING ZONE=6.650M

ENTHALPIES OF PRODUCT LIME AND ASH/CINDERS AT BOTTOM OF KILN = 21268.2 KCAL/HR

TABLE P.3 (A3)

SIMULATION OF LIFE SHAFT KILN
ANALYSIS OF THE COOLING ZONE

INPUT DATA FOR SET NO. 3 (A)

(LTHICK=0.69 M)

RESULTS OF ANALYSIS

7-68

Z	Z(M)	TG(K)	TS(K)	TH(K)	HSG	ASCZ	QSG	DELHTL
1	0.00	1111	1111	1111	1111	1111	1111	0000
2	0.00	1111	1111	1111	1111	1111	1111	0000
3	0.00	1111	1111	1111	1111	1111	1111	0000
4	0.00	1111	1111	1111	1111	1111	1111	0000
5	0.00	1111	1111	1111	1111	1111	1111	0000
6	0.00	1111	1111	1111	1111	1111	1111	0000
7	0.00	1111	1111	1111	1111	1111	1111	0000
8	0.00	1111	1111	1111	1111	1111	1111	0000
9	0.00	1111	1111	1111	1111	1111	1111	0000
10	0.00	1111	1111	1111	1111	1111	1111	0000
11	0.00	1111	1111	1111	1111	1111	1111	0000
12	0.00	1111	1111	1111	1111	1111	1111	0000
13	0.00	1111	1111	1111	1111	1111	1111	0000
14	0.00	1111	1111	1111	1111	1111	1111	0000
15	0.00	1111	1111	1111	1111	1111	1111	0000
16	0.00	1111	1111	1111	1111	1111	1111	0000
17	0.00	1111	1111	1111	1111	1111	1111	0000
18	0.00	1111	1111	1111	1111	1111	1111	0000
19	0.00	1111	1111	1111	1111	1111	1111	0000
20	0.00	1111	1111	1111	1111	1111	1111	0000
21	0.00	1111	1111	1111	1111	1111	1111	0000
22	0.00	1111	1111	1111	1111	1111	1111	0000
23	0.00	1111	1111	1111	1111	1111	1111	0000
24	0.00	1111	1111	1111	1111	1111	1111	0000
25	0.00	1111	1111	1111	1111	1111	1111	0000
26	0.00	1111	1111	1111	1111	1111	1111	0000
27	0.00	1111	1111	1111	1111	1111	1111	0000
28	0.00	1111	1111	1111	1111	1111	1111	0000
29	0.00	1111	1111	1111	1111	1111	1111	0000
30	0.00	1111	1111	1111	1111	1111	1111	0000
31	0.00	1111	1111	1111	1111	1111	1111	0000
32	0.00	1111	1111	1111	1111	1111	1111	0000
33	0.00	1111	1111	1111	1111	1111	1111	0000
34	0.00	1111	1111	1111	1111	1111	1111	0000
35	0.00	1111	1111	1111	1111	1111	1111	0000
36	0.00	1111	1111	1111	1111	1111	1111	0000
37	0.00	1111	1111	1111	1111	1111	1111	0000
38	0.00	1111	1111	1111	1111	1111	1111	0000
39	0.00	1111	1111	1111	1111	1111	1111	0000
40	0.00	1111	1111	1111	1111	1111	1111	0000
41	0.00	1111	1111	1111	1111	1111	1111	0000
42	0.00	1111	1111	1111	1111	1111	1111	0000
43	0.00	1111	1111	1111	1111	1111	1111	0000
44	0.00	1111	1111	1111	1111	1111	1111	0000
45	0.00	1111	1111	1111	1111	1111	1111	0000
46	0.00	1111	1111	1111	1111	1111	1111	0000
47	0.00	1111	1111	1111	1111	1111	1111	0000
48	0.00	1111	1111	1111	1111	1111	1111	0000
49	0.00	1111	1111	1111	1111	1111	1111	0000
50	0.00	1111	1111	1111	1111	1111	1111	0000

HEIGHT OF THE COOLING ZONE=4.60DM

TABLE No. (A2)
SIMULATION OF LIME SHAFT KILN
ANALYSIS OF THE BURNING ZONE

INPUT DATA FOR SET NO. 9 (A)
(TGO = 695 K)

P-33

RESULTS OF ANALYSIS

I	Z (M)	XF	XS	TG(K)	TF(K)	TS(K)	TT(K)	BSHLHD	DELSHT	HFS	HFG	HSG	ASBZ	AFBZ	QFS	QFG	QSG	DELHNL	P026	PC026
1	0.000	0.000	0.000	695	695	695	695	0	0	0	0	0	0	0	0	0	0	0	0	0
2	0.100	0.000	0.000	695	695	695	695	0	0	0	0	0	0	0	0	0	0	0	0	0
3	0.200	0.000	0.000	695	695	695	695	0	0	0	0	0	0	0	0	0	0	0	0	0
4	0.300	0.000	0.000	695	695	695	695	0	0	0	0	0	0	0	0	0	0	0	0	0
5	0.400	0.000	0.000	695	695	695	695	0	0	0	0	0	0	0	0	0	0	0	0	0
6	0.500	0.000	0.000	695	695	695	695	0	0	0	0	0	0	0	0	0	0	0	0	0
7	0.600	0.000	0.000	695	695	695	695	0	0	0	0	0	0	0	0	0	0	0	0	0
8	0.700	0.000	0.000	695	695	695	695	0	0	0	0	0	0	0	0	0	0	0	0	0
9	0.800	0.000	0.000	695	695	695	695	0	0	0	0	0	0	0	0	0	0	0	0	0
10	0.900	0.000	0.000	695	695	695	695	0	0	0	0	0	0	0	0	0	0	0	0	0
11	1.000	0.000	0.000	695	695	695	695	0	0	0	0	0	0	0	0	0	0	0	0	0
12	1.100	0.000	0.000	695	695	695	695	0	0	0	0	0	0	0	0	0	0	0	0	0
13	1.200	0.000	0.000	695	695	695	695	0	0	0	0	0	0	0	0	0	0	0	0	0
14	1.300	0.000	0.000	695	695	695	695	0	0	0	0	0	0	0	0	0	0	0	0	0
15	1.400	0.000	0.000	695	695	695	695	0	0	0	0	0	0	0	0	0	0	0	0	0
16	1.500	0.000	0.000	695	695	695	695	0	0	0	0	0	0	0	0	0	0	0	0	0
17	1.600	0.000	0.000	695	695	695	695	0	0	0	0	0	0	0	0	0	0	0	0	0
18	1.700	0.000	0.000	695	695	695	695	0	0	0	0	0	0	0	0	0	0	0	0	0
19	1.800	0.000	0.000	695	695	695	695	0	0	0	0	0	0	0	0	0	0	0	0	0
20	1.900	0.000	0.000	695	695	695	695	0	0	0	0	0	0	0	0	0	0	0	0	0
21	2.000	0.000	0.000	695	695	695	695	0	0	0	0	0	0	0	0	0	0	0	0	0
22	2.100	0.000	0.000	695	695	695	695	0	0	0	0	0	0	0	0	0	0	0	0	0
23	2.200	0.000	0.000	695	695	695	695	0	0	0	0	0	0	0	0	0	0	0	0	0
24	2.300	0.000	0.000	695	695	695	695	0	0	0	0	0	0	0	0	0	0	0	0	0
25	2.400	0.000	0.000	695	695	695	695	0	0	0	0	0	0	0	0	0	0	0	0	0
26	2.500	0.000	0.000	695	695	695	695	0	0	0	0	0	0	0	0	0	0	0	0	0
27	2.600	0.000	0.000	695	695	695	695	0	0	0	0	0	0	0	0	0	0	0	0	0
28	2.700	0.000	0.000	695	695	695	695	0	0	0	0	0	0	0	0	0	0	0	0	0
29	2.800	0.000	0.000	695	695	695	695	0	0	0	0	0	0	0	0	0	0	0	0	0
30	2.900	0.000	0.000	695	695	695	695	0	0	0	0	0	0	0	0	0	0	0	0	0
31	3.000	0.000	0.000	695	695	695	695	0	0	0	0	0	0	0	0	0	0	0	0	0
32	3.100	0.000	0.000	695	695	695	695	0	0	0	0	0	0	0	0	0	0	0	0	0
33	3.200	0.000	0.000	695	695	695	695	0	0	0	0	0	0	0	0	0	0	0	0	0
34	3.300	0.000	0.000	695	695	695	695	0	0	0	0	0	0	0	0	0	0	0	0	0
35	3.400	0.000	0.000	695	695	695	695	0	0	0	0	0	0	0	0	0	0	0	0	0
36	3.500	0.000	0.000	695	695	695	695	0	0	0	0	0	0	0	0	0	0	0	0	0
37	3.600	0.000	0.000	695	695	695	695	0	0	0	0	0	0	0	0	0	0	0	0	0
38	3.700	0.000	0.000	695	695	695	695	0	0	0	0	0	0	0	0	0	0	0	0	0
39	3.800	0.000	0.000	695	695	695	695	0	0	0	0	0	0	0	0	0	0	0	0	0
40	3.900	0.000	0.000	695	695	695	695	0	0	0	0	0	0	0	0	0	0	0	0	0
41	4.000	0.000	0.000	695	695	695	695	0	0	0	0	0	0	0	0	0	0	0	0	0
42	4.100	0.000	0.000	695	695	695	695	0	0	0	0	0	0	0	0	0	0	0	0	0
43	4.200	0.000	0.000	695	695	695	695	0	0	0	0	0	0	0	0	0	0	0	0	0
44	4.300	0.000	0.000	695	695	695	695	0	0	0	0	0	0	0	0	0	0	0	0	0
45	4.400	0.000	0.000	695	695	695	695	0	0	0	0	0	0	0	0	0	0	0	0	0
46	4.500	0.000	0.000	695	695	695	695	0	0	0	0	0	0	0	0	0	0	0	0	0
47	4.600	0.000	0.000	695	695	695	695	0	0	0	0	0	0	0	0	0	0	0	0	0
48	4.700	0.000	0.000	695	695	695	695	0	0	0	0	0	0	0	0	0	0	0	0	0
49	4.800	0.000	0.000	695	695	695	695	0	0	0	0	0	0	0	0	0	0	0	0	0
50	4.900	0.000	0.000	695	695	695	695	0	0	0	0	0	0	0	0	0	0	0	0	0
51	5.000	0.000	0.000	695	695	695	695	0	0	0	0	0	0	0	0	0	0	0	0	0

ASH-FUSION STARTS AT XF = 0.6967 AT HEIGHT (FROM TOP OF BURNING ZONE) = 1.970 M
HEIGHT OF THE BURNING ZONE = 2.290 M

TABLE 7.9 (E1)

TITLE: SIMULATION OF LIME SHAFT KILN
 STYLE: PREHEATING-CUM-DEVOLATILIZATION ZONE

INPUT DATA FOR SET NO. 9 (B)
 (T60 = 792 K)

RESULTS OF ANALYSIS

I	Z (M)	XF	TG(I)	TF(I)	TS(I)	TL(K)	HFS	HFG	HSG	ASPZ	AFPZ	QFS	QFG	QSG	DELTA TL
1	0.00	0.00	0.00	0.00	0.00	0.00	0.00	0.00	0.00	0.00	0.00	0.00	0.00	0.00	0.00
2	0.00	0.00	0.00	0.00	0.00	0.00	0.00	0.00	0.00	0.00	0.00	0.00	0.00	0.00	0.00
3	0.00	0.00	0.00	0.00	0.00	0.00	0.00	0.00	0.00	0.00	0.00	0.00	0.00	0.00	0.00
4	0.00	0.00	0.00	0.00	0.00	0.00	0.00	0.00	0.00	0.00	0.00	0.00	0.00	0.00	0.00
5	0.00	0.00	0.00	0.00	0.00	0.00	0.00	0.00	0.00	0.00	0.00	0.00	0.00	0.00	0.00
6	0.00	0.00	0.00	0.00	0.00	0.00	0.00	0.00	0.00	0.00	0.00	0.00	0.00	0.00	0.00
7	0.00	0.00	0.00	0.00	0.00	0.00	0.00	0.00	0.00	0.00	0.00	0.00	0.00	0.00	0.00
8	0.00	0.00	0.00	0.00	0.00	0.00	0.00	0.00	0.00	0.00	0.00	0.00	0.00	0.00	0.00
9	0.00	0.00	0.00	0.00	0.00	0.00	0.00	0.00	0.00	0.00	0.00	0.00	0.00	0.00	0.00
10	0.00	0.00	0.00	0.00	0.00	0.00	0.00	0.00	0.00	0.00	0.00	0.00	0.00	0.00	0.00
11	0.00	0.00	0.00	0.00	0.00	0.00	0.00	0.00	0.00	0.00	0.00	0.00	0.00	0.00	0.00
12	0.00	0.00	0.00	0.00	0.00	0.00	0.00	0.00	0.00	0.00	0.00	0.00	0.00	0.00	0.00
13	0.00	0.00	0.00	0.00	0.00	0.00	0.00	0.00	0.00	0.00	0.00	0.00	0.00	0.00	0.00
14	0.00	0.00	0.00	0.00	0.00	0.00	0.00	0.00	0.00	0.00	0.00	0.00	0.00	0.00	0.00
15	0.00	0.00	0.00	0.00	0.00	0.00	0.00	0.00	0.00	0.00	0.00	0.00	0.00	0.00	0.00
16	0.00	0.00	0.00	0.00	0.00	0.00	0.00	0.00	0.00	0.00	0.00	0.00	0.00	0.00	0.00
17	0.00	0.00	0.00	0.00	0.00	0.00	0.00	0.00	0.00	0.00	0.00	0.00	0.00	0.00	0.00
18	0.00	0.00	0.00	0.00	0.00	0.00	0.00	0.00	0.00	0.00	0.00	0.00	0.00	0.00	0.00
19	0.00	0.00	0.00	0.00	0.00	0.00	0.00	0.00	0.00	0.00	0.00	0.00	0.00	0.00	0.00
20	0.00	0.00	0.00	0.00	0.00	0.00	0.00	0.00	0.00	0.00	0.00	0.00	0.00	0.00	0.00
21	0.00	0.00	0.00	0.00	0.00	0.00	0.00	0.00	0.00	0.00	0.00	0.00	0.00	0.00	0.00
22	0.00	0.00	0.00	0.00	0.00	0.00	0.00	0.00	0.00	0.00	0.00	0.00	0.00	0.00	0.00
23	0.00	0.00	0.00	0.00	0.00	0.00	0.00	0.00	0.00	0.00	0.00	0.00	0.00	0.00	0.00
24	0.00	0.00	0.00	0.00	0.00	0.00	0.00	0.00	0.00	0.00	0.00	0.00	0.00	0.00	0.00
25	0.00	0.00	0.00	0.00	0.00	0.00	0.00	0.00	0.00	0.00	0.00	0.00	0.00	0.00	0.00
26	0.00	0.00	0.00	0.00	0.00	0.00	0.00	0.00	0.00	0.00	0.00	0.00	0.00	0.00	0.00
27	0.00	0.00	0.00	0.00	0.00	0.00	0.00	0.00	0.00	0.00	0.00	0.00	0.00	0.00	0.00
28	0.00	0.00	0.00	0.00	0.00	0.00	0.00	0.00	0.00	0.00	0.00	0.00	0.00	0.00	0.00
29	0.00	0.00	0.00	0.00	0.00	0.00	0.00	0.00	0.00	0.00	0.00	0.00	0.00	0.00	0.00
30	0.00	0.00	0.00	0.00	0.00	0.00	0.00	0.00	0.00	0.00	0.00	0.00	0.00	0.00	0.00

VM COMBUSTION STARTS AT XF = 0.1732 AND AT HEIGHT (FROM TOP) = 3.950 M
 HEIGHT OF THE PREHEATING-CUM-DEVOLATILIZATION ZONE = 3.950 M

